UNIVERSITÀ DEGLI STUDI DI TRIESTE

UNIVERSITÀ DEGLI STUDI DI TRIESTE

XXXIV Ciclo del Dottorato di ricerca in Fisica

M-theory geometric engineering for 5d SCFTs and Gopakumar-Vafa invariants

Settore scientifico-disciplinare FIS/02

Dottorando
Andrea Sangiovanni

Coordinatore
Prof. Francesco Longo

Supervisore di Tesi
Prof. Roberto Valandro

Anno accademico 2020/2021

Contents

Ringraziamenti

Ringraziare pubblicamente[1], per via di quell'innata (e stupida?) ritrosia ad esprimere le proprie emozioni, è operazione difficile nella propria lingua madre, figuriamoci in inglese. Per questo, scrivo qui qualche riga in italiano.

Va da sé che questo lavoro non esisterebbe senza la costante guida e supporto, nel corso di quasi quattro lunghi anni, del mio supervisore, Roberto. Per questo, e per avermi instillato il piacere della ricerca, nonché il dovere di condurla con precisione e senza superficialità[2], ti ringrazio profondamente.

Grazie Mario per i pomeriggi di svago, al contempo incredibilmente produttivi ai fini accademici, grazie Andrés per lo stimolo e l'ospitalità in questi ultimi mesi di dottorato, e grazie ai membri del dipartimento di Fisica teorica dell'ULB per avermi contestualmente accolto a Bruxelles.

Essendo frutto di un lavoro umano, questa tesi ha le sue radici nel contributo inestricabile che amici e anime affini offrono alla complessificazione e alla divagazione della mente. Per questo lato personale ed emotivamente drenante, credo che lo strumento più consono sia la lista, nell'accezione sfaccettata e intessuta di valore di Eco. Lista che icasticamente (ma significativamente) racchiude in ogni elemento un contenuto affettivo, che ne costituisce cifra unica e distintiva: grazie Sergej, Luca, Sonia, Edoardo, Clara, Caterina, Rola, Pierfrancesco, Alvise, Giulia, Chiara, Francesca, José, Anirudh, Ankur, Lorenzo, Caitlin, Jakob.

Infine, come postilla nobilissima alla lista, ringrazio immensamente la mia famiglia, Marta, Marco e Fabio[3], per le ragioni che tutti i figli e i fratelli conoscono e che non serve esplicitare, e per avermi supportato e incoraggiato da sempre, in particolare fin da quando, beh...fin da quando ero un ragazzino con una sciocca passione per le stelle e i buchi neri.

[1]Pur tenendo conto della limitatissima diffusione che interesserà questo lavoro.

[2]La responsabilità di qualsivoglia dettaglio di questa tesi che dimostri che lo studente non ha appreso del tutto questi principi va ascritto, ovviamente, a me.

[3]Cui debbo le mie scuse, per questa sviolinata.

Abstract

M-theory compactified on non-compact singular Calabi-Yau threefolds is a fertile environment for both physical and mathematical considerations: on the one hand, by dimensional reduction on the threefolds, it gives rise to five-dimensional superconformal field theories (SCFTs), in the spirit of geometric engineering; on the other side, the dynamics of M2-branes wrapped on the extra dimensions encodes topological data of the threefolds, such as their Gopakumar-Vafa (GV) invariants.

In this work, we tackle the analysis of M-theory on Calabi-Yau threefolds exhibiting *terminal* isolated singularities, namely spaces admitting a crepant resolution where only complex-dimension one (at most) exceptional loci appear. This implies that the 5d SCFT arising from M-theory has rank 0, i.e. a trivial Coulomb branch, and possibly a non-trivial Higgs branch. Furthermore, all threefolds enjoying this property can be described in the framework of ADE singularity theory.

Operating in this setting, we establish a clear-cut relationship between the M-theory compactification space and a complex scalar field, transforming in the adjoint of an appropriate ADE algebra, that captures the properties of the five-dimensional Higgs branch, as well as the information concerning the GV invariants of the corresponding threefold.

Thanks to this method, that possesses a natural interpretation in Type IIA in the A and D Lie algebra cases, we classify Higgs branches and GV invariants in a wide variety of M-theory compactifications, constructing explicit examples of simple flops of all lengths, and systematizing the analysis of the quasi-homogeneous compound Du Val threefolds. Besides, the tools we develop naturally offer a scaffolding upon which to study the role of T-brane backgrounds in the M-theory context, also lending themselves to complementary interpretations based on the tachyon condensation formalism.

Introduction

String theory as a multi-purpose tool

Since its inception during the seventies as an attempt to describe strong interactions, string theory has entirely reshaped the world of theoretical physics research, sparkling a series of developments, spanning from applications to condensed matter physics to the opening of new mathematical programs, that are still to be fully understood. The first turning point in the long history of string theory came with the "first superstring revolution" in the mid-eighties, when Green and Schwarz showed [1] that heterotic string theory is devoid of anomalies. This fact, combined with the natural emergence of a spin-2 particle from the quantization of the string, attracted a huge amount of interest, in the hope that string theory could provide the first coherent account of a theory of quantum gravity. The necessary ingredients needed for this pursuit, though, were provided in the course of the "second superstring revolution", that rocked the field in the mid-nineties. In a seminal paper [2], Witten argued that the five variants of string theory living in ten spacetime dimensions, namely Type I string theory, Type IIA and IIB, and the heterotic $SO(32)$ and $E_8 \times E_8$ string theories, were nothing but facets of a deeper theory, that came to be known as M-theory, connected by a web of dualities. Shortly after, Polchinski introduced [3] new kinds of entities into the picture of string theory, realizing that extended objects, dubbed D-branes, naturally arose as the end-points of strings, obtained imposing suitable boundary conditions on the strings equations of motion. D-branes, along with their counterparts in M-theory, have wildly broadened the theoretical power of string theory, fostering great advancements in the quest for a consistent string theory model, that should be able to reproduce the features of the Universe in all its observable (up to our present experimental precision) nuances, including the Standard model, BSM particle physics such as neutrino masses and dark matter, and the cosmological constant. The ultimate objective of this ongoing research program, also known as *string phenomenology*, is to find the correct string theory vacuum displaying the desired characteristics: to this end, constructions such as the KKLT and the LVS proposals, that make full use of the tools offered by string theory, such as brane-constructions and flux-based techniques for moduli stabilization, have been put forward with promising results, although no completely satisfactory model has been found, yet. This is also due to the mind-boggling amount of string theory vacua, that has hampered the attempts to control them, and to the tight consistency constraints imposed by string theory. Furthermore, in the recent years the Swampland program has furnished sharper tools to circumscribe the viable landscape of effective theories that uplift to consistent theories of quantum gravity[4], providing non-trivial checks and narrowing the research spectrum.

The quest for a fully detailed, consistent and predictive model of the Universe in a string theory setting follows the philosophical fil rouge that goes from the first steps of Galileo and Newton in explaining the dynamics of common objects and the Solar system, to the extreme-precision measurements and discoveries of new particles in accelerators during the late twentieth century, in an ever-increasing search for a unifying theory of Nature.

String theory, though, is not *only* a magnificent environment in which to undertake this task: in the last forty years, with an accelerating pattern in the last couple of decades, string theory has proven itself to be a multi-faceted tool, lying at the intersection of mathematics and physics, capable of seeding fruitful theoretical advancements in both realms. It is in the context of this more ample understanding of string theory that this thesis draws its motivations.

On the one hand, string theory has a long history of fostering unanticipated developments in pure mathematics, such as the application of topological quantum field theory to knot invariants [5] and the inception of mirror symmetry [6,7], to name but two chief examples. In this perspective, since the mid-nineties, thanks to the work of Gopakumar and Vafa [8–10], string theory and M-theory have lied at the crossroads of an ambitious program of classification of topological invariants of Calabi-Yau threefolds: making use of the topological string theory A-model and its M-theory translation, it was realized that invariants counting holomorphic maps from a Riemann surface to some homology class in a Calabi-Yau threefold, known as Gromov-Witten (GW) invariants, could be reformulated from a physical perspective as the counting of M2-brane BPS states wrapping those very same homology classes. The latter constitute the Gopakumar-Vafa (GV) invariants, that have played a relevant role in the physics literature, as they encode non-perturbative corrections in the effective theories arising from string compactifications. Their integrality, as opposed to the rationality of the GW invariants, has been conjectured also in relation to their physical interpretation as a BPS count, but has been proven in full generality only in the genus-0 case [11]. In turn, it is thought that the Gromov-Witten formulation is equivalent to the Donaldson-Thomas (DT) theory, that counts invariants of moduli space of sheaves on a Calabi-Yau threefold, in what is known as the MNOP conjecture[5]. Analogously, the Gopakumar-Vafa data can be converted in sheaf-theoretic language introducing the Pandharipande-Thomas (PT) invariants, that count the so-called "stable pairs" of Calabi-Yau threefolds. All in all, the web of (conjectured) relationships between invariants of Calabi-Yau threefolds can be organized as follows[6]:

[4] It should be noted, though, that the application of the Swampland program goes also beyond the realm of string theory. See e.g. the review work by [4].

[5] Shorthand for Maulik-Nekrasov-Okounkov-Pandharipande conjecture.

[6] For a review of these relationships see e.g. [12].

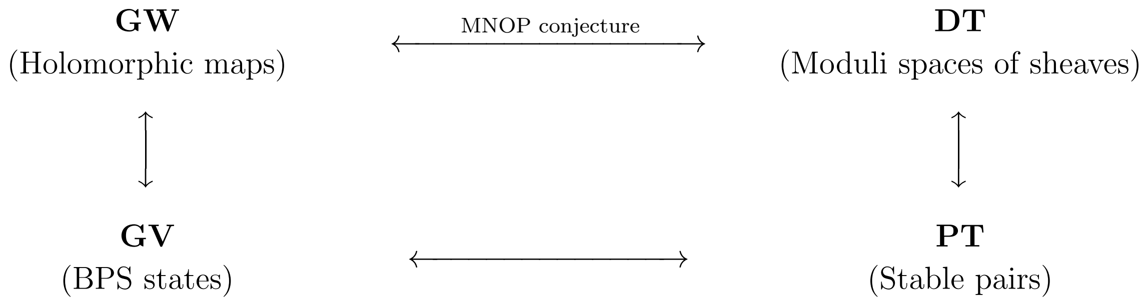

Figure 1: *Correspondences between invariants of Calabi-Yau threefolds.*

String theory has provided invaluable tools to investigate the correspondences in Figure 1, as well as to directly compute the respective invariants: in this thesis, while keeping in mind this convoluted web of dualities, we will stick to the analysis of the lower-left corner, namely of GV invariants.

In a complementary fashion with respect to its mathematical repercussions, the highly-structured geometrical underpinnings of string theory have provided unexpected ways to study and classify the general properties of quantum field theories (QFTs), which appear ubiquitously in the description of Nature, from particle physics to condensed matter theory. A comprehensive analysis of the properties of QFTs is, at present, lacking. Despite this, the subject has undergone huge progress in the course of the last decades, especially in the class of *supersymmetric* QFTs, thanks to substantial advancements in the understanding of strongly-coupled phenomena, the realization that the realm of theories admitting a Lagrangian formulation is extremely limited, and the complete overhaul of the concept of symmetry, with the introduction of higher-form symmetries, higher-group structures and non-invertible symmetries. Such theoretical achievements are deeply interconnected, and string theory has provided a framework to elucidate their properties, as well as to produce new predictions. In particular, string theory has furnished recipes to explicitly construct quantum field theories that are in some cases inaccessible from a purely field-theoretic perspective, employing the power of the extra dimensions in the non-compact limit, where gravity decouples. This program, that relates the properties of QFTs to the features of string theory on a *singular* compactification space, earned the name of *geometric engineering*, and was initiated by Katz, Klemm and Vafa in a series of seminal papers [13, 14], that employed string dualities to study $\mathcal{N} = 2$ and $\mathcal{N} = 1$ QFTs in four spacetime dimensions. In particular, the study of 4d $\mathcal{N} = 2$ QFTs has undergone huge improvement since then, following the organizing principles provided by 4d $\mathcal{N} = 2$ Super-Conformal field theories (SCFTs) and focusing on the analysis of their Coulomb and Higgs branches, as well as on the related RG flows. In such spirit, the introduction of Seiberg-Witten curves has renownedly revolutionized the study of 4d $\mathcal{N} = 2$ Coulomb branches [15, 16], later being given a string theory interpretation, and wide classes of QFTs have been studied and classified employing the class $\mathcal{S}$ construction, involving M5-branes wrapped on a Riemann surface [17, 18], and Type IIB setups on singular Calabi-Yau threefolds [19]. Such Type IIB based constructions have also allowed to engineer large classes of strongly-coupled SCFTs admitting Coulomb branch operators with fractional scaling dimensions, such as Argyres-Douglas theories[7], that were first studied from a gauge-theory perspective in [20, 21].

The geometrical setups of string theory, besides, have enabled the probing of quantum field theories in higher spacetime dimensions, such as 6d and 5d. In dimensions greater than four, the Yang-Mills gauge coupling has negative mass dimension, and hence gauge theories are non-renormalizable. At the infinite coupling limit, though, gauge theories in 6d and 5d can flow to *superconformal fixed points*, that admit no marginal deformations in 5d and in the 6d case with minimal supersymmetry. Turning on a mass deformation on the SCFT point can trigger a RG flow to some weakly-coupled gauge theory in the IR: depending on the specifics of the mass deformation, one can obtain different low-energy gauge theories which are in some sense "dual" in the UV, as they are related to the same SCFT. In this regard, string theory has set the table for a classification of 6d SCFTs with $\mathcal{N} = (2, 0)$ supersymmetry from Type IIB on ADE singularities [22–24], and with $\mathcal{N} = (1, 0)$ supersymmetry using a F-theory formulation [25–27].

The panorama on 5d SCFTs is somewhat more obscure. It has been conjectured that all 5d SCFTs arise from circle compactification of 6d SCFTs [28], but a systematic classification is still absent. The origin of the subject dates back to the work of Seiberg, Morrison and Intriligator [29–31], that showed phenomena of flavor symmetry enhancements in theories with $SU(2)$ gauge symmetry and a variable number of flavors, discovering the famous E_n theories.

In general, there exist various approaches in dealing with 5d $\mathcal{N} = 1$ SCFTs via stringy constructions. Among the chief ones, 5-branes setups arranged as (p, q)-webs in Type IIB string theory [32, 33] have allowed a direct analysis of the Coulomb and Higgs branches of vast classes of 5d SCFTs, via the parameters encoded by the movement of the branes along their transverse directions [34–43]. The SCFT limit is reached when all the components of the web collapse, yielding the singular point. These setups can often be given a toric-geometric interpretation, and more recently the introduction of generalized toric polygons (GTP) has further expanded the subject [44–46].

A complementary approach to construct 5d SCFTs comes from the reduction of *M-theory on Calabi-Yau threefolds* exhibiting a canonical singularity. There exists a beautiful dictionary between the properties of the M-theory geometry and the moduli spaces of the 5d SCFT: resolutions of the singularity correspond to the (extended[8]) Coulomb branch of the theory, whereas deformations of the singularity encode its Higgs branch. Geometrically, divisors that shrink to a point through the blow-down dictate the gauge symmetry, and their

[7]We should note here that, recently, it has been proposed to *define* Argyres-Douglas theories precisely as those theories with fractional scaling dimensions of the Coulomb branch operators.

[8]The *extended* Coulomb branch is defined including also mass deformations. We will return to its definition in the context of 5d SCFTs in Chapter 4.

volume regulates the gauge-coupling. W-bosons arise from M2-branes wrapping $\mathbb{P}^1$'s that are ruled over some curve contained in the exceptional divisors. Shrinking rigid curves correspond to mass parameters, and M2-branes wrapping such curves give rise to hypermultiplets, whose mass is controlled by the volume of the curve. The SCFT point is reached in the limit of vanishing volume of all the exceptional divisors and curves. Employing this framework, large swaths of the 5d SCFTs landscape have been explored, in the toric realm [47,48], in elliptically fibered cases or from circle reduction from 6d [28,49–57], and in a limited amount of isolated hypersurface singularities (IHS) examples [58–61].

Recently, novel techniques have been added to the toolbox for the analysis of 5d SCFTs, and in particular of their Higgs branch: through a chain of dualities from Type IIB theory to Type IIA, it is possible to construct a *magnetic quiver*, interpreted as a quiver for a 3d $\mathcal{N} = 4$ theory, whose Coulomb branch is isomorphic, save for some ungauging of $U(1)$ symmetries, to the Higgs branch of M-theory on a Calabi-Yau threefold with a canonical singularity. Magnetic quivers [62–65] have paved the way for a more in-depth analysis of the geometrical structure of the Higgs branches of 5d SCFTs [66–74]: it has been possible to detail the symplectic foliation structure of the Higgs branches via a Hasse diagram [75], whose "leaves" (i.e. points) represent different phases of the SCFT. The lines connecting points in the Hasse diagrams, which are Slodowy (transverse) slices, can be associated to a magnetic quiver, and represent theories coming from the Higgsing of the original SCFT.

Finally, the novel framework provided by generalized symmetries has offered additional tools allowing a more thorough understanding of the structure of 5d SCFTs, constraining their non-perturbative dynamics. In this regard, 5d SCFTs arising, e.g., from compactifications on generalized toric polygons and $\mathbb{C}^3$-orbifolds have been examined, also taking into account their relationships between parent 6d theories and emerging higher-group structures [76–83].

This thesis

The work that constitutes the core of this thesis lies at the intersection of the two broad research veins that we have briefly recalled, namely the mathematics program aiming at the classification and computation of invariants of Calabi-Yau threefolds, and the peculiarly physics-based quest for a deeper understanding of the structure of 5d $\mathcal{N} = 1$ SCFTs. This research area is enormous and we focus, of course, on a limited corner of the available space of unsolved problems, that is nevertheless extremely rich.

In particular, we concentrate on *rank-0* 5d $\mathcal{N} = 1$ SCFT engineered from M-theory on singular Calabi-Yau threefolds, built as isolated hypersurface singularities, i.e. from equations of the form:

$$F(x, y, z, w) = 0 \quad \subset \mathbb{C}^4, \tag{1}$$

where x, y, z, w are complex coordinates. Geometrically, rank-0 means that we are considering *terminal singularities*, i.e. singularities that admit at most complex curves in the crepant resolution, and *no exceptional divisor*. Physically, this implies that the 5d SCFTs have an empty Coulomb branch, and possibly a non-trivial Higgs branch. This choice is, of course, quite restrictive in the landscape of possible 5d $\mathcal{N} = 1$ SCFTs, but as we will see it conversely provides extremely explicit computational tools, that will allow a direct inspection of the Higgs branches of the theories of interest. A theorem by Reid [84] proves that *all* the Calabi-Yau threefolds admitting terminal isolated singularities are of compound Du Val type, namely they take the form:

$$f(x, y, z) + wg(x, y, z, w) = 0 \quad \subset \mathbb{C}^4, \tag{2}$$

where $f(x, y, z)$ is a Du Val singularity, also known as ADE singularity. Notice that (2) is a one-parameter deformation of the ADE singularity, namely a non-trivial fibration of an ADE singularity over the plane $\mathbb{C}_w$. These singularities are, except from sparse examples such as the conifold, *non-toric*.

As a result, the natural environment to undertake the study of rank-0 5d SCFTs with 8 supercharges is that of M-theory compactified on compound Du Val isolated singularities, namely one-parameter families of deformed ADE singularities. This is the setting we will work on throughout the course of the thesis.

The study of these setups, though, is not exclusively motivated by the analysis of the 5d SCFTs that arise after the M-theory dimensional reduction, and draws its relevance also from the investigation of the topological properties of the compactification threefolds, in the form of their GV invariants: indeed, as we will sketch momentarily, there exists a one-to-one correspondence between the GV invariants of a Calabi-Yau threefold with an isolated compound Du Val singularity, and the Higgs branch of the 5d $\mathcal{N} = 1$ SCFT engineered from M-theory on that very same singularity. While for toric cases there exist systematic methods such as the topological vertex [85], in the context of deformed ADE singularities GV invariants have been computed only in a very limited selection of cases, mostly in the mathematical literature [86–92].

In very broad brushes, we can schematically sum up the setup and the applications of this thesis in the following picture:

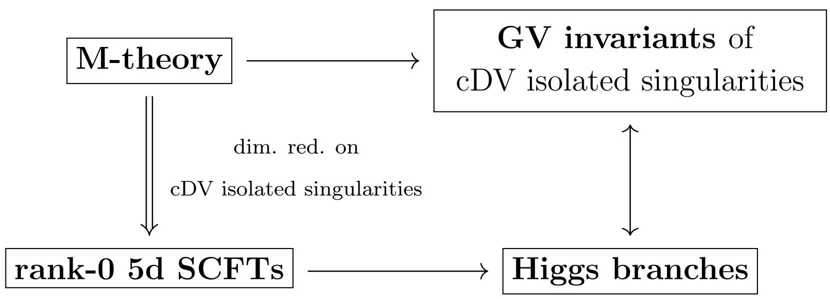

In the rest of this work, then, we lay a bipartite objective:

- Compute the Higgs branches of rank-0 5d $\mathcal{N} = 1$ SCFTs arising from M-theory compactifications on cDV isolated singularities.

- Compute the Gopakumar-Vafa (GV) invariants of Calabi-Yau threefolds built as cDV isolated singularities.

As we have said, these tasks are two faces of the same coin, and we will explicitly build the bridge between the mathematical and physical side of the story, yielding on the one hand a new physical interpretation to the GV invariants, and on the other side a systematic classification of rank-0 5d SCFT Higgs branches.

In order to tackle this set of problems, we introduce a new technique that allows extremely explicit computations. The gist of the strategy is to establish a correspondence between cDV isolated singularities, built as a one-parameter deformation of an ADE singularity of type $\mathfrak{g}$, and a complex scalar field Φ transforming in the adjoint of $\mathfrak{g}$. It is in this sense that we will talk about this setup as the "adjoint Higgs method", as all the relevant data about the GV invariants of the threefold and the Higgs branch of the 5d SCFT arising from compactification on the same threefold are encoded in such complex scalar field. Let us briefly sketch how this comes about.

Consider M-theory compactified on an ADE singularity $\mathfrak{g}$: this gives rise to an effective $\mathcal{N} = 1$ theory in 7d, that contains three real scalars ϕ_1, ϕ_2, ϕ_3 transforming in the adjoint of $\mathfrak{g}$. We can combine two of them into a complex scalar field $\Phi = \phi_1 + i\phi_2$, that controls the complex deformations of the ADE surface. If we switch on a position-dependent vev for Φ, say $\langle\Phi(w)\rangle$, where w is a complex coordinate, we are deforming the M-theory geometry, namely we are adding a w-dependent deformation term to the ADE singularity (specifically, the *Casimirs* of $\langle\Phi(w)\rangle$ control the deformation). This yields precisely a cDV singularity of the form (2). If the starting Du Val singularity is of A and D type, this has a very precise meaning in the Type IIA dual picture: M-theory on A and D singularities is dual to Type IIA with a stack of coincident D6-branes (on top of an orientifold plane, in the D case). In this context, the scalar fields ϕ_1, ϕ_2, ϕ_3 parametrize motion transverse to the branes, and turning on a vev $\langle\Phi(w)\rangle$ corresponds to a deformation of the brane-stack in the w direction, yielding a setup of branes intersecting at[9] $w = 0$.

We see then that there exists a correspondence between the deformed geometry, namely the cDV singularity on which M-theory is compactified, and the Higgs vev $\langle\Phi(w)\rangle$. This is the key observation that enables all of our subsequent reasonings[10].

$$\boxed{\text{Higgs vev } \langle\Phi(w)\rangle} \quad \Longleftrightarrow \quad \boxed{\text{cDV isolated singularity}} \tag{3}$$

In order to study the Higgs branches of the 5d SCFTs arising from M-theory compacti-

[9]Modulo some shift along the w coordinate.

[10]As we will see in the following, this correspondence is *not* one-to-one. This will yield interesting physical consequences, related to T-brane backgrounds.

fication, we can consider fluctuations φ around the background $\langle\Phi(w)\rangle$:

$$\Phi(w) = \langle\Phi(w)\rangle + \varphi(w). \tag{4}$$

Not all the fluctuations correspond to physical degrees of freedom, and they must first be gauge-fixed using the 7d gauge symmetry: the zero-modes that survive the gauge-fixing and that are localized on $w = 0$ are genuine five-dimensional degrees of freedom, and correspond to hypermultiplets in the 5d SCFT. In the Type IIA picture (whenever available), these are open string modes stretching between the D6-branes near the point $w = 0$. This computation, after suitably embedding $\langle\Phi(w)\rangle$ in an explicit matrix representation, can be carried out with straightforward linear algebra methods, and further allows to pinpoint the preserved symmetry is 5d, which is given by the stabilizer of $\langle\Phi(w)\rangle$. Combining the data about the hypermultiplets and the 5d symmetries, including their explicit action on the hypermultiplets, one can completely characterize the Higgs branch of the 5d SCFT, as a complex algebraic variety[11].

This line of reasoning also naturally entails that we can extract information about the GV invariants of the compactification threefold via the Higgs branch computation: indeed, as we are dealing with cDV singularities, which are terminal, we can consider M2-branes wrapping the exceptional curves inflated by the resolution[12]. These give rise to BPS states that descend to hypermultiplets in 5d. On the other hand, the M2-brane BPS states counting is precisely the kind of data that is encoded by the GV invariants theory of the Calabi-Yau threefold. We reach a significant conclusion: the Higgs branch data (namely, the hypermultiplets, the symmetries, and the charges under the symmetries) have a direct counterpart in terms of the geometrical data of the M-theory threefold: the GV invariants correspond to the number of hypermultiplets, the exceptional curves are in one-to-one correspondence with the continuous preserved symmetries, and the degrees of the GV invariants regulate the charges of the 5d hypers. In this fashion, we can characterize the GV invariants of cDV threefolds that are largely unexplored from this perspective.

The preceding lines rapidly sum up the main physical and mathematical idea of this work, whose fruits, though, are not as easy to reap. Given the interpretation of the Higgs branch and GV data in terms of a "adjoint Higgs background" describing the corresponding cDV singularity, in fact, one must sit down and write the Higgs background explicitly, if one wishes to use it for actual computations. This proves to be a non-trivial task.

As a consequence, much of the technical content of this work lies in developing concrete techniques to build, given a cDV geometry, the associated Higgs background. The cornerstone for this kind of task was laid by [93] and subsequently developed in [94], that introduced the concept of T-branes, namely of Higgs profiles that are not trivially diagonal. Using these ideas and employing the formalism of tachyon condensation, [95] dealt with

[11]Namely, one cannot obtain, solely employing this method, the metric on the Higgs branch.

[12]We will see, in addition, that M2-brane states at the singular point can be defined also in the absence of crepant exceptional curves.

some special cases of Du Val singularities taken from the A series, showing how to explicitly relate the Higgs background $\langle\Phi(w)\rangle$ to the M-theory geometry, namely to a cDV singularity. Analogous results for D and E singularities, as well as for more involved cases in the A series, were not, to our knowledge, present in the literature. In the course of this work, we dealt with all the aforementioned cases, showing:

1. How to explicitly relate the M-theory geometry (a cDV singularity) to an adjoint Higgs background, which in general is not diagonal, in *all* the ADE cases.

2. Employing the connection provided by 1, how to explicitly build the Higgs backgrounds for large classes of cDV singularities.

Furthermore, the seminal work of [94] has huge repercussions for our choices of Higgs backgrounds: we will see, indeed, that the correspondence between Higgs backgrounds and threefold geometries is not one-to-one, but that in general a single geometry is compatible with many inequivalent backgrounds, in the precise sense that they yield a different physics in 5d. These take the name of T-brane backgrounds, and one must be extremely careful in distinguishing them, if one wishes to correctly reproduce the 5d field theory expectations, and make contact with the existing literature in the few cases already present in the literature. As a consequence, we will devote congruent space to T-brane backgrounds throughout the thesis.

From the purely technical point of view, we have accomplished tasks 1 and 2 heavily relying on the theory of ADE Lie algebras: in particular, the nilpotent orbits and the Slodowy slices through nilpotent orbits prove themselves to be the organizing principles for the explicit construction of Higgs backgrounds. In addition, such tools naturally lead to an interpretation of the Higgs backgrounds as related to the theory of Grothendieck-Springer resolutions, which furnish an alternative to standard resolution techniques, and that further yield useful byproducts, such as the versal deformations of ADE singularities in coordinates adapted to a given partial simultaneous resolution.

In the Conclusions, we will analyze the results of this work in details; before that, we sketch here the key take-aways:

- The Higgs branches of 5d SCFTs from M-theory on cDV isolated singularities are composed of free hypers or of discrete gaugings of free hypers. The flavor symmetry is dictated by the exceptional curves in the crepant resolution of the cDV isolated singularities.

- The GV invariants of cDV isolated singularities are related to the Higgs branch data from M-theory on the same singularities.

- We have explicitly computed the Higgs branch data (and thus, the corresponding GV invariants) in large classes of cDV singularities, namely (in growing degree of generality):

- Relevant examples of cDV singularities (conifold, Reid's pagodas, Brown-Wemyss' singularity, Laufer's singularity)
- Instances of *simple flops of all lengths.*
- *All* quasi-homogeneous cDV singularities. These comprise also singularities that give rise to Argyres-Douglas theories of type $(A, \mathfrak{g})$, with $\mathfrak{g} = A, D, E$, in Type IIB compactifications.

In the next section, we briefly summarize the general structure of the thesis.

Outline

The work is divided into two parts: in **Part I**, we introduce background material and we progressively build towards the construction of explicit Higgs backgrounds associated to threefold singularities.

In **Part II**, we concretely apply the tools developed in Part I in a wide array of classes.

Part I

We start in **Chapter 1** with a brief introduction on ADE singularities, specifically adapted to our purposes, and with no presumption of completeness. We recap the structure of their resolutions and deformations, and review the concept of complete and partial simultaneous resolutions. We define compound Du Val (cDV) singularities.

In **Chapter 2**, we introduce some mathematical concepts that will be key in the reasonings of later chapters: we set in the context of ADE Lie algebras, and introduce their nilpotent orbits and Slodowy slices, exhibiting explicit examples. Thanks to these tools, we then review the theory of Grothendieck-Springer resolutions of ADE singularities, providing fully worked-out examples.

Chapter 3 is the technical core of the thesis, and we begin introducing physics into the game. We briefly retrace the logical process behind M-theory compactifications, proceeding gradually: we sketchily review M-theory on smooth manifolds, M-theory on K3 singularities, and finally we start dealing with M-theory on one-parameter deformed ADE singularities, namely cDV singularities. Introducing our original contributions, we show how the theory of Springer resolutions can help us associate a Higgs background to a cDV singularity, taking the conifold as the simplest working example. We then proceed in generalizing the strategy to encompass all singularities of A, D and E type, writing down explicitly the connection between the Higgs backgrounds and threefold equations, which is encoded in the Casimirs of the Higgs backgrounds. We conclude explaining the gauge-theory role of the Higgs backgrounds, and summing up the general recipe to construct them.

Part II

In **Chapter 4**, we get to the gnosiological nutshell of the work: we recap the definition of Gopakumar-Vafa (GV) invariants, and quickly review the main properties of 5d $\mathcal{N}=1$ SCFTs. We introduce simple threefold flops, that constitute the first class of examples we wish to analyze. These are cDV singularities admitting a single exceptional curve in the resolution: we first define them precisely, highlighting the physical meaning of their *length*.

Then, we get into the original work, showing how to extract the Higgs branch and the GV data from the Higgs background, at first relying on the simple example of the conifold. We then move on applying this technique to a few cases of simple flop examples from the A and the D series, such as Reid's pagodas, the Brown-Wemyss' singularity and Laufer's singularity, comparing results with the existing literature. Then, we explain in full generality how to explicitly construct Higgs backgrounds associated to simple flops, and introduce a novel algorithm to compute the Higgs branch and GV data, that lends itself to an efficient computer implementation. We thus exhibit concrete examples of flops of all lengths, computing their GV invariants and the Higgs branch from M-theory compactified on them, making contact, in some cases, with the existing literature. We conclude by going beyond the formalism of simple flops, exihibiting non-simple flops and non-resolvable (in a crepant fashion) singularities. This also yields the first simple examples of T-brane backgrounds.

In **Chapter 5**, we classify the Higgs branches (and consequently, the related GV invariants) of the rank-0 5d SCFTs arising from M-theory on *all* quasi-homogeneous cDV singularities. We start by recalling the classification of quasi-homogeneous cDV singularities, and introduce a refinement of our construction of Higgs backgrounds, that allows us to systematically build them for all the cases of interest, solely by looking at the cDV equation. We then proceed in writing down Tables of results for the Higgs branch and GV data. We conclude by analyzing the role of T-branes in this context.

In **Chapter 6**, we revisit the content of Chapter 4 from the perspective of tachyon condensation, that yields, in selected cases, more compact and efficient results. We conclude by displaying some useful properties of determinantal varieties in the analysis of Laufer's singularity.

In the **Conclusions**, we summarize our construction of Higgs backgrounds associated to cDV threefold isolated singularities, putting all the pieces together and providing a unitary perspective. We conclude with some final remarks on the achieved results and future perspectives.

In **Appendix A**, we give a short review of the theory of ADE Lie algebras, focused on the objectives of the main text. In **Appendix B**, we write down explicitly the deformation parameters of the exceptional singularities E_6, E_7, E_8 in terms of the Casimirs of the Higgs background. In **Appendix C** and **D**, we give some additional details about the Higgs branches of (A,A) singularities and the hierarchy of T-brane backgrounds in (A,D) singularities, respectively.

Original contributions

The original work of this thesis is distributed as follows: in Chapter 2, the fully worked-out examples of Springer resolutions; in Chapter 3, the relationship between Springer resolutions and Higgs backgrounds, as well as the connection between Higgs backgrounds and M-theory geometry, namely everything from 3.3 on (except the M-theory uplift of the brane loci in the A series); in Chapter 4, everything except the review sections about GV invariants, 5d SCFTs and the definition of simple flops; the entirety of Chapters 5 and 6, except for the brief introductory reviews about cDV singularities and tachyon condensation.

The work is for the most part based on a handful of published (or submitted, at the present time) papers, that we report here for completeness. They have been realized in collaboration with Roberto Valandro, Mario De Marco and Andrés Collinucci.

Published:

- A. Collinucci, A. Sangiovanni and R. Valandro, *Genus zero Gopakumar-Vafa invariants from open strings*, JHEP **09** (2021), 059.
- A. Collinucci, M. De Marco, A. Sangiovanni and R. Valandro, *Higgs branches of 5d rank-zero theories from geometry*, JHEP **10** (2021), 018.
- M. De Marco and A. Sangiovanni, *Higgs branches of rank-0 5d theories from M-theory on* (A_j, A_l) *and* (A_k, D_n) *singularities*, JHEP **03** (2022), 099.

Submitted for publication:

- A. Collinucci, M. De Marco, A. Sangiovanni and R. Valandro, *Flops of any length, Gopakumar-Vafa invariants, and 5d Higgs branches*, arXiv:2204.10366.
- M. De Marco, A. Sangiovanni and R. Valandro, *5d Higgs branches from M-theory on quasi-homogeneous cDV threefold singularities*, arXiv:2205.01125.

We briefly add a "historical" note: this work started as a simple exercise in the theory of Lie algebras, studying nilpotent orbits, Slodowy slices and Grothendieck-Springer resolutions, trying to work out examples of the latter in a completely explicit fashion. Unexpectedly, this led to construct the first Higgs backgrounds for cases in the D series, and to the realization that zero-modes of fluctuations around the Higgs backgrounds encode GV and Higgs branch data, inspiring the papers [96] and [97].

Subsequently, the attempt to generalize the technique in a systematic way allowed to tackle M-theory geometric engineering on (A, A) and (A, D) singularities, producing [98]. The tools and the understanding needed to write this paper paved the way for the last steps, that encompassed the generalization to exceptional singularities and all quasi-homogeneous cDV singularities, whose analysis was finalized in [99] and [100].

Part I

CHAPTER 1

Singularity theory

As was briefly mentioned in the Introduction, string theory on singular spaces is a rich and diverse environment, yielding peculiar features that lie at the core of geometric engineering of quantum field theories.

The overarching theme of this work is the analysis of the physical and mathematical properties of M-theory compactifications on some classes of *singular* Calabi-Yau threefolds.

Defining and explaining what constitutes a singularity is therefore imperative to start off, and in this chapter we will provide a short introduction to the topic without requiring extreme mathematical rigor, focusing especially on the class of ADE singularities.

We start in Section 1.1 by reviewing the very definition of singular points, we introduce ADE singularities in Section 1.2, their resolutions and deformations in Section 1.3, and we conclude mentioning some basic facts about compound Du Val singularities (which will be the main playground of this thesis) in Section 1.4.

1.1 Singularities in algebraic geometry

As a first, let us define our main objects of interest: *algebraic varieties.*

Def 1.1. *An **algebraic variety** is a set $X \subset \mathbb{C}^n$ defined as the zero locus of some polynomials F_i:*

$$X := \{(z_1, ..., z_n) \mid F_i(z_1, ..., z_n) = 0\}$$

where $(z_1, ..., z_n)$ are the coordinates on $\mathbb{C}^n$. In the rest of this work we will be interested in *singular* algebraic varieties, understood as:

Def 1.2. *An irreducible algebraic variety X of dimension m is **smooth** at a point p if the Jacobian matrix:*

$$\mathcal{J} = \left(\frac{\partial F_i}{\partial z_j} \right) \Bigg|_p$$

has rank $n - m$.

*Otherwise, the variety is said to be **singular** at p.*

Of course, singularities are not necessarily found on isolated points, but can appear on generic subvarieties of X. In the remainder of this work, though, we will focus exclusively on algebraic varieties that are singular only on isolated points.

Just to ground these definitions in intuition, an extremely trivial example of smooth variety is the circle S^1 embedded in $\mathbb{R}^2$:

$$F = 0 \quad \text{with } F = x^2 + y^2 - 1 \qquad \nabla F = 0 \Rightarrow (x, y) = (0, 0).$$

The gradient vanishes on the origin, that however does not belong to S^1, that therefore is smooth.

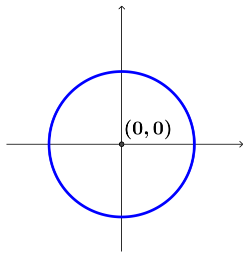

Figure 1.1: $S^1 \subset \mathbb{R}^2$ *is non-singular.*

On the other hand, a trivial example of singular variety is given by the following self-intersecting curve in $\mathbb{R}^2$:

$$F = 0 \quad \text{with } F = y^2 - x^2(x + 1),$$

where a direct computation shows that condition (1.2) is not satisfied at the origin, signalling that it is a singular point.

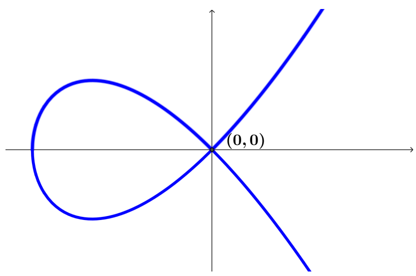

Figure 1.2: *An example of singular curve in* $\mathbb{R}^2$.

In the next section we devote our attention to a specific class of singularities, known as ADE singularities, that will be our work environment throughout all the following chapters.

1.2 ADE singularities

As is known since the seminal work of Killing and Cartan [101–105], there exists an exhaustive classification of simple Lie algebras, encompassing the so-called "classical algebras"[1] A_n, B_n, C_n, D_n, as well as a bunch of "exceptional" algebras G_2, F_4, E_6, E_7, E_8. The subscript indicates their rank. Each of these algebras can be put in one-to-one correspondence with a Dynkin diagram, allowing us to swiftly recover the properties of the algebra itself. For a lightning review of some basic Lie algebra concepts we refer to Appendix A.

In the following, we are interested in a subset of all simple Lie algebras, namely the ones in correspondence with simply-laced Dynkin diagrams. These are the A_n, D_n, E_6, E_7, E_8 algebras, belonging to the homonymous ADE classification.

For convenience, we report their Dynkin diagrams in Figure 1.3, whose origin is briefly recalled in Appendix A, and that we will profusely employ in the next analyses.

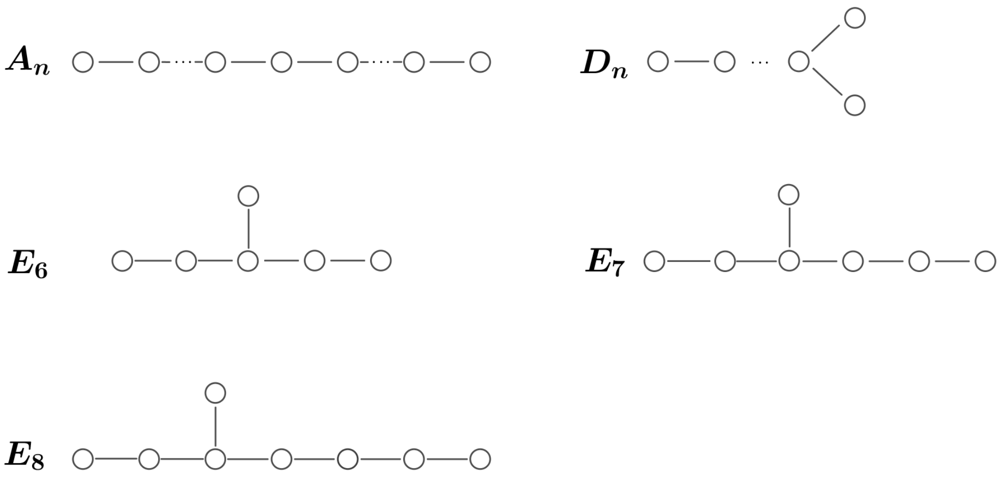

Figure 1.3: *ADE Dynkin diagrams.*

The ADE algebras play a crucial role for our discussion on singularities. There exists, indeed, a specific class of singularities known as *ADE singularities* for reasons that will be clear shortly. These constitute the work environment of all the following chapters, due to their extreme versatility in the string theory framework.

The realization of their relevance in a physical context dates back to the work of McKay [106], that discovered a surprising connection between the theory of Du Val orbifold singularities and the representation theory of the algebras in the ADE classification, in what came to be known as the *McKay correspondence*.

Du Val singularities [107] are isolated singularities in complex surfaces, that can be defined as a quotient:

$$\text{Du Val singularities:} \quad \leftrightarrow \quad \mathbb{C}^2/\Gamma$$

[1]As is usual in the physics literature, we will often mix the notions of algebra and group, unless the distinction becomes necessary.

where Γ is a finite subgroup of $SU(2)$.

This definition yields a natural classification of Du Val singularities in terms of the finite subgroups of $SU(2)$, which in turn are in correspondence with the algebras in the ADE classification:

$$\begin{aligned} A_n &= \mathfrak{sl}(n+1) \\ D_n &= \mathfrak{so}(2n) \\ E_n &= \mathfrak{e}(n) \end{aligned} \tag{1.1}$$

where n is the rank of the algebra.

Du Val singularities can also be defined as hypersurfaces in $\mathbb{C}^3$, zero-loci of the polynomials:

$$\begin{aligned} A_n: &\qquad x^2 + y^2 + z^{n+1} = 0 \\ D_n: &\qquad x^2 + zy^2 + z^{n-1} = 0 \\ E_6: &\qquad x^2 + y^3 + z^4 = 0 \\ E_7: &\qquad x^2 + y^3 + yz^3 = 0 \\ E_8: &\qquad x^2 + y^3 + z^5 = 0 \end{aligned} \tag{1.2}$$

It can be shown that these surfaces are singular at the origin, and that their canonical bundle is trivial, and so that they are local $K3$ surfaces.

In the next sections, we are going to get a hands-on understanding of the relationship between the Dynkin diagrams in Figure 1.3 and the surfaces (1.2), introducing the concepts of *deformation* and *resolution* of a singularity.

1.3 "Smoothing" singularities

Consider a surface in $\mathbb{C}^n$ with an isolated singularity: in the following paragraph we are going to illustrate, in broad brushes, two ways of "smoothing" out the singular locus, either by modifying its complex structure, *deforming* it, or by "substituting" the singular locus via a birational map, *resolving* the singularity.

1.3.1 Deformations

As a first, we describe *deformations*, that act by modifying the complex structure of the surface.

To give a more mathematically grounded idea of this concept, fix a general surface S inside $\mathbb{C}^n$, defined by the zero locus of a polynomial F:

$$S: \quad F(z_1, \ldots, z_n) = 0. \tag{1.3}$$

Now define the ring:

$$R_{\text{def}} = \frac{\mathbb{C}[z_1, ..., z_n]}{\left(\frac{\partial F}{\partial z_1}, ..., \frac{\partial F}{\partial z_n}\right)}, \tag{1.4}$$

and a basis $(g_1, ..., g_k)$ of R_{def}.

Then we say that the surface S_{versal} in $\mathbb{C}^{n+k}$ defined by:

$$S_{\text{versal}}: \quad F + \sum_{i=1}^{k} \mu_i g_i = 0, \tag{1.5}$$

with μ_i some complex parameters is the semi-universal, or *versal*, deformation of the singularity.

The parameters μ_i span the deformation space Def (S), and we can write the versal deformation S_{versal} as a family of surfaces S' in $\mathbb{C}^n$ fibered over the deformation space Def $(S) = \mathbb{C}^k$:

$$\begin{array}{c} S_{\text{versal}} \subset \text{Def}\,(S) \times \mathbb{C}^n \\ \downarrow \\ \text{Def}\,(S) \end{array} \tag{1.6}$$

The fiber S' over a point of the deformation space Def (S) is a deformation of S in 1.3: it is easy to verify, applying the definition 1.2, that for a generic point of Def (S) the surface S' is non-singular.

Moreover, the deformation space Def (S), where the coefficients μ_i live, is intimately related to the Weyl theory of the corresponding ADE singularity.

Letting $\mathcal{T}$ be the Cartan subalgebra and $\mathcal{W}$ the Weyl group of the Lie algebra under consideration, one can show that the deformation space is made up of variables that are invariant under the action of the *whole* Weyl group, that is:

$$\text{Def}\,(S) = \mathcal{T}/\mathcal{W}. \tag{1.7}$$

We could then rewrite (1.6) as:

$$\begin{array}{c} S_{\text{versal}} \subset \mathcal{T}/\mathcal{W} \times \mathbb{C}^n \\ \downarrow \\ \mathcal{T}/\mathcal{W} \end{array} \tag{1.8}$$

Having set up this machinery, let us show an explicit example.

Take the simplest singularity in the ADE classification, namely the $A_1 = \mathfrak{sl}(2)$ case.

The surface $S \subset \mathbb{C}^3$ reads:

$$S: \qquad x^2 + y^2 + z^2 = 0, \tag{1.9}$$

and has a unique isolated singularity at the origin.

A basis of R_{def} is given by $\mu \in \mathbb{C}$. As a result, the versal deformation S_{versal} lives in:

$$\begin{array}{c} S_{\text{versal}} \subset \mathbb{C} \times \mathbb{C}^3 \\ \downarrow \\ \mathbb{C} \end{array} \tag{1.10}$$

and the fiber explicitly reads:

$$S' : \qquad x^2 + y^2 + z^2 = \mu \quad \subset \mathbb{C}^3, \tag{1.11}$$

where μ is a constant. We can also immediately verify that, for generic $\mu \neq 0$, the deformed A_1 singularity in 1.11 is non-singular.

The total space of 1.10 is the versal deformation S_{versal}: it is a non-singular threefold and it can be described as a family of deformed A_1 singularities, fibered on the plane spanned by μ, whose value precisely fixes the deformation. Explicitly, it is given by:

$$S_{\text{versal}} : \qquad x^2 + y^2 + z^2 = \mu \quad \subset \mathbb{C}^4, \tag{1.12}$$

where now μ is a coordinate.

1.3.2 Resolutions

Another independent way to smooth out the singularity on the origin of S is the *resolution*, an operation that modifies the Kähler structure of the surface.

By resolving the singularity we effectively "remove" the singular point, replacing it with an exceptional locus that either smooths the singularity, or replaces it with a "milder" singular locus.

More precisely, a resolution of S with a singularity on a point p is a *birational* map π:

$$\pi : \quad \tilde{S} \to S. \tag{1.13}$$

The fact that π is birational means that it is an isomorphism on $S \setminus p$, and replaces the singular point with:

$$\pi^{-1}(p) = E, \tag{1.14}$$

where E is called exceptional locus. In the rest of this work, we will focus on the case in which the exceptional locus is a collection of $\mathbb{P}^1$'s.

There are plenty of ways to resolve singularities, and here we will briefly show a technique based on matrix factorizations[2]. In the following chapter, however, we will devote our

[2]Matrix factorizations (MFs, for short) are a vast and deep topic (see e.g. [108] for the original reference, and [109] for a physics-oriented review). In this work, however, we will just scratch the surface with some basic applications.

attention to the so-called Grothendieck-Springer resolutions, that will act as the inspirational foundation for our physics considerations.

Consider, again, the singular surface (1.9) in $\mathbb{C}^3$. First, notice that it can be concisely written (after an immediate change of coordinates $x = \frac{u+v}{2}, y = \frac{u-v}{2i}$) as:

$$\det M = \det \begin{pmatrix} u & z \\ z & v \end{pmatrix} = uv - z^2 = 0. \tag{1.15}$$

Then, embed it into the space $\mathbb{C}^3 \times \mathbb{P}^1$, subject to the constraint:

$$\begin{pmatrix} u & z \\ z & v \end{pmatrix} \cdot \begin{pmatrix} s_0 \\ s_1 \end{pmatrix} = 0, \tag{1.16}$$

where $[s_0, s_1] \in \mathbb{P}^1$.

Let us examine the solutions of (1.16):

- $s_0 = s_1 = 0$ is not allowed, as they are coordinates in a projective space.
- the only possibility is that the rank of M is non-maximal, that is $uv - z^2 = 0$.

At this point, we have two possibilities:

- $\text{rk}M = 1$, meaning that $(u, v, z) \neq (0, 0, 0)$. This implies that there exists a unique $[s_0, s_1]$ that solves the equation.
- $\text{rk}M = 0$, that is we are on top of the origin $(u, v, z) = (0, 0, 0)$. In this case, all $[s_0, s_1] \in \mathbb{P}^1$ satisfy the constraint.

We can see, as a result, that each point different from the origin corresponds to a single point in $\mathbb{P}^1$, and that on the other hand the origin, the former singular point, has now been substituted by the whole $\mathbb{P}^1$.

This is an example of a *birational* equivalence: the starting singular surface is isomorphic to the resolved one, apart from the singular point, that has been substituted by a sphere.

A similar procedure can be carried out to resolve all the ADE singularities in the classification (1.2): in this way, it can be proven that *the resolution of the ADE singularities is a birational map that substitutes the singular point with a collection of complex curves isomorphic to* $\mathbb{P}^1$*, intersecting with a pattern given by the Dynkin diagram pertaining to the corresponding ADE algebra.*

In the next section we see how to use both the tools of the deformation and of the resolution, constructing *simultaneous resolutions.*

1.3.3 Simultaneous resolutions of deformed families

Let us go back to the deformed family (1.12): for a generic non-zero μ the family is a smooth threefold. However, the fiber on top of the point $\mu = 0$ (i.e. the central fiber) is still singular, and so we might want to be able to resolve it. It turns out that a resolution of the central fiber exists, but that it cannot be "glued" in a smooth fashion with the rest of the family (1.12) [110].

What we want to do, instead, is perform a *simultaneous* resolution of S_{versal}, meaning an operation that, when restricted to the central fiber, reduces to the standard resolution.

In order to achieve this result we must recall the fact that the deformation space Def (S) is spanned by parameters that are invariant under the action of the Weyl group associated to the ADE singularity (1.7). In our A_1 case, we can write the explicit action of $\mathcal{W}$ on the Cartan subalgebra $\mathcal{T}$, described by a single variable t:

$$\mathcal{W} : t \to -t. \tag{1.17}$$

We must then have $\mu = t^2$, as the complex variable μ in S_{versal} is Weyl-invariant, that is: $\mu \in \mathcal{T}/\mathcal{W}$.

As a result, we can perform a base change, pulling back from the coordinate μ to its covering space spanned by t, which is Weyl-covariant:

$$\phi : \widetilde{\text{Def}(S)} \to \text{Def}(S) : t \mapsto \mu = t^2. \tag{1.18}$$

Applying this map to the family S_{versal} we get:

$$\tilde{S}_{\text{versal}} : \quad x^2 + y^2 + z^2 = t^2, \tag{1.19}$$

which is nothing but the famous equation of the conifold, which is singular at the origin.

Finally using the form (1.19) we can simultaneously resolve the deformed A_1 family, obtaining a smooth surface in $\mathcal{T} \times \mathbb{C}^3$.

This can be done rewriting the conifold using the formalism of matrix factorizations, as previously shown for the non-deformed A_1 case:

$$\text{det}M = \det \begin{pmatrix} u & z+t \\ z-t & v \end{pmatrix} = uv - z^2 + t^2 = 0. \tag{1.20}$$

and then embedding it into $\mathbb{C}^4 \times \mathbb{P}^1$, subject to the condition:

$$\begin{pmatrix} u & z+t \\ z-t & v \end{pmatrix} \cdot \begin{pmatrix} s_0 \\ s_1 \end{pmatrix} = 0. \tag{1.21}$$

Reasoning along the lines of the non-deformed A_1 case, it is easily shown that equation (1.21) describes a surface that is birationally equivalent to the conifold, except for the singular point that has been substituted by a $\mathbb{P}^1$, smoothing out the singularity.

Diagramatically, this reads as:

$$\begin{array}{ccccc} \mathcal{Z}_{\mathcal{T}} & \xrightarrow{\pi} & \tilde{S}_{\text{versal}} & \rightarrow & S_{\text{versal}} \\ & \searrow & \downarrow & & \downarrow \\ & & \mathcal{T} & \xrightarrow{\phi} & \mathcal{T}/\mathcal{W} \end{array} \tag{1.22}$$

where the map $\pi : \mathcal{Z}_{\mathcal{T}} \to \tilde{S}_{\text{versal}}$ is the complete simultaneous resolution of the deformed A_1 family.

Let us recap the operations we have performed so far:

- Consider the A_1 singular surface S, defined in equation (1.9).
- Deform the singularity, generating the family S_{versal}, and pull it back on the covering space dictated by the action of the Weyl group, obtaining the deformed A_1 singularity $\tilde{S}_{\text{versal}}$ in Weyl covariant coordinates.
- Simultaneously resolve the family $\tilde{S}_{\text{versal}}$, which is singular.
- The end result is a family $\mathcal{Z}_{\mathcal{T}}$, that is birationally equivalent to $\tilde{S}_{\text{versal}}$: on every point different than the origin of $\text{Def}(S) \times \mathbb{C}^3$ they are isomorphic, while the origin has been superseded by a $\mathbb{P}^1$, smoothing out the singularity of the central fiber.
  $\mathcal{Z}_{\mathcal{T}} \to \tilde{S}_{\text{versal}}$ is the *complete simultaneous resolution of the deformed family*, meaning that all the singularities in the family (even in the fibers) have been smoothed out.

The reasoning outlined above is general and can be applied to all the ADE singularities, and we now retrace the above mentioned steps for the general cases.

First, we start from the singular surfaces in $\mathbb{C}^3$ defined in (1.2).

Then we write down the versal deformation of the singularities in terms of Weyl-invariant coordinates μ_i, defined on $\mathcal{T}/\mathcal{W}$. This produces the deformed families:

$$\begin{aligned} A_n : &\quad x^2 + y^2 + z^{n+1} + \sum_{i=2}^{n+1} \sigma_i z^{n+1-i} = 0 \\ D_n : &\quad x^2 + y^2 z + z^{n-1} + \sum_{i=1}^{n-1} \delta_{2i} z^{n-1-i} + 2\tilde{\delta}_n y = 0 \\ E_6 : &\quad x^2 + y^3 + z^4 + \epsilon_2 y z^2 + \epsilon_5 y z + \epsilon_6 z^2 + \epsilon_8 y + \epsilon_9 z + \epsilon_{12} = 0 \\ E_7 : &\quad x^2 + y^3 + y z^3 + \tilde{\epsilon}_2 y^2 z + \tilde{\epsilon}_6 y^2 + \tilde{\epsilon}_8 y z + \tilde{\epsilon}_{10} z^2 + \tilde{\epsilon}_{12} y + \epsilon_{14} z + \tilde{\epsilon}_{18} = 0 \\ E_8 : &\quad x^2 + y^3 + z^5 + \hat{\epsilon}_2 y z^3 + \hat{\epsilon}_8 y z^2 + \epsilon_{12} z^3 + \hat{\epsilon}_{14} y z + \hat{\epsilon}_{18} z^2 + \hat{\epsilon}_{20} y + \hat{\epsilon}_{24} z + \hat{\epsilon}_{30} = 0 \end{aligned} \tag{1.23}$$

where we have specified the coordinates μ_i with distinct names for every A, D, E class (using σ_i for A, $\delta_i, \tilde{\delta}_i$ for D and $\epsilon, \tilde{\epsilon}, \hat{\epsilon}$ for E). The deformed families (1.23) admit no simultaneous resolution.

Now we can take the pull back of the deformation parameters from $\mathcal{T}/\mathcal{W}$ to the covering space $\mathcal{T}$. In this way we can write the generic deformation for each ADE case:

$$\begin{aligned}
A_n: &\quad x^2+y^2+\prod_{i=1}^{n+1}(z+t_i)=0 \quad \sum_{i=1}^{n+1}t_i=0\\
D_n: &\quad x^2+y^2z+\frac{\prod_{i=1}^{n}(z+t_i^2)-\prod_{i=1}^{n}t_i^2}{z}+2\prod_{i=1}^{n}t_iy=0\\
E_6: &\quad x^2+y^3+z^4+\epsilon_2yz^2+\epsilon_5yz+\epsilon_6z^2+\epsilon_8y+\epsilon_9z+\epsilon_{12}=0\\
E_7: &\quad x^2+y^3+yz^3+\tilde{\epsilon}_2y^2z+\tilde{\epsilon}_6y^2+\tilde{\epsilon}_8yz+\tilde{\epsilon}_{10}z^2+\tilde{\epsilon}_{12}y+\epsilon_{14}z+\tilde{\epsilon}_{18}=0\\
E_8: &\quad x^2+y^3+z^5+\hat{\epsilon}_2yz^3+\hat{\epsilon}_8yz^2+\epsilon_{12}z^3+\hat{\epsilon}_{14}yz+\hat{\epsilon}_{18}z^2+\hat{\epsilon}_{20}y+\hat{\epsilon}_{24}z+\hat{\epsilon}_{30}=0
\end{aligned} \tag{1.24}$$

where the t_i are coordinates on the covering space $\mathcal{T}=\widetilde{\mathrm{Def}(S)}$ and now the $\epsilon_i, \tilde{\epsilon}_i, \hat{\epsilon}_i$ are functions of the t_i [111]. Analogously to the conifold case, the deformed families (1.24), defined on the deformation space $\mathcal{T}$, admit a complete simultaneous resolution, namely a resolution that on the central fiber inflates all the nodes in the corresponding ADE Lie algebra.

Let us take a closer look to the structure of the deformed ADE families: it can be shown that, if all the t_is are different from zero, the surfaces (1.24) admit n non-trivial spheres S_i^2, arranged via their intersection form in the same fashion as the structure of the Dynkin diagram of the corresponding singularity.

In addition, we can relate the volume of such spheres to the deformation parameters t_i in the Cartan subalgebra. In general, the volume V_i of the sphere S_i^2 is given by the integral of the holomorphic 2-form Ω:

$$\alpha_i=\int_{S_i^2}\Omega, \tag{1.25}$$

where we have used the symbols α_i to explicitly state the correspondence between the spheres (and their volumes) and the simple roots of the corresponding Lie algebra, as their intersection pattern is exactly the same and is given by the Dynkin diagram.

The relationship between the volumes and the deformation parameters is then given by[3]

$$\begin{aligned}
A_n: &\quad \alpha_i=t_i-t_{i+1} \quad i=1,\dots,n\\
D_n: &\quad \alpha_i=t_i-t_{i+1} \quad i=1,\dots,n-1 \quad \text{and} \quad \alpha_n=t_{n-1}+t_n\\
E_n: &\quad \alpha_i=t_i-t_{i+1} \quad i=1,\dots,n-1 \quad \text{and} \quad \alpha_n=-t_1-t_2-t_3
\end{aligned} \tag{1.26}$$

It is critical to note that the Weyl group acts on the root system accordingly to the Lie algebra, inducing in turn an action on the Weyl-covariant deformation parameters t_i of the Cartan subalgebra.

Moreover, it is evident that when all the t_is vanish, so do the volumes of the spheres corresponding to the simple roots, thus obtaining a singular space. It is precisely on this point

[3] In the following we will interchangeably use, when no confusion might arise, the terms "root", "node", "sphere", keeping in mind the correspondence between roots, Dynkin diagrams and inflated spheres in the simultaneous resolution.

that the machinery of the simultaneous resolution comes into play: by looking at the diagram (1.22) we notice that $\mathcal{Z}_{\mathcal{T}}$ is isomorphic to $\tilde{S}_{\text{versal}}$ on every point where all the t_is are generic: on the other hand, if all the t_is are null, $\mathcal{Z}_{\mathcal{T}}$ inflates a bunch of 2-cycles arranged exactly as the Dynkin diagram of the corresponding ADE. We should notice, though, a difference with respect to the basic A_1 case that acted as a template: for some carefully chosen values of the parameters t_i there could be other points, or even curves, where subsingularities of the whole ADE singularity under consideration appear. For example, there are A_1 singular points inside the versal deformation of the A_3 singularity turning up on some loci in the space spanned by the t_is. What is relevant, in the end, is that the simultaneous resolution takes care of *all* of these singularities, smoothing them out.

In this way the families (1.24) are in fact simultaneously resolved on *all* of their points, origin and subsingular points included, leaving no room for other 2-cycles (meaning that the deformation, for the points different from the origin, the resolution, for the origin, and a combination of the two for the subsingular points have "inflated" all the possible non-trivial two-spheres). We remark that this was possible because we have expressed the deformed families in terms of the Weyl-covariant coordinates.

1.3.4 Partial simultaneous resolutions

Pulling back the deformed ADE families of rank n from $\mathcal{T}/\mathcal{W}$ to $\mathcal{T}$ is not the only allowed choice to obtain a simultaneous resolution. In fact, we can perform a base change and pick a set of n deformation parameters ϱ_i belonging to the quotient $\mathcal{T}/\mathcal{W}'$, with $\mathcal{W}'$ a subgroup of the whole Weyl group, producing a $(n+2)$-dimensional hypersurface admitting a *partial simultaneous resolution*, where only the 2-cycles corresponding to roots that are *invariant* with respect to $\mathcal{W}'$ get inflated.

Let us clarify this statement with an example: consider the A_3 singular surface, whose complete simultaneous resolution would yield three spheres intersecting in the shape of the A_3 Dynkin diagram. Say, though, that we want to only admit the resolution of the central sphere, corresponding to root α_2. In order to achieve this, we must express the deformed A_3 family in coordinates that are invariant under the subgroup $\mathcal{W}'$ that acts on the external roots. Explicitly, $\mathcal{W}'$ acts as the permutations $S_2 \times S_2$ on the parameters (t_1, t_2) and (t_3, t_4) respectively. Defining the symmetric polynomials:

$$\sigma_i(z_1, ..., z_n) = \sum_{j_1,...,j_i \text{ distinct}} z_{j_1} \cdot ... \cdot z_{j_i}, \tag{1.27}$$

we find that the $\mathcal{W}'$-invariant deformation space of the A_3 family is spanned by the coordinates:

$$\sigma_i(t_1, t_2) \quad \text{and} \quad \tilde{\sigma}_i(t_3, t_4) \tag{1.28}$$

which are nothing but the symmetric polynomials of degree $i = 1, 2$ in the parameters (t_1, t_2) and (t_3, t_4). Moreover, the condition $\sum_{i=1}^{n+1} t_i = 0$ valid for the A_n deformations enforces

$\sigma_1 = -\tilde{\sigma}_1$. Passing from the parameters t_i in (1.24) to the new coordinates $\sigma_i, \tilde{\sigma}_i$ we get the hypersurface:

$$\text{deformed } A_3 : \quad x^2 + y^2 + \left(z^2 + \sigma_1 z + \sigma_2\right)\left(z^2 + \tilde{\sigma}_1 z + \tilde{\sigma}_2\right) = 0, \tag{1.29}$$

which is an example of a flop of length 1, with which we will deal in closer detail later on.

The deformed A_3 family (1.29) admits only the resolution of the central node of the corresponding Dynkin diagram, be it on the origin of the deformation space or appearing in a subsingularity. This happens because we have explicitly written the family in term of coordinates that are Weyl-invariant under $\mathcal{W}'$ generated by the external roots. Had we chosen a different $\mathcal{W}'$, we would have found a different allowed simultaneous resolution. In later chapters, we will see this concretely, showing why there might be obstructions that allow to write the equation of the family only in the shape (1.29) and not in the form (1.24), that would yield a complete simultaneous resolution, as it is written in term of coordinates in $\mathcal{T}$.

It is in this sense that we talk of *partial simultaneous resolution*: in the central fiber we have only inflated the 2-cycle related to the central root. The fact that we have *not* resolved the external nodes of the A_3 Dynkin diagram generates a leftover $A_1 \times A_1$ singularity[4]. Pictorially, we can represent the resolved fiber on the origin using a colored Dynkin diagram, where dark dots correspond to resolved 2-cycles, and the white ones to shrunk ones:

$\boldsymbol{A_3}$ 

Figure 1.4: *Partial resolution of A_3.*

In general, given a deformed ADE family expressed in terms of Weyl-invariant parameters $\mathcal{T}/\mathcal{W}$, the family corresponding to some partial simultaneous resolution can be obtained by pulling back $\mathcal{T}/\mathcal{W}$ to $\mathcal{T}/\mathcal{W}'$, with $\mathcal{W}'$ the Weyl group generated by the nodes of the Dynkin diagram that are *not* being resolved by the partial simultaneous resolution. This happens according to the diagram:

$$\begin{array}{ccccc} \mathcal{Z}_{\mathcal{T}/\mathcal{W}'} & \stackrel{\pi}{\to} & \hat{S}_{\text{versal}} & \to & S_{\text{versal}} \\ & \searrow & \downarrow & & \downarrow \\ & & \mathcal{T}/\mathcal{W}' & \stackrel{\phi}{\to} & \mathcal{T}/\mathcal{W} \end{array} , \tag{1.30}$$

where $\mathcal{Z}_{\mathcal{T}/\mathcal{W}'} \to \hat{S}_{\text{versal}}$ is the partial simultaneous resolution of the deformed ADE family, which is written in terms of coordinates ϱ_i parametrizing $\mathcal{T}/\mathcal{W}'$.

Let us sum up the possible base changes we have introduced so far: we have first written the versal deformation of the ADE singularities in terms of coordinates $\mu_i \in \mathcal{T}/\mathcal{W}$,

[4]This is a general feature of partial simultaneous resolutions: there is a leftover singularity in the central fiber given by the Dynkin nodes that have not been resolved.

producing $(n+2)$-dimensional non-singular hypersurfaces. Performing a base change to the coordinates $t_i \in \mathcal{T}$ produces $(n+2)$-dimensional singular hypersurfaces admitting a *complete simultaneous resolution*, while picking an intermediate choice with coordinates $\varrho_i \in \mathcal{T}/\mathcal{W}'$ produces a partial simultaneous resolution. In Figure 1.5, we summarize the possible base changes that can be done at the level of the $(n+2)$-dimensional family. Schematically, this reads:

	$\mathcal{T}$	$\longrightarrow$	$\mathcal{T}/\mathcal{W}'$	$\longrightarrow$	$\mathcal{T}/\mathcal{W}$
1)	t_i	$\longmapsto$		$\longmapsto$	$\mu_i(t_j)$
2)	t_i	$\longmapsto$	$\varrho_i(t_j)$		
3)			ϱ_i	$\longmapsto$	$\mu_i(\varrho_j)$

Figure 1.5: *Three possible base changes: 1) from $\mathcal{T}$ to $\mathcal{T}/\mathcal{W}$, 2) from $\mathcal{T}$ to $\mathcal{T}/\mathcal{W}'$, 3) from $\mathcal{T}/\mathcal{W}'$ to $\mathcal{T}/\mathcal{W}$.*

1.4 Compound Du Val threefolds

In the course of this work, we will be exclusively interested in analyzing threefolds built as one-parameter deformations of ADE singularities: to obtain such objects, we can consider a family of deformed ADE singularities, fibered over $\mathcal{T}/\mathcal{W}, \mathcal{T}/\mathcal{W}'$ or $\mathcal{T}$, and impose a dependence of the deformation parameters on a single complex coordinate $w \in \mathbb{C}_w$. We further require[5] that the deformation vanishes on top of $w = 0$, meaning that the fiber on $w = 0$ reduces to the standard Du Val singularity. Taking a look at (1.24), it is easy to realize that such requirements impose that these one-parameter deformed ADE singularities take the form:

$$x^2 + P_{\mathfrak{g}}(y, z) + wg(x, y, z, w) = 0 \tag{1.31}$$

[5]In almost all cases: in Section 4.6.3, we will analyze Laufer's singularity, that does not satisfy this property. Still, it is possible to rewrite Laufer's singularity to satisfy this framework, although in a form that is less suitable for the analysis of Chapter 4.

with g an arbitrary polynomial, and where $P_{\mathfrak{g}}$ classifies the ADE singularity:

$$\begin{aligned}
P_{A_n} &= y^2 + z^{n+1} \\
P_{D_n} &= zy^2 + z^{n-1} \\
P_{E_6} &= y^3 + z^4 \\
P_{E_7} &= y^3 + yz^3 \\
P_{E_8} &= y^3 + z^5
\end{aligned} \tag{1.32}$$

Singularities of the form (1.31) are called *compound Du Val (cDV) singularities*. These will be the form of *all* the singularities we will deal with in the following chapters. A crucial property of cDV singularities that we will use in the following is the fact, proven by [84], that *all* Gorenstein threefold isolated terminal singularities are of cDV form. Here, by "terminal", we mean that the singularity either admits no crepant resolution, or admits a small crepant resolution (namely, a crepant resolution that inflates only one-dimensional complex curves).

CHAPTER 2

Nilpotent orbits theory of ADE Lie algebras

In this chapter we review the mathematical underpinnings of the theory of nilpotent orbits of ADE Lie algebras, examining some key concepts, such as Slodowy slices through nilpotent orbits, that will be widely employed in the rest of the work. This is the subject of Section 2.1.

In addition, the introduction of the nilpotent orbits formalism naturally leads to a new method to resolve ADE singularities, known as the Grothendieck-Springer (or just Springer, for conciseness) resolutions.

The usefulness of Springer resolutions comes in the fact that they will inspire our treatment of Higgs fields to deal with threefolds arising from deformed ADE singularities, dictating how such Higgs fields can be explicitly constructed[1]. Although it is possible to inspect the physics without any reference to Springer resolutions, as we will mainly do in the following, we think that it is instructive, to more thoroughly understand the reasoning behind those constructions, as well as to infer some of their properties, to start where all of this work began, i.e. from Springer resolutions.

In addition, Springer resolutions furnish a natural way to construct explicitly deformed ADE families related to complete or partial simultaneous resolutions, mapping the versal deformation depending on parameters in $\mathcal{T}/\mathcal{W}$ to some quotient $\mathcal{T}/\mathcal{W}'$ admitting a simultaneous resolution.

In this perspective, in Section 2.2 we review the general theory for complete Springer simultaneous resolutions, providing simple working examples for both the A and the D series (thus adding a slight contribution to the already existing mathematical literature, which is perfectly rigorous but oftentimes lacks concrete instances of the main concepts). Then, in Section 2.3 we focus our attention on partial Springer simultaneous resolutions, again considering simple cases in the A and D series, highlighting the connections to the deformed ADE singularities introduced in Chapter 1.

Main references for this chapter are the classic book by Collingwood and McGovern [112],

[1]As of now, this must be taken with a grain of salt: Springer resolutions are a useful tool to identify Higgs backgrounds, although we have no rigorous proof of the procedure. On the other hand, we will show in Chapter 3 a logically independent way, based on field-theoretic arguments, to get to the same results in an alternative fashion.

along with crystal clear lectures by Henderson [113] and Yun [114]. For Springer resolutions, we also refer to the original work of Springer [115], and its generalization to the Grothendieck-Springer resolution in [116] and [117].

As we have mentioned, we start by recapping the main tenets of the nilpotent orbits formalism of Lie algebra elements.

2.1 Nilpotent orbits and Slodowy slices of ADE Lie algebras

2.1.1 The nilpotent cone

Consider a Lie algebra $\mathfrak{g}$, and a faithful representation:

$$\rho : \quad \mathfrak{g} \mapsto \mathrm{End}(V), \tag{2.1}$$

with V some finite dimensional vector space. Then we say that an element $\mathrm{x} \in \mathfrak{g}$ is nilpotent if and only if $\rho(\mathrm{x})$ is a nilpotent endomorphism of x. If $\rho(\mathrm{x})$ is a matrix representation endowed with the usual matrix product, this simply means that $\rho(\mathrm{x})^k = 0$ for some finite k.

As the next basic step we define the action of the adjoint group G_{ad}, defined as the exponentiation of the Lie algebra $\mathfrak{g}$, on $\mathfrak{g}$ itself seen as a vector space. Given an element $g \in \mathfrak{g}$ and $G \in G_{\mathrm{ad}}$ such action reads:

$$g \longrightarrow G \cdot g \cdot G^{-1} \in \mathfrak{g}. \tag{2.2}$$

The action of the adjoint group defines the *adjoint orbits*, each orbit being a set of elements in $\mathfrak{g}$ up to the conjugation (2.2).

Furthermore, given a nilpotent element x, we define the *nilpotent orbit through* x as the set of elements connected to x by the adjoint action:

$$\mathcal{O}_{\mathrm{x}} = G_{\mathrm{ad}} \cdot \mathrm{x} = \{G \cdot \mathrm{x} \cdot G^{-1} \ | \ G \in G_{\mathrm{ad}}\}. \tag{2.3}$$

The union of all nilpotent orbits or, equivalently, the set of all nilpotent elements, constitutes the *nilpotent cone* $\mathcal{N}$ of the Lie algebra $\mathfrak{g}$.

We can now define the *adjoint quotient map* χ that associates an element $\mathrm{x} \in \mathfrak{g}$ with n polynomials in x, invariant under G_{ad}:

$$\chi : \mathfrak{g} \to \mathbb{C}^n : \mathrm{x} \mapsto (\chi_1(\mathrm{x}), \cdots, \chi_n(\mathrm{x})), \tag{2.4}$$

with n the rank of the Lie algebra $\mathfrak{g}$. The polynomials χ are related to the Casimirs[2] of $\mathfrak{g}$, which are in turn in correspondence with the traces of powers of x.

[2]Here we call "Casimirs" of $\mathfrak{g}$ of rank n a set of n independent polynomials built from elements of $\mathfrak{g}$ that are invariant under the action of the Weyl group $\mathcal{W}$ of $\mathfrak{g}$. For further details, we refer to Appendix A.

The fibers of this map are:

$$\chi^{-1}(u) = \{\mathrm{x} \in \mathfrak{g} \mid \chi_1(\mathrm{x}) = u_1, \cdots, \chi_n(\mathrm{x}) = u_n\}, \tag{2.5}$$

with $u = (u_1, \ldots, u_n) \in \mathbb{C}^n$. Roughly speaking we can interpret the fiber $\chi^{-1}(u)$ as all the elements in $\mathfrak{g}$ with coefficients $\{u_i, i = 1, \ldots, n\}$ in the characteristic polynomial (this is precisely so in the $\mathfrak{sl}(n)$ case, while some generalizations apply in the D and E algebras, as we will see in later chapters). It follows immediately that $\mathcal{N} = \chi^{-1}(0)$, because all the coefficients vanish for nilpotent elements.

We now state a relevant theorem by Kostant, that allows us to investigate the structure of the nilpotent cone:

Prop 2.1. (Kostant) *For any $u \in \mathbb{C}^n$, the fiber $\chi^{-1}(u)$:*

- *consists of finitely many adjoint orbits (only one for generic u),*
- *contains a unique dense orbit, and is hence irreducible,*
- *has codimension n in $\mathfrak{g}$, and is hence a complete intersection,*

where by *irreducible* we mean that the fiber cannot be written as the union of more than one algebraic variety.

It follows that the nilpotent cone $\mathcal{N} = \chi^{-1}(0)$ is a finite union of nilpotent orbits, with a unique dense orbit that we call $\mathcal{O}_{\text{reg}}$, the *principal (or regular) nilpotent orbit.* The trivial null orbit $\{0\}$, instead, is the one of minimal dimension and is represented by the null element in $\mathfrak{g}$. There exists a partial order $\leq$ for the nilpotent orbits, defined by stating that $\mathcal{O}' \leq \mathcal{O}$ if $\mathcal{O}' \subseteq \overline{\mathcal{O}}$, where $\overline{\mathcal{O}}$ indicates the closure of $\mathcal{O}$. It is immediate to show that the regular (null) nilpotent orbit is at the top (bottom) of this partial ordering.

Other relevant orbits, that will be useful in the following, are the *subregular nilpotent orbit* $\mathcal{O}_{\text{subreg}}$ and the *minimal nilpotent orbit* $\mathcal{O}_{\text{min}}$. They satisfy:

$$\begin{aligned} &\mathcal{O}_{\text{subreg}} < \mathcal{O}_{\text{reg}} \quad \text{with no other } \mathcal{O} \text{ such that } \mathcal{O}_{\text{subreg}} < \mathcal{O} < \mathcal{O}_{\text{reg}}, \\ &\{0\} < \mathcal{O}_{\text{min}} \quad \text{with no other } \mathcal{O} \text{ such that } \{0\} < \mathcal{O} < \mathcal{O}_{\text{min}}. \end{aligned} \tag{2.6}$$

Summing up, the dimensions of the aforementioned nilpotent orbits are:

Orbit	Dimension
$\mathcal{O}_{reg}$	$\dim(\mathfrak{g}) - \text{rank}(\mathfrak{g})$
$\mathcal{O}_{subreg}$	$\dim(\mathfrak{g}) - \text{rank}(\mathfrak{g}) - 2$
$\mathcal{O}_{min}$	a

(2.7)

with a the number of positive roots in $\mathfrak{g}$ not orthogonal (w.r.t. the usual scalar product defined through the Killing form, as detailed in Appendix A) to the highest root of $\mathfrak{g}$.

Let us immediately give a concrete example of all these constructs.

Consider the Lie algebra $A_3 = \mathfrak{sl}(4)$ in its standard matrix representation. Then, it can be shown that the regular, subregular and minimal nilpotent orbits can be represented by the elements:

$$
\begin{aligned}
\mathrm{x}_{\text{reg}} &= \begin{pmatrix} 0 & 1 & 0 & 0 \\ 0 & 0 & 1 & 0 \\ 0 & 0 & 0 & 1 \\ 0 & 0 & 0 & 0 \end{pmatrix}, \qquad \dim(\mathcal{O}_{\text{reg}}) = 12, \\
\mathrm{x}_{\text{subreg}} &= \begin{pmatrix} 0 & 1 & 0 & 0 \\ 0 & 0 & 1 & 0 \\ 0 & 0 & 0 & 0 \\ 0 & 0 & 0 & 0 \end{pmatrix}, \qquad \dim(\mathcal{O}_{\text{subreg}}) = 10, \\
\mathrm{x}_{\text{min}} &= \begin{pmatrix} 0 & 1 & 0 & 0 \\ 0 & 0 & 0 & 0 \\ 0 & 0 & 0 & 0 \\ 0 & 0 & 0 & 0 \end{pmatrix}, \qquad \dim(\mathcal{O}_{\text{min}}) = 6.
\end{aligned}
\tag{2.8}
$$

It is evident from this example that there is some kind of relationship between nilpotent orbits and the structure of Jordan decompositions. In the following subsection we will make this connection precise, sketchily following the review work of [112].

2.1.2 Nilpotent orbits classification

In this section we want to briefly outline an efficient way to classify nilpotent orbits of a generic ADE Lie algebra $\mathfrak{g}$. For simplicity, we will heavily rely on the matrix representations of the A and D series, while details for the exceptional cases will be given in later chapters.

The starting point is a theorem by Jacobson and Morozov, connecting a generic nilpotent element x with its so-called standard triple:

Prop 2.2. (Jacobson-Morozov) *Given a non-vanishing nilpotent element* $\mathrm{x} \in \mathfrak{g}$*, there exists a standard triple whose nilpositive element is* x*,*

where a standard triple is defined as a triple $\{\mathrm{x}, \mathrm{y}, H\}$ of elements in $\mathfrak{g}$, respectively called nilpositive, nilnegative and Cartan element, satisfying the relations of the $\mathfrak{su}(2)$ algebra:

$$
[\mathrm{x}, \mathrm{y}] = H, \qquad [H, \mathrm{x}] = 2\mathrm{x}, \qquad [H, \mathrm{y}] = -2\mathrm{y}. \tag{2.9}
$$

It can be shown that each inequivalent standard triple (equivalence being defined by conjugation under G_{ad}) is in correspondence with a distinct nilpotent orbit. Furthermore, as we will see in Appendix A, we can decompose every element in $\mathfrak{g}$ as a sum of the Cartan and root generators. In turn, considering the A_n and D_n cases, it can be proven that standard triples are in correspondence with (possibly only some) partitions of $n+1$ and $2n$ respectively. This happens in the following way: each partition of $n+1$ or $2n$ dictates, via a precise dictionary, which root generators must be switched on to build the nilpositive element x and which Cartans must be turned on in H, thus completely constraining the standard triple.

On the practical side, the classification of nilpotent orbits for the A and D series goes as:

- Choose a Lie algebra $\mathfrak{g}$ from the A_n and D_n series.
- Choose one of the allowed partitions of $n+1$ (for the A_n case) or $2n$ (for the D_n case). This choice identifies the nilpotent orbit.
- Associate to the chosen partition, using the dictionary, the corresponding root and Cartan generators.
- Sum all the above root generators together, obtaining the nilpositive element x, and all the Cartan generators, obtaining H. x is the canonical representative of the chosen nilpotent orbit.

Let us start illustrating this procedure in the A_n series, which yields a straightforward construction.

2.1.3 A_n nilpotent orbit classification

It can be shown, using the properties of the Jordan decomposition (for details and proof of these constructions we again refer to [112]), that nilpotent orbits in the A_n series are classified by *all* the partitions of $n+1$. A generic partition of $n+1$ into k parts can be labeled as:

$$\boldsymbol{d} = [d_1, d_2, \dots, d_k], \qquad \text{with } d_1 + d_2 + \ldots + d_k = n+1. \tag{2.10}$$

We want now to understand which root and Cartan generators must be switched on to build x and H respectively, i.e. to build a standard triple associated to the nilpotent orbit. The dictionary between the partitions and the root and Cartan generators is as follows (modulo Weyl transformations on the root system):

$$\begin{aligned} \mathrm{x} &= \begin{pmatrix} J_{d_1} & 0 & 0 & \dots & 0 \\ 0 & J_{d_2} & 0 & \dots & 0 \\ \vdots & \vdots & \vdots & \ddots & \vdots \\ 0 & 0 & 0 & \dots & J_{d_k} \end{pmatrix}, \\ H &= \begin{pmatrix} h_{d_1} & 0 & 0 & \dots & 0 \\ 0 & h_{d_2} & 0 & \dots & 0 \\ \vdots & \vdots & \vdots & \ddots & \vdots \\ 0 & 0 & 0 & \dots & h_{d_k} \end{pmatrix}, \end{aligned} \tag{2.11}$$

where J_{d_i} are Jordan blocks of size d_i, and h_{d_i} are blocks of the kind:

$$h_{d_i} = \begin{pmatrix} d_i - 1 & 0 & 0 & \dots & 0 \\ 0 & d_i - 3 & 0 & \dots & 0 \\ \vdots & \vdots & \vdots & \ddots & \vdots \\ 0 & 0 & 0 & \dots & -d_i + 1 \end{pmatrix} . \tag{2.12}$$

We see that in order to build x, the dictionary basically prescribes to add a Jordan block of size d_i for every chunk d_i of the partition, yielding a very simple and intuitive rule[3]. We emphasize, as we will make extensive use of this fact when tackling Springer resolutions, that the 1 entries in the Jordan blocks of x correspond to the generators of the simple roots of A_n, as detailed in Appendix A. Moreover, once we have chosen a partition $\boldsymbol{d}$ and built representatives x and H of the standard triple, also the nilnegative element y is fixed by the $\mathfrak{su}(2)$ algebra (2.9).
Finally, we can explicitly give the partitions corresponding to the principal, subregular and minimal nilpotent orbit in a Lie algebra A_n:

Orbit	Partition
$\mathcal{O}_{reg}$	$[n+1]$
$\mathcal{O}_{subreg}$	$[n,1]$
$\mathcal{O}_{min}$	$[2,1^{n-1}]$

(2.13)

Let us illustrate the above construction with a concrete example: consider the algebra $A_3 = \mathfrak{sl}(4)$. There are 5 distinct partitions of 4, and therefore there are 5 distinct nilpotent orbits:

$$\mathcal{O}_{[4]} \qquad \mathcal{O}_{[3,1]} \qquad \mathcal{O}_{[2^2]} \qquad \mathcal{O}_{[2,1^2]} \qquad \mathcal{O}_{[1^4]}, \tag{2.14}$$

where we have used exponents as shorthand for a repeated number. Focusing on, say, partition $[2,2]$, we can build explicit representatives x and H of the standard triple:

$$\mathrm{x} = \begin{pmatrix} 0 & 1 & 0 & 0 \\ 0 & 0 & 0 & 0 \\ 0 & 0 & 0 & 1 \\ 0 & 0 & 0 & 0 \end{pmatrix}, \qquad H = \begin{pmatrix} 1 & 0 & 0 & 0 \\ 0 & -1 & 0 & 0 \\ 0 & 0 & 1 & 0 \\ 0 & 0 & 0 & -1 \end{pmatrix}, \tag{2.15}$$

where we explicitly see that the partition $[2,2]$ has given rise to two Jordan blocks of size 2. Having settled the A_n case, we can now quickly review how the story goes in the D_n series, providing some explicit examples.

[3]Switching the order of Jordan blocks corresponds to a Weyl transformation on the root system, and the order of blocks in H changes accordingly.

2.1.4 D_n nilpotent orbit classification

As we have done in the previous subsection, we would like to have an easy way to classify nilpotent orbits in the $D_n = \mathfrak{so}(2n)$ series, connecting partitions of $2n$ to nilpotent orbits and standard triples. A slight complication, though, immediately arises: not all partitions of $2n$ label nilpotent orbits of $\mathfrak{so}(2n)$. A partition:

$$\boldsymbol{d} = [d_1, d_2, \ldots, d_k], \qquad \text{with } d_1 + d_2 + \ldots + d_k = 2n, \tag{2.16}$$

is a "good" partition of $2n$, meaning that it labels a nilpotent orbit, *if and only if its even parts enter the partition with even multiplicity*[4]. As a result, for the $\mathfrak{so}(2n)$ cases we can always subdivide partitions into chunks of the kind:

$$\{u, u\} \quad \text{for any } u, \qquad \{2s+1, 2t+1\} \quad \text{for any } s, t, \tag{2.17}$$

where we take $s > t$ as a labeling convention.

Having specified the allowed partitions, we can state the dictionary connecting them to explicit standard triples of $\mathfrak{so}(2n)$ made up of canonical representatives of the respective nilpotent orbit. Though surely tedious, the dictionary between partition chunks and root generators goes as:

- for chunks of type $\{u, u\}$ choose a block of consecutive indices $\{m+1, \ldots, m+u\}$. Then the root generators associated to this chunk are:

$$\{e_{m+1} - e_{m+2}, \ldots, e_{m+u-1} - e_{m+u}\}$$

- for chunks of type $\{2s+1, 2t+1\}$ choose a block of consecutive indices $\{m+1, \ldots, m+s+t+1\}$. The root generators associated to this chunk are:

$$\{e_{m+1} - e_{m+2}, \ldots, e_{m+s} - e_{m+s+1}, e_{m+s} + e_{m+s+1}, \ldots, e_{m+s+t} + e_{m+s+t+1}\}$$

To explicitly build the nilpositive element x of the standard triple, one has to subdivide the chosen partitions into chunks of the above kinds, find which root generators are attached to each chunk, and finally sum all such root generators, yielding x. As regards H, the story goes almost exactly as in the A_n case: first, one orders the chunks in partition $\boldsymbol{d}$ according to the construction of x. Then the cartan element H in the standard basis of $\mathfrak{so}(2n)$ is made of blocks of the following form, one for each chunk:

$$H = \begin{pmatrix} D & 0 \\ 0 & -D \end{pmatrix}, \tag{2.18}$$

[4] A subtlety, that we will never use in practical applications, arises for very even partitions, i.e. partitions made up of only even parts: in such cases, each partition labels two different nilpotent orbits.

with D a diagonal matrix given by:

$$D = \begin{pmatrix} d_i - 1 & 0 & 0 & \dots & 0 \\ 0 & d_i - 3 & 0 & \dots & 0 \\ \vdots & \vdots & \vdots & \ddots & \vdots \\ 0 & 0 & 0 & \dots & -d_i + 1 \end{pmatrix}. \tag{2.19}$$

As the last piece of useful data, we give the explicit partitions for the principal, subregular and minimal nilpotent orbits of D_n:

Orbit	Partition
$\mathcal{O}_{reg}$	$[2n-1, 1]$
$\mathcal{O}_{subreg}$	$[2n-3, 3]$
$\mathcal{O}_{min}$	$[2^2, 1^{2n-4}]$

(2.20)

In order to get a grasp on this seemingly abstruse construction, let us show an explicit example.

Consider D_4, the simplest non-trivial algebra in the D_n series different from A_n cases. We now know that nilpotent orbits of D_4 are labelled by partitions of $2 \times 4 = 8$ in which even parts appear even times (or do not appear at all). The allowed nilpotent orbits are then:

$$\begin{array}{cccccc} \mathcal{O}_{[7,1]} & \mathcal{O}_{[5,3]} & \mathcal{O}_{[5,1^3]} & \mathcal{O}^{I}_{[4^2]} & \mathcal{O}^{II}_{[4^2]} & \mathcal{O}_{[3^2,1^2]} \\ \mathcal{O}_{[3,2^2,1]} & \mathcal{O}_{[3,1^5]} & \mathcal{O}^{I}_{[2^4]} & \mathcal{O}^{II}_{[2^4]} & \mathcal{O}_{[2^2,1^4]} & \mathcal{O}_{[1^8]} \end{array}, \tag{2.21}$$

where the superscripts I and II label the two orbits corresponding to very even partitions, according to footnote (4).

Now we want to write an explicit standard triple for such orbits. Given its importance in later chapters, we choose the $\mathcal{O}_{[7,1]}$ nilpotent orbit, i.e. the principal orbit. Notice that the partition $[7,1]$ is made up of only one chunk of the type $\{2s+1, 2t+1\}$. Therefore, the dictionary between partitions and root and Cartan generators listed above tells us that the chunk $[7,1]$ is associated to the root generators (choosing $m = 0$ as the starting point for counting indices):

$$\{e_1 - e_2, e_2 - e_3, e_3 - e_4, e_3 + e_4\}. \tag{2.22}$$

Taking a look at the explicit presentation of root generators in Appendix A we can immediately construct the nilpositive element x of the standard triple: summing all these root generators we get[5]:

$$
\mathrm{x}_{[7,1]} = \left(\begin{array}{cccc|cccc}
0 & 1 & 0 & 0 & 0 & 0 & 0 & 0 \\
0 & 0 & 1 & 0 & 0 & 0 & 0 & 0 \\
0 & 0 & 0 & 1 & 0 & 0 & 0 & 1 \\
0 & 0 & 0 & 0 & 0 & 0 & -1 & 0 \\
\hline
0 & 0 & 0 & 0 & 0 & 0 & 0 & 0 \\
0 & 0 & 0 & 0 & -1 & 0 & 0 & 0 \\
0 & 0 & 0 & 0 & 0 & -1 & 0 & 0 \\
0 & 0 & 0 & 0 & 0 & 0 & -1 & 0
\end{array}\right). \tag{2.24}
$$

As regards the Cartan element H of the standard triple, we proceed as outlined above. There is only one chunk in the partition, namely $[7,1]$, and as a result we find that H is given by:

$$
H_{[7,1]} = \left(\begin{array}{cccc|cccc}
6 & 0 & 0 & 0 & 0 & 0 & 0 & 0 \\
0 & 4 & 0 & 0 & 0 & 0 & 0 & 0 \\
0 & 0 & 2 & 0 & 0 & 0 & 0 & 0 \\
0 & 0 & 0 & 0 & 0 & 0 & 0 & 0 \\
\hline
0 & 0 & 0 & 0 & -6 & 0 & 0 & 0 \\
0 & 0 & 0 & 0 & 0 & -4 & 0 & 0 \\
0 & 0 & 0 & 0 & 0 & 0 & -2 & 0 \\
0 & 0 & 0 & 0 & 0 & 0 & 0 & 0
\end{array}\right). \tag{2.25}
$$

It is easy to see that, given x and H, there exists a nilnegative element y that completes the standard triple of the nilpotent orbit $[7,1]$ closing the $\mathfrak{su}(2)$ algebra (2.9).

Having given an explicit recipe for computing nilpotent orbits and standard triples for the A_n and D_n series, we can move on and continue our path towards a concrete hands-on treatment of Springer resolutions. In the next section we deal with another key ingredient for this task, the so-called Slodowy slices.

2.1.5 Slodowy slices

The Jacobson-Morozov theorem (2.2) associates to every nilpotent element x in $\mathfrak{g}$ a standard triple spanning a $\mathfrak{su}(2)$ algebra. Restating the theorem in a slightly different fashion helps us define the Slodowy slice.

[5] Here, we are representing matrices M of D_4 in the standard basis of $\mathfrak{so}(2n)$ that we define in detail in Appendix A:

$$
\left\{ M = \begin{pmatrix} Z_1 & Z_2 \\ Z_3 & -Z_1^t \end{pmatrix} \mid Z_2, Z_3 \text{ antisymmetric} \right\}. \tag{2.23}
$$

Prop 2.3. (Jacobson-Morozov, revisited) *Given a non-vanishing nilpotent element* $\mathrm{x} \in \mathcal{N}$*, there exists a nilpotent element* $\mathrm{y} \in \mathcal{N}$*, such that they satisfy a* $\mathfrak{su}(2)$ *algebra*:

$$[[\mathrm{x}, \mathrm{y}], \mathrm{x}] = 2\mathrm{x}, \qquad [[\mathrm{x}, \mathrm{y}], \mathrm{y}] = -2\mathrm{y}. \tag{2.26}$$

y belongs to the nilpotent orbit $\mathcal{O}_{\mathrm{x}}$ passing through x, and although the choice of y is not unique it can be proven that, given a $\mathrm{y}' \neq \mathrm{y}$ satisfying (2.3), it is connected to y by a G_{ad} transformation that leaves x unchanged.

We can now define the *Slodowy slice* $\mathcal{S}_{\mathrm{x}}$ through x as:

$$\mathcal{S}_{\mathrm{x}} = \{\mathrm{z} \in \mathfrak{g} \mid [\mathrm{z} - \mathrm{x}, \mathrm{y}] = 0\}, \tag{2.27}$$

where again a different choice for y changes the Slodowy slice only up to a G_{ad} action. Thanks to a theorem by Kostant and Slodowy, the Slodowy slice can be thought as a subspace of $\mathfrak{g}$ transverse to the nilpotent orbit $\mathcal{O}_{\mathrm{x}}$ passing through x, whose dimension is hence given by

$$\dim(\mathcal{S}_{\mathrm{x}}) = \dim(\mathfrak{g}) - \dim(\mathcal{O}_{\mathrm{x}}). \tag{2.28}$$

Pictorially, we can think of the geometrical setup in $\mathfrak{g}$ described so far, with the Slodowy slice transversally intersecting the orbit $\mathcal{O}_{\mathrm{x}} \subset \mathcal{N}$, as:

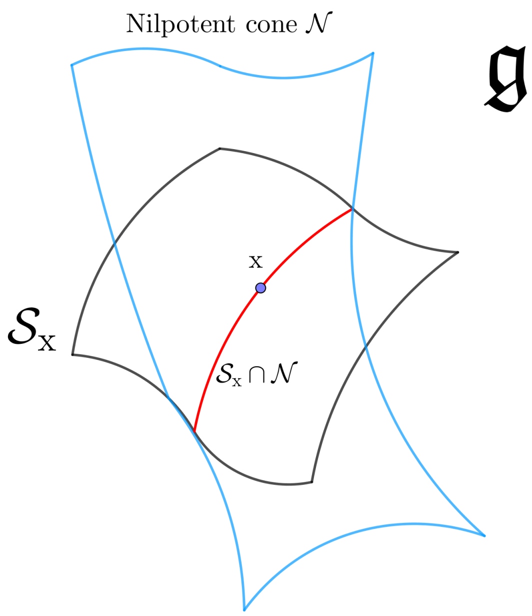

Figure 2.1: *Intersection between Slodowy slice and nilpotent cone.*

Having introduced Slodowy slices, we are finally in the correct place to establish the main theorem of this chapter, that will allow us to perform complete and partial resolutions of ADE singularities. It is due to Brieskorn [118], and reads:

Prop 2.4. (Brieskorn) *Given an algebra $\mathfrak{g}$ in the ADE classification, and an element* x *belonging to the subregular nilpotent orbit of $\mathfrak{g}$, the intersection of the Slodowy slice through* x *and the nilpotent cone is isomorphic to the ADE singularity related to $\mathfrak{g}$, i.e.*

$$\mathcal{S}_{subreg} \cap \mathcal{N} \cong \mathbb{C}^2/\Gamma, \tag{2.29}$$

with Γ the subgroup of $SU(2)$ identifying the ADE Lie algebra.
Moreover, the family given by the intersection of the Slodowy slice through x *with the fiber of the quotient adjoint map (2.5) is isomorphic to the versal deformation of the corresponding ADE singularity, namely:*

$$\mathcal{S}_{subreg} \cap \chi^{-1}(u) \cong \textit{versal def of } \mathbb{C}^2/\Gamma. \tag{2.30}$$

Let us clarify the meaning of the theorem by giving some intuition. What the isomorphism (2.29) is telling us is that we can describe an ADE singularity with a formalism relying solely on nilpotent orbits inside the corresponding Lie algebra: taking a look at Figure 2.1, the ADE singular surface is represented by the red curve, which is precisely the intersection of the Slodowy slice through x with the fiber $\chi^{-1}(0)$ of the quotient adjoint map corresponding to vanishing Casimirs of the algebra, i.e. the nilpotent cone $\mathcal{N} = \chi^{-1}(0)$. In this view, the nilpotent element x itself is in correspondence with the singular point, that is the origin in the algebraic definition of the ADE surface (1.2). In addition, taking the intersection of the Slodowy slice with a generic fiber $\chi^{-1}(u)$ of the quotient adjoint map, namely going outside the nilpotent cone and roaming through the Slodowy slice, we get a deformed ADE singularity[6]. Varying u, one gets a family of deformed ADE singularities over $\mathcal{T}/\mathcal{W}$.

What we want to do next is exploit the formalism developed up to now to simultaneously resolve, be it completely or partially, the deformed families $\mathcal{S}_{\text{subreg}} \cap \chi^{-1}(u)$. As a bonus, Springer resolutions will also allow to naturally define deformed ADE families corresponding to complete and partial simultaneous resolutions.

In the next section we give the general recipe for complete resolutions, and then immediately delve into explicit examples.

2.2 Complete Springer resolutions

As previously hinted, we can employ the tools furnished by Slodowy slices to perform a simultaneous complete resolution of the family $\mathcal{S}_{\text{subreg}} \cap \chi^{-1}(u)$ parameterized by the coordinates u_i, with the special case $\{u_i = 0 \quad \forall i\}$ being the undeformed singularity, i.e. simply $\mathbb{C}^2/\Gamma$. In this section, we are letting u vary along $\mathbb{C}^n = \mathcal{T}/\mathcal{W}$, and hence we are considering the full versal deformation of the ADE singularity.

The technique allowing us to perform such a task is the Grothendieck-Springer simultaneous resolution, that plays with the following ingredients:

[6]This implies that the parameters u_i are related by an invertible change of coordinates to the versal deformation parameters μ_i introduced in Chapter 1.

- Elements $\mathrm{x} \in \mathcal{S}_{\text{subreg}} \cap \chi^{-1}(u)$.
- Borel subalgebras $\mathfrak{b}$ (for a quick recap of Borel subalgebras aimed at our purposes, see Appendix A).
- The closed subvariety $\mathcal{B}$ of $\mathfrak{g}$ formed by all Borel subalgebras.

Putting all these pieces together, the resolution is given by the projection map:

$$\pi : \mathcal{S}_{\text{subreg}} \widetilde{\cap \chi^{-1}}(u) \to \mathcal{S}_{\text{subreg}} \cap \chi^{-1}(u), \tag{2.31}$$

where we have:

$$\mathcal{S}_{\text{subreg}} \widetilde{\cap \chi^{-1}}(u) = \{(\mathrm{x}, \mathfrak{b}) \in \mathcal{S}_{\text{subreg}} \times \mathcal{B} \mid \mathrm{x} \in \mathfrak{b}\}. \tag{2.32}$$

Intuitively speaking, the resolution consists in associating to each element $\mathrm{x} \in \mathcal{S}_{\text{subreg}} \cap \chi^{-1}(u)$ the variety of Borel subalgebras that contain x itself. This means that the fiber over x, the *Springer fiber*, is:

$$\pi^{-1}(\mathrm{x}) = \{\text{Borel subalgebras containing x}\}. \tag{2.33}$$

From a diagrammatic point of view, the resolution goes as follows (with $\mathcal{T}$ the Cartan subalgebra and $\mathcal{W}$ the Weyl group of $\mathfrak{g}$):

$$\begin{array}{ccc} \mathcal{S}_{\text{subreg}} \widetilde{\cap \chi^{-1}}(u) & \xrightarrow{\pi} & \mathcal{S}_{\text{subreg}} \cap \chi^{-1}(u) \\ \downarrow{\scriptstyle \phi} & & \downarrow{\scriptstyle \chi} \\ \mathcal{T} & \xrightarrow{p} & \mathcal{T}/\mathcal{W} \end{array} , \tag{2.34}$$

where ϕ is a map extracting the eigenvalues of an element of the Lie algebra $\mathfrak{g}$ and expanding them in a basis of the Cartan subalgebra $\mathcal{T}$, χ is the adjoint quotient map defined in (3.86), i.e. the map extracting the Casimirs of an element in $\mathfrak{g}$, and p is a map from the Cartan subalgebra $\mathcal{T}$ to the invariant coordinates on $\mathcal{T}/\mathcal{W}$.

Notice that the resolved space $\mathcal{S}_{\text{subreg}} \widetilde{\cap \chi^{-1}}(u)$ is mapped to the *full* Cartan subalgebra, whereas the starting family $\mathcal{S}_{\text{subreg}} \cap \chi^{-1}(u)$ is mapped to the Cartan subalgebra quotiented by the full Weyl group. In practice this means that the resolved ADE singularity will be written in terms of Weyl *covariant* coordinates if we look at $\mathcal{S}_{\text{subreg}} \widetilde{\cap \chi^{-1}}(u)$, whereas the projection to $\mathcal{S}_{\text{subreg}} \cap \chi^{-1}(u)$ is expressed with Weyl *invariant* coordinates, exactly as we have seen in the course of Chapter 1.

The fundamental technical step needed in order to perform concrete computations is the correspondence, valid if we restrict to the A_n case (we will deal with the D_n case in due time), between the variety $\mathcal{B}$ spanned by Borel subalgebras and the set of complete *flags* $\mathcal{F}$, defined as:

$$\mathcal{F} := \left\{0 \subset V_1 \subset V_2 \subset \cdots \subset V_n \subset \mathbb{C}^{n+1} \;\middle|\; \dim V_i = i\right\}. \tag{2.35}$$

The idea of the Springer resolution is then to define the fiber of the resolution map $\pi^{-1}(\mathrm{x})$ as the variety of flags that are preserved by $\mathrm{x} \in \mathcal{S}_{\text{subreg}} \cap \chi^{-1}(u)$ itself, where x acts on each space composing a flag as a matrix in the fundamental representation. In other words, the Springer fibers are:

$$\pi^{-1}(\mathrm{x}) = \{\text{Flags preserved by x}\}. \tag{2.36}$$

Summing up the procedure we have outlined so far, in order to find the simultaneous resolution of $\mathcal{S}_{\text{subreg}} \cap \chi^{-1}(u)$ we should go through the following (completely mechanical) steps:

- Consider an ADE Lie algebra $\mathfrak{g}$, compute its subregular nilpotent orbit and choose a specific element x belonging to the orbit.
- Compute the Slodowy slice $\mathcal{S}_{\text{subreg}}$ through x.
- Write the intersection of the Slodowy slice with the fibers of the adjoint quotient map $\mathcal{S}_{\text{subreg}} \cap \chi^{-1}(u)$.
- For each element x of $\mathcal{S}_{\text{subreg}} \cap \chi^{-1}(u)$, find *all* the complete flags in $\mathcal{F}$ preserved by x, that is the complete flags such that $\mathrm{x}(V_i) \subseteq V_i, \quad \forall i$.
  On the nilpotent cone $\mathcal{N}$ this last relation becomes $\mathrm{x}(V_i) \subseteq V_{i-1}, \quad \forall i$. For each x, call $\mathfrak{f}$ the set of flags that it preserves.
- The simultaneous resolution of the ADE singularity of type $\mathfrak{g}$ is then given by the map (2.31), with:

$$\widetilde{\mathcal{S}_{\text{subreg}} \cap \chi^{-1}(u)} = \{(\mathrm{x}, \mathfrak{f}) \in \mathcal{S}_{\text{subreg}} \times \mathcal{F}\}. \tag{2.37}$$

Although apparently rather involved, the above strategy to infer the simultaneous resolution of an ADE singularity is computationally straightforward. In order to concretely ground these ideas, we show an explicit example, considering the A_2 Lie algebra.

2.2.1 Complete Springer resolution of A_2

The first ingredient we need is the subregular nilpotent orbit of A_2: taking a look at table (2.13) we see that $\mathcal{O}_{\text{subreg}}$ is in correspondence with the partition $[2,1]$ which can be represented by the element:

$$\mathrm{x} = \begin{pmatrix} 0 & 1 & 0 \\ 0 & 0 & 0 \\ 0 & 0 & 0 \end{pmatrix}. \tag{2.38}$$

A suitable y satisfying (2.9) can hence be chosen as:

$$
\mathrm{y} = \begin{pmatrix} 0 & 0 & 0 \\ 1 & 0 & 0 \\ 0 & 0 & 0 \end{pmatrix}. \tag{2.39}
$$

Performing a straightforward linear algebra computation, the Slodowy slice $\mathcal{S}_{\text{subreg}}$ through x turns out to be given by the matrices:

$$
\mathcal{S}_{\text{subreg}} = \left\{ \begin{pmatrix} a & 1 & 0 \\ b & a & c \\ d & 0 & -2a \end{pmatrix} \;\middle|\; a, b, c, d \in \mathbb{C} \right\}. \tag{2.40}
$$

The computation of the characteristic polynomial of the matrices in $\mathcal{S}_{\text{subreg}}$ gives (calling u_1 and u_2 the coefficients of the polynomial, which are also the Casimirs of $\mathcal{S}_{\text{subreg}}$):

$$
\begin{aligned}
u_1 &= 3a^2 + b, \\
u_2 &= 2a(b - a^2) + cd.
\end{aligned} \tag{2.41}
$$

If we restrict to the nilpotent cone, that is to $\chi^{-1}(0)$, we find:

$$
\mathcal{S}_{\text{subreg}} \cap \mathcal{N} = \left\{ \begin{pmatrix} a & 1 & 0 \\ -3a^2 & a & c \\ d & 0 & -2a \end{pmatrix} \;\middle|\; 8a^3 = cd \right\}, \tag{2.42}
$$

where we notice that the constraint equation $8a^3 = cd$ is exactly the A_2 singular surface, as expected from theorem (2.4).

If, on the other hand, we take $u_i \neq 0$ we get:

$$
\mathcal{S}_{\text{subreg}} \cap \chi^{-1}(u) = \left\{ \begin{pmatrix} a & 1 & 0 \\ b & a & c \\ d & 0 & -2a \end{pmatrix} \;\middle|\; 8a^3 - cd - 2au_1 + u_2 = 0 \right\}, \tag{2.43}
$$

with the constraint equation being the semiuniversal deformation of the A_2 singularity, the coordinates u_1 and u_2 representing the Weyl-invariant parameters deformation living on $\mathcal{T}/\mathcal{W}$.

We are now interested in performing a simultaneous complete resolution in the general case $\mathcal{S}_{\text{subreg}} \cap \chi^{-1}(u)$. It is convenient, for a more intuitive understanding of the structure of the Springer fibers, to subdivide the analysis according to the region of the space $\mathcal{S}_{\text{subreg}} \cap \chi^{-1}(u)$ we are considering.

- $\boldsymbol{u_i \neq 0 \ \ \forall i}$

The matrices in (2.40) possess 3 distinct eigenvectors (i.e. vectors spanning subspaces preserved by the action of (2.40)) v_1, v_2, v_3, functions of a, b, c, d.

We would like to build flags of the kind (2.35) out of these vectors. As we will also see for more involved cases, it is more convenient to use the Jordan form of the matrix in order to compute the preserved flags (noting that we could reconstruct the original preserved flags conjugating by the action of some element in G_{ad}). In this case the Jordan form is nothing but a diagonal matrix with the eigenvalues as entries, and with the vectors of the canonical basis e_1, e_2, e_3 as eigenvectors. It is clear that the spaces spanned by some combination of them satisfy $\mathrm{x}(V_i) \subseteq V_i, \quad \forall i$. As a result, all the possible invariant subspaces we can build using e_1, e_2, e_3 are:

$$\begin{aligned} 1-\dim: &\quad <e_1> \ , \ <e_2> \ , \ <e_3> \\ 2-\dim: &\quad <e_1, e_2> \ , \ <e_1, e_3> \ , \ <e_2, e_3> \\ 3-\dim: &\quad \mathbb{C}^3 \end{aligned} \tag{2.44}$$

Clearly, given a choice of a 1-dim subspace, we have two options for a 2-dim subspace such that $V_1 \subset V_2$, so we obtain a total of $3 \times 2 \times 1 = 3!$ combinations, with each combination being a different flag.

We have shown, as a result, that if all the u_i differ from 0, each point x in $\mathfrak{g}$ corresponds to 6 points in the Springer fiber.

We can readily notice that the deformed surface (2.43), expressed as a function of the deformation parameters $u_i \in \mathcal{T}/\mathcal{W}$, which are the Casimirs of $\mathcal{S}_{\text{subreg}}$, can be rewritten in terms of its eigenvalues, which in general are Weyl-covariant, and thus are coordinates on $\mathcal{T}$.

In order to do so we stick to the case of generic u_is, so that we can diagonalize the matrices of the Slowody slice (2.43). Calling the eigenvalues ξ_1, ξ_2, ξ_3 we can write:

$$\begin{pmatrix} a & 1 & 0 \\ b & a & c \\ d & 0 & -2a \end{pmatrix} \sim \begin{pmatrix} \xi_1 & 0 & 0 \\ 0 & \xi_2 & 0 \\ 0 & 0 & \xi_3 \end{pmatrix} \qquad \text{with} \quad \xi_1 + \xi_2 + \xi_3 = 0. \tag{2.45}$$

This is exactly equivalent to choosing a flag of the kind:

$$F = \{0 \subset \ <v_1> \ \subset \ <v_1, v_2> \ \subset \ <v_1, v_2, v_3> \ = \mathbb{C}^3\}, \tag{2.46}$$

provided that v_1, v_2, v_3 are the eigenvectors relative to the eigenvalues ξ_1, ξ_2, ξ_3 respectively.

We can now express the Casimirs u_i in terms of the eigenvalues ξ_i, obtaining:

$$\begin{aligned} u_1 &= \xi_1^2 + \xi_2^2 + \xi_1 \xi_2, \\ u_2 &= -\xi_1 \xi_2 (\xi_1 + \xi_2). \end{aligned} \tag{2.47}$$

Once inserted back into the expression (2.43) of the versal deformation of A_2, the relations (2.47) yield the usual presentation (1.24) in terms of coordinates on $\mathcal{T}$, once we substitute $\xi_i \leftrightarrow t_i$.

This is a remarkable point: we have seen that the Springer resolution, employing the tool of Slodowy slices, offers a natural way to map the deformed A_2 family fibered on $\mathcal{T}/\mathcal{W}$ to the family on $\mathcal{T}$, with a completely automatic computation. This feature recurs in all deformed ADE cases, and works also in the case of partial simultaneous resolutions, as we will see momentarily.

- $\boldsymbol{u_i = 0 \quad \forall i}$ **and** $\boldsymbol{(a,b,c,d) \neq (0,0,0,0)}$

  This choice equals going on top of the nilpotent cone, but outside of the origin (which is the A_2 singular point). In this region we can put the matrices (2.42) in the following Jordan form:

$$\begin{pmatrix} 0 & 1 & 0 \\ 0 & 0 & 1 \\ 0 & 0 & 0 \end{pmatrix}, \tag{2.48}$$

which preserves the single flag:

$$F = \{0 \subset \ < e_1 > \ \subset \ < e_1, e_2 > \ \subset \mathbb{C}^3\}. \tag{2.49}$$

We see then that the Springer fiber over the nilpotent cone is composed of a single point.

- $\boldsymbol{u_i = 0 \quad \forall i}$ **and** $\boldsymbol{(a,b,c,d) = (0,0,0,0)}$

  We are on top of the singular point. The matrix (2.40) corresponding to this point is:

$$\mathrm{x} = \begin{pmatrix} 0 & 1 & 0 \\ 0 & 0 & 0 \\ 0 & 0 & 0 \end{pmatrix}. \tag{2.50}$$

In the canonical basis we have $\mathrm{Ker}(\mathrm{x}) =< e_1, e_3 >$ and $\mathrm{Im}(\mathrm{x}) =< e_1 >$.
We can then see that we get two possible flags:

$$\begin{aligned} F_1 &= \{< \alpha e_1 + \beta e_3 > \ \subset \ \ \mathrm{Ker}(\mathrm{x}) \subset \mathbb{C}^3\}, \\ F_2 &= \{\mathrm{Im}(\mathrm{x}) \subset \ < e_1, \alpha e_2 + \beta e_3 > \ \subset \mathbb{C}^3\}, \end{aligned} \tag{2.51}$$

with α and β some complex parameters. Therefore, these two families of flags correspond to two $\mathbb{P}^1$'s, and their intersection is:

$$F_1 \cap F_2 = \{< e_1 > \ \subset \ < e_1, e_3 > \ \subset \mathbb{C}^3\}, \tag{2.52}$$

which is a single point. In other words, we have obtained two 2-spheres intersecting at one point, exactly as expected for the resolution of the A_2 singularity.

- We conclude the analysis of the Springer fibers by studying a class of A_1 subsingularities in the A_2 deformation, thus showing that the Grothendieck-Springer resolution is indeed a *complete simultaneous resolution*, where all the singular fibers of the deformed family are smoothed out.
  We recall that the generic deformation for a A_2 singularity can also be written as (1.24):

$$(2a + t_1)(2a + t_2)(2a + t_3) - cd = 0 \qquad \text{with} \quad t_1 + t_2 + t_3 = 0, \tag{2.53}$$

where t_1 and t_2 are the deformation parameters. We now consider specific slices of the deformation space, giving rise to A_1 subsingularities. The conditions to be imposed on the t_is turn out to be:

$$(A) \;\; t_1 = t_2 \equiv t, \qquad (B) \;\; t_1 = -2t_2 \equiv -2t, \qquad (C) \;\; t_2 = -2t_1 \equiv -2t, \tag{2.54}$$

where all the choices are related by the action of the Weyl group on the parameters t_i.

It is relevant to recall that, for a generic value of the t_is in the deformed surface (2.53), there are three (not independent) 2-cycles with non-zero volume, representing the simple roots α_i of the A_2 algebra and the other positive roots[7]. The volumes α_i of these spheres can be written accordingly to equation (1.26):

$$\alpha_i = t_i - t_{i+1}, \qquad \text{with} \quad \sum_{i=1}^{3} t_i = 0. \tag{2.55}$$

As a result the three cases (2.54) correspond to shrinking the volumes of one of the positive roots, thus leaving only one inflated sphere (because the other two become trivially coincident), representing the remaining A_1 algebra. The volumes of the three roots are:

$$(A) \;\; \begin{cases} \alpha_1 = 0 \\ \alpha_2 = 3t \\ \alpha_1 + \alpha_2 = 3t \end{cases} \qquad (B) \;\; \begin{cases} \alpha_1 = -3t \\ \alpha_2 = 0 \\ \alpha_1 + \alpha_2 = -3t \end{cases} \qquad (C) \;\; \begin{cases} \alpha_1 = 3t \\ \alpha_2 = -3t \\ \alpha_1 + \alpha_2 = 0 \end{cases} \tag{2.56}$$

Inserting the constraints (2.54) in the deformed surface (2.53) we find in all the three cases:

$$8a^3 - 6at^2 - 2t^3 - cd = 0. \tag{2.57}$$

Comparing this equation with (2.43) we note that the Casimirs of the Slodowy slice

[7] In the case of A_2 the positive roots are $\alpha_1, \alpha_2, \alpha_1 + \alpha_2$.

u_1 and u_2 depend on the deformation parameters t_i, and should satisfy:

$$\begin{cases} u_1 = 3t^2 \\ u_2 = -2t^3 \end{cases} \implies \begin{cases} 3a^2 + b = 3t^2 \\ 2a(b-a^2) + cd = -2t^3 \end{cases} . \tag{2.58}$$

Moreover, noticing that the surface (2.57) is singular at the point $(a, c, d) = (-\frac{t}{2}, 0, 0)$, and using the relations (2.58) we should find constraints on b, c, d, which turn out to be:

$$c = d = 0, \qquad b = 9a^2. \tag{2.59}$$

In this way we have obtained the subregion of the Slodowy slice of A_2 (2.40) whose elements are A_1 singular points, because their Casimirs satisfy (2.58):

$$\mathcal{S}^{A_1}_{\text{subreg}} = \left\{ \left(\begin{array}{ccc} a & 1 & 0 \\ 9a^2 & a & 0 \\ 0 & 0 & -2a \end{array} \right) \middle| \; a \in \mathbb{C} \right\}. \tag{2.60}$$

These matrices have three non-zero eigenvalues, two of which are equal:

$$\text{Eigenvalues: } (-2a, -2a, 4a). \tag{2.61}$$

They correspond to three distinct eigenvectors:

$$v_1 = \begin{pmatrix} 0 \\ 0 \\ 1 \end{pmatrix}, \quad v_2 = \begin{pmatrix} -\frac{1}{3a} \\ 1 \\ 0 \end{pmatrix}, \quad v_3 = \begin{pmatrix} \frac{1}{3a} \\ 1 \\ 0 \end{pmatrix}. \tag{2.62}$$

We can therefore diagonalize $\mathcal{S}^{A_1}_{\text{subreg}}$, putting them in the form:

$$\mathcal{S}^{A_1}_{\text{subreg}} \sim \left(\begin{array}{ccc} -2a & 0 & 0 \\ 0 & -2a & 0 \\ 0 & 0 & 4a \end{array} \right), \tag{2.63}$$

with eigenvectors e_1, e_2, e_3 in the canonical basis.

With these vectors we can build only three families of flags that are preserved by the diagonal matrices (2.63):

$$\begin{aligned} F_1 &= \{0 \subset <\alpha e_1 + \beta e_2> \subset <e_1, e_2> \subset \mathbb{C}^3\}, \\ F_2 &= \{0 \subset <e_3> \subset <e_3, \alpha e_1 + \beta e_2> \subset \mathbb{C}^3\}, \\ F_3 &= \{0 \subset <\alpha e_1 + \beta e_2> \subset <\alpha e_1 + \beta e_2, e_3> \subset \mathbb{C}^3\}. \end{aligned} \tag{2.64}$$

These flags corresponds to three non-intersecting $\mathbb{P}^1$'s, each copy representing one of the Weyl-related cases (2.54):

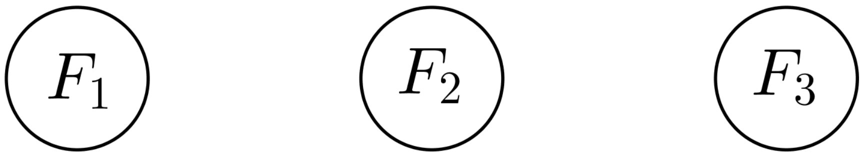

This is in exact correspondence with what we expected from the analysis of the volumes of the roots in (2.56): choosing the Casimirs u_i of the Slodowy slice in such a way to produce an algebraic equation exhibiting subsingularities, automatically triggers a Springer simultaneous resolution smoothing out the very same subsingularities. We see then that there exists a close relationship between Casimirs of the Slodowy and allowed Springer simultaneous resolution: the eigenvalues of the Slodowy slice (2.63) are in one-to-one correspondence with the deformation parameters (2.54) living in $\mathcal{T}$ that define the subsingularities; in turn, the eigenvalues of the Slodowy slice completely predict the Springer simultaneous resolution, via the flags preserved by the form (2.63). This relationship will be a key fact in constructing adjoint Higgses corresponding to threefolds built as deformed ADE singularities, as we will see in Chapter 3.

Summary

Summing up the results of this first example, the Grothendieck-Springer simultaneous resolution for the family $\mathcal{S}_{\text{subreg}} \cap \chi^{-1}(u)$ has yielded the following results:

- For all $u_i \neq 0$, i.e. on a generic point of the deformed A_2 family, the Springer fiber contains $3! = 6$ distinct points, consistently with the number of elements in the full Weyl group of A_2.

- For all $u_i = 0$ and $(a, b, c, d) \neq (0, 0, 0, 0)$, i.e. on top of the nilpotent cone, corresponding to the undeformed A_2 singularity, the Springer fiber contains a single point.

- For all $u_i = 0$ and $(a, b, c, d) = (0, 0, 0, 0)$, i.e. on the singular fiber of the deformed A_2 family, the Springer fiber contains two $\mathbb{P}^1$'s intersecting at a single point.

- Finally, on the A_1 singular points of the form (2.60) the fiber contains three non-intersecting copies of a $\mathbb{P}^1$, related by the action of the Weyl group.

The multiplicity of the Springer fibers is in perfect agreement with the diagram (2.34), that tells us that the resolved fibers will depend on Weyl covariant coordinates living in $\mathcal{T}$, and will be related to each other by Weyl transformations.

The structure of the complete simultaneous resolutions can finally be intuitively represented graphically, highlighting the content of the Springer fibers:

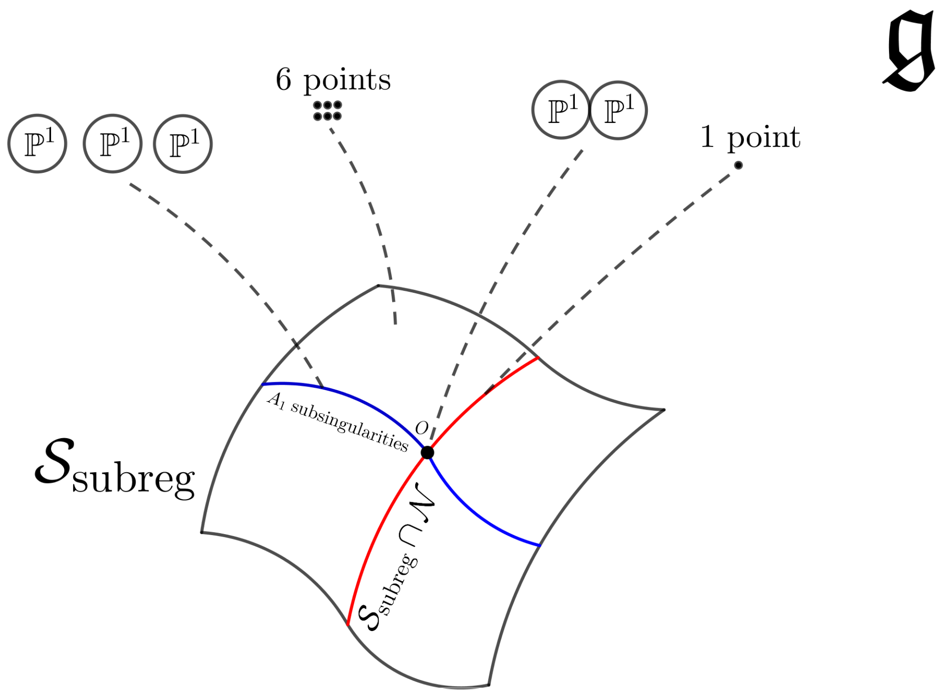

Figure 2.2: *Content of the Springer fibers in the complete resolution of the A_2 singularity.*

We conclude this section underlining the aspects of the Grothendieck-Springer resolutions that will be relevant for the physics of theories geometrically engineered by ADE singularities: in our example we have examined in great detail the *complete* resolution of the A_2 deformed family. In order to do so, we have associated to each element of the family the *complete* flags that it preserves, which are in correspondence with the *Borel* subalgebras of A_2. As reviewed in Appendix A, Borel subalgebras can be decomposed into the sum of a Cartan subalgebra $\mathfrak{h}$, which is nothing but a diagonal Levi subalgebra $\mathcal{L}$, and some nilpotent subalgebra $\mathfrak{n}$. In general, a Levi subalgebra $\mathcal{L}$ is defined by a choice of simple roots Θ, and is generated by:

$$\mathcal{L} = \mathfrak{h} \oplus \langle \Theta \rangle, \tag{2.65}$$

where $\langle \Theta \rangle$ are the roots (that can be both positive and negative) generated by the set Θ. For further details on this definition we refer to Appendix A.

In our A_2 example we can decompose $\mathfrak{b}$ as a sum of the trivial Levi subalgebra $\mathcal{L} = \mathfrak{h}$ and some nilpotent part:

$$\mathfrak{b} = \begin{pmatrix} * & * & * \\ 0 & * & * \\ 0 & 0 & * \end{pmatrix} = \underbrace{\begin{pmatrix} * & 0 & 0 \\ 0 & * & 0 \\ 0 & 0 & * \end{pmatrix}}_{\mathcal{L}} + \underbrace{\begin{pmatrix} 0 & * & * \\ 0 & 0 & * \\ 0 & 0 & 0 \end{pmatrix}}_{\mathfrak{n}}. \tag{2.66}$$

This decomposition is not casual: notice that a generic element of the A_2 deformed family can always be put in a diagonal form with distinct eigenvalues, according to the equivalence (2.45). This is possible because we have not constrained in any way the deformation parameters, thus allowing a *complete* simultaneous resolution. Such diagonal form precisely corresponds to the shape of the Levi subalgebra $\mathcal{L}$ contained in the Springer fibers. As a result, we see that the following chain of correspondences holds:

$$\text{generic x} \in A_2\text{-deformed family} \quad \longleftrightarrow \quad \underbrace{\begin{pmatrix} \xi_1 & 0 & 0 \\ 0 & \xi_2 & 0 \\ 0 & 0 & \xi_3 \end{pmatrix}}_{\text{diagonalized matrix}} \quad \longleftrightarrow \quad \underbrace{\begin{pmatrix} * & 0 & 0 \\ 0 & * & 0 \\ 0 & 0 & * \end{pmatrix}}_{\text{Levi subalgebra in the Springer fiber}}$$

The coordinates ξ_i, which are the Casimirs of the diagonal blocks of the Levi on the r.h.s. (in the following, we will call them *partial Casimirs*), span the Cartan subalgebra $\mathcal{T}$, and this is why the family written in terms of the ξ_i admits a complete simultaneous resolution.

This is the central fact that will inspire our physical constructions in the ensuing chapters: performing a complete resolution constrains the shape of the Levi subalgebra in the Springer fibers, which comes equipped with its Casimirs, and we will show that this in turn fixes the structure of the Higgs field that geometrically engineers 5d theories arising from the compactification of M-theory on an ADE deformed singularity. We further argue that this equivalence holds for all kind of resolutions: *partial* simultaneous resolutions correspond to larger Levi subalgebras, and thus to different structures of the Higgs field.

Before getting into the details of partial Springer resolutions and fully explain the details of the general construction, we now briefly show a last example of complete resolution, taking into account the subtleties given by the D_n series.

2.2.2 Complete Springer resolution of D_4

To set the stage for the analysis of the complete simultaneous Springer resolution of a singularity in the D_n series, let us consider the simplest non trivial example, given by D_4. As for the A_2 case, the recipe to resolve the singularity is simple: first we find the Slodowy slice passing through an element of the subregular nilpotent orbit of D_4, then intersect the Slodowy slice with the fibers of the adjoint quotient map, producing the D_4 deformed family, and finally we compute the Borel subalgebras containing each point of the family, thus finding the fibers of the resolution. Keeping in mind such steps, let us briefly show the main points of the computation, with specific attention devoted to the computation of preserved flags, which is the point differing from the A_n case.

Taking a look at table (2.20) the subregular nilpotent orbit of $D_4 \equiv \mathfrak{so}(8)$ corresponds to the partition $[5,3]$. Following the dictionary outlined in section (2.1.4) we immediately find the following canonical representative x for the subregular orbit, along with its companion y satisfying the usual $\mathfrak{su}(2)$ commutation relations:

$$\mathrm{x} = \begin{pmatrix} 0 & 1 & 0 & 0 & 0 & 0 & 0 & 0 \\ 0 & 0 & 1 & 0 & 0 & 0 & 1 & 0 \\ 0 & 0 & 0 & 0 & 0 & -1 & 0 & 1 \\ 0 & 0 & 0 & 0 & 0 & 0 & -1 & 0 \\ 0 & 0 & 0 & 0 & 0 & 0 & 0 & 0 \\ 0 & 0 & 0 & 0 & -1 & 0 & 0 & 0 \\ 0 & 0 & 0 & 0 & 0 & -1 & 0 & 0 \\ 0 & 0 & 0 & 0 & 0 & 0 & 0 & 0 \end{pmatrix}, \qquad \mathrm{y} = \begin{pmatrix} 0 & 0 & 0 & 0 & 0 & 0 & 0 & 0 \\ 4 & 0 & 0 & 0 & 0 & 0 & 0 & 0 \\ 0 & 4 & 0 & 2 & 0 & 0 & 0 & 0 \\ -2 & 0 & 0 & 0 & 0 & 0 & 0 & 0 \\ 0 & 0 & 0 & 0 & 0 & -4 & 0 & 2 \\ 0 & 0 & -2 & 0 & 0 & 0 & -4 & 0 \\ 0 & 2 & 0 & -2 & 0 & 0 & 0 & 0 \\ 0 & 0 & 2 & 0 & 0 & 0 & -2 & 0 \end{pmatrix}. \tag{2.67}$$

The Slodowy slice through x then is:

$$\mathcal{S}_{\text{subreg}} = \begin{pmatrix} 0 & 1 & 0 & 0 & 0 & 0 & 0 & 0 \\ b_1 & 0 & 1 & 0 & 0 & 0 & 1 & 0 \\ b_2 & b_3 & 0 & b_4 & 0 & -1 & 0 & 1 \\ -2b_1+2b_3-b_4 & 0 & 0 & 0 & 0 & 0 & -1 & 0 \\ 0 & b_5 & b_2 & b_6 & 0 & -b_1 & -b_2 & 2b_1-2b_3+b_4 \\ -b_5 & 0 & -2b_1+\frac{5b_3}{3}-\frac{b_4}{3} & -b_2 & -1 & 0 & -b_3 & 0 \\ -b_2 & 2b_1-\frac{5b_3}{3}+\frac{b_4}{3} & 0 & b_1-\frac{4b_3}{3}-\frac{b_4}{3} & 0 & -1 & 0 & 0 \\ -b_6 & b_2 & -b_1+\frac{4b_3}{3}+\frac{b_4}{3} & 0 & 0 & 0 & -b_4 & 0 \end{pmatrix}, \tag{2.68}$$

where the b_is are complex parameters.

The Lie algebra $\mathfrak{so}(8)$ possesses 4 Casimir invariants, given by[8]:

$$u_i = \mathrm{Tr}\,(\mathcal{S}^i_{\text{subreg}}) \quad \text{for } i = 2, 4, 6, \qquad \tilde{u}_4 = \mathrm{Pfaff}(\mathcal{S}_{\text{subreg}}). \tag{2.69}$$

Computing them explicitly and putting ourselves on top of the nilpotent cone (that is, where all the $u_i = 0$) we find that the intersection of the Slodowy slice with the nilpotent cone yields the canonical presentation (1.2) of the D_4 singularity:

$$\mathcal{S}_{\text{subreg}} \cap \mathcal{N} = \left\{ \text{matrices in } \mathcal{S}_{\text{subreg}} \;\middle|\; 81b_2^2 - 500b_3\left(2b_3^2 + b_4b_3 - b_4^2\right) = 0 \right\}, \tag{2.70}$$

where by a trivial translation and renaming we obtain the form (1.2):

$$81b_2^2 - 500b_3\left(2b_3^2 + b_4b_3 - b_4^2\right) \quad \sim \quad x^2 + zy^2 - z^3 = 0. \tag{2.71}$$

The completely deformed D_4 family (1.23), on the other hand, is obtained by letting the u_is be non-vanishing. After appropriate rescalings and renamings, the final (admittingly ugly) result is:

$$\mathcal{S}_{\text{subreg}} \cap \chi^{-1}(u) = \{\text{matrices in } \mathcal{S}_{\text{subreg}} \mid P(x, y, z, u_i) = 0\}, \tag{2.72}$$

[8]For further details on the Casimir invariants, we refer to Appendix A.

with:

$$
\begin{aligned}
&P(x,y,z,u_i) = \\
&= x^2+zy^2-z^3-z^2\left(2\sqrt[3]{2}\;3^{2/3}u_2\right)+z\left(-3\sqrt[3]{\frac{3}{2}}u_2^2-6\;2^{2/3}\sqrt[3]{3}u_4+144\;2^{2/3}\sqrt[3]{3}\tilde{u}_4\right)+ \\
&y\left(-6\;2^{2/3}\sqrt[3]{3}u_4+3\sqrt[3]{\frac{3}{2}}u_2^2-48\;2^{2/3}\sqrt[3]{3}\tilde{u}_4\right)+\left(-15u_2^3+108u_2u_4+288u_2\tilde{u}_4-192u_6\right).
\end{aligned}
\tag{2.73}
$$

Using this expression it is then possible to explicitly relate the parameters u_i with the usual deformation parameters $\delta_{2i}, \tilde{\delta}_4$ of the D_4 deformed family (1.23).

At this point we have all the material needed in order to perform the complete simultaneous Springer resolution: in the last step we have to find the Borel subalgebra that contains each point of the deformed family, i.e. each matrix of $\mathcal{S}_{\text{subreg}} \cap \chi^{-1}(u)$, which will be then identified with the Springer fibers. As we did in the A_n case, for ease of computation we would like to relate the Borel variety $\mathcal{B}$ formed by the Borel subalgebras of D_n with some kind of flag variety $\mathcal{F}$, encoding the flags that are preserved, in some to be defined sense, by the elements of $\mathcal{S}_{\text{subreg}} \cap \chi^{-1}(u)$.

It turns out that the flags we are looking for in the D_n case must be *isotropic flags*, that assume the form:

$$
\mathcal{F} = \{0 \subset V_1 \subset \ldots \subset V_{n-1} \subset V_n \subset V_{n-1}^{\perp} \subset \ldots \subset V_1^{\perp} \subset \mathbb{C}^{2n}\} \qquad \text{with} \qquad V_n = V_n^{\perp}, \tag{2.74}
$$

where perpendicularity is defined with respect to the following quadratic form q and bilinear product $B(v,w)$, where v,w are vectors in $\mathbb{C}^{2n}$:

$$
q = \begin{pmatrix} 0 & \mathbb{1}_{n\times n} \\ \mathbb{1}_{n\times n} & 0 \end{pmatrix}, \qquad B(v,w) = \frac{1}{2}\left(q(v+w)-q(v)-q(w)\right). \tag{2.75}
$$

Specifying to the D_4 case at hand, in order to build the Springer fibers we must look for preserved flags of the kind:

$$
\mathcal{F} = \{0 \subset V_1 \subset V_2 \subset V_3 \subset V_4 \subset V_3^{\perp} \subset V_2^{\perp} \subset V_1^{\perp} \subset \mathbb{C}^8\} \qquad \text{with} \qquad V_4 = V_4^{\perp} \tag{2.76}
$$

Using the presentation (2.68) we find the following flags, depending on the examined point of the deformed family:

- On a generic point of the deformed family (2.68), that is for arbitrary deformation parameters u_i, we find 8 eigenvectors:

$$
v_1, v_2, v_3, v_4, v_5, v_6, v_7, v_8. \tag{2.77}
$$

They are all orthogonal with respect to each other, except:

$$\begin{aligned}&(v_1, v_2)\\&(v_3, v_6)\\&(v_4, v_5)\\&(v_7, v_8)\end{aligned} \tag{2.78}$$

So we can build the following number of flags:

$$\#\text{ of flags}: \qquad 8\times6\times4\times2 = 384, \tag{2.79}$$

where we notice that 384 is exactly twice the order of the Weyl group of D_4, which is 192.

Why do we find twice the number of flags that we would expect from a complete resolution of a D_4 singularity? The reason is that, following [119] and [112], the D_4 group acts transitively on the flags, except when a flag contains a maximal isotropic subspace of dimension half the total dimension of the complex space (i.e. subspaces of dimension 4, in our case). In such cases there are two distinct orbits, that are linked by a transformation with negative determinant (for example, a series of reflections in non-isotropic vectors).

As a result, in the case of the complete resolution, that involves complete isotropic flags, we always have a doubling of the number of flags[9].

Finally, if we want to understand whether two flags involving maximal isotropic subspaces W and W' belong to the same orbit we should compute the codimension of their intersection $W\cap W'$ inside W and W': if this codimension is even they belong to the same orbit, and viceversa if the codimension is odd.

- On top of the nilpotent cone, namely on the D_4 singular surface, we can reason exactly as in the preceding paragraph, finding only a single preserved flag.
- On the origin of the deformed D_4 family, namely on the point corresponding to the singular fiber, we find 8 families of flags, each isomorphic to a $\mathbb{P}^1$ subdivided into two

[9] We should additionally notice that this fact is connected to the presence of two possible nilpotent orbits for very even partitions in the D_n cases. In D_4, indeed, we have the nilpotent orbits $\mathcal{O}^{I}_{[4,4]}$ and $\mathcal{O}^{II}_{[4,4]}$.

sets intersecting exactly in the shape of the D_4 Dynkin diagram, as anticipated:

$$F_1 = \{0 \subset\ < \alpha e_1 + \beta e_4 > \ \subset\ < e_1, e_4 > \ \subset\ < e_1, e_2, e_4 > \ \subset\ < e_1, e_2, e_3, e_4 > \ \subset$$
$$< e_1, e_2, e_3, e_4, e_7 > \ \subset\ < e_1, e_2, e_3, e_4, e_6, e_7 > \ \subset\ < e_1, e_2, e_3, e_4, e_6, e_7, \beta e_5 - \alpha e_8 > \ \subset \mathbb{C}^8\},$$
$$F_2 = \{0 \subset\ < e_1 > \ \subset\ < e_1, \alpha e_2 + \beta e_4 > \ \subset\ < e_1, e_2, e_4 > \ \subset\ < e_1, e_2, e_3, e_4 > \ \subset$$
$$< e_1, e_2, e_3, e_4, e_7 > \ \subset\ < e_1, e_2, e_3, e_4, e_7, \beta e_6 - \alpha e_8 > \ \subset\ < e_1, e_2, e_3, e_4, e_6, e_7, e_8 > \ \subset \mathbb{C}^8\},$$
$$F_3 = \{0 \subset\ < e_1 > \ \subset\ < e_1, e_2 > \ \subset\ < e_1, e_2, \alpha e_3 + \beta e_4 > \ \subset\ < e_1, e_2, e_3, e_4 > \ \subset$$
$$< e_1, e_2, e_3, e_4, \beta e_7 - \alpha e_8 > \ \subset\ < e_1, e_2, e_3, e_4, e_7, e_8 > \ \subset\ < e_1, e_2, e_3, e_4, e_6, e_7, e_8 > \ \subset \mathbb{C}^8\},$$
$$F_4 = \{0 \subset < e_1 > \subset < e_1, e_2 - e_4 > \subset < e_1, e_2 - e_4, \alpha e_7 + \beta e_2 > \subset\ < e_1, e_2 - e_4, \alpha e_7 + \beta e_2, \alpha e_3 - \beta(e_6 + e_8) > \ \subset$$
$$< e_1, e_2, \alpha(e_6 + e_8) - \beta e_3, e_4, e_7 > \ \subset\ < e_1, e_2, e_3, e_4, e_6 + e_8, e_7 > \ \subset\ < e_1, e_2, e_3, e_4, e_6, e_7, e_8 > \ \subset \mathbb{C}^8\},$$
$$F_5 = \{0 \subset\ < \alpha e_1 + \beta e_4 > \ \subset\ < e_1, e_4 > \ \subset\ < e_1, e_2, e_4 > \ \subset\ < e_1, e_2, e_4, e_7 > \ \subset$$
$$< e_1, e_2, e_3, e_4, e_7 > \ \subset\ < e_1, e_2, e_3, e_4, e_6, e_7 > \ \subset\ < e_1, e_2, e_3, e_4, e_6, e_7, \beta e_5 - \alpha e_8 > \ \subset \mathbb{C}^8\},$$
$$F_6 = \{0 \subset\ < e_1 > \ \subset\ < e_1, \alpha e_2 + \beta e_4 > \ \subset\ < e_1, e_2, e_4 > \ \subset\ < e_1, e_2, e_4, e_7 > \ \subset$$
$$< e_1, e_2, e_3, e_4, e_7 > \ \subset\ < e_1, e_2, e_3, e_4, e_7, \beta e_6 - \alpha e_8 > \ \subset\ < e_1, e_2, e_3, e_4, e_6, e_7, e_8 > \ \subset \mathbb{C}^8\},$$
$$F_7 = \{0 \subset\ < e_1 > \ \subset\ < e_1, e_2 > \ \subset\ < e_1, e_2, \alpha e_3 + \beta e_4 > \ \subset\ < e_1, e_2, \alpha e_3 + \beta e_4, \beta e_7 - \alpha e_8 > \ \subset$$
$$< e_1, e_2, e_3, e_4, \beta e_7 - \alpha e_8 > \ \subset\ < e_1, e_2, e_3, e_4, e_7, e_8 > \ \subset\ < e_1, e_2, e_3, e_4, e_6, e_7, e_8 > \ \subset \mathbb{C}^8\},$$
$$F_8 = \{0 \subset\ < e_1 > \ \subset\ < e_1, e_2 - e_4 > \ \subset\ < e_1, e_2 - e_4, \alpha e_7 + \beta e_2 > \ \subset\ < e_1, e_2, e_4, e_7 > \ \subset$$
$$< e_1, e_2, \alpha(e_6 + e_8) - \beta e_3, e_4, e_7 > \ \subset\ < e_1, e_2, e_3, e_4, e_6 + e_8, e_7 > \ \subset\ < e_1, e_2, e_3, e_4, e_6, e_7, e_8 > \ \subset \mathbb{C}^8\}.$$

Their intersection pattern can be explicitly computed, yielding two copies of the D_4 Dynkin diagram:

Again, the fact that we have *two* sets of spheres intersecting in the shape of the D_4 Dynkin diagram is due to the fact that the flags preserve an isotropic subspace of dimension half that of the total complex space $\mathbb{C}^8$, thus doubling the counting.

Having settled the discussion for the Springer complete simultaneous resolution of both A_n and D_n cases, we can finally concentrate our attention to partial simultaneous resolutions, which can be thought of as particular cases of complete Springer resolutions, and that will be the actual tool massively employed in the following more physically-oriented chapters.

2.3 Partial Springer resolutions

In this section, we focus our efforts onto *partial* Springer simultaneous resolutions, that involve as key ingredients the so-called *parabolic subalgebras* of a Lie algebra $\mathfrak{g}$. For a quick reminder of how parabolic subalgebras of an ADE Lie algebra arise, we refer to Appendix A. Here we concentrate exclusively on their practical applications.

Parabolic subalgebras $\mathfrak{p}$ of a Lie algebra $\mathfrak{g}$ can be sketchily defined as those subalgebras that contain a Borel subalgebra $\mathfrak{b}$. Practically speaking, each parabolic subalgebra is related to a choice of positive roots $\Theta \in \Delta_{\text{simple roots}}$ (with $\Delta_{\text{simple roots}}$ the set of all simple roots of $\mathfrak{g}$). The corresponding parabolic subalgebra $\mathfrak{p}_\Theta$ can be built taking the Cartan and root generators of the standard Borel subalgebra and adding the generators of all the roots (both positive and negative) generated by Θ.

In the case of the $\mathfrak{sl}(n)$ algebras the standard Borel subalgebra is represented in the fundamental representation by the upper triangular matrices, and the generators associated to the simple roots $\alpha_i = e_i - e_{i+1}$ are represented by the matrices $X_{i,i+1}$ defined in Appendix A. Parabolic subalgebras are built by adding these matrices (depending on what choice of the simple roots we make) to the Borel subalgebra, as we will show in a concrete example in Section 2.3.1.

The commutative diagram encoding the partial resolution is very similar to the one of the complete Springer resolution (2.34):

$$\begin{array}{ccc} \widehat{\mathcal{S}_{\text{subreg}} \cap \chi^{-1}(u)} & \xrightarrow{\pi} & \mathcal{S}_{\text{subreg}} \cap \chi^{-1}(u) \\ \downarrow \phi_P & & \downarrow \chi \\ \mathcal{T}/\mathcal{W}' & \xrightarrow{p} & \mathcal{T}/\mathcal{W} \end{array} . \tag{2.80}$$

Differently from the complete resolution case, ϕ_P is a map that takes an element in $\mathfrak{g}$ and extracts its $\mathcal{W}'$-invariant partial Casimirs, with $\mathcal{W}'$ the Weyl group corresponding to the simple roots belonging to Θ.

As we have seen in the case of complete resolutions, Borel subalgebras are in one-to-one correspondence with complete flags, that is flags that possess a subspace for each complex dimension between 0 and n, because these are exactly the flags preserved by the action of the Borel subalgebra.

Analogously, the variety of parabolic subalgebras is in one-to-one correspondence with the set of *partial flags*, which are flags "lacking" one or more dimensions in the flag, meaning that there is no subspace of that dimension preserved by the parabolic subalgebra.

A partial Springer resolution of an ADE singularity can therefore be performed along the same routes as a complete resolution, provided that one makes the substitutions:

$$\begin{aligned} \text{Borel subalgebras} &\longleftrightarrow \text{Parabolic subalgebras} \\ \text{Complete flags} &\longleftrightarrow \text{Partial flags} \end{aligned} \tag{2.81}$$

As a result, the recipe to explicitly compute the partial simultaneous resolution of an ADE singularity can be performed as follows:

- Consider an ADE Lie algebra $\mathfrak{g}$, compute its subregular nilpotent orbit and choose a specific element x belonging to the orbit.
- Compute the Slodowy slice $\mathcal{S}_{\text{subreg}}$ through x.
- Write the intersection of the Slodowy slice with the fibers of the adjoint quotient map $\mathcal{S}_{\text{subreg}} \cap \chi^{-1}(u)$.
- Choose a set Θ of simple roots in $\mathfrak{g}$: the roots that are *not* generated by Θ will correspond to the resolved 2-cycles in the partial simultaneous resolution.
- Identify the parabolic subalgebra corresponding to the choice of the roots, and compute which subspace-dimensions are not present in the partial flags preserved by the parabolic subalgebra. Call $\mathcal{P}$ the set of partial flags with these dimensions missing.
- For each element x of $\mathcal{S}_{\text{subreg}} \cap \chi^{-1}(u)$, find *all* the *partial* flags in $\mathcal{P}$ preserved by x, that is the partial flags such that $\text{x}(V_i) \subseteq V_i, \quad \forall i$.
  On the nilpotent cone $\mathcal{N}$ this last relation becomes $\text{x}(V_i) \subseteq V_{i-1}, \quad \forall i$. For each x, call $\mathfrak{p}$ the set of flags that it preserves.
- The simultaneous resolution of the ADE singularity of type $\mathfrak{g}$ is then given by the map π in (2.80), with:
$$\widetilde{\mathcal{S}_{\text{subreg}} \cap \chi^{-1}(u)} = \{(\text{x}, \mathfrak{p}) \in \mathcal{S}_{\text{subreg}} \times \mathcal{P}\}. \tag{2.82}$$

In this recipe, we have used the word "choose" referring to the set of simple roots Θ that dictate the pattern of 2-cycles that will arise after the resolution: it is paramount to notice that a "choice" is possible only in the case of an ADE singularity deformed with *generic* parameters u_i. In the more concrete and informative cases of the following chapters, we will make constrained choices of the deformation parameters, that will automatically also fix the choice of Θ.

Having set up the machinery for partial Springer resolutions, we can proceed in showing two explicit examples, once again picking simple cases in the A_n and D_n series.

2.3.1 Partial Springer resolution of A_2

In this section, we examine the partial Springer resolution of the deformed A_2 family, completing the work started in section (2.2.1) with the complete resolution.

The main ingrendient in a partial Springer resolution is the choice of simple roots Θ, that determines the parabolic subalgebras that constitute the Springer fibers. It is easy, employing the rules of Appendix A, to classify all parabolic subalgebras of A_2 (in compliance with the notation of [112] we indicate with a $*$ the non vanishing entries in the matrices):

Θ	Parabolic subalgebra
α_1	$\begin{pmatrix} * & * & * \\ * & * & * \\ 0 & 0 & * \end{pmatrix}$
α_2	$\begin{pmatrix} * & * & * \\ 0 & * & * \\ 0 & * & * \end{pmatrix}$
α_1, α_2	$\begin{pmatrix} * & * & * \\ * & * & * \\ * & * & * \end{pmatrix}$

As an example of partial simultaneous resolution let us choose the parabolic subalgebra associated to $\Theta = \alpha_1$: it is easily shown that this subalgebra does not admit any invariant 1-dim subspace. As a result the partial flags we must be looking for, in order to obtain the partial resolution, should "skip" the 1-dim subspace. In other words the partial flags $\mathcal{P}_{\alpha_1}$ are of the form:

$$\mathcal{P}_{\alpha_1} = \{0 \subset V_2 \subset \mathbb{C}^3\}. \tag{2.83}$$

A similar reasoning goes for the parabolic subalgebra related to $\Theta = \alpha_2$, except that in this case there is no 2-dim subspace:

$$\mathcal{P}_{\alpha_2} = \{0 \subset V_1 \subset \mathbb{C}^3\}. \tag{2.84}$$

Recalling that, in order to build the fibers of the resolution, for each element x in the Slodowy slice we should have $\mathrm{x}(V_i) \subseteq V_i \quad \forall i$, we obtain for each root a family of partial flags isomorphic to $\mathbb{P}^1$ on the origin of the A_2 deformed family where x has the form (2.38):

$$\begin{aligned} P_{\alpha_1} &= \{0 \subset \; < e_1, \alpha e_2 + \beta e_3 > \; \subset \mathbb{C}^3\}, \\ P_{\alpha_2} &= \{0 \subset \; < \alpha e_1 + \beta e_3 > \; \subset \mathbb{C}^3\}. \end{aligned} \tag{2.85}$$

P_{α_1} corresponds to the partial simultaneous resolution where we have resolved only the 2-cycle corresponding to α_2, and viceversa for P_{α_2}.

Furthermore, if we pick the parabolic subalgebra corresponding to both α_1 and α_2 we find that no subspace of $\mathbb{C}^3$ is left unchanged: as a result no 2-cycle is resolved, and so we have effectively no resolution.

Finally, for generic u_i, namely outside the nilpotent cone, we can perform the computation as follows. We have shown that in the complete resolution we obtain $3! = 6$ distinct points, corresponding to the flags:

$$\begin{aligned}
F_1 &= \{0 \subset \ < e_1 > \ \subset \ < e_1, e_2 > \ \subset \mathbb{C}^3\}, \\
F_2 &= \{0 \subset \ < e_1 > \ \subset \ < e_1, e_3 > \ \subset \mathbb{C}^3\}, \\
F_3 &= \{0 \subset \ < e_2 > \ \subset \ < e_1, e_2 > \ \subset \mathbb{C}^3\}, \\
F_4 &= \{0 \subset \ < e_2 > \ \subset \ < e_2, e_3 > \ \subset \mathbb{C}^3\}, \\
F_5 &= \{0 \subset \ < e_3 > \ \subset \ < e_2, e_3 > \ \subset \mathbb{C}^3\}, \\
F_6 &= \{0 \subset \ < e_3 > \ \subset \ < e_1, e_3 > \ \subset \mathbb{C}^3\}.
\end{aligned} \tag{2.86}$$

Once we pass to the partial resolution corresponding, for example, to the root $\alpha_1 \in \Theta$ (the other case is completely analogous), only 3 flags remain:

$$\begin{aligned}
F_1 &= \{0 \subset \ < e_1, e_2 > \ \subset \mathbb{C}^3\}, \\
F_2 &= \{0 \subset \ < e_1, e_3 > \ \subset \mathbb{C}^3\}, \\
F_3 &= \{0 \subset \ < e_2, e_3 > \ \subset \mathbb{C}^3\}.
\end{aligned} \tag{2.87}$$

The ratio behind this change in the preserved flags is clear when comparing the commutative diagrams of the partial (2.80) and complete (2.34) resolution: while the completely resolved A_2 family gets mapped to the full Cartan subalgebra $\mathcal{T}$, thus getting $|\mathcal{W}| = |S_3| = 3! = 6$ points, for the partial resolution the map goes to the quotiented Cartan subalgebra $\mathcal{T}/\mathcal{W}'$, with $\mathcal{W}' = S_2$, that leaves only 3 points.

We would finally like to relate the total Casimirs of the Slodowy slice $u_i \in \mathcal{T}/\mathcal{W}$ appearing in (2.43) with coordinates adapted to the partial Springer simultaneous resolution we are performing, namely we want to find the map from $\mathcal{T}/\mathcal{W}$ to $\mathcal{T}/\mathcal{W}'$, where $\mathcal{W}'$ is dictated by the partial resolution. To this end, we:

- Consider the maximal Levi subalgebra contained in the parabolic subalgebra associated to the roots in Θ. For example, choosing $\alpha_1 \in \Theta$, the suitable subalgebra is the boxed one:

$$\begin{pmatrix} \boxed{\begin{matrix} * & * \\ * & * \end{matrix}} & \begin{matrix} * \\ * \end{matrix} \\ \begin{matrix} 0 & 0 \end{matrix} & \boxed{*} \end{pmatrix} \qquad = A_1 \oplus \langle \alpha_2^* \rangle \tag{2.88}$$

  where the A_1 addend refers to the non-resolved α_1 node, and $\langle \alpha_2^* \rangle$ is the $U(1)$ generated by the resolved node α_2.

- Compute the Casimir invariants of the simple and Cartan addends in the Levi subalgebra on a generic point of the Slodowy slice, that for generic u_i can be diagonalized:

$$\begin{pmatrix} \boxed{\begin{matrix} \xi_1 & 0 \\ 0 & \xi_2 \end{matrix}} & \begin{matrix} 0 \\ 0 \end{matrix} \\ \begin{matrix} 0 & 0 \end{matrix} & \xi_3 \end{pmatrix} \tag{2.89}$$

- These invariants under $\mathcal{W}'$ will provide new coordinates parameterizing the deformed surface corresponding to a partial resolution in which only the roots not belonging to Θ are blown-up. If we chose $\alpha_1 \in \Theta$ we would obtain:

$$\begin{aligned} &\begin{cases} \xi_1 \\ \xi_2 \end{cases} \Rightarrow \begin{cases} \sigma_1 = \xi_1 + \xi_2 \\ \sigma_2 = \xi_1 \xi_2 \end{cases} \\ &\ \xi_3 \quad \Rightarrow \ \tilde{\sigma}_1 = \xi_3 = -\sigma_1 \end{aligned} \tag{2.90}$$

  In this case the versal deformation (2.43) rearranges as:

$$8a^3 + 2a(-\sigma_1^2 + \sigma_2) - \sigma_1 \sigma_2 = 0, \tag{2.91}$$

  where σ_1 and σ_2 are invariant coordinates with respect to the Weyl group $\mathcal{W}'$. By construction, equation (2.91) is a deformed A_2 family admitting only the partial simultaneous resolution of the node corresponding to the root α_2. We have thus shown that the formalism of the Springer resolution, computing the Casimirs of the simple addends in the Levi subalgebra, naturally reproduces the deformed A_2 family, mapping from $\mathcal{T}/\mathcal{W}$ to $\mathcal{T}/\mathcal{W}'$.

Let us conclude the analysis of partial Springer resolutions by examining the D_4 case.

2.3.2 Partial Springer resolution of D_4

In this section, we briefly show how to perform a partial simultaneous Springer resolution of the deformed D_4 family where only the central node gets resolved. The motivation to perform such a computation will become crystal clear in the following chapters, where we will profusely employ the results of this section.

Once again, the starting point is the choice of simple roots Θ, that correspond to 2-cycles that will *not* be resolved in the Springer fiber. Considering the D_4 Dynkin diagram:

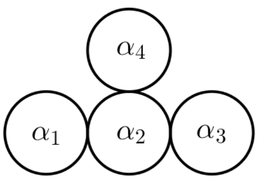

we pick:

$$\Theta = \{\alpha_1, \alpha_3, \alpha_4\}, \tag{2.92}$$

so that only the central node will be resolved by the partial resolution. Now we have to compute the parabolic subalgebra $\mathfrak{p}_\Theta$ corresponding to the choice (2.92).
The most general Borel subalgebra of D_4 reads:

$$\mathfrak{b} = \left(\begin{array}{cccc|cccc} * & * & * & * & 0 & * & * & * \\ 0 & * & * & * & * & 0 & * & * \\ 0 & 0 & * & * & * & * & 0 & * \\ 0 & 0 & 0 & * & * & * & * & 0 \\ \hline 0 & 0 & 0 & 0 & * & 0 & 0 & 0 \\ 0 & 0 & 0 & 0 & * & * & 0 & 0 \\ 0 & 0 & 0 & 0 & * & * & * & 0 \\ 0 & 0 & 0 & 0 & * & * & * & * \end{array}\right). \tag{2.93}$$

In order to compute $\mathfrak{p}_\Theta$ we have to add to the Borel subalgebra $\mathfrak{b}$ all the matrix representatives corresponding to the roots generated by the external nodes $\alpha_1, \alpha_3, \alpha_4 \in \Theta$ (2.93). Picking the appropriate matrix representatives with the aid of Appendix A the result is:

$$\mathfrak{p}_\Theta = \left(\begin{array}{cccc|cccc} * & * & * & * & 0 & * & * & * \\ * & * & * & * & * & 0 & * & * \\ 0 & 0 & * & * & * & * & 0 & * \\ 0 & 0 & * & * & * & * & * & 0 \\ \hline 0 & 0 & 0 & 0 & * & * & 0 & 0 \\ 0 & 0 & 0 & 0 & * & * & 0 & 0 \\ 0 & 0 & 0 & * & * & * & * & * \\ 0 & 0 & * & 0 & * & * & * & * \end{array}\right). \tag{2.94}$$

It is easy to show that the matrices in $\mathfrak{p}_\Theta$ preserve only partial flags of the form:

$$\mathcal{F} = \{0 \subset V_2 \subset V_6 \subset \mathbb{C}^8\}. \tag{2.95}$$

We notice that these flags do not contain a maximal isotropic subspace (i.e. a V_4), and so we do *not* expect to find the doubling of flags that we have observed in 2.2.2, according to [119].

Indeed a short computation shows that there is a unique family of partial flags of the form (2.95) that is preserved on the origin of the Slodowy slice (2.68), namely on the point possessing a singular D_4 fiber:

$$F_{\text{central node}} = \{0 \subset \, < e_1, \alpha e_2 + \beta e_4 > \, \subset \, < e_1, e_2, e_3, e_4, e_7, \beta e_6 - \alpha e_8 > \, \subset \mathbb{C}^8\}. \tag{2.96}$$

Geometrically, this flag, that is isomorphic to $\mathbb{P}^1$, corresponds to the central node that is resolved by the partial resolution.

Instead, on a generic point of the Slodowy slice outside the origin, we get a total of:

$$\#\text{ of flags}: \qquad \frac{8\times 6}{2} = 24, \tag{2.97}$$

that exactly corresponds to the quotients of the cardinality of the full Weyl group and the Weyl group generated by the roots that are not being resolved by the partial resolution:

$$24 = \frac{|\mathcal{W}|}{|\mathcal{W}'|} = \frac{|\mathcal{W}|}{|S_2\times S_2\times S_2|}. \tag{2.98}$$

Finally, as in the case of the A_2 deformed family, one would like to be able to reconstruct the algebraic expression of the D_4 deformed family allowing the resolution of the central node, defined in (1.24), by computing the Casimirs of appropriate simple addends in the Levi subalgebra corresponding to $\mathfrak{p}_\Theta$. The Levi subalgebra in question reads:

$$\mathcal{L}_\Theta = \left(\begin{array}{cccc|cccc} * & * & 0 & 0 & 0 & 0 & 0 & 0 \\ * & * & 0 & 0 & 0 & 0 & 0 & 0 \\ 0 & 0 & * & * & 0 & 0 & 0 & * \\ 0 & 0 & * & * & 0 & 0 & * & 0 \\ \hline 0 & 0 & 0 & 0 & * & * & 0 & 0 \\ 0 & 0 & 0 & 0 & * & * & 0 & 0 \\ 0 & 0 & 0 & * & 0 & 0 & * & * \\ 0 & 0 & * & 0 & 0 & 0 & * & * \end{array}\right) = A_1\oplus A_1\oplus A_1\oplus\langle\alpha_2^*\rangle, \tag{2.99}$$

where the A_1 addends refer to the external nodes, while $\langle\alpha_2^*\rangle$ corresponds to the resolved central node.

With this knowledge, we can rewrite the Levi subalgebra (2.99) in a more explicit form:

$$\mathcal{L}_\Theta = \left(\begin{array}{cccc|cccc} d+k & b_1 & 0 & 0 & 0 & 0 & 0 & 0 \\ b_2 & d-k & 0 & 0 & 0 & 0 & 0 & 0 \\ 0 & 0 & f+c & b_3 & 0 & 0 & 0 & b_5 \\ 0 & 0 & b_4 & f-c & 0 & 0 & -b_5 & 0 \\ \hline 0 & 0 & 0 & 0 & -d-k & -b_2 & 0 & 0 \\ 0 & 0 & 0 & 0 & -b_1 & -d+k & 0 & 0 \\ 0 & 0 & 0 & b_6 & 0 & 0 & -f-c & -b_4 \\ 0 & 0 & -b_6 & 0 & 0 & 0 & -b_3 & -f+c \end{array}\right). \tag{2.100}$$

The advantage of such a generic decomposition is that it displays the Casimirs of the Levi subalgebra (2.99) in a manifest way. It is easy to show that indeed such Casimirs are:

$$\begin{aligned} c_1 &= k^2+b_1b_2 \\ c_3 &= c^2+b_3b_4 \\ c_4 &= f^2+b_5b_6 \\ c_2 &= d \end{aligned}, \tag{2.101}$$

and that they are related to the Casimirs of the full matrix $\mathcal{L}_\Theta$ by:

$$\begin{aligned} u_2 &= \mathrm{Tr}(\mathcal{L}_\Theta^2) = 4c_1+4c_2+4c_3+4c_4 \\ u_4 &= \mathrm{Tr}(\mathcal{L}_\Theta^4) = 4c_1^2+4c_2^2+4c_3^2+4c_4^2+24c_1c_4+24c_2c_3 \\ u_6 &= \mathrm{Tr}(\mathcal{L}_\Theta^6) = 4c_1^3+4c_2^3+4c_3^3+4c_4^3+60c_1^2c_4+60c_2^2c_3+60c_3^2c_2+60c_4^2c_1 \\ \tilde{u}_4 &= \mathrm{Pfaff}(\mathcal{L}_\Theta) = c_1c_2-c_1c_3-c_2c_4+c_3c_4 \end{aligned} \tag{2.102}$$

By diagonalizing the Levi subalgebra (for generic u_i) in the shape:

$$\mathcal{L}_\Theta^{\mathrm{diag}} = \left(\begin{array}{cccc|cccc} \xi_1 & 0 & 0 & 0 & 0 & 0 & 0 & 0 \\ 0 & \xi_2 & 0 & 0 & 0 & 0 & 0 & 0 \\ 0 & 0 & \xi_3 & 0 & 0 & 0 & 0 & 0 \\ 0 & 0 & 0 & \xi_4 & 0 & 0 & 0 & 0 \\ \hline 0 & 0 & 0 & 0 & -\xi_1 & 0 & 0 & 0 \\ 0 & 0 & 0 & 0 & 0 & -\xi_2 & 0 & 0 \\ 0 & 0 & 0 & 0 & 0 & 0 & -\xi_3 & 0 \\ 0 & 0 & 0 & 0 & 0 & 0 & 0 & -\xi_4 \end{array}\right), \tag{2.103}$$

it is immediate to exhibit the relationship between the Casimirs (2.101) and the $\mathcal{W}'$-invariant deformation parameters in the D_4 deformed family (1.24). In the case we are considering, namely the resolution of the central node, a choice of coordinates depending on the ξ_i that are invariant under the Weyl group $\mathcal{W}'$ generated by the external nodes is:

$$\begin{aligned} \sigma_1 &= \xi_1+\xi_2, \quad \sigma_2 = \xi_1\xi_2 \\ \tilde{\sigma}_1 &= \xi_3+\xi_4, \quad \tilde{\sigma}_2 = \xi_3\xi_4 \end{aligned} \tag{2.104}$$

We can then show that:

$$\begin{aligned} c_1 &= \frac{\sigma_1^2}{4}-\sigma_2 \\ c_3 &= \frac{\tilde{\sigma}_1^2}{4}-\tilde{\sigma}_2 \\ c_4 &= \frac{\tilde{\sigma}_1^2}{4} \\ c_2 &= \frac{\sigma_1}{2} \end{aligned}, \tag{2.105}$$

thus completing the bridge between the Springer resolution and the theory of deformed singularities in the D_4 case.

2.3.3 Remark: constructing ADE families admitting arbitrary partial simultaneous resolutions

In the few examples we have presented in the preceding sections, we have considered versal deformations of ADE singularities, defined as the intersection of the Slodowy slice through the subregular nilpotent orbit with the fibers of the adjoint quotient map:

$$\text{versal deformation of ADE}: \qquad \mathcal{S}_{\text{subreg}} \cap \chi^{-1}(u), \tag{2.106}$$

where the $u = (u_1, \ldots, u_n)$ parametrize $\mathcal{T}/\mathcal{W}$.

We have recalled that if we wish to construct a family admitting some partial resolution dictated by the Weyl subgroup $\mathcal{W}'$, we have to consider the flags preserved by the Slodowy slice in correspondence with some parabolic subalgebra, predicted by $\mathcal{W}'$. Parabolic subalgebras are, in turn, in one to one correspondence with Levi subalgebras. This amounts to changing coordinates from $\mathcal{T}/\mathcal{W}$ to $\mathcal{T}/\mathcal{W}'$. Generically, the Levi subalgebra will be the sum of simple addends $\mathcal{L}_h$ and of generators $\mathcal{H}$ in the Cartan subalgebra:

$$\mathcal{L} = \bigoplus_h \mathcal{L}_h \oplus \mathcal{H}. \tag{2.107}$$

The key point of our analysis is that the Springer resolution automatically provides the change of coordinates from $\mathcal{T}/\mathcal{W}$ to $\mathcal{T}/\mathcal{W}'$: we have shown that computing the Casimirs of the Slodowy slice relative to the simple and Cartan addends of the Levi subalgebra (2.107) corresponding to the Springer resolution *automatically* furnishes coordinates adapted to $\mathcal{T}/\mathcal{W}'$.

This turns out to be particularly useful for the case of the exceptional singularities, in which explicitly building families corresponding to a given partial resolution $\mathcal{T}/\mathcal{W}'$, e.g. employing the tools of [111], can be a rather cumbersome and time-consuming computation. We show how this works in Appendix B.

CHAPTER 3

M-theory geometric engineering

In the course of this chapter we finally reap the physical implications of the mathematical tools that have been introduced in Chapter 1 and 2.

The arena for our considerations is constituted by M-theory placed on top of Calabi-Yau threefolds, built from one-parameter families of deformed ADE singularities, of the form (1.23). Before dealing with the analysis of such intricate cases, we adopt a gradual perspective and proceed through a step by step approach:

- First, in Section 3.1 we quickly describe the theories arising from the compactification of M-theory on a *smooth* Calabi-Yau threefold. This will allow us to motivate the need for *singular* Calabi-Yau's in order to obtain interesting physical phenomena.

- Then, in Section 3.2 we proceed in briefly reviewing how to characterize M-theory on top of singular K3 surfaces, that can be described locally by the ADE singularities (1.2), producing seven-dimensional gauge theories, extracting the corresponding IIA description in terms of stacks of D6-branes and $O6^-$-planes, whenever possible.

- Finally, in Section 3.3 we fiber the K3 surfaces over a complex line in a non-trivial fashion, yielding the one-parameter deformed ADE families (Calabi-Yau threefolds) that are the backbone of our M-theory constructions. Making use of the M-theory/Type IIA duality, we flesh out the details of the corresponding D6-brane at angles and $O6^-$-plane system (whenever possible) in terms of a Higgs field valued in the adjoint of the gauge group, highlighting the role of Slodowy slices and Springer resolutions. Of chief interest for our discussions will be the five-dimensional theories that arise from the modes localized at the intersections of the D6-branes.
  In later chapters we will systematically draw the consequences of these M-theory setups, in particular computing the Gopakumar-Vafa invariants of the examined CY threefolds, and studying the Higgs branches of the 5d theories arising from M-theory geometric engineering.

3.1 M-theory on smooth CY threefolds

As a baby step towards the analysis of 5d theories geometrically engineered by M-theory on deformed ADE singularities, let us start from the simpler setup of M-theory on top of a *smooth* Calabi-Yau threefold, that has been examined in detail shortly after the very discovery of M-theory [120].

At low energies, M-theory is described by 11-dimensional supergravity, which is only made up of the supergravity multiplet, with bosonic components:

$$\begin{array}{ll} g_{MN} & \text{graviton} \\ C_{MNR} \equiv C_3 & \text{3-form gauge field} \end{array} \quad \text{with: M,N,R} = 1,\ldots,11 \; . \tag{3.1}$$

The three-form gauge field is related to a four-form field strength G_4 by $G_4 = dC_3$, and satisfies the equations of motion:

$$d{*}G_4 = \frac{1}{2} G_4 \wedge G_4. \tag{3.2}$$

We can now consider the compactification of 11d supergravity on a generic smooth *compact* manifold M_6 (large compared to the Planck scale) characterized by the Hodge numbers $h^{1,1}$ and $h^{2,1}$.

Using Kaluza-Klein reduction on the metric and the three-form gauge field it can be shown [120] that the effective theory in five dimensions is a $\mathcal{N} = 1$ theory made up of a supergravity multiplet, $h^{1,1}-1$ abelian gauge fields, as well as $h^{2,1}+1$ hypermultiplets uncharged under the abelian gauge fields. We briefly recall that in five dimensions the (bosonic component of the) $\mathcal{N} = 1$ vector multiplet is made of a real scalar and a spin-1 field, while the hypermultiplets contain a doublet of complex scalars (charged under the R-symmetry).

Introducing the index $\mu = 1, \ldots, 5$ and the vielbein index a the field content of 11d supergravity dimensionally reduced to 5d can be summed up as follows (omitting the fermionic fields):

$$\begin{array}{lll} \text{Supergravity multiplet:} & (A_\mu, e^a_\mu) & \\ h^{1,1}-1 \text{ vector multiplets:} & (\phi^A, A^A_\mu) & A = 1, \ldots, h^{1,1}-1 \\ h^{2,1}+1 \text{ hypermultiplets:} & (\phi^m) & m = 1, \ldots, 2(h^{2,1}+1) \end{array} \tag{3.3}$$

The resulting $\mathcal{N} = 1$ theory in five dimensions is rather uninteresting from a physical point of view: it features a bunch of abelian gauge fields A^A_μ, along with some uncharged complex scalar fields ϕ^m. On the other hand the Standard Model and, more generally, more compelling quantum field theories, feature non-abelian gauge fields, as well as charged light particles. The absence of these selling points in the context of M-theory compactified on a smooth threefold requires a change of setting, and motivates taking into account singular manifolds.

3.2 M-theory on singular K3 surfaces

In this paragraph we start introducing singular manifolds into the game of M-theory compactifications: we consider placing M-theory on top of a K3 surface with isolated point-like ADE singularities, and examine the 7d low-energy description of this theory by means of the duality with Type IIA. To this end, we follow the pedagogical expositions of [121, 122].

The most relevant novelties of this setup originate near the singularity, where we will see that new degrees of freedom, related to non-abelian gauge symmetries, arise [123, 124]. As a consequence, for our purposes we can focus on a local patch near the singularity of the K3 surface. This can be achieved by taking an infinite volume limit, such that gravity gets decoupled from the theory: this means that we are considering a non-compact K3 surface, and that we can concentrate exclusively on the gauge symmetry sector appearing at the singularity.

One of the main tools used to analyze M-theory on local K3 surfaces displaying ADE singularities is the M-theory/Type IIA duality, that we briefly review in the next section. For the sake of clarity, we focus on singularities from the A series, although the discussion can be generalized to encompass also the D cases.

3.2.1 M-theory/Type IIA duality

As is known since the pioneering work of [2], the non-perturbative limit of Type IIA string theory is given by M-theory, that at low-energies is well approximated by 11d supergravity. In particular, M-theory compactified on a circle is dual to Type IIA, where the size of the circle regulates the string coupling g_s. We can summarize this correspondence with the following diagram:

$$\begin{array}{ccc} \text{M-theory} & \xrightarrow{\text{low-energy limit}} & \text{11d SUGRA} \\ \Big\downarrow{\scriptstyle \text{small } g_s} & & \Big\downarrow{\scriptstyle \text{KK reduction on } S^1} \\ \text{Type IIA} & \xrightarrow{\text{low-energy limit}} & \text{10d SUGRA} \end{array}$$

In order to see the relationship between M-theory and Type IIA explicitly, we can write the 11d metric as follows:

$$ds_{11}^2 = e^{-2\varphi/3} ds_{10}^2 + e^{4\varphi/3}\left(dx^{11} + C_M dx^M\right)^2 , \tag{3.4}$$

where x^{11} is the direction along the circle. If the S^1 is fibered over the 10d spacetime one has a non-trivial connection C_M. $e^{\frac{4\varphi}{3}}$ is the size of the S^1. In the dual language, φ is the dilaton field, and C_M is the Type IIA 1-form with 10-dimensional index $M = 1, \dots, 10$.

Furthermore, we see that any object that satisfies the Type IIA equations of motion involving the dilaton, the Type IIA 1-form and the 10d metric must uplift in M-theory to pure geometry, as they all appear in the 11d SUGRA metric (3.4).

This is precisely the case for D6-branes[1]: they are a solution of the 10d e.o.m. and act as

[1] As well as for O6-planes, though for the moment we will not be concerned with them.

a source for the dilaton, the 1-form and the metric. Consequently, a flat D6-brane embedded in Type IIA with flat 10d spacetime uplifts in M-theory to a pure geometric background, given by the direct product of flat 7d spacetime and a *Taub-NUT* space [125]:

$$\begin{aligned} ds^2_{11} &= \underbrace{ds^2_{\mathbb{R}^{6,1}}}_{\text{flat space}} + \underbrace{H d\vec{r}^2 + H^{-1}\left(dx^{11} + \vec{j}\cdot d\vec{r}\right)^2}_{\text{Taub-NUT}} \\ \text{with:} \quad \nabla\times\vec{j} &= -\nabla H, \qquad e^{\varphi} = H^{-3/4}, \qquad H = 1 + \frac{1}{2}\frac{R}{|\vec{r}|}, \qquad R = g_s\sqrt{\alpha'}. \end{aligned} \tag{3.5}$$

The point $\vec{r} = (r_1, r_2, r_3) = 0$ is the *center* of the Taub-NUT space, and corresponds in Type IIA to the location of the D6-brane in the three directions transverse to its worldvolume.

The Taub-NUT space is a non-compact 2 complex-dimensional space endowed with $SU(2)$ holonomy, implying that it is also hyper-Kähler. Indeed, $\vec{j} = (j_1, j_2, j_3)$ appearing in (3.5) is the vector of the three Kähler forms of the Taub-NUT. Moreover, the Taub-NUT can be described as a $\mathbb{C}^*$-*fibration*, the fiber being parametrized by r_3 along with the circle described by x^{11}, that naturally defines a S^1-fibration over $\mathbb{R}^3$, spanned by $\vec{r} = (r_1, r_2, r_3)$ with the S^1 fiber shrinking to zero size precisely on $\vec{r} = 0$: this signals the presence of a defect, namely the D6-brane. Furthermore, the Taub-NUT space is smooth, provided that x^{11} has periodicity $2\pi R$ (with R a constant), which equals the statement that it is the coordinate parametrizing the S^1-fiber. The fact that the Taub-NUT is a S^1-fibration is the key observation allowing us to pass from M-theory to type IIA, as the S^1 plays the role of the M-theory circle of (3.4). From the physical standpoint, the size of the S^1 regulates the string coupling g_s.

More generally, a setup of $n+1$ parallel and non-coincident D6-branes uplifts in M-theory to a purely geometric background, described by a *multi-center Taub-NUT* space [126, 127]:

$$\begin{aligned} ds^2_{11} &= \underbrace{ds^2_{\mathbb{R}^{6,1}}}_{\text{flat space}} + \underbrace{H d\vec{r}^2 + H^{-1}\left(dx^{11} + \vec{j}\cdot d\vec{r}\right)^2}_{\text{multi-center Taub-NUT}} \\ \text{with:} \quad \nabla\times\vec{j} &= -\nabla H \qquad e^{\varphi} = H^{-3/4} \qquad H = 1 + \frac{1}{2}\sum_{i=1}^{n+1}\frac{R}{|\vec{r}-\vec{r}_i|} \qquad R = g_s\sqrt{\alpha'}. \end{aligned} \tag{3.6}$$

The multi-center Taub-NUT retains the properties of its single-center cousin: it is a smooth 2 complex-dimensional hyper-Kähler space with $SU(2)$ holonomy, that can be described as a S^1-fibration over $\mathbb{R}^3$. The S^1-fiber degenerates on the $n+1$ points $\vec{r} = \vec{r}_i$ (also called centers), that pinpoint the D6-brane locations.

From the homological point of view, the multi-center Taub-NUT admits n non-trivial compact 2-cycles $\alpha_i, i = 1, \dots n$, as can be seen in the following way: consider a path along the $\mathbb{R}^3$ base connecting two of the centers, say $\vec{r}_i$ and $\vec{r}_j$, $i \neq j$. The S^1-fiber on the extreme points of the path has zero size, whereas it acquires a non-vanishing radius in the interior of the path: we see then that the path in the base times the fiber is topologically equivalent to a 2-sphere. In this fashion, one can build $\frac{n(n+1)}{2}$ spheres, of which only n are inequivalent.

Furthermore, these 2-spheres can be chosen in such a way as to intersect in the shape of the A_n Dynkin diagram, with the nodes of the Dynkin diagram corresponding to the spheres, and the connecting lines to the intersection points.

Consider now collapsing the centers $\vec{r}_i$ on the same value $\vec{r}$: the resulting space is not smooth anymore, but develops a A_n singularity. The way to see this is that the coordinate x^{11}, to retain its $2\pi R$ periodicity after the collapse of the centers, must be modded by $\mathbb{Z}_{n+1}$, precisely in the same way as $\mathbb{C}^2/\mathbb{Z}_{n+1}$ produces a A_n singularity, thanks to the McKay correspondence reviewed in Chapter 1. On the Type IIA side, this equals superimposing the D6-branes on top of each other. In the next section, we will see that this gives rise to a $U(n+1)$ gauge group generated by the stack of branes. This also elucidates the correspondence between M-theory on A_n singularities and the resulting effective theory, that exhibits precisely a non-abelian $SU(n+1)$ gauge group.

In this picture, *resolving* the singularity means moving the centers of the Taub-NUT along the same direction r_3 in the $\mathbb{C}^*$-fiber: this produces a set of n 2-spheres, arranged as the A_n Dynkin diagram, entirely contained in the $\mathbb{C}^*$-fiber. If all the points $\vec{r}_i$ are collinear, this can be obtained by fixing the hyper-Kähler metric, and using the $SO(3)$ rotating the three Kähler forms to choose a complex structure such that all the centers are along r_3. Moreover, we see that these spheres have zero holomorphic volume (because the non-vanishing holmorphic 2-form Ω, of Hodge type $(1,1)$, has only one leg along the fiber). On the other hand, if all the points $\vec{r}_i$ are on a plane, we can tune the complex structure in a way that separates the centers along the plane $\mathbb{R}^2$ spanned by (r_1, r_2) producing the *deformation* of the A_n singularity; this generates n 2-spheres with one leg along $\mathbb{R}^2$ and one leg along the $\mathbb{C}^*$-fiber, with non-vanishing holomorphic volume. Resolution and deformation of the A_n singularities have a direct counterpart in Type IIA, that we examine in the next section.

3.2.2 M-theory on ADE singularities

Our aim is to review the physics of M-theory compactified on local K3 surfaces displaying the ADE singularities classified in (1.2). In the preceding section, we have established a correspondence between M-theory on a $n+1$-center Taub-NUT space and Type IIA with $n+1$ parallel non-coincident D6-branes. When the centers of the Taub-NUT collapse on the same point, a A_n singularity arises, corresponding in Type IIA to the D6-branes moving on top of each other. We would like to extract the physical content of these setups.

As was mentioned above, the Taub-NUT space features n non-trivial compact 2-cycles, that give rise to n normalizable harmonic 2-forms $\omega_i, i = 1, \dots, n$, via Poincaré duality. In addition, the Taub-NUT sports an additional normalizable harmonic 2-form ω_0. The Taub-NUT is a ALF space, that in the limit $R \to \infty$ becomes asymptotic at infinity to the ALE space described by the $\mathbb{C}^2/\mathbb{Z}_{n+1}$ singularity [128].

Consider now the smooth phase, in which all the centers are separated. As we are working in a low-energy regime where gravity is decoupled, thanks to the fact that the singular K3 surface is non-compact, the only perturbative objects we have to consider are modes coming from the M-theory 3-form C_3, the Kähler form J and the holomorphic 2-form Ω along the normalizable 2-forms ω_i. We can thus dimensionally reduce C_3 on the 2-forms $\omega_i, i = 0, \dots n$:

$$C_3 = \sum_{i=0}^{n} A_i \wedge \omega_i, \tag{3.7}$$

where A_i are $U(1)$ gauge bosons depending only on the coordinates of the $\mathbb{R}^{6,1}$ orthogonal to the Taub-NUT. Thus, reducing C_3 on the Taub-NUT space yields $n+1$ $U(1)$ massless gauge fields in 7d. On the type IIA side, which is made up of $n+1$ D6-branes lying on $\mathbb{R}^{6,1}$ and located on the centers $\vec{r}_i$ in the transverse directions, the A_i correspond to the worldvolume $U(1)$'s of D6-branes. A combination of these $U(1)$'s can be taken as the center of mass $U(1)$ of the D6-brane system. From a group-theoretic perspective, the n $U(1)$ gauge fields with non-trivial action are turned on along the Cartan generators of the A_n algebra, whereas A_0 corresponds to the center of mass $U(1)$. The reduction of Kähler and the holomorphic 2-forms gives, respectively, real scalars ξ_i and complex scalars ζ_i, that are geometric moduli controlling the volume of the 2-spheres, and that end up with the A_i in the 7d vector multiplets.

On the non-perturbative side, we must also take into account the presence of M2-branes in the M-theory description. In the Taub-NUT space with generic $\vec{r}_i$, the M2-branes can wrap the corresponding 2-spheres: it can be proven [129] that the resulting particles in the 7d theory on $\mathbb{R}^{6,1}$ have the correct quantum numbers to be massive vector bosons, the mass being proportional to the volume of the 2-spheres. Recalling that the intersection pattern of the 2-spheres is dictated by the A_n Dynkin diagram, we see that the M2-branes can wrap all the 2-cycles α_i, or combinations thereof, that are 2-spheres filling all the entries in the A_n root system[2]. M2-branes wrapping the 2-spheres with opposite orientation encode opposite roots in the root system. Such M2-branes are of course charged under C_3, and as a consequence the massive vectors are also charged under the $U(1)^{n+1}$ generators, in the right way to correspond to the leftover A_n-algebra generators, as we now explain.

The charges with respect to the Cartan generators can be explicitly computed as the integral of the Poincaré dual 2-form ω_i corresponding to the Cartan generator over the 2-cycle wrapped by the M2-brane (say β_j, with $\beta_j \in \Delta$, the root system of A_n):

$$q_{ij} = \int_{\beta_j} \omega_i = \int_{\text{Taub-NUT}} \alpha_i \cdot \beta_j. \tag{3.8}$$

If we restrict the charge computation to the cycles dual to simple roots we find:

$$q_{ij} = \int_{\alpha_j} \omega_i = \int_{\text{Taub-NUT}} \alpha_i \cdot \alpha_j = -A_{ij}, \tag{3.9}$$

which is the Cartan matrix of the A_n Lie algebra, that encodes the weights of the adjoint

[2]This happens because the α_i are 2-spheres, and a combination $\alpha_i + \alpha_j$ is a 2-sphere in the K3 if $\alpha_i + \alpha_j$ is a root of A_n.

representation of A_n. We see then that the charges of the states arising from M2-branes wrapping the exceptional $\mathbb{P}^1$'s correspond to weight vectors in the adjoint representation, and thus are compatible with the structure of the A_n Lie algebra. The fact that M2-branes with opposite orientations play the role of opposite roots is a consequence of the fact that they possess opposite weight vectors.

The Cartan generators obtained from the reduction of C_3 and the M2-brane states, that correspond to the root system of A_n, fill the adjoint representation of the A_n Lie algebra:

$$\dim(A_n) = \underbrace{\overbrace{n}^{C_3 \text{ reduction}}}_{\text{Cartan}} + \underbrace{\overbrace{|\Delta|}^{\text{M2-brane states}}}_{\text{roots}} \quad . \tag{3.10}$$

In the 7d $\mathcal{N} = 1$ effective theory arising from M-theory on the Taub-NUT space, if we focus on a local patch containing its centers, we find a set of n massless vector fields A_i corresponding to the Cartan generators, as well as $|\Delta|$ massive W-bosons arising from the M2-brane states. The fact that they are massive is a consequence of the non-zero volume of the wrapped 2-spheres in the multi-center Taub-NUT.

In the *singular limit*, in which the volumes of the 2-spheres shrink to zero, the W-bosons become massless and the gauge group in 7d enhances to the full non-abelian $SU(n+1)$. This is precisely what is observed in Type IIA, as we are now going to review.

3.2.3 The Type IIA perspective and the M-theory uplift

Let us now examine the physics from the Type IIA perspective.

The generators arising from the reduction of C_3 descend to strings with both ends on the same D6-brane, while the M2-branes wrapped on the 2-spheres in the Taub-NUT geometry descend, by compactification on the M-theory circle, to strings stretching between different D6-branes as in Figure 3.1.

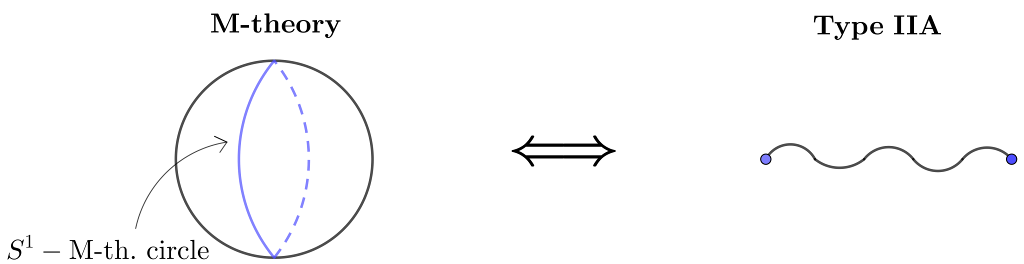

Figure 3.1: *M2-branes wrapped on the M-theory circle descend to strings in Type IIA. The end-points of the strings are points in M-theory where the S^1-fiber collapses.*

The first are massless, whereas the latter possess a mass which is proportional to the distance between the D6-branes.

In Type IIA, the singular limit is taken by coalescing the $n+1$ D6-branes located on the points $\vec{r}_i$ into a single stack. Here, the W-bosons given by strings stretching between branes become massless, and the full $SU(n+1)$ symmetry is realized[3].
Pictorially, we can represent the singular limit as in Figure 3.2.

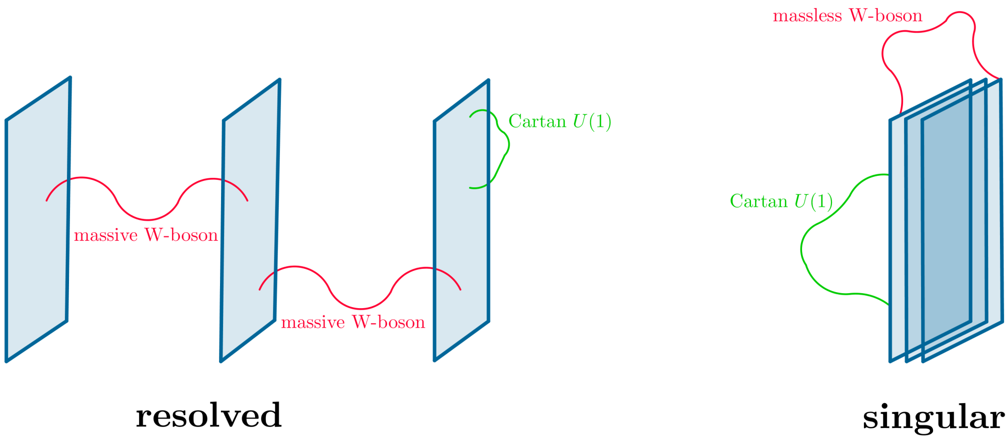

Figure 3.2: *D6-brane configuration in type IIA: resolved and singular phases.*

In this setting the movement of the D6-brane stack in the directions $\vec{r} = (r_1, r_2, r_3)$ transverse to its worldvolume are parameterized by three real scalars in the adjoint representation ϕ_i, with $i = 1, 2, 3$, which are the lowest components of the vector multiplets related to the D6-branes. Picking an appropriate choice of complex structure, we can conjure up two of these real scalars into a single adjoint-valued complex scalar field:

$$\Phi = \phi_1 + i\phi_2. \tag{3.11}$$

Φ parameterizes the configuration of the D6-branes along a complex direction, say z. Pictorially, we have:

	$\mathbb{R}^{6,1}$	$\mathbb{C}_z$	ϕ_3
D6	$\times$	$\cdot$	$\cdot$

Table 3.1: *IIA setup dual to M-th. on* $\mathbb{R}^{6,1} \times ADE$.

Switching on a diagonal and constant vev for Φ and ϕ_3 separates the branes along the

[3]More precisely, this would yield a $U(n+1)$ gauge group, although the overall center of mass $U(1)$ can always be decoupled, leaving only $SU(n+1)$.

transverse directions, Higgsing the group $U(n+1)$ to $U(1)^{n+1}$:

$$\Phi = \begin{pmatrix} v_1 & & & \\ & v_2 & & \\ & & \ddots & \\ & & & v_{n+1} \end{pmatrix}, \quad \phi_3 = \begin{pmatrix} \tilde{v}_1 & & & \\ & \tilde{v}_2 & & \\ & & \ddots & \\ & & & \tilde{v}_{n+1} \end{pmatrix} : \quad U(n+1) \to U(1)^{n+1}, \tag{3.12}$$

where the $v_i \in \mathbb{C}$ and $\tilde{v}_i \in \mathbb{R}$ are constants. This process has a direct counterpart in the multi-center Taub-NUT geometry we have previously examined: switching on a constant vev for Φ equals separating the centers along a plane $\mathbb{R}^2$ that does not contain the $\mathbb{C}^*$-fiber, spanned by r_3 and the S^1, thus corresponding to a deformation of the A_n singularity. Conversely, a constant vev for ϕ_3, which is a real scalar, translates into separating the centers along the real line parametrized by r_3, contained in the $\mathbb{C}^*$-fiber, resolving the singularity.

The brane locus Δ along the z direction can be computed as the zero locus of the characteristic polynomial of Φ, namely $\Delta(z) = 0$, with:

$$\Delta(z) = (z - v_1) \cdot \ldots \cdot (z - v_{n+1}), \tag{3.13}$$

that clearly shows the separation of the branes along z. In the case of A_n singularities, the M-theory uplift of the D6-brane locus (3.13) can be understood highlighting the structure of the deformed A family as a $\mathbb{C}^*$-fibration. Let us immediately clarify this statement, considering the A_1 singularity. Its defining equation reads:

$$x^2 + y^2 = z^2. \tag{3.14}$$

M-theory reduced on (3.14) gives a 7d $\mathcal{N} = 1$ theory with gauge group $SU(2)$. Let us now make the connection between M-theory and type IIA manifest. Making the change of coordinates $x = u + iv$, $y = u - iv$, we get:

$$uv = z^2. \tag{3.15}$$

The above equation admits various $\mathbb{C}^* \cong S^1 \times \mathbb{R}$ actions. For our purposes, we choose the one that acts only on the u and v coordinates, namely:

$$\mathbb{C}^*\text{-action}: \quad (u, v, z) \to (\lambda u, \lambda^{-1} v, z). \tag{3.16}$$

We see then that (3.15) can be interpreted as $\mathbb{C}^*$-fibration[4]. The S^1 inside the $\mathbb{C}^*$ plays the role of the M-theory circle.

By the M-theory/Type IIA duality, the locus where the $\mathbb{C}^*$-fiber degenerates, that is when $uv = 0$, is precisely the D6-brane locus:

$$\Delta = z^2. \tag{3.17}$$

[4]Indeed, fixing z and considering the equation $uv = \text{const}$ precisely highlights the $\mathbb{C}^*$-fiber.

Notice that we could write the A_1 singularity (3.14) as:

$$uv = \det(z\mathbb{1} - \Phi), \tag{3.18}$$

where in this case Φ is trivial because the D6-branes are coincident (namely, Φ is the 2×2 null matrix). Turning on a non-trivial diagonal constant vev for Φ we would get:

$$\Delta(z) = (z - v)(z + v), \tag{3.19}$$

that ends up in M-theory as:

$$uv = z^2 - v^2 = z^2 + k, \tag{3.20}$$

where we have renamed $k \equiv -v^2$, as v is just a constant. Notice that (3.20) is non-singular, which is expected as by turning on a vev we are separating the branes, deforming the A_1 singularity.

Summing up the well-known results of this section, we have briefly reviewed how M-theory placed on top of a K3 surface locally modeled by an ADE singularity gives rise to a 7d $\mathcal{N} = 1$ theory with gauge group given by the singularity on the K3[5].

In the next section, we focus on M-theory compactified on Calabi-Yau threefolds of a special kind, namely built as one-parameter deformations of the ADE singularities we have considered up to now.

3.3 M-theory on deformed ADE singularities

In the course of this section, we lay down the basic construction that constitutes the core of the present work. The arena hosting our reasoning is M-theory compactified on a Calabi-Yau threefold displaying an isolated singularity, and giving rise to an effective theory in five spacetime dimensions. We focus on a specific class of Calabi-Yau threefolds: we pick the deformed ADE singularities reviewed in (1.23), and choose a dependence of the deformation parameters on a single complex variable w, in such a way that the resulting hypersurface is singular at a point. Let us make the simplest of examples, writing down the equation of the conifold. It is a deformation of the A_1 singularity lying in $\mathbb{C}^4$, where the deformation parameters (1.24) have been chosen as $t_1 = -t_2 = w$:

$$\text{Conifold:} \quad \underbrace{x^2 + y^2 + z^2}_{A_1 \text{ sing}} = \underbrace{w^2}_{\text{def}} \quad \subset \mathbb{C}^4. \tag{3.21}$$

Notice that for fixed w we obtain a deformed non-singular A_1 singularity. This can be straightforwardly generalized to all the other classes of deformed ADE singularities, and hence we see that our compactification spaces can be interpreted as one-parameter families of deformed ADE singularities, the parameter being w. These kinds of singular spaces are

[5]We have shown this explicitly in the A case, although the result holds also for the D and E series.

isolated hypersurface singularities (IHS), i.e. they are expressed by a hypersurface equation in some complex ambient space (in our case, $\mathbb{C}^4$), and possess a point-like singularity, that can be conventionally put at the origin of the ambient space. IHS have been investigated from multiple angles in the recent physical literature, focusing on M-theory and Type IIB compactifications and studying the resulting lower-dimensional effective theories in 5d and 4d (see e.g. [58–61, 130, 131] for a few recent examples). We stress that, although one-parameter families of deformed ADE singularities constitute only a tiny subset of all possible IHS, they display a wide range of phenomena of both physical and mathematical interest.

It is widely believed [58] that M-theory placed on top of a singular one-parameter family of ADE singularities gives rise to a $\mathcal{N} = 1$ five-dimensional superconformal field theory (SCFT). The field theoretic data of the 5d SCFTs is by construction related to the geometrical properties of the compactification space that originates them. As a result, if one finds a way to study the physical content of the five-dimensional theories, non-trivial information about the threefold singularity can be retrieved, furnishing a physical counterpart to mathematical features of interest in their own terms. For our intents, we will see how 5d SCFTs arising from deformed ADE singularities encode in a natural fashion the so-called Gopakumar-Vafa (GV) invariants of the compactification threefolds. In the remainder of this work we focus on the context:

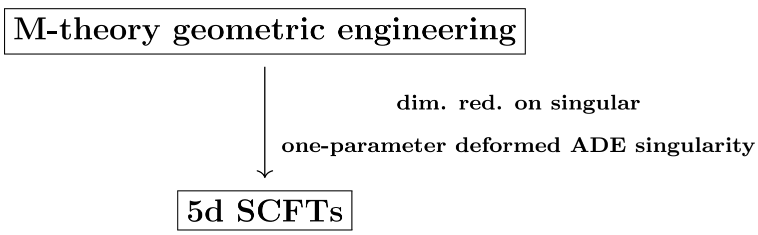

Figure 3.3: *Schematic context of the work.*

We aim at accomplishing two interconnected objectives:

1. Give a physics-grounded method to classify Gopakumar-Vafa invariants of non-compact Calabi-Yau threefolds with isolated singularities, built as one-parameter families of ADE singularities.

2. Study 5d SCFTs (in particular, extract their Higgs branch) arising from M-theory engineered on one-parameter families of deformed ADE singularities, exhibiting an isolated singularity.

In this respect, the main tool that will allow us to deal with problems 1 and 2 is the fact that we will be able to associate to every one-parameter deformed ADE singularity a Higgs field background valued in the adjoint of the corresponding Lie algebra, that completely encodes the physics that we are interested in.

Before dealing with the details of the mathematical definition of GV invariants and the features of 5d SCFTs, to which we will come in the following chapters, we devote the rest of this chapter to fleshing out the common method that will allow us to tackle the two aforementioned key problems, seeing how the techniques based on Slodowy slices and on the Springer resolution outlined in Chapter 2 furnish a guiding principle in constructing explicit Higgs backgrounds. In the following sections we tackle this task in an ordered fashion, going through the A, D, E cases separately, and summing up our results at the end of the chapter.

3.4 M-theory on deformed A_n singularities

In Section 3.2, we have reviewed how M-theory placed on top of ADE singularities gives rise to a $\mathcal{N} = 1$ theory in 7d with gauge group corresponding to the ADE type. In this and the subsequent sections, we go further and show how to describe a setup arising from M-theory on one-parameter deformed ADE singularities, as defined at the beginning of Section 3.3. We tackle this task both in the deformed A_n and D_n singularities, that admit a low-energy description in type IIA in terms of D6-branes and O6$^-$-planes, and in the deformed E_6, E_7, E_8 cases, that are intrinsically non-perturbative and admit no brane counterpart in Type IIA. Let us start from the most accessible cases, namely the deformed A_n singularities.

3.4.1 M-theory on deformed A_n singularities: the type IIA setup

Consider the D6-brane setup described in Section 3.2.3. There, we have reviewed how turning on a constant vev for the scalars describing motion transverse to the D6-brane stack separates the branes and Higgses the 7d gauge group.

A completely different dynamics can instead be produced if the Higgs scalars Φ and ϕ_3 acquire a vev that varies along the brane world-volume. To fix ideas, suppose that we turn on a dependence of the vevs on a complex parameter w, that spans two real directions along the brane worldvolume. In such a case, the vev $\Phi(w)$ separates the branes putting them at angles, and intersections among different branes can arise, depending on the specific tuning of the vev. We can rewrite (3.13) as:

$$\Delta(z, w) = (z - v_1(w)) \cdot \ldots \cdot (z - v_{n+1}(w)). \tag{3.22}$$

The D6-branes now fill a common flat $\mathbb{R}^{4,1}$ spacetime, and can intersect in the extra dimensions:

	$\mathbb{R}^{4,1}$	$\mathbb{C}_w \vert \mathbb{C}_z$	$\mathbb{R}$
D6	$\times$	2 $\dim_{\mathbb{R}}$	$\cdot$

Table 3.2: *IIA setup with D6-branes at angles.*

Let us see how this works in a simple example involving the A_1 singularity. We consider turning on a vev $\Phi(w)$ that depends on a complex coordinate w on the D6-brane worldvolume.

Let us switch on the simplest of such vevs:

$$\Phi(w) = \begin{pmatrix} w & 0 \\ 0 & -w \end{pmatrix}. \tag{3.23}$$

The brane locus gets modified and becomes:

$$\Delta(z, w) = (z-w)(z+w). \tag{3.24}$$

This is a type IIA statement. Its M-theory counterpart can be understood recalling, from Section 3.2.3, that the M-theory geometry in the A_n cases is a $\mathbb{C}^*$-fibration, with the D6-brane location dictating its degeneracy locus.

Turning on brane worldvolume-dependent vevs we are modifying the compactification space of M-theory, which is no more merely a A_n singularity. More precisely, a non-trivial $\Phi(w)$ *deforms* the A_n singularity and produces a threefold, adding terms dependent on the parameter w. Uplifting the brane locus to M-theory, we obtain:

$$uv = (z-w)(z+w) = z^2 - w^2, \tag{3.25}$$

that is singular at $(u, v, z, w) = (0, 0, 0, 0)$, because now no invertible redefinition of w is possible. Going back to the variables x and y it is immediate to see that (3.25) is precisely the equation of the conifold.

This is the key point that builds a bridge between M-theory and type IIA:

M-theory placed on top of a one-parameter deformed A_n singularity descends to a setup of D6-branes at angles in Type IIA: the M-theory geometry is a $\mathbb{C}^*$-fibration that degenerates above the D6-brane locus $\Delta = 0$. Explicitly, the relation is given by:

$$\boxed{\text{IIA brane locus:} \quad \Delta(z, w) = 0} \quad \longleftrightarrow \quad \boxed{\text{M-th. geometry:} \quad uv = \Delta(z, w) = \det(z\mathbb{1} - \Phi(w))}, \tag{3.26}$$

where the $\mathbb{C}^*$-action leaves z and w unaffected:

$$\mathbb{C}^*\text{-action}: \quad (u, v, z, w) \to (\lambda u, \lambda^{-1} v, z, w). \tag{3.27}$$

In addition, notice that the M-theory geometry in (3.26) depends on the Casimirs of the Higgs background $\Phi(w)$, via its characteristic polynomial. We pick the following canonical choices of the Casimirs of a Higgs background $\Phi(w)$ living in the A_n algebra:

$\boldsymbol{A_n}$
$k_i = \mathrm{Tr}(\Phi^{i+1}), \quad i = 1, \dots, n$

(3.28)

Relation (3.26) allows us to rewrite M-theory on a one-parameter family of deformed ADE singularities in terms of the Higgsing of a $\mathcal{N} = 1$ supersymmetric 7d gauge theory. As we will see, this statement can also be extended to the D series (admitting a Type IIA dual) and to the E_6, E_7, E_8 cases, that have no Type IIA counterpart.

3.4.2 Higgs vs geometry: T-branes

In the example of the previous section we have seen how the conifold, which is a deformation of a A_1 singularity, arises as the M-theory uplift of a D6-brane configuration with brane locus $\Delta = z^2 - w^2$, that can be encoded by a Higgs field $\Phi(w)$ dependent on the brane-worldvolume coordinates. There is, however, a subtlety that will prove crucial in more involved examples. Notice that in equation (3.26) the characteristic polynomial of $\Phi(w)$, which is a matrix in the adjoint of A_n, appears on the right hand side. It is a known mathematical fact, though, that the characteristic polynomial of a matrix does not completely fix the entries of the matrix. For example, in the conifold we could have chosen the following Higgs $\Phi(w)$, different from (3.23), but that possesses the same characteristic polynomial:

$$\Phi(w) = \begin{pmatrix} 0 & 1 \\ w^2 & 0 \end{pmatrix}. \tag{3.29}$$

It is therefore clear that both (3.23) and (3.29), despite being different (although, in this simple case, we could simply diagonalize (3.29) and put it into the form (3.23)), give rise to the same M-theory geometry. Let us clarify what we precisely mean by "different": when we switch on a vev $\Phi(w)$, the $SU(2)$ stack of branes[6] gets deformed into two branes, located along the loci $z - w = 0$ and $z + w = 0$. This breaks the 7d gauge group into the stabilizer of the Higgs vev $\Phi(w)$:

$$\text{7d gauge group } G \quad \xrightarrow{\text{turn on } \Phi(w)} \quad G \cdot \Phi(w) \cdot G^{-1} = \Phi(w). \tag{3.30}$$

Notice that for $w \neq 0$ (3.23) breaks $G = SU(2)$ to $U(1)$, and that instead (3.29), as w varies over the base of the fibration, completely breaks $G = SU(2)$. Moreover, on top of $w = 0$ (3.23) preserves the whole $SU(2)$, whereas (3.29), thanks to its constant entry, breaks all the $SU(2)$. It is in this sense that the two Higgses we have considered are not physically equivalent.

Of course this is no new phenomenon, and the peculiar upper-triangular shape of (3.29) on $w = 0$ has earned this kind of Higgses the name "T-branes", originated in [93], popularized in [94] and subsequently studied in a deluge of work [95, 109, 132–148]. In general, T-branes are bound states of branes that, despite giving rise to the same geometry in the M-theory dual as their diagonal Higgs cousins, encode a different physics. It is in this sense that T-branes add information to a D6-brane configuration, that therefore cannot be considered as a mere geometrical feature. In other words, the same M-theory geometry (or, equivalently, Type IIA brane locus), is in general compatible with many different brane configurations, yielding inequivalent physics. Therefore, in order to fully specify the physical content of a theory, one has first to fix the geometry, and then a T-brane background, be it trivial (in the case of diagonal Higgs) or non-trivial.

[6]We neglect the center of mass $U(1)$, as it is never broken by the scalar vevs.

3.4.3 Springer resolutions come into play

The reasoning of the previous section sparks some immediate questions: given an M-theory geometry, which (if any) T-brane states are allowed? Is there a guiding principle to determine them? It turns out that the theory of Springer resolutions, introduced in Chapter 2, provides systematic answers to these questions. Let us see how this comes about, going once again back to the conifold.

In the preceding lines, we have built the conifold as a deformed A_1 singularity, written as the M-theory uplift of the brane locus $\Delta(z, w) = z^2 - w^2$. We have also shown that such brane locus is compatible with two inequivalent choices of Higgses, (3.23) and (3.29). We have noticed this point by guesswork, as the conifold is a very simple geometry, but, in order to face much more generic cases, it is desirable to have a more grounded guiding principle. In order to find a possible recipe for the construction of the Higgs backgrounds (3.23) and (3.29), consider the complete and partial Springer resolutions of the A_1 singularity, whose formalism has been introduced in Chapter 2.

Let us briefly recall how Springer resolutions work summing up in a flash the content of Chapter 2: given an ADE singularity, pick an element x in the subregular nilpotent orbit of the algebra, and consider the Slodowy slice passing through x. Then, the intersection of the Slodowy slice with the adjoint quotient map (that parametrizes the Casimirs of the Slodowy slice) gives back the versal deformation of the chosen ADE singularity. To perform a *complete* simultaneous resolution, one can consider the versal deformation point by point (recalling that every point is an element in the Lie algebra): the fiber of the resolution map is given by all the Borel subalgebras that contain the base point itself. Carrying out this computation for all the points of the versal deformation, one obtains the whole preimage of the resolution map, and therefore the complete simultaneous resolution of the deformed family. If, on the other hand, one wishes to perform a *partial* simultaneous resolution, the fibers are made up of all the parabolic subalgebras of a certain conjugacy class that contain the base point. The conjugacy class is chosen according to the sought-after partial resolution, and implies a choice of simple roots Θ, corresponding to the nodes of the ADE Dynkin diagram that are not being resolved. Finally, in Chapter 2 we have also seen how choosing a complete or partial resolution fixes a choice of coordinates that are invariant under the Weyl group $\mathcal{W}'$ corresponding to the nodes that are *not* resolved, by using the block-diagonal decomposition of the Levi subalgebra contained in the Borel or parabolic subalgebras involved in the Springer resolution: this furnishes the pull-back map from the standard versal deformation coordinates appearing in the Casimirs of the Slodowy slice (which are invariant under the whole Weyl group $\mathcal{W}$, indicated with u_i in Chapter 2) and the correct invariant coordinates under $\mathcal{W}'$, that we call ϱ_i. Notice that in the case of the complete resolution we have $\mathcal{W}' = \emptyset$ and the "invariant coordinates" are precisely the t_i in the versal deformations (1.24), which encode the volumes of the inflated $\mathbb{P}^1$'s via (1.26).

Deformed A_1 example

After this quick recap of the Springer resolution machinery, we can look at what happens when we try to apply it at the A_1 singularity, skipping all the unnecessary details (for the complete formalism, we refer to Chapter 2): assume that we picked up an element in the subregular nilpotent orbit of the algebra A_1, and that we have built the Slodowy slice passing through it. Intersecting it with the adjoint quotient map, we correctly recover the versal deformation of A_1:

$$x^2+y^2 = z^2+u, \tag{3.31}$$

where u is the sole independent Casimir of the Slodowy slice. To perform a simultaneous complete resolution of the family, one has to find, point by point on the deformed family, all the Borel subalgebras containing the chosen point, seen as an element of the Lie algebra. In the case of A_1, the Borel subalgebras take the shape (for a review of Borel and Levi subalgebras, we refer to Appendix A):

$$\mathfrak{b} = \begin{pmatrix} * & * \\ 0 & * \end{pmatrix}. \tag{3.32}$$

As shown in Appendix A, Borel subalgebras $\mathfrak{b}$ can always be decomposed into a sum of the Cartan subalgebra $\mathfrak{h}$ and a nilpotent part $\mathfrak{n} = [\mathfrak{b}, \mathfrak{b}]$:

$$\mathfrak{b} = \mathfrak{h} \oplus \mathfrak{n}. \tag{3.33}$$

In the case of A_1, $\mathfrak{h}$ is simply given by the (traceless) diagonal elements, and it is the trivial Levi subalgebra corresponding to the choice of simple roots $\Theta = \emptyset$ (recalling from Chapter 2 that Θ is made up of the roots corresponding to nodes in the Dynkin diagram that are *not* being resolved):

$$\mathfrak{h} = \begin{pmatrix} * & 0 \\ 0 & * \end{pmatrix}. \tag{3.34}$$

The shape of (3.34) is the same as the one of the Higgs background for the conifold (3.23), but for now we could consider this fact as a mere coincidence. Also notice that (3.34) tells us which are the correct invariant coordinates when performing the complete simultaneous resolution. In this case we are resolving the only inflatable 2-cycle in the A_1 singularity, and therefore $\mathcal{W}' = \emptyset$. Calling w the invariant coordinate under $\mathcal{W}'$, that appears in the entries of (3.34), we can connect it with the Casimir of the A_1 algebra that appears in (3.31):

$$\mathfrak{h} = \begin{pmatrix} w & 0 \\ 0 & -w \end{pmatrix} \quad \Rightarrow \quad \text{Casimir of } \mathfrak{h} \propto u = w^2, \tag{3.35}$$

where the Casimir of $\mathfrak{h}$ has been computed as Casimir $= \mathrm{Tr}(\mathfrak{h} \cdot \mathfrak{h})$. Substituting the expression of the Casimir u into the versal deformation of A_1 (3.31) we immediately recover the equation of the conifold. What happens if, on the other hand, we choose to perform a partial Springer resolution, i.e. for the A_1 case a "resolution" where no node is resolved?

For such a case, the theory of Springer resolution tells us that we have to pick the subset of simple roots that are not being resolved, which is trivially:

$$\Theta = \alpha, \tag{3.36}$$

where α is the only simple root of A_1. Then, the fibers of the resolution are given by the elements of the Slodowy slice contained in the parabolic subalgebras $\mathfrak{p}$ built from Θ, which are:

$$\mathfrak{p}_\Theta = \mathcal{L}_\Theta = \begin{pmatrix} * & * \\ * & * \end{pmatrix}, \tag{3.37}$$

which is just the A_1 algebra. We have also highlighted the fact that $\mathfrak{p}_\Theta$ coincides with the associated Levi subalgebra $\mathcal{L}_\Theta$ (recall that the parabolic subalgebra $\mathfrak{p}_\Theta$ contains the standard Borel subalgebra $\mathfrak{b}$, as well as all the roots $\langle\Theta\rangle$ generated by the choice of simple roots Θ, while the Levi subalgebra $\mathcal{L}_\Theta$ contains only the roots in $\langle\Theta\rangle$. Hence, for the A_1 case $\mathfrak{p}_\Theta$ and $\mathcal{L}_\Theta$ coincide).

Notice that in the case (3.37) the invariant coordinate under $\mathcal{W}'$, which is $\mathbb{Z}_2$, is given by the Casimir of $\mathcal{L}_\Theta$, which is the Casimir u of the A_1 algebra. As a result, this choice of partial resolution exactly corresponds to the deformed family (3.31), which is non-singular and therefore does not admit any inflatable $\mathbb{P}^1$. What is of chief interest for our physical discussion, is that the shape of the Levi subalgebra (3.37) resembles the non-diagonal Higgs background (3.29). We can see, indeed, that we could rewrite (3.29) as:

$$\Phi = \begin{pmatrix} 0 & 1 \\ w^2 & 0 \end{pmatrix} = \begin{pmatrix} 0 & 1 \\ u & 0 \end{pmatrix}, \tag{3.38}$$

where we notice that the only independent Casimir of Φ is precisely u, the invariant coordinate predicted by the partial Springer resolution. We remark that (3.38) is holomorphically diagonalizable outside $w \neq 0$, and thus can be put in the form (3.35), thus going back to the choice of Levi (3.34). This cannot be done for all w, but only for $w \neq 0$: it is in this sense that (3.35) and (3.38) are indeed "different". Hence, if we wish to embed a Higgs background in (3.37), and not in one of its subalgebras, we must stick to the form (3.38). Nevertheless, holomorphic diagonalization will not be possible in general, as we will see in the analysis of the next chapters.

3.4.4 Higgs backgrounds and Springer resolutions in A_n cases

Let us summarize what we have found so far, employing the tool of Springer resolutions and the theory of Weyl-invariant coordinates: given a one-parameter deformation of an A_n Lie algebra, there seems to be a *correspondence between the subalgebra in which the Higgs background that encodes the M-theory uplift of the D6-brane locus lives, and the Levi subalgebra corresponding to a complete or partial resolution.* We have defined Levi subalgebras in (2.65), with additional details in Appendix A. This is consistent with the analysis of Springer resolutions in Chapter 2: there, given a A_n singularity, we have shown a correspondence between the eigenvalues of the Slodowy slice $\mathcal{S}_{\text{subreg}}$ through its subregular nilpotent orbit, and the Springer resolution. In the present context, by turning on a w-dependent vev for Φ we are deforming the A_n singularity, which is equivalent to fixing some non-vanishing Casimirs for $\mathcal{S}_{\text{subreg}}$. Finally, fixing the Casimirs predicts the corresponding Springer resolution. All in all, we have a correspondence:

$$\begin{array}{ccc} \text{Casimirs of } \mathcal{S}_{\text{subreg}} & \longleftrightarrow & \text{Casimirs of } \Phi \\ \updownarrow & & \updownarrow \\ \text{Springer resolution} & \longleftrightarrow & \text{Levi subalgebra containing } \Phi \end{array} \tag{3.39}$$

As of now we have exclusively dealt with the case of the conifold, but another point strikes the attention: the Higgs in the case of the complete Springer resolution preserves a single $U(1)$ outside the origin, whereas the Higgs corresponding to the partial Springer resolution completely breaks the group. This indicates that the number of preserved $U(1)$'s is in correspondence with the number of resolved nodes. This is of course no coincidence from the quantum field theory perspective, as we will see in Section 3.7 that the Kähler parameter of the resolution precisely appears in the vector multiplet of the preserved 7d gauge group. Furthermore, the Levi subalgebra associated to the Springer resolution dictates which are the correct invariant coordinates with which to write the deformed family. We can schematically rearrange the information we have gathered so far in the conifold case:

Higgs background	**Levi subalgebra**	**Resolution**
$\Phi = \begin{pmatrix} w & 0 \\ 0 & -w \end{pmatrix}$	$\begin{pmatrix} * & 0 \\ 0 & * \end{pmatrix}$	1 resolved node ($U(1)$ preserved)
$\Phi = \begin{pmatrix} 0 & 1 \\ w^2 & 0 \end{pmatrix}$	$\begin{pmatrix} * & * \\ * & * \end{pmatrix}$	No resolution (no $U(1)$ preserved)

(3.40)

We must stress, at this point, that the example of the conifold has some limitations: we have seen, indeed, that the defining equation of the conifold can be obtained directly as the M-theory uplift of a D6-brane locus described by a *diagonal* holomorphic Higgs background (3.23). Therefore, it may seem artificial (although completely consistent) to introduce the possibility of non-diagonal Higgs backgrounds, such as (3.29), yielding no resolution, whereas it is well known that the conifold admits a simultaneous resolution of the node of the A_1 algebra from which it arises. It may be the case, though, that for some deformations of ADE singularities *no diagonal holomorphic Higgs background exists.* In other words, for some M-theory geometries there might not exist a corresponding D6-brane locus that can be obtained as the characteristic polynomial (in the deformed A_n cases) of a diagonal holomorphic Higgs background, the only option being furnished by a non-diagonal one[7]. As the authors of [94] remark, one may well try and diagonalize such non-diagonal Higgs, at the cost of introducing non-holomorphic eigenvalues on the diagonal. This points to the fact that a non-monodromic behaviour has been introduced, considerably complicating the field theory analysis.

It is in this context that the work presented in the following chapters offers new ways to look at the kind of geometries that cannot be obtained from diagonal Higgses: we will show how, given such a geometry, the theory of Springer resolutions can play the role of guiding principle to explicitly construct a holomorphic, not necessarily diagonal, Higgs background $\Phi(w)$, with which concrete computations can be performed. This is, although, no trivial task, and we will see how each letter in the ADE classification displays different hurdles. While the deformed A_n cases are quite straightforward, also thanks to the amount of work already present in the literature, a description for deformed D and E series is, to our knowledge, completely lacking. In the next pages, we will first show how to construct Higgs backgrounds for D6-brane loci of the deformed D_n singularities, employing an O6$^-$-plane inducing an orientifold projection, and how to explicitly build their M-theory uplift. The E_6, E_7, E_8 cases, instead, do not admit a perturbative description in type IIA in terms of a system of D6-branes and O6$^-$-planes, and different methods to extract their M-theory uplift must be devised.

Before dealing with the above-mentioned cases, in the next section we delve deeper into the properties of the Higgs background $\Phi(w)$.

3.4.5 The field-theoretic construction of Higgs backgrounds

In the preceding sections, we have introduced the complex scalar field $\Phi(w)$, controlling the deformations of a stack of D6-branes along two real transverse directions. Moreover, we have seen in (3.26) that the Casimirs of such Higgs background are related to the explicit shape of the M-theory geometry, which is a deformed A_n singularity.

In this section we flesh out some properties of the Higgs background $\Phi(w)$, showing how to dictate its shape, that must be compatible with the M-theory geometry, via gauge-theoretic arguments. This approach is complementary to the Springer resolution perspective, and we will use it profusely in the next chapters.

Recall that in the type IIA side, motion transverse to the D6-brane stack is parametrized by three scalars ϕ_i, $i = 1, 2, 3$, where the first two get rearranged in the Higgs background $\Phi = \phi_1 + i\phi_2$ whose vev defines the singular geometry. The vev for Φ *need not* necessarily be diagonal, namely in general we allow:

$$[\phi_1, \phi_2] \neq 0 \quad \Rightarrow \quad \left[\Phi, \Phi^\dagger\right] \neq 0. \tag{3.41}$$

Physically, this amounts to switching on a non-vanishing background flux F_2 along $\mathbb{C}_w$, in the direction $\left[\Phi, \Phi^\dagger\right]$ of the algebra, which is along the Cartan subalgebra.

Giving a vev to the last scalar field ϕ_3, instead, corresponds to resolving the singularity,

[7] Indeed, in the following chapters we will mostly encounter examples of this kind.

as its eigenvalues are the Kähler parameters that encode the volumes of the resolved 2-cycles: as we will later see in more detail, its modes end up in the 7d vector multiplet that contains the gauge bosons that survive the breaking induced by Φ. This fact can be expressed by the D-term relation between Φ and ϕ_3:

$$[\Phi, \phi_3] = 0. \tag{3.42}$$

Equation (3.42) tells us that if we switch on a vev for ϕ_3 along the Cartan generators dual to the simple roots that we wish to resolve, that we define as[8]

$$\mathcal{H} = \langle \alpha_1^*, \dots, \alpha_f^* \rangle \tag{3.43}$$

then the Higgs background Φ must live in the subalgebra commuting with ϕ_3. This means that:

$$\Phi(w) \in \mathcal{L} = \bigoplus_h \mathcal{L}_h \oplus \mathcal{H}, \tag{3.44}$$

where $\mathcal{L}$ is a Levi subalgebra and $\mathcal{L}_h$ are simple Lie algebras.

In the example of the conifold, this implies that if we pick ϕ_3 along the Cartan generator dual to the only root in the A_1 system, namely $\mathcal{H} = \langle \alpha^* \rangle$:

$$\phi_3 = \begin{pmatrix} 1 & 0 \\ 0 & -1 \end{pmatrix}, \tag{3.45}$$

we end up with a Higgs background Φ of the form:

$$\Phi = \begin{pmatrix} * & 0 \\ 0 & * \end{pmatrix}. \tag{3.46}$$

If, instead, we pick ϕ_3 to be trivially null, we find:

$$\Phi = \begin{pmatrix} * & * \\ * & * \end{pmatrix}. \tag{3.47}$$

Notice that the two choices for the Higgs background reproduce the ones we found using the Springer resolution in Section 3.4.4. As a result, we see that there is a correspondence between the roots that are not being resolved, that we called Θ in the formalism of Springer resolutions, and the Cartan generators switched on in ϕ_3, dual to the roots $\overline{\Theta}$. It is obvious then that we have:

$$\overline{\Theta} = \Delta_{\text{simple roots}} \backslash \Theta,$$

where $\Delta_{\text{simple roots}}$ is the set of simple roots of A_1.

[8]The α_i are the simple roots of the considered ADE algebra. The α_i^* can be operatively defined as those Cartan generators orthogonal to *all* the simple roots except α_i. They can be readily computed using the explicit matrix representations of simple roots detailed in Appendix A.

3.4.6 Higgs backgrounds for A_n cases: summary

Let us recap the key takeaways from the discussion of the previous sections:

- We have started from M-theory on one-parameter deformed A_n singularities, described in the dual Type IIA picture by a setup of D6-branes intersecting at angles.

- The motion transverse to the D6-branes is controlled by three scalars ϕ_1, ϕ_2, ϕ_3: we have conjured up two of them into the complex scalar $\Phi(w) = \phi_1 + i\phi_2$. This complex scalar plays the role of the Higgs backround, and its Casimirs regulate the D6-brane locus, and hence also the M-theory geometry, via (3.26). This enables us to establish a correspondence between a given M-theory geometry and a Higgs background.

- Such correspondence, though, is not one-to-one, as there can be many different Higgs backgrounds yielding the same M-theory geometry. These multiple choices are known as *T-brane backgrounds*. In the following, given a one-parameter deformed A_n singularity, we will always associate to it (except when explicitly specified) the Higgs background that breaks the 7d gauge symmetry in the *least* brutal way, namely the Higgs background that inflates the *maximal* amount of nodes in the corresponding A_n Dynkin diagram.

- The guide to build such Higgs backgrounds is provided by the theory of Springer resolutions and the field-theoretic arguments of Section 3.4.5.

In conclusion, in the next page we gather in a schematic way all the information we need to build Higgs backgrounds in the deformed A_n cases, a task that we will systematically undertake in later chapters.

Consider a threefold X, built as a one-parameter deformation of a A_n singularity. In M-theory, we can always rewrite this geometry as:

$$uv = \Delta(z, w) = \det(z\mathbb{1} - \Phi(w)), \tag{3.48}$$

where w is the deformation parameter. $\Phi(w)$ is the holomorphic Higgs background, not necessarily diagonal, whose characteristic polynomial (that depends on its Casimirs) defines the brane locus $\Delta(z, w) = 0$ on the Type IIA side.
Given the maximal allowed simultaneous resolution admitted by X (namely, the resolution inflating the largest amount of nodes), consider the Cartan generators dual to the resolved roots, defined as:

$$\mathcal{H} = \langle \alpha_1^*, \ldots, \alpha_f^* \rangle. \tag{3.49}$$

The minimal subalgebra containing a holomorphic vev for the Higgs background $\Phi(w)$ is then:

$$\mathcal{L} = \bigoplus_h \mathcal{L}_h \oplus \mathcal{H}, \tag{3.50}$$

with $\mathcal{L}_h$ simple Lie algebras. Generically, the Higgs background can also be embedded into larger subalgebras containing $\mathcal{L}$: these will correspond to T-brane states.
Finally, (3.48) depends on the Casimirs of Φ. For generic A_n cases, we pick the following canonical choices of the Casimirs of a Higgs background Φ living in the A_n algebra:

$$\begin{array}{c} \boldsymbol{A_n} \\ \hline k_i = \mathrm{Tr}(\Phi^{i+1}), \;\; i = 1, \ldots, n \end{array} \tag{3.51}$$

In the following chapters we will dive into reaping the full results from these guiding principles, examining a variety of different cases involving deformed A_n singularities.

We are now ready to complete the program of analyizing all the one-parameter deformed ADE singularities, dealing with the D and the E cases.

3.5 M-theory on deformed D_n singularities

In this section, we tackle the case of one-parameter families of deformed D_n singularities, expanding the recipe based on Springer resolutions presented in the deformed A_n examples.

Before dealing with the M-theory uplift, let us start from the Type IIA side: a setup made up only of D6-branes is not sufficient to reproduce the features of deformed D_n singularities, and we must introduce O6$^-$-planes into the picture. This is not unexpected, as orientifold planes are known to generate D_n groups on stacks of D6-branes. We take the D6-branes to live on the target space $\overline{X}_2 = \mathbb{C}^2[\xi, w]$, where w will end up being the deformation parameter in the M-theory uplift of the D_n brane locus. This means that the D6-branes fill the flat five-dimensional spacetime and span a curve inside $\mathbb{C}^2[\xi, w]$. Consider now an orientifold action on $\mathbb{C}^2[\xi, w]$, acting as:

$$\sigma : (\xi, w) \longrightarrow (-\xi, w)\,. \tag{3.52}$$

This leaves the divisor $\xi = 0$ invariant. On the worldsheet, the action is $\Omega_p(-1)^{F_L}$, where Ω_p is the worldsheet parity and F_L is the space-time fermion number in the left-moving sector. As we did in the A_n cases, we wish to describe the full CY threefold X in M-theory, which is explicitly defined as a one-parameter deformation of a D_n singularity, as a $\mathbb{C}^*$-fibration over the brane locus of Type IIA. More precisely, as we have introduced an orientifold action exchanging the sign of the coordinate ξ, the CY threefold will be defined as a $\mathbb{Z}_2$-quotient of a $\mathbb{C}^*$-fibration. We can sum up this construction in a commutative diagram:

$$\begin{array}{ccc} \overline{X} & \xrightarrow{\mathbb{Z}_2} & X \\ {\scriptstyle \mathbb{C}^*}\big\downarrow & & \big\downarrow{\scriptstyle \mathbb{C}^*} \\ \overline{X}_2 & \xrightarrow{\mathbb{Z}_2} & X_2 \end{array}, \tag{3.53}$$

where $\overline{X}_2$ is a double cover of X_2 (which is isomorphic to $\mathbb{C}^2$), in which the orientifold action exchanges the sign of ξ. We can describe explicitly the $\mathbb{Z}_2$-quotient as:

$$\pi_{\mathbb{Z}_2} : \overline{X}_2 \longrightarrow \mathbb{C}^2 \tag{3.54}$$

$$(\xi, w) \mapsto (z := \xi^2, w)\,. \tag{3.55}$$

This means that we can describe X_2 redundantly as a hypersurface:

$$X_2 := \quad \mathbb{C}[\xi, w, z]/(\xi^2 - z), \tag{3.56}$$

where we have explicitly quotiented by the orientifold-invariant relation $\xi^2 = z$.

3.5.1 M-theory uplift of deformed D_n singularities

We can now analyze how this setup translates into the M-theory language. In M-theory, $\Omega_p(-1)^{F_L}$ acts as the inversion on the M-theory circle S^1. As in the A_n case, the M-theory circle belongs to the $\mathbb{C}^* = \mathbb{R} \times S^1$ fiber in the $\mathbb{C}^*$-fibration $\overline{X}$ over $\overline{X}_2$. The general structure of a $\mathbb{C}^*$-fibration can be written as:

$$uv = K, \tag{3.57}$$

for some polynomial K. Given this form, the circle inversion is tantamount to the exchange $u \leftrightarrow v$. As a consequence, we expect that the most general M-theory geometry $\overline{X}$ before the $\mathbb{Z}_2$-quotient is represented by the equation:

$$(x + i\xi y)(x - i\xi y) = P(\xi^2, w) - 2yQ(\xi^2, w) \quad \subset \mathbb{C}[x, y, \xi, w], \tag{3.58}$$

where we define $u = (x+i\xi y)$ and $v = (x-i\xi y)$ in order to correctly reproduce the circle inversion under the orientifold action. The factor of 2 in front of $Q(\xi^2, w)$ is conventional, and its usefulness will become momentarily clear. Implementing the $\mathbb{Z}_2$-quotient encoded by the relation (3.56) we finally find the CY threefold X expressed as a $\mathbb{C}^*$-fibration:

$$x^2+zy^2-P(z,w)+2yQ(z,w) = 0 \quad \subset \mathbb{C}[x,y,z,w]. \tag{3.59}$$

Proceeding analogously to the deformed A_n cases, we can look for the D6-brane locus by inspecting where the $\mathbb{C}^*$-fiber in (3.59) degenerates. This can be done by computing the discriminant of $zy^2-P(z,w)+2Q(z,w)y$ with respect to y, yielding:

$$\Delta(z,w) = Q(z,w)^2+zP(z,w). \tag{3.60}$$

We immediately see that on top of a point (z,w) satisfying $\Delta(z,w) = 0$ the expression for X becomes the difference of two squares:

$$x^2+zy_0^2 = 0, \tag{3.61}$$

for some y_0, that on the double cover where $\xi^2 = z$ becomes of the form $uv = 0$, which is precisely the degeneration of a $\mathbb{C}^*$-fibration, as we have seen in the A_n cases.

As of now, we have solely described the $\mathbb{C}^*$-structure of the CY threefold encoding one-parameter deformed D_n singularities, describing the D6-brane locus in presence of a O6$^-$-plane, but we have not dealt yet with the the connection between the M-theory geometry and the Higgs background $\Phi(w)$ describing the motion transverse to the D6-branes. Let us now address this issue, always keeping in mind the A_n case as a template.

In a fashion analogous to Section 3.4, M-theory placed on top of a D_n singularity gives rise to a $\mathcal{N} = 1$ 7d theory with gauge group $SO(2n)$, accounted for in Type IIA by a stack of D6-branes on top of an orientifold plane[9]. The three scalars ϕ_1, ϕ_2, ϕ_3 parametrizing directions transverse to the branes are arranged in a complex scalar $\Phi = \phi_1+i\phi_2$ and a real scalar ϕ_3, as in the A_n case. The deformation of the D_n singularity is encoded by a non-trivial vev for $\Phi(w)$, dependent on a complex parameter w that spans the brane worldvolume in the extra dimensions. The connection between the properties of $\Phi(w)$ and the explicit D6-brane locus, as well as its M-theory uplift, is slightly more involved in comparison to the A_n case. More specifically, given a Higgs background $\Phi(w)$ the D6-brane locus in the double cover $\overline{X}_2$ can be obtained as:

$$\Delta(\xi^2, w) = \det(\xi+\Phi(w)). \tag{3.62}$$

Tracking the locus through the M-theory uplift, we end up with the double cover $\overline{X}$ of the

[9]More rigorously, we only know for certain that the gauge algebra in 7d is $\mathfrak{so}(2n)$. In order to precisely fix the group, one should carefully consider the possible choices allowed by the global structure of the compactification space [76, 149]. We will return to this ambiguity in Chapter 4.

CY threefold, which depends on the characteristic polynomial of Φ, as well as its Pfaffian:

$$x^2+\xi^2y^2-\frac{\det(\xi\mathbb{1}+\Phi(w))-\mathrm{Pfaff}^2(\Phi(w))}{\xi^2}+2y\,\mathrm{Pfaff}(\Phi(w))=0. \tag{3.63}$$

Notice that this expression is analogous to (3.58), with the due identifications:

$$P(\xi^2,w)=\frac{\det(\xi\mathbb{1}+\Phi(w))-\mathrm{Pfaff}^2(\Phi(w))}{\xi^2}, \qquad Q(\xi^2,w)=\mathrm{Pfaff}(\Phi(w)). \tag{3.64}$$

We stress that, although not at first sight, $P(\xi^2,w)$ is devoid of poles, as the subtraction of $\mathrm{Pfaff}^2(\Phi(w))$ eliminates any term not proportional to ξ^2. Performing the $\mathbb{Z}_2$-quotient we obtain the full expression for the CY threefold X:

$$x^2+zy^2-\frac{\sqrt{\det(z\mathbb{1}+\Phi^2)}-\mathrm{Pfaff}^2(\Phi)}{z}+2y\,\mathrm{Pfaff}(\Phi)=0, \tag{3.65}$$

which is once again devoid of poles.

The remarkable point, that connects the D_n case to the A_n case, is that the threefold equation depends exclusively on the Casimirs of Φ, via its characteristic polynomial and Pfaffian. Our canonical choice for the Casimirs of $\Phi\in D_n$ is as follows:

$$\begin{array}{c} \boldsymbol{D_n} \\ \hline \tilde{k}_i=\mathrm{Tr}(\Phi^{2i}),\;\; i=1,\dots,n-1 \\ \tilde{k}_n=\mathrm{Pfaff}(\Phi) \end{array} \tag{3.66}$$

At this point, we have at our disposal the explicit structure of the $\mathbb{C}^*$-fibration, as well as the full expression for the M-theory geometry of a deformed D_n singularity in terms of the Type IIA Higgs background $\Phi(w)$. The last ingredient we need to start and do actual computations is a hands-on recipe for building Higgs backgrounds explicitly: as in the A_n cases, the blueprint for this task is given by the complete and partial Springer simultaneous resolutions.

In order to see how this works in practice, let us fix ideas working on the simplest D_n case, namely a one-parameter deformed D_4 singularity.

3.5.2 Springer resolutions of D_4: the Brown-Wemyss singularity

Let us consider a singular hypersurface in $\mathbb{C}^4$ that has been extensively studied in the mathematical community [92], trying to employ the machinery of Springer resolution to garner some phyisical intuition.

The defining equation of the Brown-Wemyss singularity[10] reads:

$$x^2+zy^2-(z-w)\left(zw^2+(z-w)^2\right)=0 \quad\subset\mathbb{C}^4. \tag{3.67}$$

[10] In later chapters, we will give more details about such singularity, including its physical repercussions.

It is easy to check that it is a deformed D_4 singularity and that it admits a unique isolated singularity of D_4 type at the origin. Our aim is to build a Higgs background Φ such that it reproduces equation (3.67), via the formula (3.65) that relates the shape of the Higgs with the explicit threefold equation.

In principle, in order to perform this construction letting Springer resolutions be the guide, one should try and look for a Higgs background in the most constrained Levi subalgebra of $D_4 = \mathfrak{so}(8)$, which is made up only of the Cartan generators and corresponds to a complete resolution of the singularity. If no holomorphic Higgs of such shape can be found, it means that a complete resolution is obstructed by the choice of the specific w-deformation of D_4 that yields the Brown-Wemyss threefold, and that therefore one should look next to a slightly bigger Levi subalgebra, namely one involving a choice of a simple root, besides the Cartan generators. The procedure then runs until a suitable Higgs has been found: the Levi subalgebra in which it resides predicts the allowed partial resolution.

In the Brown-Wemyss singularity case, it turns out that the minimal Levi subalgebra that contains an holomorphic Higgs reproducing (3.67) is the one given by the choice:

$$\Theta = \{\alpha_1, \alpha_3, \alpha_4\}, \tag{3.68}$$

recalling that α_2 is the central root of the D_4 Dynkin diagram (see Figure 3.4 for some graphical intuition). This means that the maximal resolution allowed by the Brown-Wemyss singularity inflates exclusively the central node of the D_4 singularity at the origin.

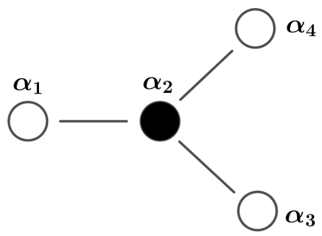

Figure 3.4: *Partial resolution of the Brown-Wemyss threefold: only the central node can be resolved.*

Translating this information into a constraint on the shape of the Higgs field, we find that Φ should be of the following form, that we have encountered in Section 2.3.2:

$$\mathcal{L} = \left(\begin{array}{cccc|cccc} * & * & 0 & 0 & 0 & 0 & 0 & 0 \\ * & * & 0 & 0 & 0 & 0 & 0 & 0 \\ 0 & 0 & * & * & 0 & 0 & 0 & * \\ 0 & 0 & * & * & 0 & 0 & * & 0 \\ \hline 0 & 0 & 0 & 0 & * & * & 0 & 0 \\ 0 & 0 & 0 & 0 & * & * & 0 & 0 \\ 0 & 0 & 0 & * & 0 & 0 & * & * \\ 0 & 0 & * & 0 & 0 & 0 & * & * \end{array}\right), \tag{3.69}$$

where the $*$ entries satisfy the usual conditions of the algebra $\mathfrak{so}(8)$ and where we can notice that all the roots generated by the set Θ have been switched on.

The result (3.69) could have been equivalently obtained as follows: consider the maximal allowed resolution of the Brown-Wemyss threefold, inflating only the central node of the D_4 Dynkin diagram. In the language of Section 3.4.5, this means taking a choice:

$$\mathcal{H} = \langle \alpha_2^* \rangle, \tag{3.70}$$

with α_2 the trivalent root of D_4. As a consequence, the Higgs background should live in the commutant of $\mathcal{H}$, which takes precisely the form (3.69).

The form (3.69) is the farthest that the Springer resolution can bring us: from here on, we must tune the $*$ entries so as to recover the Brown-Wemyss threefold by means of equation (3.65). An easy try and test shows that the correct form reads:

$$\Phi = \left(\begin{array}{cccc|cccc} 0 & 1 & 0 & 0 & 0 & 0 & 0 & 0 \\ -w & -w & 0 & 0 & 0 & 0 & 0 & 0 \\ 0 & 0 & 0 & 1 & 0 & 0 & 0 & 1 \\ 0 & 0 & -\frac{w}{4} & 0 & 0 & 0 & -1 & 0 \\ \hline 0 & 0 & 0 & 0 & 0 & w & 0 & 0 \\ 0 & 0 & 0 & 0 & -1 & w & 0 & 0 \\ 0 & 0 & 0 & \frac{w}{4} & 0 & 0 & 0 & \frac{w}{4} \\ 0 & 0 & -\frac{w}{4} & 0 & 0 & 0 & -1 & 0 \end{array}\right). \tag{3.71}$$

Finally, inserting (3.71) into (3.65) immediately yields the expected Brown-Wemyss threefold (3.67).

A quick computation shows that the only continuous group preserved by Φ is a single $U(1)$, signaling, exactly as in the A_n cases, that a partial resolution inflating only a single node is allowed by the shape of Φ.

We should also note that, as it happened for the A_n cases, this is not the only allowed Higgs background that correctly encodes the Brown-Wemyss equations: indeed less natural Higgses, residing in larger Levi subalgebras, may exist and give rise to (3.67) via their Casimirs: these are additional T-brane backgrounds. All these extra Higgses, though, live in Levi subalgebras that correspond to a partial resolution with *less* resolved nodes with respect to the choice (3.71). In later chapters we will give a physical interpretation also to this kind of Higgs backgrounds.

Before summarizing the main takeaways of this section, let us check explicitly the relationship between the threefold equation of the deformed D_4 singularities admitting a resolution of the central node and the Casimirs of the Higgs background Φ. In this perspective, we recall that we have already encountered the shape (3.69) of the Levi subalgebra in equation (2.99), during the analysis of Springer resolutions. In that section we showed how the Casimirs of the full matrix (3.69) are related to the partial Casimirs of the $\mathfrak{sl}(2)\oplus\mathfrak{sl}(2)\oplus\mathfrak{sl}(2)\oplus\mathfrak{u}(1)$ algebra, where the $\mathfrak{sl}(2)$ factors correspond to the non-resolved nodes, and the $\mathfrak{u}(1)$ term accounts for the resolution of the central node. In this way, we see that the equation that defines the threefold (3.65) depends on the Casimirs of $\Phi(w)$, and thus also on the partial Casimirs related to the specific resolution pattern, that is fixed by the allowed choice of Springer resolution.

We will encounter many more examples of this line of reasoning in the following chapters, allowing an explicit connection between the Weyl theory of the singularity and the structure of the Higgs background.

We can at last conclude this section on deformed D_n singularities with a summary of our finds:

Consider a threefold X, built as a one-parameter deformation of a D_n singularity. In M-theory, we can always rewrite this geometry as:

$$x^2+zy^2-\frac{\sqrt{\det(z\mathbb{1}+\Phi(w)^2)}-\text{Pfaff}^2(\Phi(w))}{z}+2y\,\text{Pfaff}(\Phi(w))=0, \tag{3.72}$$

where w is the deformation parameter. $\Phi(w)$ is the holomorphic Higgs background, not necessarily diagonal, whose characteristic polynomial (that depends on its Casimirs) defines the brane locus $\Delta(z,w)=0$ on the Type IIA side.
Given the maximal allowed simultaneous resolution admitted by X (namely, the resolution inflating the largest amount of nodes), consider the Cartan generators dual to the resolved roots, defined as:

$$\mathcal{H}=\langle\alpha_1^*,\ldots,\alpha_f^*\rangle. \tag{3.73}$$

The minimal subalgebra containing a holomorphic vev for the Higgs background $\Phi(w)$ is then:

$$\mathcal{L}=\bigoplus_h \mathcal{L}_h\oplus\mathcal{H}, \tag{3.74}$$

with $\mathcal{L}_h$ simple Lie algebras. Generically, the Higgs background can also be embedded into larger subalgebras containing $\mathcal{L}$: these will correspond to T-brane states.
Our canonical choice of Casimirs for $\Phi\in D_n$ reads:

$$\begin{array}{c}\boldsymbol{D_n}\\ \hline \tilde{k}_i=\text{Tr}(\Phi^{2i}),\;\; i=1,\ldots,n-1\\ \tilde{k}_n=\text{Pfaff}(\Phi)\end{array} \tag{3.75}$$

3.6 M-theory on deformed E_6, E_7, E_8 singularities

In this section, we put under the magnifying lens the ADE singularities of exceptional type E_6, E_7, E_8, furnishing a description of the Higgs backgrounds associated to the threefolds arising from their one-parameter deformations.

The first and most relevant difference with respect to the A_n and D_n cases is that one-parameter families of exceptional singularities *do not* admit a perturbative description in terms of D6-branes and orientifold planes. As a result, if we wish to introduce a Higgs background field Φ describing our geometrical setup, it cannot physically correspond to the displacement of some D6-branes. This can be seen directly from the M-theory geometry, which in our cases reads:

$$\begin{aligned}
E_6: &\quad x^2+z^4+y^3+\epsilon_2(w)yz^2+\epsilon_5(w)yz+\epsilon_6(w)z^2+\epsilon_8(w)y+\epsilon_9(w)z+\epsilon_{12}(w)=0\\
E_7: &\quad x^2+y^3+yz^3+\tilde{\epsilon}_2(w)y^2z+\tilde{\epsilon}_6(w)y^2+\tilde{\epsilon}_8(w)yz+\tilde{\epsilon}_{10}(w)z^2+\tilde{\epsilon}_{12}(w)y+\epsilon_{14}(w)z+\tilde{\epsilon}_{18}(w)=0 \quad ,\\
E_8: &\quad x^2+y^3+z^5+\hat{\epsilon}_2(w)yz^3+\hat{\epsilon}_8(w)yz^2+\epsilon_{12}(w)z^3+\hat{\epsilon}_{14}(w)yz+\hat{\epsilon}_{18}(w)z^2+\epsilon_{20}(w)y+\hat{\epsilon}_{24}(w)z+\hat{\epsilon}_{30}(w)=0
\end{aligned} \tag{3.76}$$

where we have explicitly introduced a dependence on the $\epsilon, \tilde{\epsilon}, \hat{\epsilon}$ deformation coefficients appearing in (1.24) on a complex parameter w.

The fact that only a non-perturbative description of such geometries is possible is reflected by the fact that the threefolds (3.76) do not admit a $\mathbb{C}^*$-fibration, that constituted the key tool allowing us to reduce M-theory on a S^1 and build its Type IIA counterpart. Nevertheless, the one-parameter families of E_6, E_7, E_8 singularities admit an elliptic fibration, and hence we can consider F-theory compactified on them: further reducing the resulting 6d theory on a circle, we end up with an effective theory in 5d. In this picture, the Higgs background $\Phi(w)$ is the adjoint Higgs on the stack of non-perturbative 7-branes. Let us rephrase this procedure in the M-theory language: M-theory on the E singularities gives rise to a 7d $\mathcal{N}=1$ theory with E gauge group (up to subtleties on the global form), and this theory possesses three adjoint scalars ϕ_1, ϕ_2, ϕ_3. Combining two of them into the complex scalar $\Phi = \phi_1 + i\phi_2$ we build the Higgs background $\Phi(w)$ that describes a non-trivial fibration of the starting E singularity on the $\mathbb{C}_w$ plane. From here we can proceed analogously as for the A and D cases, with no reference to D6-branes or O6$^-$-planes.

As a consequence of the fact that no $\mathbb{C}^*$-fibration is available, we should recur to slightly different methods, compared with the A_n and D_n cases, to relate Higgs backgrounds living in the exceptional algebras and the corresponding threefold equations.

Let us outline the strategy to tackle such cases. Our first objective is to relate these Higgs backgrounds to an explicit threefold equation of the form (3.76). We will show that the punchline is that it is indeed possible to perform this task, and that there exists a precise relationship between the Casimirs of the Higgs background $\Phi \in E_6, E_7, E_8$ and the deformation parameters $\epsilon, \tilde{\epsilon}, \hat{\epsilon}$ in (3.76).

For our purposes in the following chapters, it is convenient to fix the representation in which Φ lives, namely the fundamental of E_6 and the adjoint of E_7 and E_8:

$$\begin{array}{c|c} \boldsymbol{E_6} & \mathbf{27} \\ \boldsymbol{E_7} & \mathbf{133} \\ \boldsymbol{E_8} & \mathbf{248} \end{array} . \tag{3.77}$$

We pick a choice of the Casimirs of Φ as [150,151]:

$$\begin{array}{c|ll} \boldsymbol{E_6} & c_i = \mathrm{Tr}(\Phi^i) & \text{for } i = 2,5,6,8,9,12 \\ \boldsymbol{E_7} & \tilde{c}_i = \mathrm{Tr}(\Phi^i) & \text{for } i = 2,6,8,10,12,14,18 \\ \boldsymbol{E_8} & \hat{c}_i = \mathrm{Tr}(\Phi^i) & \text{for } i = 2,8,12,14,18,20,24,30 \end{array} , \tag{3.78}$$

where it is relevant to notice that the degrees of the Casimirs reflect the powers of the volume parameters t_i (1.26) appearing in them, that in turn correspond to the degrees of the $\epsilon_i, \tilde{\epsilon}_i, \hat{\epsilon}_i$ parameters in (3.76). The exact relationship between Casimirs and versal deformation parameters is analyzed step-by-step in Appendix B, and the resulting threefold equations can be written in the form:

$$\begin{aligned} E_6: &\quad x^2+y^3+z^4+f_6(z,y,c_i(w)) = 0, \\ E_7: &\quad x^2+y^3+yz^3+f_7(z,y,\tilde{c}_i(w)) = 0, \\ E_8: &\quad x^2+y^3+z^5+f_8(z,y,\hat{c}_i(w)) = 0. \end{aligned} \tag{3.79}$$

where we notice the appearance of the Casimirs of the Higgs background $\Phi(w)$.

Once that the Higgs-threefold relationship is settled, we can proceed in employing the theory of Springer resolutions to gather intel on the concrete shape of the Higgs backgrounds. As in the A_n and D_n cases, once a resolution pattern is known, one can consider the Levi subalgebra of E_6, E_7, E_8 generated by the roots that are *not* being resolved, and embed the Higgs background in that Levi subalgebra. This takes care of the resolution side of the story. Then, a case-by-case tuning of the coefficients of the Levi subalgebra must be enforced in order to produce the threefold equation that one wishes to study. Of course, this strategy can also be reverse-engineered, using Springer resolutions to build a Higgs background with some desired resolution pattern, and then computing the threefold that corresponds to such a Higgs.

Due to the intricacy of the cases involving exceptional algebras, we refrain to show the construction of Higgs backgrounds, leaving this work for Chapers 4 and 5. As we did in the A_n and D_n cases, we quickly summarize the recipe to build explicit Higgs backgrounds in the E_6, E_7, E_8 cases:

Consider a threefold X, built as a one-parameter deformation of a E_6, E_7, E_8 singularity, defined by the equations:

$$\begin{array}{ll} E_6: & x^2+y^3+z^4+\epsilon_2(w)yz^2+\epsilon_5(w)yz+\epsilon_6(w)z^2+\epsilon_8(w)y+\epsilon_9(w)z+\epsilon_{12}(w)=0 \\ E_7: & x^2+y^3+yz^3+\tilde{\epsilon}_2(w)y^2z+\tilde{\epsilon}_6(w)y^2+\tilde{\epsilon}_8(w)yz+\tilde{\epsilon}_{10}(w)z^2+\tilde{\epsilon}_{12}(w)y+\epsilon_{14}(w)z+\tilde{\epsilon}_{18}(w)=0 \\ E_8: & x^2+y^3+z^5+\hat{\epsilon}_2(w)yz^3+\hat{\epsilon}_8(w)yz^2+\epsilon_{12}(w)z^3+\hat{\epsilon}_{14}(w)yz+\hat{\epsilon}_{18}(w)z^2+\epsilon_{20}(w)y+\hat{\epsilon}_{24}(w)z+\hat{\epsilon}_{30}(w)=0 \end{array}, \tag{3.80}$$

where w is the deformation parameter.
In M-theory, we can always rewrite the deformation parameters $\epsilon_i, \tilde{\epsilon}_i, \hat{\epsilon}_i$ of these geometries in terms of the Casimirs of a Higgs background $\Phi(w)$ (as detailed in Appendix B), which is not necessarily diagonal.
Given the maximal allowed simultaneous resolution admitted by X (namely, the resolution inflating the largest amount of nodes), consider the Cartan generators dual to the resolved roots, defined as:

$$\mathcal{H} = \langle \alpha_1^*, \ldots, \alpha_f^* \rangle. \tag{3.81}$$

The minimal subalgebra containing a holomorphic vev for the Higgs background $\Phi(w)$ is then:

$$\mathcal{L} = \bigoplus_h \mathcal{L}_h \oplus \mathcal{H}, \tag{3.82}$$

with $\mathcal{L}_h$ simple Lie algebras. Generically, the Higgs background can also be embedded into larger subalgebras containing $\mathcal{L}$: these will correspond to T-brane states.
Our canonical choice of Casimirs for $\Phi \in E_6, E_7, E_8$ reads:

$$\begin{array}{l|l} \boldsymbol{E_6} & c_i = \mathrm{Tr}(\Phi^i) \;\; \text{for } i = 2,5,6,8,9,12 \\ \boldsymbol{E_7} & \tilde{c}_i = \mathrm{Tr}(\Phi^i) \;\; \text{for } i = 2,6,8,10,12,14,18 \\ \boldsymbol{E_8} & \hat{c}_i = \mathrm{Tr}(\Phi^i) \;\; \text{for } i = 2,8,12,14,18,20,24,30 \end{array}. \tag{3.83}$$

3.7 M-theory on ADE singularities and the Higgs background Φ

Throughout the rest of this work, we consider M-theory on an ALE surface with an ADE singularity, of the shape that we have fleshed out in the previous sections. In this section, we reprise the content of Section 3.4.5 and state the general procedure that takes us from a K3 with an ADE singularity to a one-parameter deformed ADE singularity yielding a theory in five dimensions, via the Higgsing provided by the background $\Phi(w)$.

Consider a K3 with an ADE singularity: the fact that the compactification space is non-compact assures that gravity is decoupled. As we have previously reviewed, the effective theory in 7d is a SYM theory with three adjoint scalars and group $G = A, D, E$ with $\mathcal{N} = 1$ supersymmetry. One can break half of the supercharges by switching on a BPS vev for the scalar fields in the following way:

- Take the 7d spacetime to be $\mathbb{R}^5 \times \mathbb{C}$. Call w the local coordinate on $\mathbb{C}$.
- Choose two of the three real scalars and construct a complex scalar in the adjoint. We then have the complex adjoint scalar $\Phi = \phi_1 + i\phi_2$ and the real adjoint scalar ϕ_3.
- Take a holomorphic w-dependent vev for Φ.

This breaks the Lorentz group to $SO(4,1)$, that acts by rotation on the extended $\mathbb{R}^5$. The 7d gauge group is broken to the stabilizer of Φ. The 7d $\mathcal{N}=1$ vector multiplet was made up by the gauge field A_M ($M = 0, 1, ..., 6$) and the three scalars ϕ_i ($i = 1, 2, 3$); after giving a vev to Φ, only a 5d $\mathcal{N}=1$ vector multiplet (A_μ, ϕ_3) in the subalgebra $\mathcal{H}$ that commutes with Φ survives (these vector multiplets still propagate in 7d, and are then seen as background vector multiplets from the 5d point of view).

From the geometric point of view, we have deformed the ADE singularity; the deformation parameters are related to the Casimirs of Φ and depend on w: we have hence obtained a threefold that is an ALE fibration over the plane $\mathbb{C}_w$. The precise relationship between the Casimirs of Φ and the M-theory uplift, that corresponds to the compactification threefold, has been elucidated in Sections 3.4.6, 3.5.2, 3.6, both in the cases with Type IIA dual (A and D deformed singularities) and in the intrinsically non-perturbative cases (E_6, E_7, E_8 deformed singularities).

Whenever the M-theory uplift can be described as a $\mathbb{C}^*$-fibration, namely in the A and D cases, we can build the Type IIA dual in terms of D6-branes, whose transverse directions are parametrized by ϕ_1, ϕ_2, ϕ_3. Hence Φ describes a deformation of the D6-brane stack along the (z, w) directions:

	$\mathbb{R}^{4,1}$	$\mathbb{C}_w \vert \mathbb{C}_z$	ϕ_3
D6	$\times$	2 $\dim_{\mathbb{R}}$	$\cdot$

(3.84)

The vev of Φ should also satisfy some BPS equations, whose solutions preserve a 5d Poincaré symmetry and half of the original supersymmetries. Hence we can describe the spectrum after Higgsing in terms of $\mathcal{N}=1$, $d=5$ supermultiplets:

- The massless deformations of A_μ ($\mu = 0, ..., 4$) and of ϕ_3 make up vector multiplets in the adjoint of $\mathcal{H}$. These are background vector multiplets from the 5d perspective, as these fields propagate in 7d.
- Let us consider the massless deformations of Φ and A_5, A_6. As we will see in detail in the next chapter, there are localized Φ-modes at $w = 0$ that organize in hypermultiplets charged under $\mathcal{H}$ and that propagate in 5d. The massless deformations of A_5, A_6 are along $\mathcal{H} \subseteq \mathcal{T}$ and sit together with zero modes of Φ in background (the fields propagate in 7d) hypermultiplets that are neutral under $\mathcal{H}$.

The field ϕ_3 in the background vector multiplet satisfies $[\phi_3, \Phi] = 0$, as $\phi_3 \in \mathcal{H}$. Recall from Section 3.4.6 that in the 7d theory a vev for $\phi_3 \in \mathcal{T}$ corresponds geometrically to blowing up the simple roots of the corresponding ADE algebra. Hence the fact that the 5d ϕ_3 lives in $\mathcal{H} \subseteq \mathcal{T}$ tells us that only part of the simple roots can be blown up in the ALE fibration over $\mathbb{C}_w$ (i.e. after Higgsing Φ). This is dual to the statement that the choice of Levi subalgebra encodes which are the resolved roots, via the Springer resolution formalism. Furthermore, the vev of the 5d ϕ_3 gives the size of the exceptional $\mathbb{P}^1$'s of the simultaneous resolution of the threefold. If the simple roots that are resolved in $w = 0$ are $\alpha_1, \ldots, \alpha_f$, then

$$\mathcal{H} = \langle \alpha_1^*, \ldots, \alpha_f^* \rangle, \tag{3.85}$$

where the α_i^* are elements in some basis of the Cartan algebra $\mathcal{T}$ that is dual to the simple roots.

From a physical perspective, the vev of ϕ_3 gives rise to a mass term for the hypermultiplets in the five-dimensional theory.

In the next section, we recap the relationship between Higgs backgrounds and threefold equations, built as one-parameter deformations of ADE singularities, revisiting part the content of Sections 3.4.6, 3.5.2, 3.6 in a slightly different light.

3.8 The threefold equation from Φ and Slodowy slices

In the preceding sections, we have shown the correspondence between threefold equations, i.e. the geometries on which M-theory is compactified, and the Higgs background obtained from the adjoint fields that parametrize the deformations of the 7d theory built from M-theory on the corresponding ADE singularity. In this section, we recap these results, reproducing them using the formalism of Slodowy slices.

As a starting point, we consider the adjoint quotient map, introduced in (2.4), that associates an element x of the ADE algebra $\mathfrak{g}$ of rank n with n independent polynomials χ_i, whose value gives a point in $\mathcal{T}/\mathcal{W}$:

$$\chi : \quad \mathfrak{g} \to \mathcal{T}/\mathcal{W} : \mathrm{x} \mapsto (\chi_1(\mathrm{x}), \cdots, \chi_n(\mathrm{x})). \tag{3.86}$$

The polynomials $\chi_i(\mathrm{x})$ are the Casimirs of $\mathfrak{g}$ and are defined in the following way. By choosing a representation of the Lie algebra $\mathfrak{g}$, x can be put in a matrix form. Its Casimirs are then given by specific invariant polynomials of this matrix: for the A and D series, we have seen that the canonical Casimirs of x are (with x a matrix in the fundamental/vector representation):

$\boldsymbol{A_n}$	$\boldsymbol{D_n}$
$\chi_i^A(\mathrm{x}) = \mathrm{Tr}(\mathrm{x}^{i+1}),\ \ i = 1, \ldots, n$	$\chi_i^D(\mathrm{x}) = \mathrm{Tr}(\mathrm{x}^{2i}),\ \ i = 1, \ldots, n-1$
	$\chi_n^D(\mathrm{x}) = \mathrm{Pfaff}(\mathrm{x})$

(3.87)

For the exceptional algebras E_n, one takes x in the following representations: **27** for E_6, **133** for E_7 and **248** for E_8. One then defines the Casimirs of x as [150, 151]:

$$\begin{array}{l|l} \boldsymbol{E_6} & \chi_i^{E_6}(\mathrm{x}) = \mathrm{Tr}(\mathrm{x}^{k_i}) \quad \text{for } k_i = 2,5,6,8,9,12 \\ \boldsymbol{E_7} & \chi_i^{E_7}(\mathrm{x}) = \mathrm{Tr}(\mathrm{x}^{k_i}) \quad \text{for } k_i = 2,6,8,10,12,14,18 \\ \boldsymbol{E_8} & \chi_i^{E_8}(\mathrm{x}) = \mathrm{Tr}(\mathrm{x}^{k_i}) \quad \text{for } k_i = 2,8,12,14,18,20,24,30 \end{array} , \tag{3.88}$$

and $i = 1, ..., n$.

The crucial fact for us is the following (that we recall from Chapter 2):
Given an algebra $\mathfrak{g}$ in the ADE classification, and an element $\mathrm{x} \in \mathcal{O}_{\text{subreg}}$, the intersection of the Slodowy slice through x with the fiber of the adjoint quotient map (3.86) is isomorphic to the versal deformation of the corresponding ADE singularity, namely:

$$\mathcal{S}_{\text{subreg}} \cap \chi^{-1}(u) \cong \text{versal deformation of } \mathbb{C}^2/\Gamma_{\text{ADE}}, \tag{3.89}$$

where u is a point in $\mathcal{T}/\mathcal{W} \simeq \mathbb{C}^n$ with coordinates u_i.

The isomorphism (3.89) is telling us that the coefficients of the monomials in the versal deformation can be written in terms of the coordinates u_i related to the polynomials χ_i.

We now want to describe the ALE families of deformed ADE singularities over $\mathbb{C}_w$. We have constructed them by the choice of a Higgs field $\Phi(w)$, that through its Casimirs is telling us how the deformation is performed on top of each point of $\mathbb{C}_w$. In other words, take $w \in \mathbb{C}_w$; to see which is the deformed ALE surface over w, we pick $\Phi(w)$ and compute its Casimirs $\chi_i(\Phi)$. Their values select a specific point $u \in \mathcal{T}/\mathcal{W}$ and then a specific deformed ALE surface (with precise volumes of the non-holomorphic spheres (2.55)). The equation of the threefold is obtained imposing the relations

$$\chi_i(\mathcal{S}_{\text{subreg}}) = \chi_i(\Phi(w)) \,, \qquad i = 1, ..., n, \tag{3.90}$$

with $\chi_i(\mathrm{x})$ defined in (3.87) and (3.88), and substituting the resulting $\chi_i(\mathcal{S}_{\text{subreg}})$ into the expressions defining $\mathcal{S}_{\text{subreg}} \cap \chi^{-1}(\chi_i(\mathcal{S}_{\text{subreg}}))$.

In general, if we keep $\Phi(w)$ unspecified, (3.90) gives us the versal deformations of the ADE singularity, with deformation parameters depending on the Casimirs of Φ. We have worked out these relations for all the ADE algebras. For the A_n and D_n singularities, one obtains (up to coordinate redefinition) the compact forms of Sections 3.4.6 and 3.5.2:

$$A_n : \qquad x^2 + y^2 + \det(z\mathbb{1} - \Phi) = 0 \tag{3.91}$$

and

$$D_n : \qquad x^2 + zy^2 - \frac{\sqrt{\det(z\mathbb{1} + \Phi^2)} - \mathrm{Pfaff}^2(\Phi)}{z} + 2y\,\mathrm{Pfaff}(\Phi) = 0. \tag{3.92}$$

For the E_n singularities the expression of the deformation parameters $\epsilon_i, \tilde{\epsilon}_i, \hat{\epsilon}_i$ (appearing in (1.24)) in terms of the Casimirs (3.88) are given in Appendix B.

Hence, given a Higgs field $\Phi(w)$, one obtains the threefold equation by simply computing its Casimirs and then inserting them into the relations (3.91) and (3.92) for the A and D cases, or using the formulae in Appendix A for the E cases.

A_3 example

Let us immediately clarify the definitions given so far with a simple example.

Consider the A_3 Lie algebra, and a nilpotent element x lying in its subregular nilpotent orbit. The element x and its Slodowy slice are

$$\mathrm{x} = \begin{pmatrix} 0 & 1 & 0 & 0 \\ 0 & 0 & 1 & 0 \\ 0 & 0 & 0 & 0 \\ 0 & 0 & 0 & 0 \end{pmatrix}, \qquad \mathcal{S}_{\text{subreg}} = \left\{ \begin{pmatrix} a & 1 & 0 & 0 \\ b & a & 1 & 0 \\ c & b & a & d \\ e & 0 & 0 & -3a \end{pmatrix} \;\middle|\; a,b,c,d,e \in \mathbb{C} \right\}. \tag{3.93}$$

The Casimirs of the Slodowy slice read (3.93):

$$\begin{aligned} \chi_1(\mathcal{S}_{\text{subreg}}) &= 6a^2+2b, \\ \chi_2(\mathcal{S}_{\text{subreg}}) &= -8a^3+4ab+c, \\ \chi_3(\mathcal{S}_{\text{subreg}}) &= 21a^4+6a^2b+3ac+2b^2+de. \end{aligned} \tag{3.94}$$

We now compute $\mathcal{S}_{\text{subreg}} \cap \chi^{-1}(u)$:

$$\begin{cases} 6a^2+2b = u_1 \\ -8a^3+4ab+c = u_2 \\ 21a^4+6a^2b+3ac+2b^2+de = u_3 \end{cases} \Rightarrow -cd = (3a)^4 - u_1(3a)^2 + u_2(3a) - u_3 + \frac{u_1^2}{2}, \tag{3.95}$$

that is the usual presentation of the deformed A_3 singularity: if we set $u = c, v = -d, z = 3a$, we obtain

$$uv = z^4 - u_1 z^2 + u_2 z - u_3 + \frac{u_1^2}{2} \tag{3.96}$$

that matches (1.23) (up to an invertible redefinition of the coordinates in $\mathcal{T}/\mathcal{W}$).[11]

Now let us see the correspondence between Casimirs of the Levi and Casimirs of the Higgs explicitly, producing a threefold equation.

Take the following Higgs field in A_3:

$$\Phi = \begin{pmatrix} \varrho_2 & 1 & & \\ \varrho_1 & \varrho_2 & & \\ & & -\varrho_2 & 1 \\ & & \varrho_3 & -\varrho_2 \end{pmatrix}, \tag{3.97}$$

[11] The match works for $\sigma_2 = u_1, \sigma_3 = u_2, \sigma_4 = u_3 - u_1^2/2$.

and compute its Casimirs:

$$\begin{aligned}\chi_1(\Phi) &= \varrho_1+\varrho_3+2\varrho_2^2\\ \chi_2(\Phi) &= 2\varrho_2(\varrho_1-\varrho_3)\\ \chi_3(\Phi) &= \frac{1}{2}(\varrho_1+\varrho_3+2\varrho_2^2)^2-(\varrho_2^2-\varrho_1)(\varrho_2^2-\varrho_3)\end{aligned} \tag{3.98}$$

We substitute u_i with $\chi_i(\Phi)$ in (3.96), obtaining

$$uv = \left((z+\varrho_2)^2-\varrho_1\right)\left((z-\varrho_2)^2-\varrho_3\right). \tag{3.99}$$

One can check that the same equation can be obtained using directly (3.91). Finally, choosing a dependence of the $\varrho_i = \varrho_i(w)$, we obtain the equation of a threefold, which is a one-parameter deformation of the A_3 singularity.

In the next section, we finally recap the general recipe, for all the ADE cases, to explicitly build the Higgs backgrounds whose role we have examined so far.

3.9 Summary: the recipe to build Higgs backgrounds

Before driving towards the analysis of the physical relevance of the Higgs backgrounds we have learnt to build, it is instructive to pause for a moment and review the general recipe, for the A_n, D_n and E_6, E_7, E_8 cases, to explicitly realize the Higgs backgrounds of interest.

There are two possible starting points: either we are in possession of a threefold equation X that we aim to study, built as a one-parameter family of deformed ADE singularities (with parameter w), or we are not. In the first case, the general recipe goes as:

- Suppose that the maximal resolution pattern[12] of the threefold equation is known a priori[13].
- Given a resolution pattern inflating only the roots $\alpha_1, \ldots, \alpha_f$ of the corresponding algebra $\mathfrak{g}$, construct the Levi subalgebra that corresponds to such resolution using the Springer formalism. In general, the Levi subalgebra will be a sum of simple factors and of elements in the Cartan, dual to the roots $\alpha_1, \ldots, \alpha_f$:

$$\mathcal{L} = \bigoplus_h \mathcal{L}_h \oplus \mathcal{H}, \tag{3.100}$$

  where $\mathcal{L}_h$ are simple Lie algebras. We now want to select a vev for $\Phi(w)$ that allows the (simultaneous) resolution only of a choice of simple roots $\alpha_1, \ldots, \alpha_f$ of $\mathfrak{g}$. Rephrased

[12] I.e. the resolution inflating the maximal amount of unobstructed nodes in the corresponding ADE Dynkin diagram.

[13] If the threefold is non-singular, we can still go on with the construction thinking of it as if it were non-resolvable.

in the field theory language of Section 3.4.5, $\Phi(w)$ must be compatible with switching on a vev for ϕ_3 along the subalgebra

$$\mathcal{H} = \langle \alpha_1^*, ...\alpha_f^* \rangle . \tag{3.101}$$

Since $[\Phi(w), \phi_3] = 0$, then $\Phi(w)$ must live in the commutant of $\mathcal{H}$, that is precisely the Levi subalgebra (3.100).[14]

Summing up, the choice of the blown up simple roots selects an abelian subalgebra $\mathcal{H} \subset \mathfrak{g}$. This defines a Levi subalgebra $\mathcal{L} \subset \mathfrak{g}$, and $\Phi(w)$ should live in $\mathcal{L}$, according to the analysis based on Springer resolutions we have performed in the preceding sections:

$$\Phi(w) \in \mathcal{L} = \bigoplus_h \mathcal{L}_h \oplus \mathcal{H} \tag{3.102}$$

with $\mathcal{L}_h$ simple Lie algebras.

- Build a Higgs background $\Phi(w)$ in the newly-found Levi subalgebra, and fine-tune its coefficients in order to reproduce the threefold equation.

- The Casimir invariants of the Higgs field $\Phi(w)$ tell us how the ALE fiber is deformed, according to the correspondence between Casimirs and threefold equation established in Sections 3.4.6, 3.5.2, 3.6 for all the A, D, E cases.

- *Caveat (1)*: in case the resolution pattern of the threefold is not known, a recursive procedure must be employed: one attempts to build a Higgs background in the smallest Levi subalgebra, namely the one corresponding to a complete resolution. If this is not possible, a larger Levi subalgebra, corresponding to a partial resolution, is chosen, and the algorithm runs until a holomorphic Higgs reproducing the threefold equation is found. The Levi in which such Higgs lives determines the resolution pattern a posteriori

- *Caveat (2)*: we will see in Chapter 5 that in large classes of one-parameter deformed ADE singularities, namely for quasi-homogeneous cDV singularities, a quicker and more efficient way of extracting the Levi subalgebra (3.100) can be employed. In other words, in those cases we will be able to glean the resolution pattern solely by looking at the threefold equation. Furthermore, we will see how maximal subalgebras of (3.100) enter into the game.

- *Caveat (3)*: in general, the Higgs background is not unique, and T-brane backgrounds, either with different choices of coefficients in the Higgs entries, or less resolved 2-cycles (or a combination of the two phenomena) might be possible. In later chapters we will

[14] At the level of the effective 7d theory, the vev $\Phi(w)$ breaks the gauge algebra to its commutant $\mathcal{H}$. It is important that $\mathcal{H}$ is a subspace of the Cartan subalgebra of $\mathfrak{g}$. In fact, if the preserved algebra contained a simple factor $\mathfrak{g}'$, the vev $\Phi(w)$ would not deform the ADE singularity completely, but the fiber over generic w would have a singularity of type $\mathfrak{g}'$, i.e. X would have a non-isolated singularity.

see how to explicitly deal with such backgrounds, learning how to distinguish them on physical grounds.

On the other hand, we might wish to build a Higgs background encoding some physical properties of particular interest, without starting from a pre-established threefold. In this case, different techniques can be employed to build the Higgs background, but the core reasoning remains the same: Springer resolutions dictate which is the shape of the Higgs so as to achieve some resolution pattern. We shall see examples of such constructions in Chapter 4.

Part II

CHAPTER 4

GV invariants and 5d SCFTs from M-theory on simple threefold flops

In the course of this chapter we start reaping the fruits of the machinery that has been introduced in the course of the past pages. Our interest is devoted on a two-fold avenue:

- On the mathematical side, we are interested in computing the Gopakumar-Vafa (GV) invariants of classes of non-toric threefolds displaying isolated singularities, built as one-parameter families of ADE singularities.

- On the physical side, we aim at characterizing, as complex algebraic varieties, the Higgs branches of the 5d superconformal field theories (SCFTs) geometrically engineered by M-theory on the above-mentioned deformed ADE singularities.

The two aspects are better to be treated in an all-encompassing formalism, as they are intimately related to the same physical counterpart, namely the counting of BPS M2-brane states, as we will momentarily see. Schematically, we will proceed as follows:

(1) Fix a threefold X built as a one-parameter family of ADE singularities, and construct the associated Higgs background, following the recipe of Section 3.9.

(2) Compute the five-dimensional localized fluctuations of the Higgs background, as well as the unbroken flavor and gauge symmetries in 5d.

(3) Relate the above data to the GV invariants of the deformed family, and to the Higgs branch content of the 5d SCFT arising from M-theory on X.

Point (1) has been extensively introduced in the previous chapter: we are hence left to address point (2) and (3) explicitly. We will do this focusing on a class of deformed ADE families, known as *simple threefold flops*.

The chapter is organized as follows: in Section 4.1 we briefly review the definition of Gopakumar-Vafa invariants; in Section 4.2 we recap the most relevant properties of 5d SCFTs from M-theory geometric engineering; in Section 4.3 we state the main physical properties of the Higgs background Φ; in Section 4.4 we introduce the simple flops, namely the main singularities we will deal with in this chapter. In Section 4.5 and 4.6 we first show how to compute localized 5d modes and preserved symmetries for simple flops in the A and D series, characterizing their Higgs branch and GV invariants.

In 4.7 we pause and add some ingredients to the mix: we explain how we explicitly choose Higgs backgrounds for simple flops of all lengths and we introduce a new and more efficient algorithm to compute localized five-dimensional modes, corresponding to the GV and Higgs branch data. This will make computations compact and completely auotmatizable, via a Mathematica code. We then employ this procedure to analyze simple flops of lengths from 1 to 6 in Section 4.8, and conclude in Section 4.9 with some examples that go beyond the flops environment.

4.1 Gopakumar-Vafa invariants

The definition of the Gopakumar-Vafa topological invariants, first introduced in [8–10], is intimately related to the curve-counting problem in algebraic geometry, and in particular to the theory of Gromov-Witten invariants. A crystal clear pedagogical summary of the topic, approached from a physical perspective, is displayed e.g. in [152]. In this section, we quickly review the definition of GV invariants, focusing on their physical origin.

Gromov-Witten (GW) invariants are topological invariants counting holomorphic maps from a Riemann surface into a Calabi-Yau threefold target space. Such maps are not always easy to count, as their images are sometimes holomorphic curves in the target space, but sometimes they correspond to points, or to multicovered curves. Mathematically, this is translated into evaluating the properties of the moduli space of stable maps, from the Riemann surface to homology classes in the Calabi-Yau threefold, with marked points[1]. In general, GW invariants are rational numbers. In Figure 4.1 we sketch the geometrical setting that we are reviewing.

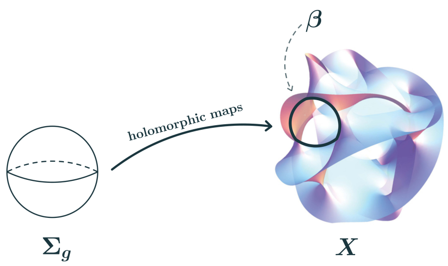

Figure 4.1: *GW invariants count holomorphic maps from a Riemann surface Σ_g of genus g to homology classes β in a Calabi-Yau threefold X.*

From the physical point of view, GW invariants possess a very precise meaning, as they

[1]Here, stability means that the automorphism group preserving the marked points is finite. For further details we refer to [152].

capture the non-perturbative part of the partition function of the topological string. Let us briefly sketch how this comes about.

The topological A-model [153] is a simplified model of closed strings that counts holomorphic maps from the worldsheet into a Calabi-Yau threefold target space. It has a striking relevance for physical considerations, as the A-model encodes corrections to the four-dimensional low-energy theory arising from Type IIA compactifications on compact Calabi-Yau threefolds. It can be shown [154] that the terms in the 4d effective action that are affected by the contributions due to the topological string amplitudes involve the Riemann tensor and ($2g-2$ copies of) the field strength of the graviphoton, which appears as the lowest component of the graviton multiplet. These terms take the form:

$$\int d^4x F_g(\mathbf{t}) R_+^2 F_+^{2g-2}, \tag{4.1}$$

where $\mathbf{t} = B+iJ$ is the complexified Kähler form, R_+ is the self-dual part of the Riemann tensor, and F_+ is the self-dual part of the field strength of the graviphoton. $F_g(\mathbf{t})$ is the genus g amplitude computed from the topological string. One can prove that the *full* expression for these terms, encompassing all non-perturbative contributions, is entirely characterized by the topological string partition function $F(\mathbf{t})$. Hence, after giving a vev $F_+ = g_s$ to the graviphoton field strength, with g_s the string coupling, the expression (4.1) summed over all-genus amplitudes takes the form:

$$\int d^4x R_+^2 F(\mathbf{t}), \tag{4.2}$$

where $F(\mathbf{t})$ is the total free energy for the A-model topological string. Explicitly, it can be written as a genus-sum of the form:

$$F(\mathbf{t}) = \sum_{g=0} F_g(\mathbf{t}) g_s^{2-2g} \,. \tag{4.3}$$

This sum splits

$$F(\mathbf{t}) = F_p(\mathbf{t}) + F_{GW}(\mathbf{t}) \tag{4.4}$$

into a perturbative part $F_p(\mathbf{t})$ and a worldsheet instanton part $F_{GW}(\mathbf{t})$. The perturbative part is a cubic polynomial in $\mathbf{t}$, and the non-perturbative part is a sum over exponentials. We will come to their physical interpretation momentarily.

Now, let us define a basis

$$[c_i] \in H_2^{\text{cpt}}(X, \mathbb{Z}) \,, \tag{4.5}$$

for the second homology of the Calabi-Yau threefold X with compact support. A general curve class can be written as $\beta = \sum_i d_i [c_i]$; we can also expand $\mathbf{t} = \sum_i t_i [c_i]^\vee$, where $\int_{c_i} [c_j]^\vee = \delta_i^j$. Defining a vector $\mathbf{d} = [d_1, \ldots, d_s]$, we can write the non-perturbative sum as follows:

$$F_{GW}(\mathbf{t}) = \sum_{g\geq 0}\sum_{\mathbf{d}} N^g_{\mathbf{d}} e^{-\mathbf{d}\cdot\mathbf{t}}, \tag{4.6}$$

where g is again the genus and $\mathbf{d}$ labels the classes in the threefold target space X. In (4.6), $N^g_{\mathbf{d}}$ is the Gromov-Witten invariant at degree $\mathbf{d}$ and genus g, which computes the virtual dimension of the moduli space of holomorphic maps from the worldsheet into the target space. As a result, the non-perturbative part of the topological string amplitude is completely characterized by the Gromov-Witten invariants of the compactification threefold.

Now, we would like to restate the Gromov-Witten generating series (4.6), obtained from the topological string, in terms of the physics of the 4d effective field theory obtained by the reduction of Type IIA.

In order to do so, one recurs to the formulation of Gopakumar and Vafa, [8–10], in which one looks not at the topological string, but at M-theory on the same CY threefold, employing its duality to Type IIA string theory. The key observation is that the topological string partition function (4.4) should be equivalently obtained from integrating out the degrees of freedom of Type IIA string theory, in a suitable fashion. Thus, we should be able to retrace the origin of the terms (4.1) from the 4d field theory perspective.

In this respect, notice that (4.1) is an amplitude involving graviton legs, as well as $2g-2$ graviphoton legs. In order to properly evaluate it, we should consider loop contributions from all the particles that are charged under the graviphoton. Such particles are precisely accounted for by D2-branes in the full Type IIA string theory.

These D2-branes may be wrapped on some curve of the Calabi-Yau threefold in the class $\beta \in H_2^{\mathrm{cpt}}(X,\mathbb{Z})$, or may wrap a trivial class. After a careful computation, one can show that unwrapped D2-branes and massless modes take care of reproducing the perturbative part of (4.4). We are most interested, though, on the non-perturbative contribution, due to wrapped D2-branes. These correspond to BPS states in the four-dimensional effective field theory, with mass given by the integral of the Kähler form J over the wrapped class β:

$$m = \frac{1}{g_s}\int_\beta J. \tag{4.7}$$

Being BPS, their charge q under the graviphoton equals their mass, namely $q = m$.

In M-theory, the D2-branes translate into wrapped M2-branes: actually, to every M2-brane there corresponds an infinite number of D2-branes, labelled by their momentum along the M-theory circle.

Resumming the contributions of the BPS states from D2-branes wrapped on the curve β, one can compute explicitly the amplitudes in (4.1) at all loops, and rewrite the Gromov-Witten generating function as a series depending on the BPS spectrum. This equals rearranging the non-perturbative part of the topological string free energy into an object that counts curves in the target space. Explicitly, (4.6) is recast into the form:

$$F_{GV}(\mathbf{t}, g_s) = \sum_{k=1}^{\infty} \sum_{g=0}^{\infty} \sum_{\mathbf{d}} \frac{n_{\mathbf{d}}^g}{k} (2\sin(kg_s/2))^{2g-2} e^{-k\mathbf{d}\cdot\mathbf{t}}, \quad (4.8)$$

where k is related to the momentum of the wrapped D2-branes along the M-theory circle. The function (4.8) now has a dependence on g_s. Formally we have the equivalence:

$$F_{GV}(\mathbf{t}, g_s) = F_{GW}(\mathbf{t}, g_s). \quad (4.9)$$

In (4.8), we are summing over homology classes $\beta \in H_2^{\text{cpct}}(X, \mathbb{Z})$ with compact support, i.e. over *degrees* $\mathbf{d} \in \mathbb{Z}$, and genera g. In addition, the degree represents a multiplicity of a homology class. The numbers $n_\beta^g \equiv n_{\mathbf{d}}^g$ are the *Gopakumar-Vafa invariants*, which are conjectured to be integers (and proven to be such in the genus 0 case [11]), in contrast with the rational Gromov-Witten invariants. Here, g denotes the genus of the curve in the class $\mathbf{d}$: this is *not* the genus of the Riemann surface Σ_g in the definition of the Gromov-Witten invariants[2].

All in all, we have reviewed the established GV/GW relationship:

$$\boxed{\text{GW (rational)}} \quad \longleftrightarrow \quad \boxed{\text{GV (integers)}} \quad (4.10)$$

Despite numerous attempts throughout the years, and great progress fostered by the connection of the theory of Gopakumar and Vafa to the properties of moduli spaces of sheaves in the PT/GV correspondence, a fully satisfactory mathematical formulation of GV invariants is, at present, lacking [12].

Nevertheless, from the physical viewpoint the integrality conjecture for GV invariants stands on reasonably firm ground, as it stems from the fact that, as we have seen in M-theory, these integers are counting BPS states that are realized as M2-branes wrapping holomorphic curves, that correspond to the D2-brane BPS states in Type IIA. Notice that β runs over all classes, and can therefore also run over multiples of a generator of H_2, i.e. possess a degree $\mathbf{d}$ with entries higher than 1. Those are interpreted as *bound states* of coincident M2-branes wrapping a curve. In the course of this work we will explicitly see the appearance of these bound states, as well as their physical meaning.

Each M2-state wrapping a holomorphic curve gives rise to a single particle state in the 5d effective field theory. In order to deduce what kind of super-multiplet describes such a particle, we refer to Witten's analysis, [129], which extracts the spin of the lowest component of the superfield by studying the moduli space of the holomorphic curve. The upshot for the purposes of this work is that a rigid curve gives rise to a *hypermultiplet* in the 5d theory arising from dimensional reduction of M-theory on a threefold singularity. By "rigid", we mean either a curve with a negative normal bundle, or one with some higher

[2]Unfortunately, this slight abuse of notation is vastly employed in the literature. More rigorously, we should denote $N_{\mathbf{d}}^g$ the GW invariants, and $n_{\mathbf{d}}^{g'}$ the GV invariants, where g and g' refer to the domain and the image curve (in the map $\Sigma_g \longrightarrow \beta \in H_2$), respectively.

order obstruction, such that its moduli space is a point. We will study situations with normal bundles $\mathcal{O}(-1)\oplus\mathcal{O}(-1)\,,\mathcal{O}(0)\oplus\mathcal{O}(-2)$ and $\mathcal{O}(1)\oplus\mathcal{O}(-3)$. In all cases, the curves will be rigid, so we will only have hypermultiplet content in our 5d theories.

The fact that the M2-brane BPS states, which are counted by GV invariants, give rise to hypermultiplets in 5d, is the key fact that allows us to investigate the Higgs branches of the 5d SCFTs arising from M-theory on one-parameter families of deformed ADE singularities. In the next section, we briefly recap the main properties that are relevant for our analysis.

4.2 5d SCFTs from singular threefolds: a lightning review

One of the key advancements in geometric engineering of the recent years is the realization that M-theory placed on top of a threefold with an isolated singularity gives rise to a superconformal field theory (SCFT) in five spacetime dimensions with $\mathcal{N}=1$ supersymmetry [29–31]. This is a remarkable statement, as it provides a way to investigate 5d SCFTs, which are generically challenging to study from a purely field-theoretic perspective. Furthermore, this is precisely the setting we are working in, as we are considering the dimensional reduction of M-theory on one-parameter singular families of deformed ADE singularities, that constitute a subclass of singular threefolds[3].

In general, in five spacetime dimensions the superconformal algebra with 8 supercharges is made up of the conformal group $SO(2,5)$, the R-symmetry group $SU(2)_R$, and a possible additional global symmetry group. As we briefly reviewed in Section 3.1, in five dimensions the lowest component of vector multiplets is made up of a *real* scalar, while the lowest components of hypermultiplets consist of a doublet of complex scalars, which are exchanged under $SU(2)_R$.

As we have seen in Section 3.2, M-theory on a singular K3 surface gives rise to a $\mathcal{N}=1$ theory with ADE gauge group in 7d. Analogously, M-theory on a singular threefold X can generate a 5d theory with ADE gauge group, and possibly some flavor symmetry. As a result, in general we might have to consider a 5d SCFT with both vector and hypermultiplets. Whenever we set to zero the vevs of the hypermultiplets, leaving only the real scalars of the vector multiplets switched on, we are probing the so-called Coulomb Branch of the 5d SCFT. On a generic point of the Coulomb Branch, the gauge group G is higgsed to a collection of abelian gauge factors $U(1)^r$, with r being the rank of G, and the $SU(2)_R$ symmetry is preserved.

On the other hand, if the real scalars in the vector multiplets are fixed to zero, letting the complex scalars in the hypermultiplets vary, we are roaming across the Higgs branch of the 5d SCFT, breaking the R-symmetry group $SU(2)_R$.

These moduli spaces have a neat interpretation in terms of the geometry of the singular

[3]For a precise definition of the so-called "canonical" singularities, that include our cases, we refer to [58].

threefold X, defined as a hypersurface equation in $\mathbb{C}^4$:

$$F(x,y,z,w)=0 \quad \subset \mathbb{C}^4 \tag{4.11}$$

on which M-theory is being reduced. In particular, the Coulomb Branch is in correspondence with the *resolutions* of the singularity, whereas the Higgs branch is encoded by the *deformation* theory of the singularity:

$$\begin{aligned} \textbf{Extended Coulomb Branch} &\leftrightarrow \quad \textbf{Resolutions} \text{ of } X \equiv X_{\text{res}} \\ \textbf{Higgs branch} \qquad\quad &\leftrightarrow \textbf{Deformations} \text{ of } X \equiv X_{\text{def}}, \end{aligned} \tag{4.12}$$

where we have introduced the *Extended* Coulomb Branch, that comprises also the mass deformations encoding the flavor symmetries. Let us delve deeper into the geometrical features of the resolutions and deformations of X, examining their physical counterpart.

The structure of X_{res} dictates the gauge and flavor symmetries in the underlying five-dimensional field theory. In particular, the exceptional divisors give rise to abelian gauge fields in the effective theory describing the Coulomb Branch. In general, for threefolds with an isolated singularity, we can write down the fiber of the singular point via its pre-image through the resolution map π:

$$\pi^{-1}(0)=\bigcup_{i=1}^{r} S_i, \tag{4.13}$$

where the S_i are a set of r exceptional divisors. By reducing the M-theory 3-form C_3 on the Poincaré duals of such divisors we find r massless abelian gauge bosons in five dimensions, yielding an effective description of the Coulomb Branch, on top of a generic value of the moduli, as a rank r $U(1)^r$ abelian theory. In addition, the resolution can also inflate a bunch of f 2-cycles, dual to non-compact divisors arising from the resolution, that reduce to non-Cartier divisors after the blow-down. Reduction of C_3 on the duals of such non-compact divisors generates vectors that do not propagate in five dimensions, due to the non-compactness of the divisor. As a consequence, these are interpreted as the bosons associated to flavor symmetries in five dimensions.

Summing up, we can write down the main cohomological objects of interest for the resolved singularity X_{res} [29–31, 59, 155, 156]:

$$\begin{aligned} &H_1(X_{\text{res}},\mathbb{R})=0 \qquad H_3(X_{\text{res}},\mathbb{R})=b_3 \\ &H_2(X_{\text{res}},\mathbb{R})=r+f \ \ H_4(X_{\text{res}},\mathbb{R})=r \end{aligned}, \tag{4.14}$$

where we have indicated that in general there can be b_3 non-trivial 3-cycles (although they will never appear in the cases under our scrutiny).

Keeping in mind these general features of threefold resolutions, in the following we will be exclusuively concerned with *rank-zero* theories, namely threefolds whose crepant resolution inflates no exceptional divisor (i.e. $r=0$), but possibly produces exceptional complex curves (that is, $f \geq 0$). In these cases, we speak of "small resolution". Working in this context, we expect that M-theory on such threefolds will produce five-dimensional theories with a trivial Coulomb Branch, and in general a non-trivial Higgs branch, subject to some flavor symmetries, depending on the value of f.

In particular, the Higgs branch of a 5d SCFT is a hyper-Kähler cone, characterized by its quaternionic dimension $d_{\mathbb{H}}$. As the Higgs branch moduli are the scalars in the hypermultiplets of the theory, we see that the dimension counting is sensible, as every 5d hypermultiplet contributes to the Higgs branch with two complex scalars, yielding a moduli space of quaternionic dimension.

As we have previously mentioned, the Higgs branch is geometrically encoded in the deformations of the singular threefold. In particular, the smooth deformed threefold X_{def} possesses a number of three-spheres S^3_i, with $i = 1, \dots \mu$, where μ is Milnor number of the threefold, which is the dimension of the coordinate ring:

$$\mu = \dim \frac{\mathbb{C}[x, y, z, w]}{(\partial_x F, \partial_y F, \partial_z F, \partial_w F)} \tag{4.15}$$

and that can be computed with standard methods [130]. One can then compute periods of the nowhere-vanishing holomorphic 3-form of the CY threefold Ω_3 on such three-spheres, obtaining a scalar in five spacetime dimensions:

$$q_i = \int_{S^3_i} \Omega_3. \tag{4.16}$$

Not all these scalars, though, are moduli of the 5d Higgs branch: only the ones corresponding to independent dynamical complex structure moduli, i.e. to *normalizable* deformations, span the Higgs branch. In particular, μ comprises both f *unpaired* compact 3-cycles (where f is the number of exceptional complex curves in X_{res}), as well as $2\hat{r}$ *paired* compact 3-cycles, namely:

$$\mu = 2\hat{r} + f. \tag{4.17}$$

Physically speaking, only $\hat{r}$ hypers corresponding to paired deformations are actual Higgs branch moduli, and hence the Higgs branch quaternionic dimension reads [19, 130, 157]:

$$d_{\mathbb{H}} = \hat{r} + f. \tag{4.18}$$

This coincides with the expected number of hypermultiplets in five dimensions. Besides, this can also be rewritten as a function of the Milnor number and of the number f of 2-cycles inflated by the small resolution:

$$d_{\mathbb{H}} = \frac{\mu + f}{2}. \tag{4.19}$$

In the next section we flesh out the physical details of our M-theory setups yielding rank-0 SCFTs in 5d, emphasizing the role of the Higgs field Φ that we have explored in Chapter 3.

4.3 The physical meaning of Φ

In the following sections, we will tackle the study of M-theory reduced on Calabi-Yau threefolds built as one-parameter families of deformed ADE singularities. As we have seen, this kind of setup geometrically engineers 5d theories. In particular, we will see that the singularity structure determines the spectrum of the 5d theory, and specifically its Higgs branch:

- The flavor group is given by the small resolution $U(1)$'s, corresponding to the f 2-cycles inflated by the resolution (one would get a simple group factor G when allowing non-isolated singularities and if one has a G-type singularity along a curve). Physically, this is the continuous symmetry left unbroken by the vev of Φ.

- The gauge group is given by compact divisors: in the setup we are considering this never happens. One would need a more severe degeneration of the ALE surface at the origin (e.g. the ALE surface should split into several components, while in our cases the ALE surface just develops a singularity). On the other hand, there can be discrete gaugings coming from the stabilizer of Φ.

- As we reviewed in Section 4.1, M2-branes wrapping the exceptional curves, which are rigid, give rise to hypermultiplets in 5d dimensions, charged under the flavor group. The number of hypermultiplets of charges $(d_1, ..., d_f)$ under the $U(1)^f$ flavor symmetry is the genus 0 GV invariant of degrees $(d_1, ..., d_f)$. Pictorially, we have the correspondences:

$$\begin{aligned} \text{Genus 0 GV invariants} \quad &\Leftrightarrow \quad \text{\# of hypermultiplets in 5d} \\ \text{Degrees of GV invariants} \quad &\Leftrightarrow \quad \text{flavor charges of hypermultiplets} \end{aligned}$$

Putting all this information together, namely identifying the number of hypermultiplets, the flavor and discrete groups, as well as their explicit actions on the hypermultiplets, we can completely characterize the Higgs branches of the 5d theory under consideration, as complex algebraic varieties. This is the physical core of this work, to which we will dedicate most of the subsequent efforts.

In this regard, all the heavy machinery we introduced in the previous chapters, relying on Slodowy slices and Springer resolutions, was needed in order to explicitly build a Higgs background Φ for all the cases of ADE deformed singularities, allowing us to extract the aforementioned physical observables.

In the next sections, we will concretely employ this technique in the case of simple threefold flops, a large class of deformed ADE families exhibiting interesting physical properties, that we introduce in the next pages.

4.4 Higgs branch and GV invariants: simple flops

One-parameter deformations of ADE surfaces with an isolated singularity admitting a small crepant simultaneous resolution blowing up a single $\mathbb{P}^1$ are known as simple threefold flops. In the language of Section 4.2, we have only an exceptional rigid complex curve, and so:

$$r = 0, \qquad f = 1. \tag{4.20}$$

Hence, M-theory on simple threefold flops geometrically engineers rank-0 5d $\mathcal{N} = 1$ SCFTs with $U(1)$ flavor group (and possibly some discrete gauging group, as we will see later).

Simple flops appear ubiquitously both in the physical and mathematical literature [87–92,158–160], and encode *all* the properties of more general deformed ADE singularities that we will encounter in this work. They are classified by the *length* invariant, that we will momentarily define.

For these reasons, they constitute the protagonists of the next sections, that, as we have delineated at the beginning of this chapter, have as main objectives:

- The characterization of the GV invariants of simple threefold flops of all lengths.
- The computation of the Higgs branch of 5d $\mathcal{N} = 1$ SCFTs arising from M-theory geometric engineering on simple threefold flops of all lengths.

Let us start by reviewing some additional details about the classification of simple flops.

4.4.1 Simple flops and their *length*

The fact that simple flops admit only a partial simultaneous resolution inflating a single $\mathbb{P}^1$ means, as a consequence of the Weyl theory introduced in Chapter 1, that we can write them as deformed ADE singularities with the deformations parametrized by coordinates $\varrho_i \in \mathcal{T}/\mathcal{W}'$. $\mathcal{W}'$ is the Weyl group generated by all the roots that are not inflated by the small simultaneous resolution, corresponding to the white nodes in Figure 4.2, and choosing a dependence $\varrho_i(w)$ produces a threefold. As a consequence, the simple threefold flops can generically be written as a hypersurface of the form:

$$F\left(x, y, z, \varrho_1(w), ..., \varrho_n(w)\right) = 0, \tag{4.21}$$

where $F\left(x, y, z, \varrho_1, ..., \varrho_n\right) = 0$ is the defining equation of the $(n+2)$-dimensional family built as the versal deformation of an ADE singularity (n is the rank of the ADE algebra). In the language of Section 3.4.5, in order to produce a simultaneous resolution inflating a single node (namely, a simple flop) we must switch on a vev for ϕ_3 along:

$$\mathcal{H} = \langle \alpha_c^* \rangle, \tag{4.22}$$

where α_c^* is the resolved node.

From a mathematical point of view, threefold simple flops can be classified according to a variety of invariants.

The first, and coarsest, invariant that can be associated to a simple flop is the normal bundle $\mathcal{N}_{\mathbb{P}^1}$ to the exceptional $\mathbb{P}^1$. Laufer [161] showed that $\mathcal{N}_{\mathbb{P}^1}$ can be only of three types:

$$\mathcal{O}(-1)\oplus\mathcal{O}(-1), \qquad \mathcal{O}(0)\oplus\mathcal{O}(-2), \qquad \mathcal{O}(1)\oplus\mathcal{O}(-3). \tag{4.23}$$

The conifold (3.25) is the only example admitting a small resolution inflating an exceptional $\mathbb{P}^1$ with normal bundle $\mathcal{N}_{\mathbb{P}^1} = \mathcal{O}(-1)\oplus\mathcal{O}(-1)$. The Reid's pagodas [162], that we will analyze momentarily, locally classify all cases with $\mathcal{N}_{\mathbb{P}^1} = \mathcal{O}(0)\oplus\mathcal{O}(-2)$. Finally, all the other simple flops inflate a $\mathbb{P}^1$ with normal bundle $\mathcal{N}_{\mathbb{P}^1} = \mathcal{O}(1)\oplus\mathcal{O}(-3)$. Although useful, the normal bundle is not a sufficiently refined invariant to distinguish the different physical properties of the simple flops that we are going to scrutinize.

A rich classification of simple flops can be obtained employing the so-called *length* invariant, first introduced in [163]. Consider a singular deformed ADE singularity X and a small simultaneous resolution inflating a single $\mathbb{P}^1$, given by the map π:

$$Y \xrightarrow{\pi} X \quad \text{with:} \quad \pi^{-1}(p) = \mathbb{P}^1, \tag{4.24}$$

where p is the singular point of X. Then, we can define the length of a flop as an invariant related to a multiplicity that can be attributed to the exceptional $\mathbb{P}^1$. If, e.g., one pulls back the skyscraper sheaf corresponding to the singular point of the conifold w.r.t. the blow-down map, one will get the structure sheaf of the exceptional curve:

$$\pi^*(\mathcal{O}_p) = \mathcal{O}_{\mathbb{P}^1}\,, \tag{4.25}$$

where the length l is the multiplicity of $\mathcal{O}_{\mathbb{P}^1}$ (namely, in the case of the conifold, $l = 1$).

It was proven (see [111]) that the length of a simple flop can only assume discrete values ranging from 1 to 6, and that examples of any length indeed exist, i.e. there are cases in which the pull-back of the skyscraper sheaf reads:

$$\pi^*(\mathcal{O}_p) = \mathcal{O}_{\mathbb{P}^1}^{\oplus l} \quad \text{with } l = 1, \ldots, 6. \tag{4.26}$$

Even though the above definition may appear rather obscure, the length has a very concrete physical meaning: as we will see later, when we geometrically engineer 5d SCFTs from M-theory on simple threefold flops described as deformed ADE singularities, we find that the length of the simple flop is nothing but the *maximal flavor charge* of the 5d hypermultiplets arising from M2 branes wrapped on the exceptional $\mathbb{P}^1$.

From a Lie-algebraic point of view, the length of a simple flop corresponds to the dual Coxeter label of the node of the Dynkin diagram that is being resolved by the small si-

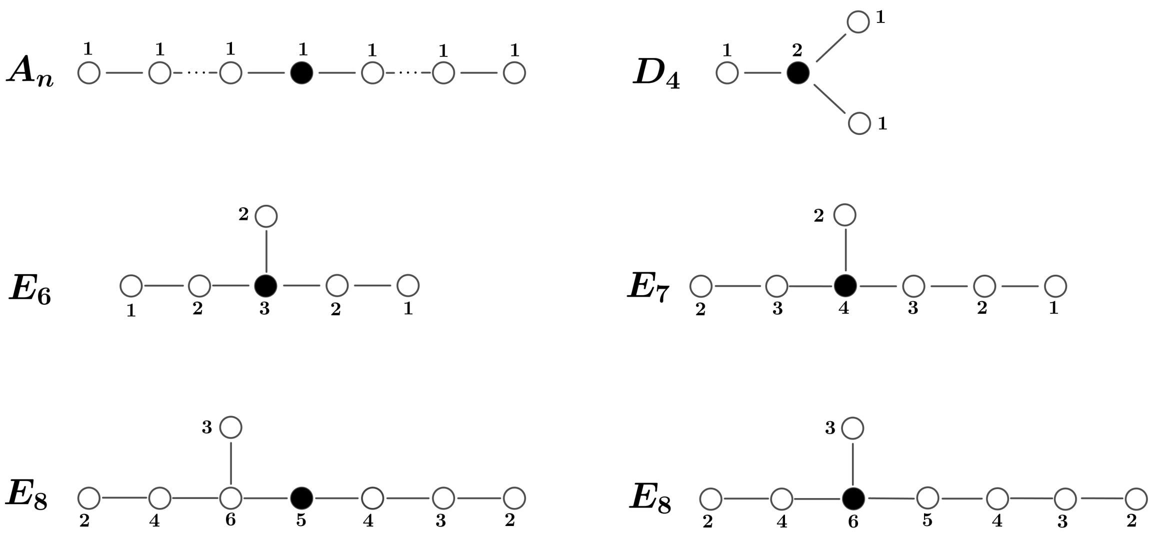

Figure 4.2: *ADE Dynkin diagrams and dual Coxeter labels of the nodes.*

multaneous resolution. Given an ADE algebra $\mathfrak{g}$ of rank n, a set of simple roots α_i, with $i = 1, \ldots n$, and the highest root θ, the dual Coxeter label of a node is the multiplicity of the corresponding simple root in the decomposition of the highest root. In other words, given a node corresponding to a simple root α_{i_0} and the decomposition of the highest root

$$\theta = \mathfrak{q}_{\alpha_1}\alpha_1 + \ldots + \mathfrak{q}_{\alpha_{i_0}}\alpha_{i_0} + \ldots + \mathfrak{q}_{\alpha_n}\alpha_n \tag{4.27}$$

then $\mathfrak{q}_{\alpha_{i_0}}$ is the dual Coxeter label of the node. As we will use this fact extensively in the explicit constructions of simple threefold flops of length up to 6, it is useful to report the Dynkin diagrams of all the ADE cases, along with the dual Coxeter labels of their nodes in Figure 4.2, where we have highlighted in black the nodes that are being resolved in the simple threefold flops that we will analyze in the following sections.

The classification of simple threefold flops based on the length can be further refined introducing the Gopakumar-Vafa (GV) invariants [8–10]. These invariants can be used to distinguish between simple flops of the same length[4].

We will see that the flavor charges in the 5d SCFT from M-theory on the simple flops correspond to the degrees of the GV invariants of the simple flops, namely:

$$n_d^{g=0} = \#\ \text{5d hypers with charge } d \text{ under the flavor group generated by the resolved node,} \tag{4.28}$$

[4] Even though we will not use this notion in this thesis, it is worth mentioning an even subtler invariant that can be associated to a simple flop, namely its contraction algebra. It has been proven [92] that there exist simple flops with the same normal bundle, same length, same Gopakumar-Vafa invariants and *different* contraction algebra. Physically, the contraction algebra can be understood, for example, as describing the quiver relations of the theory on a D3 brane in type IIB probing the singularity, and explicit constructions of contraction algebras at all lengths can be found in [91].

where d labels the class of the resolved curve of the simple flop.

As the charges are related to the dual Coxeter labels, we have a web of correspondences:

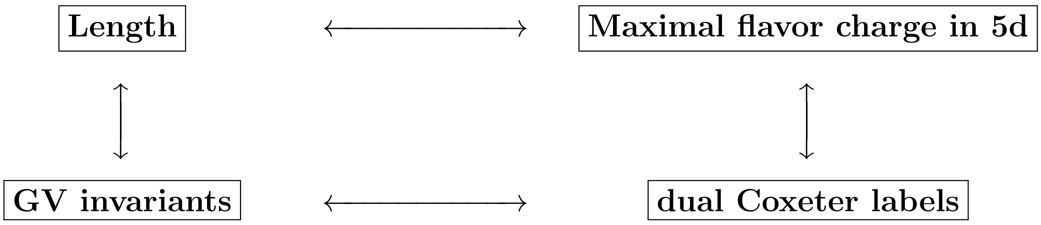

Figure 4.3: *Correspondences between invariants of flops, physical flavor charges and Lie algebra labels.*

We will explicitly witness these phenomena in the explicit computations of the next sections.

We start in the upcoming section by looking at how to carry out the zero-mode computation, as well as the identification of the preserved flavor group in 5d, in all details, starting from the example of the conifold.

4.5 Simple flops of length 1

4.5.1 The conifold example

In this section, we introduce the simplest possible example of simple flop, computing the Higgs branch of the 5d theory engineered by M-theory on the conifold. We will also see how this equals computing the GV invariants of the conifold singularity.

We define the conifold as the following hypersurface in $\mathbb{C}^4$ (of the form (4.21)):

$$uv = z^2 - w^2 \quad \subset \quad \mathbb{C}^4[u, v, z, w] \,. \tag{4.29}$$

As we have seen, it is a one-parameter family (with parameter w) of deformed A_1 Du Val singularities.

The conifold admits one normalizable deformation

$$uv = z^2 - w^2 + \mu \,, \quad \text{with} \quad \mu \in \mathbb{C} \,. \tag{4.30}$$

This mode sits in $H^3(X, \mathbb{C})$, where X is the threefold defined in (4.30). After deforming, a 3-sphere A is created, and the dual non-compact 3-cycle B intersects A at a point. In terms of the holomorphic 3-form Ω_3, we can think of the value of μ as the period

$$\mu := \int_A \Omega_3 \,. \tag{4.31}$$

In terms of Poincaré dual 3-forms α and β, we have that

$$\int_X \alpha\wedge\beta = 1. \tag{4.32}$$

The supergravity C_3-field can thus be reduced along these forms as

$$C_3 = a\alpha + b\beta\,, \tag{4.33}$$

where (a, b) form a pair of real Wilson lines for the 3-form. We can now combine all four real degrees of freedom (μ, a, b) into a single five-dimensional hypermultiplet. The Higgs branch for this theory is a single-centered Taub-Nut space, of quaternionic dimension *one*:

$$\mathcal{M}_{\text{HB}} = \text{TN}_1 \cong \mathbb{H}\,. \tag{4.34}$$

This is a special case of the multi-centered hyper-Kähler Taub-NUT space we have already encountered in the study of stacks of D6-branes. Here this space describes a branch of the moduli space.

Let us see how this result comes about using our techniques employing the duality between M-theory on $\mathbb{C}^*$-fibered threefolds and IIA string theory in the presence of D6-branes. In this case, the $uv = \ldots$ form of our hypersurface shows us that the conifold is indeed $\mathbb{C}^*$-fibered, and that the circle in $\mathbb{C}^* \cong \mathbb{R}\times S^1$ collapses wherever the r.h.s. vanishes, i.e. over the reducible locus

$$\text{D6}-\text{locus}: \quad (z-w)(z+w) = 0\,. \tag{4.35}$$

As we have seen in Section 3.4.6, the M-theory uplift is given by a $\mathbb{C}^*$-fibration that collapses over the spectral curve of Φ as follows:

$$uv = \det\left(z\mathbb{1}_2 - \Phi\right) = z^2\,. \tag{4.36}$$

In this case, the geometry is that of a local K3 with an A_1-singularity times a complex plane generated by w. This describes 7d $\mathcal{N} = 1$ SYM. Now consider switching on the following position-dependent vev for the Higgs background Φ:

$$\Phi = \begin{pmatrix} w & 0 \\ 0 & -w \end{pmatrix}, \tag{4.37}$$

where we have chosen it to lie along the Cartan subalgebra, i.e. the Levi subalgebra corresponding to the simultaneous Springer resolution of the only node of the A_1 Dynkin diagram. In the approach of Section 3.9, we are switching on a vev for ϕ_3 along the algebra:

$$\mathcal{H} = \langle \alpha^* \rangle, \tag{4.38}$$

where α is the only root of A_1. This implies, according to the principles outlined in Section

3.9, that we must switch on a vev for Φ along the Levi subalgebra

$$\mathcal{L} = \langle \alpha^* \rangle = \mathcal{H}, \tag{4.39}$$

which is precisely the case for (4.37).

The vev (4.37) breaks $SU(2) \mapsto U(1)$, although the group enhances back to $SU(2)$ at the origin $(w, z) = (0, 0)$. Explicitly, the 5d flavor group is given by the stabilizer of Φ, and reads:

$$G_{5d} = \begin{pmatrix} \lambda & 0 \\ 0 & \lambda^{-1} \end{pmatrix}. \tag{4.40}$$

Now we have two intersecting branes, and the M-theory geometry is given by the threefold:

$$uv = z^2 - w^2 \quad \subset \quad \mathbb{C}^4 . \tag{4.41}$$

As a consequence, supersymmetry is broken to eight supercharges. In order to compute the hypermultiplets in the 5d theory, we use the linearized equations of motion in holomorphic gauge for the fluctuation field φ of the Higgs, as explained in the seven-brane case in [94]:

$$\partial \varphi = 0 \qquad \varphi \sim \varphi + [\Phi, g] , \tag{4.42}$$

where g are complexified matrices in A_1, i.e. $g \in \mathfrak{sl}(2)$.

Equation (4.42) is the key formula that allows us to find localized zero-modes in a systematic, and purely linearly-algebraic, way. Physically, it is telling us that the 5d hypermultiplets can be computed as the zero-modes of fluctuations of the Higgs background $\Phi(w)$, that are localized near $z = w = 0$ after the gauge fixing, i.e. that are genuinely five-dimensional. Whenever a Type IIA interpretation is available (namely, in the A and D cases, as we will see) such zero-modes correspond to open string states stretching between the D6-branes.

Going back to the computation, and parametrizing both the fluctuation and gauge parameter as follows:

$$\varphi = \begin{pmatrix} \varphi_0 & \varphi_+ \\ \varphi_- & -\varphi_0 \end{pmatrix}, \qquad g = \tfrac{1}{2} \begin{pmatrix} g_0 & g_+ \\ g_- & -g_0 \end{pmatrix}, \tag{4.43}$$

we deduce that

$$\varphi \sim \varphi + w \begin{pmatrix} 0 & g_+ \\ -g_- & 0 \end{pmatrix}. \tag{4.44}$$

This tells us a few things. First, that we can have 7d fluctuations given by φ_0. Most importantly, that the fluctuations $\varphi_\pm$ are defined up to any multiple of w. This means that they are localized on the $(w, z) = (0, 0)$ locus, and are therefore genuinely 5d dynamical fields:

$$\varphi_\pm \in \mathbb{C}[w]/(w) \cong \mathbb{C} . \tag{4.45}$$

It is also immediate to check that φ_+ and φ_- have charge ± 1 under the flavor group (4.40).

As a result, we checked that the Higgs branch of the conifold is:

$$\mathcal{M}_{\rm HB} = \mathbb{C}^2. \tag{4.46}$$

We can also see this explicitly from the deformation theory of the conifold singularity: the pair (φ_+, φ_-) forms a free hypermultiplet, as expected. If we switch on a vev for this pair, namely:

$$\Phi(w) \to \Phi(w) = \begin{pmatrix} w & \varphi_+ \\ \varphi_- & -w \end{pmatrix}, \tag{4.47}$$

then the M-theory geometry deforms as follows:

$$uv = z^2 - w^2 - \varphi_+\varphi_- \,. \tag{4.48}$$

Therefore, we see that there is a projection from the full hypermultiplet moduli space onto the complex structure moduli space of the conifold

$$\pi : (\varphi_+, \varphi_-) \longrightarrow \mu := \varphi_+\varphi_- \,. \tag{4.49}$$

This map defines the Higgs branch as a $\mathbb{C}^*$-fibration over the complex structure moduli space, whereby the fibers contain the data about the C_3 Wilson lines. From the brane perspective this is understood from the fact that there is an action

$$(\varphi_+, \varphi_-) \mapsto (\lambda\varphi_+, \lambda^{-1}\varphi_-)\,, \tag{4.50}$$

where λ is a parameter in the complexified flavor group $U(1)_{\mathbb{C}} \cong \mathbb{C}^*$. So, if we recombine the two D6-branes, we will get a single brane in the shape of a throat (diffeomorphic to a cylinder), as it can be seen from the right hand side of (4.48). One can then define two Wilson lines for the worldvolume gauge field: one along the compact 1-cycle, and one along the non-compact 1-cycle. This uplifts in M-theory to the two Wilson lines of the supergravity C_3 form on the S^3, and its dual non-compact 3-cycle.

The Higgs branch computation we have carried out has also a topological meaning for the conifold hypersurface, as counting open string states between the D6-branes uplifts in M-theory to counting BPS states coming from M2-branes wrapped on the exceptional 2-cycle, which are nothing but the genus 0 GV invariants. As a result, we have reproduced the result [86] that the GV invariant of the conifold is:

$$n^{g=0}_{d=1} = 1\,. \tag{4.51}$$

It is of genus 0 because we are wrapping 2-cycles isomorphic to $\mathbb{P}^1$, and of degree 1 because of the charge of the hypermultiplets under the flavor group.

Notice that there is a correspondence between the flavor charge of the hyper under (4.40), which is 1, the length of the simple flop corresponding the conifold, the degree of the conifold

GV invariant and the dual Coxeter label of the A_1 Dynkin diagram (all equal to 1), as we anticipated in Figure 4.3.

4.5.2 More general deformed A_n singularities

The conifold presented in the previous section is a particular example of a family of A-type ALE spaces, parametrized by the parameter w. At $w = 0$ the equation (4.29) describes an ALE surface with a A_1 singularity at the origin; at generic value of w the singularity is deformed.

Let us generalize it to an A_{n-1} type ALE family. In Chapter 1 we have seen that the generic A_{n-1} singularity has the form:

$$uv = z^n. \tag{4.52}$$

Its versal deformation is

$$uv = z^n + \sum_{i=2}^{n} (-1)^i \sigma_i z^{n-i}. \tag{4.53}$$

This space is a fibration with fiber given by the (deformed) A_{n-1} surface and base the space $\mathcal{T}/\mathcal{W}$ of gauge invariant coordinates σ_i $(i = 2, ..., n)$[5] on the Lie algebra $\mathfrak{sl}(n)$, where $\mathcal{T}$ is the Cartan subalgebra and $\mathcal{W}$ the Weyl group. The space (4.53) is non-singular. However, as we reviewed in Chapter 1, by making a *base change*, one can obtain a singular space whose resolution blows up a subset of the roots of the central ALE fiber.

For generic n, making a base change from $\mathcal{T}/\mathcal{W}$ to $\mathcal{T}$, hence obtaining the expression in equation (1.24), resolves all the simple roots of A_{n-1} in the central fiber. One can also make a partial simultaneous resolution in which the base change maps the base $\mathcal{T}/\mathcal{W}$ to $\mathcal{T}/\mathcal{W}'$, where $\mathcal{W}' \subset \mathcal{W}$. In this case, the resolution of the family blows up the roots that are left invariant by $\mathcal{W}'$, in the central fiber. The base of the fibration is now parametrized by the $n-1$ $\mathcal{W}'$ invariants, that we call ϱ_i $(i = 1, ..., n-1)$.

In this section, we wish to construct a variety with a small resolution blowing up a single $\mathbb{P}^1$, namely a simple flop. To this end, one chooses a Weyl subgroup $\mathcal{W}'$ that leaves only one simple root of the A_{n-1} root system invariant.

The M-theory threefolds are obtained from these families by making the invariant coordinates ϱ_i depend (linearly)[6] on the parameter w.

From the Springer resolution perspective, this means switching on a vev for the Higgs background Φ in the Levi subalgebra corresponding to the simultaneous resolution of only one of the roots, say α_c. In the field-theory language, this implies turning on a vev for ϕ_3,

[5] The invariant σ_i is the i-th elementary symmetric polynomial in the eigenvalues of an element of the Lie algebra.

[6] Other dependences are indeed possible. However, we will stick to linear in order to avoid creating further singularities in the resulting threefolds.

with $[\Phi, \phi_3] = 0$, along the Cartan corresponding to the resolved root, i.e.

$$\mathcal{H} = \langle \alpha_c^* \rangle. \tag{4.54}$$

As we have seen in Section 3.4.5, a vev for ϕ_3 corresponds to the resolution of the singularity of the family in M-theory, that is the resolution of the roots of the ALE fiber left invariant by $\mathcal{W}'$, compatibly with the Springer resolution picture. Hence, the generic field Φ corresponding to a given partial simultaneous resolution is an element of the Lie algebra that commutes with the Cartan generators dual to the resolvable roots of the central fiber.

Let us exhibit a concrete example, taking into consideration the Dynkin diagram of A_{n-1}: say that we want a simultaneous resolution of the simple root α_c $(1 \leq c \leq n-1)$. Then ϕ_3 must live along the Cartan

$$\phi_3 \propto \begin{pmatrix} \frac{1}{c}\mathbb{1}_c & 0 \\ 0 & -\frac{1}{n-c}\mathbb{1}_{n-c} \end{pmatrix}, \tag{4.55}$$

and the generic Φ relative to the simultaneous resolution of α_c must live in the Levi subalgebra that commutes with $\langle \alpha_c^* \rangle$:

$$\mathcal{L} = A_{c-1} \oplus A_{n-c-1} \oplus \langle \alpha_c^* \rangle. \tag{4.56}$$

Explicitly, it will be of the form:

$$\Phi = \begin{pmatrix} \Phi_{c\times c} & 0 \\ 0 & \Phi_{(n-c)\times(n-c)} \end{pmatrix} \in \mathfrak{sl}(n). \tag{4.57}$$

The Casimirs of such Higgs field are the ϱ_i $(i = 1, ..., n-1)$ $\mathcal{W}'$-invariant coordinates, where $\mathcal{W}'$ is the Weyl subgroup that leaves the simple root α_c invariant. For the moment, we take each block to be in the shape of a *reconstructible Higgs* (following the nomenclature of [94])[7], that can be written (up to a gauge transformation) in a canonical form that depends directly on the "partial" Casimirs $\hat{\varrho}_i$. In particular, for a $\mathfrak{u}(m)$ block we have [94]:

$$\Phi_{m\times m} = \begin{pmatrix} 0 & 1 & 0 & \cdots & 0 \\ 0 & 0 & 1 & 0 & 0 \\ \vdots & 0 & \ddots & \ddots & 0 \\ 0 & 0 & 0 & 0 & 1 \\ (-1)^{m-1}\hat{\varrho}_m & (-1)^{m-2}\hat{\varrho}_{m-1} & \cdots & -\hat{\varrho}_2 & 0 \end{pmatrix} \tag{4.58}$$

with $\hat{\varrho}_j$ $(j = 2, ..., m)$ the Casimirs of $\Phi_{m\times m}$. The Casimirs ϱ_i $(i = 1, ..., n-1)$ of the block-diagonal total Φ are given by the collection of $\hat{\varrho}_j$'s of each block and the Casimir $\hat{\rho}$ related to the Cartan $\langle \alpha_c^* \rangle$. Consequently, the total Casimirs σ_i's can be written as functions of the

[7] This choice is by no means necessary, and simply ensures that no terminal singularities remain after the partial simultaneous resolution of the singularity.

partial Casimirs ϱ_i's.

Given the total Φ, whose entries depend on the Casimirs σ_i, we have shown that the M-theory uplift that describes the family equation (4.53) is produced by:

$$uv = \det\left(z\mathbb{1}_n - \Phi\right). \tag{4.59}$$

When we make the choice $\sigma_i = \sigma_i(w)$, we obtain the equation of a threefold. It is of the form of a $\mathbb{C}^*$-fibration. The D6-brane locus is then given by

$$\Delta_{D6} \equiv \det\left(z\mathbb{1}_n - \Phi(w)\right) = 0. \tag{4.60}$$

In the next section, we specialize the mode computation to a particularly relevant class of threefold hypersurface singularities, known as *Reid's pagodas* [162].

4.5.3 Reid's pagodas

Reid's pagodas are a class of singular CY threefolds that admit simple flops, meaning that only one exceptional $\mathbb{P}^1$ is produced. It is defined as the following hypersurface:

$$uv = z^{2k} - w^2 \qquad \subset \qquad \mathbb{C}^4[u, v, z, w]. \tag{4.61}$$

This geometry admits k normalizable deformations, and hence we expect the Higgs branch to be quaternionic k-dimensional. However, it is very difficult to explicitly construct the Higgs branch starting from this threefold data. We know from the supergravity analysis, that it is given by a $(\mathbb{C}^*)^k$-fibration over $\mathbb{C}^k$, whereby the base corresponds to complex structure moduli deformations, and the fiber corresponds to periods of C_3 on the various 3-cycles created by the deformations. But getting the global data of this variety is not straightforward.

Let us apply what we have learnt in the preceding sections. The threefold (4.61) is an ALE family that is singular at the origin, where the ALE fiber develops an A_{2k-1} singularity. Resolving the singularity blows up one exceptional $\mathbb{P}^1$, i.e. we have a simple flop. The root of the singular central fiber that is simultaneously resolved is[8] α_k. We then have:

$$\mathcal{H} = \langle \alpha_k^* \rangle. \tag{4.62}$$

This M-theory background is reduced in IIA to a system of $2k$ D6-branes Higgsed by a Φ of the form (4.57) with $n = 2k$ and $c = k$. The $\mathcal{W}'$-invariant Casimirs are:

$$\varrho_i = \begin{cases} \hat{\varrho}_i^{(1)}, & i = 2, \dots, k \\ \hat{\varrho}_i^{(2)}, & i = 2, \dots, k \\ \hat{\rho} & \end{cases}, \tag{4.63}$$

[8]In the convention that α_1 is the left root in the Dynkin diagram of A_{2k-1}, α_2 is the next one and so on.

where the superscripts refer to the Casimirs of the two blocks in (4.57), and $\hat{\rho}$ is the Casimir of the Cartan. Moreover, to obtain (4.61) one makes the choice

$$\hat{\rho} = \hat{\varrho}_j^{(1)} = \hat{\varrho}_j^{(2)} = 0 \;\text{ for }\; j = 2, ..., k-1 \qquad \text{and} \qquad \hat{\varrho}_k^{(1)} = -\hat{\varrho}_k^{(2)} = w.$$

Hence

$$\Phi = \begin{pmatrix} J_+ & 0 \\ 0 & J_- \end{pmatrix}, \qquad \text{where} \qquad J_\pm := \begin{pmatrix} 0 & 1 & & \\ & & \ddots & \\ & & & 1 \\ \pm w & & \dots & 0 \end{pmatrix}_k . \tag{4.64}$$

$J_\pm$ is the $k \times k$ Jordan block plus $(\pm w)$ in the $(k,1)$-entry.

The D6-branes live on a divisor in $\mathbb{C}^2$ given by:

$$\det(z \cdot \mathbb{1}_{2k} - \Phi) \equiv z^{2k} - w^2 = (z^k + w)(z^k - w) = 0\,. \tag{4.65}$$

Notice that this is again reducible, like for the conifold. However, the two components do not intersect transversely, so the open string spectrum will not be obvious.

The first thing we want to study is the effective gauge group in five dimensions. We will see that it is a discrete group. Our background vev breaks the original seven-dimensional worldvolume $SU(2k)$ gauge symmetry to a subgroup. Here we assume that before switching on the vev (4.64), the M-theory background is a A_{2k-1} ALE space, leading to a seven-dimensional gauge theory with $SU(2k)$ group. In other words the dual type IIA string coupling has been sent to infinity. With a different choice of discrete data one may start with the gauge group $SU(2k)/\mathbb{Z}_{2k}$ and obtain a different preserved group[9].

Choosing $SU(2k)$ for the global form, we find that the preserved group is given by the following $2k \times 2k$ matrices

$$\begin{pmatrix} e^{i\alpha_1}\,\mathbb{1}_k & 0 \\ 0 & e^{i\alpha_2}\,\mathbb{1}_k \end{pmatrix} \in U(1)_1 \times U(1)_2 \qquad \text{with} \qquad \alpha_1 + \alpha_2 = \frac{2\pi n}{k} \qquad n = 0, 1, ..., k-1\,. \tag{4.66}$$

Therefore, our background Higgses as follows:

$$SU(2k) \longrightarrow U(1) \times \mathbb{Z}_k\,. \tag{4.67}$$

It is generated by a continuous $U(1)$ subgroup $(n = 0)$ and a $\mathbb{Z}_k$ subgroup, that we can take to be

$$\mathbb{Z}_k : \begin{pmatrix} e^{2\pi i n/k} \cdot \mathbb{1}_k & \\ & \mathbb{1}_k \end{pmatrix}, \quad n = 0, \dots, k-1\,. \tag{4.68}$$

[9]See [76, 149] for a clear exposition of these choices, and [164, 165] for the seminal work.

Had we chosen $SU(2k)/\mathbb{Z}_{2k}$ for the global form, we would have simply obtained the Higgsing:

$$SU(2k)/\mathbb{Z}_{2k} \longrightarrow U(1), \tag{4.69}$$

and no discrete group.

So far, we have discussed the seven-dimensional perspective, and the product (4.67), obtained with the $SU(2k)$ global form, is the gauge group. In order to deduce the five-dimensional flavor and gauge symmetries, we proceed in two steps: first we compactify all directions transverse to the matter locus on a torus. This yields a 5d theory with *gauge group* $U(1)\times\mathbb{Z}_k$. Now we take a decompactification limit. This will ungauge the continuous $U(1)$ factor as the volume tends to infinity. The discrete part, however, having no gauge coupling, will remain gauged from the 5d perspective. To summarize:

$$U(1)_{\text{gauge}}\times(\mathbb{Z}_k)_{\text{gauge}} \longrightarrow U(1)_{\text{flavor}}\times(\mathbb{Z}_k)_{\text{gauge}}\,. \tag{4.70}$$

Here, one might wonder, whether the full flavor group could be bigger. However, since the IIA setup is built entirely with D-branes, where all flavor (ungauged) groups are derived from the open string picture, we claim that the above group captures the full flavor group. Now we wish to understand the Higgs branch. This consists in all possible deformations of the background Higgs field, modulo linearized gauge transformations

$$\varphi \sim \varphi+[\Phi, g]\,, \tag{4.71}$$

for any broken generator $g \in \mathfrak{sl}(2k)$. Let us write g and φ in the block form

$$g = \begin{pmatrix} \alpha & \beta \\ \gamma & \delta \end{pmatrix}, \qquad \varphi = \begin{pmatrix} \varphi^\alpha & \varphi^\beta \\ \varphi^\gamma & \varphi^\delta \end{pmatrix} \tag{4.72}$$

where each block is a $k\times k$ matrix and $\text{Tr}\alpha = \text{Tr}\delta = 0$. Then

$$[\Phi, g] = \begin{pmatrix} [J_+, \alpha] & J_+\beta-\beta J_- \\ J_-\gamma-\gamma J_+ & [J_-, \delta] \end{pmatrix}. \tag{4.73}$$

We see that, due to the block-diagonal form of the Higgs vev, α only affects the φ^α block of φ, β only φ^β, etc. This means that, in the computation of the deformations, we can work out each block individually.

Let us do it explicitly for $k = 1$. We have

$$\varphi^\alpha \sim \varphi^\alpha+\begin{pmatrix} \alpha_{21}-\alpha_{12}w & -2\alpha_{11} \\ 2\alpha_{11}w & -\alpha_{21}+\alpha_{12}w \end{pmatrix}. \tag{4.74}$$

We can use α_{11}, α_{21} to fix the first line to zero:

$$\varphi^\alpha \sim \begin{pmatrix} 0 & 0 \\ \varphi^\alpha_{21} & \varphi^\alpha_{22} \end{pmatrix} + \begin{pmatrix} 0 & 0 \\ \varphi^\alpha_{12} w & \varphi^\alpha_{11} \end{pmatrix} . \tag{4.75}$$

We see that we do not have further freedom to localize the second line, hence we do not obtain localized modes from this block. The same is true for the block related to δ. Instead, localized modes come from the off-diagonal blocks. Let us consider the block φ^β and let us define its entries in the following convenient way

$$\varphi^\beta = \begin{pmatrix} \varphi^\beta_L + \varphi^\beta_R & \varphi^\beta_{12} \\ \varphi^\beta_{21} & -\varphi^\beta_L + \varphi^\beta_R \end{pmatrix} . \tag{4.76}$$

Let us see how much we can gauge fix

$$\varphi^\beta \sim \begin{pmatrix} \varphi^\beta_L + \varphi^\beta_R & \varphi^\beta_{12} \\ \varphi^\beta_{21} & -\varphi^\beta_L + \varphi^\beta_R \end{pmatrix} + \begin{pmatrix} \beta_{21} + \beta_{12} w & \beta_{22} - \beta_{11} \\ (\beta_{22} + \beta_{11}) w & -\beta_{21} + \beta_{12} w \end{pmatrix} . \tag{4.77}$$

We see that we can fix to zero φ^β_{12} and φ^β_L by respectively choosing $(\beta_{22} - \beta_{11})$ and β_{21}, obtaining

$$\varphi^\beta \sim \begin{pmatrix} \varphi^\beta_R & 0 \\ \varphi^\beta_{21} & \varphi^\beta_R \end{pmatrix} + \begin{pmatrix} \beta_{12} w & 0 \\ (\beta_{22} + \beta_{11}) w & \beta_{12} w \end{pmatrix} . \tag{4.78}$$

We then obtain the two modes localized on the ideal (w), i.e.

$$\varphi^\beta_R, \varphi^\beta_{21} \in \mathbb{C}[w]/(w) \cong \mathbb{C}. \tag{4.79}$$

These modes have charge $+1$ with respect to the $U(1)$ flavor symmetry. Analogously we obtain two modes with $U(1)$ charge -1 from the block φ^γ.[10]

For generic k we have the same pattern. After gauge fixing we are left with k constant modes in the charge $+1$ block φ^β

$$\varphi^\beta \sim \begin{pmatrix} \varphi^\beta_k & 0 & 0 & 0 & 0 & 0 \\ \vdots & & & & & \vdots \\ \varphi^\beta_3 & \dots & \dots & \varphi^\beta_k & 0 & 0 \\ \varphi^\beta_2 & \varphi^\beta_3 & \dots & \dots & \varphi^\beta_k & 0 \\ \varphi^\beta_1 & \varphi^\beta_2 & \varphi^\beta_3 & \dots & \dots & \varphi^\beta_k \end{pmatrix} \tag{4.80}$$

with entries $\varphi^\beta_j \in \mathbb{C}[w]/(w) \cong \mathbb{C}$ $(j = 1, ..., k)$. Analogously, we get k constant modes in the

[10] As done for the conifold, one can switch on a vev for the localized modes. The deformed threefold is then $uv = \det(z\mathbb{1}_4 - \Phi(w) - \varphi)$. This provides the projection map from the Higgs branch to the deformation space of the Pagoda with $k = 2$.

charge -1 block φ^γ. This gives a total of **k hypermultiplets**.

In order to fully characterize the structure of the Higgs branch, however, we have to take into account the *discrete gauge group* we found in (4.67). More specifically, let us see how the $\mathbb{Z}_k$ discrete gauge group acts on our zero-modes:

$$\mathbb{Z}_k : \begin{pmatrix} 0 & \varphi^\beta \\ \varphi^\gamma & 0 \end{pmatrix} \mapsto \begin{pmatrix} 0 & e^{2\pi n i/k}\varphi^\beta \\ e^{-2\pi n i/k}\varphi^\gamma & 0 \end{pmatrix}. \tag{4.81}$$

We can conclude that the Reid's pagoda of degree k has a k-dimensional Higgs branch with the following orbifold geometry:

$$\mathcal{M}_{\text{HB}} = \mathbb{H}^k/\mathbb{Z}_k\,. \tag{4.82}$$

This generalizes the result found in [59][11], and agrees with the dimension counting of formula (4.19). The flavor symmetry of this theory will be the 7d gauge symmetry modulo the discrete 5d gauge group, so in this case:

$$G_{\text{flavor}} = U(1)/\mathbb{Z}_k\,. \tag{4.83}$$

Note that, even though there are k hypermultiplets, the flavor symmetry is of rank one. This implies that we can only switch on one real mass, if we are to think of real masses as background vev's in the usual way. The fact that only one real mass is available perfectly matches the fact that the corresponding M-theory threefold only admits a simple flop, i.e. only a single curve is inflated by the simultaneous resolution[12].

Finally, the outcome of the Higgs branch computation perfectly matches the known result that Reid's pagodas have the following GV invariants [86,89]:

$$n^{g=0}_{d=1} = k\,, \tag{4.84}$$

and zero for all other classes and genera, where the degree $d = 1$ is in correspondence with the fact that the hypermultiplets in the Higgs branch have charge 1 under the flavor $U(1)$, and that all the dual Coxeter labels of the A_n Dynkin diagrams are equal to 1.

This also implies that *any* simple flop constructed as a deformation of a singularity from the A series admits hypers in 5d with charge at most 1.

[11] Notice that this happens only when we send the string coupling to infinity (ALE fibration in M-theory) and we make a specific choice for the discrete data at the boundary.

[12] On the other hand, we could have expected the usual $Sp(2k)$ symmetry enjoyed by k hypers. There might be some obstructions in the metric of the Higgs branch that prevent this symmetry to manifest itself, or some other unknown phenomenon restricting the allowed symmetry (that, we remark, is compatible with the presence of only one mass parameter in the theory). At present, the definitive interpretation of this fact is, to our knowledge, still to be fleshed out.

4.6 Simple flops of length 2

4.6.1 Families of D_n-surfaces

In this section we discuss threefolds that are one-parameter families of D_n-type ALE surfaces. As before, we call this parameter w. At the origin of the parameter space the surface develops a D_n singularity, while on generic points this singularity is fully deformed. These examples were developed from the matrix factorizations viewpoint in [90] and from the Non-Commutative-Crepant-Resolution (NCCR) viewpoint in [91].

We focus on singularities that admit only a partial resolution, inflating a single $\mathbb{P}^1$ corresponding to the central node of the D_n Dynkin diagram. These are also known as a simple flops of length 2, as the dual Coxeter label of the central node in the D series is precisely equal to 2, as can be seen in Figure 4.2.

In order to exhibit such a property, the family should have a point-like singularity at $w = 0$. The resolution of such a singularity restricted to the central fiber should be the standard resolution of the trivalent node in the Dynkin diagram of D_n.

To construct these threefolds explicitly one proceeds exactly as we did for the deformed A_n singularities: one starts with the complete family of D_n-type ALE surfaces over the space $\mathcal{T}/\mathcal{W}$:

$$x^2+y^2z+z^{n-1}+\sum_{i=1}^{n-1}\delta_{2i}z^{n-1-i}+2\tilde{\delta}_n y = 0. \tag{4.85}$$

This $(n+2)$-dimensional family (n-dimensional base plus 2-dimensional fiber) is non-singular even though the fiber at the origin has a D_n-singularity.

We now want to simultaneously resolve only the trivalent node of the Dynkin diagram of D_n, in order to generate a flop of length two [90]. To do this, one takes $\mathcal{W}'$ the Weyl subgroup corresponding to all the other simple roots [111, 159]. These generate a $A_{n-3}\oplus A_1\oplus A_1$ subalgebra of D_n and the corresponding Weyl subgroup is $S_{n-2}\times\mathbb{Z}_2\times\mathbb{Z}_2$. This subalgebra corresponds to the breaking of[13] $SO(2n)$ to $U(n-2)\times SO(4)$, that would be produced by a Higgs ϕ_3 along the Cartan generator dual to the trivalent root. The Weyl invariant coordinates are the Casimirs σ_i ($i = 1, ..., n-2$) of $U(n-2)$ and the Casimirs ϖ_1 and ϖ_2 of $SO(4)$.

Now, to obtain a threefold with a flop of length two one just needs to take the $\mathcal{W}'$ invariants to depend (linearly) on the parameter w, in such a way that at $w = 0$ all of them vanish, i.e., now $\sigma_i = \sigma_i(w)$ and $\varpi_{1,2} = \varpi_{1,2}(w)$.

The IIA setups that engineer these flops of length two involve not only D6-branes, but also O6$^-$-planes. These are defined such that a stack of n D6/image-D6 pairs lie on top of the O6$^-$-plane and carry a $SO(2n)$ gauge group. The adjoint scalar fields ϕ_i ($i = 1, 2, 3$) are therefore anti-symmetric $2n\times 2n$ matrices. It will be more convenient, however, to work in

[13] Later, we will mention again a subtlety in the choice of the global form of the 7d gauge group.

a basis of $\mathfrak{so}(2n)$ such that the Higgs has the following block diagonal structure:

$$\phi_i = \begin{pmatrix} Z_1 & Z_2 \\ Z_3 & -Z_1^t \end{pmatrix}, \qquad \text{with} \quad Z_2^t = -Z_2\,, Z_3^t = -Z_3\,. \tag{4.86}$$

In this basis the matrices G of $SO(2n)$ are such that

$$G{\cdot}\mathcal{Q}{\cdot}G^t = \mathcal{Q} \qquad \text{where} \qquad \mathcal{Q} = \left(\begin{array}{c|c} 0 & \mathbb{1}_n \\ \hline \mathbb{1}_n & 0 \end{array}\right). \tag{4.87}$$

The M-theory threefold is an ALE fibration, where the fibration is generated by w-dependent deformations of the fiber. The (simultaneous) resolution is given by a constant vev for ϕ_3 along the Cartan dual to the (simultaneously) resolved roots, namely:

$$\mathcal{H} = \langle \alpha_c^* \rangle, \tag{4.88}$$

with α_c the trivalent node of D_n. In the Springer resolution formalism, this is equivalent to turning on a Higgs field in the Levi subalgebra corresponding to the non-resolved roots, i.e. all apart from the trivalent node, as we did in the D_4 case in Section 2.3.2:

$$\mathcal{L} = A_{n-3} \oplus A_1 \oplus A_1 \oplus \langle \alpha_c^* \rangle, \tag{4.89}$$

Since $[\Phi, \phi_3] = 0$, Φ should live in the adjoint representation of $U(n-2) \times SO(4) \subset SO(2n)$. The Higgs field is then the following $2n \times 2n$ matrix (in the basis (4.86))

$$\Phi = \left(\begin{array}{cc|cc} \Phi_{U(n-2)} & & & \\ & a & & b \\ \hline & & -\Phi^t_{U(n-2)} & \\ & c & & -a^t \end{array}\right) \tag{4.90}$$

where the block $\Phi_{SO(4)} = \begin{pmatrix} a & b \\ c & -a^t \end{pmatrix}$, with b, c antisymmetric 2×2 matrices, is a field in the adjoint of $SO(4)$, while $\Phi_{U(n-2)}$ is in the adjoint of $U(n-2)$.

The fields $\Phi_{SO(4)}$ and $\Phi_{U(n-2)}$ depend on the Casimirs of the corresponding groups; in particular $\varpi_2 = \text{Pfaff}(\Phi_{SO(4)})$ and $\varpi_1 = \frac{1}{2}\text{Tr}\Phi^2_{SO(4)} + 2\varpi_2$ for the $SO(4)$ block, and $\sigma_1, \ldots, \sigma_{n-2}$ for the $U(n-2)$ block. We have seen in Section 3.5.2 that the M-theory threefold can be expressed in terms of the IIA Higgs field as:

$$x^2 + zy^2 - \frac{\sqrt{\det(z\mathbb{1} + \Phi^2)} - \varpi_2^2 \sigma_{n-2}^2}{z} + 2\varpi_2 \sigma_{n-2} y = 0. \tag{4.91}$$

We have also seen that this is a $\mathbb{C}^*$-fibration, in which the $\mathbb{C}^*$-fiber degenerates over the

D6-brane locus (given by the discriminant of the quadric in y):

$$\Delta_{D6} \equiv \sqrt{\det(z\mathbb{1}+\Phi^2)} = 0. \tag{4.92}$$

The O6$^-$-plane locus is at $z=0$ (where the coefficient of y^2 vanishes). The type IIA target space is a double cover of the base of the $\mathbb{C}^*$-fibration, that can be given by the equation $\xi^2 = z$.

For the following, it is more convenient to exchange rows and columns to bring Φ into the form

$$\Phi = \left(\begin{array}{cc|c} \Phi_{U(n-2)} & & 0 \\ & -\Phi^t_{U(n-2)} & \\ \hline & & \Phi_{SO(4)} \end{array}\right). \tag{4.93}$$

In this basis, the elements g of the algebra $\mathfrak{so}(2n)$ satisfy:

$$gQ+Qg^t = 0, \qquad \text{with} \qquad Q = \left(\begin{array}{cc|cc} 0 & \mathbb{1}_{n-2} & & \\ \mathbb{1}_{n-2} & 0 & & \\ \hline & & 0 & \mathbb{1}_2 \\ & & \mathbb{1}_2 & 0 \end{array}\right). \tag{4.94}$$

Each block can be written (by a gauge transformation) in a canonical form, where the entries directly depend on the Casimirs. In particular, for the $U(n-2)$ block we have the form (4.58). For the $SO(4)$ block, one can use that $\mathfrak{so}(4) = \mathfrak{su}(2)\oplus\mathfrak{su}(2)$ to obtain the canonical form

$$\Phi_{SO(4)} = \begin{pmatrix} 0 & 1 & 0 & -\frac{\varpi_1}{4} \\ \frac{\varpi_1}{4}-\varpi_2 & 0 & \frac{\varpi_1}{4} & 0 \\ 0 & 1 & 0 & \varpi_2-\frac{\varpi_1}{4} \\ -1 & 0 & -1 & 0 \end{pmatrix}, \tag{4.95}$$

where the Casimirs of the two $SU(2)$ are $\frac{\varpi_1}{4}$ and $\varpi_2-\frac{\varpi_1}{4}$.

4.6.2 Brown-Wemyss threefold

In this section we focus our attention on a one-parameter family of deformed D_4 singularities, i.e. $n=4$, characterizing its GV invariants, as well as the Higgs branch of the 5d theory obtained by compactifying M-theory upon the singularity. Moreover we will set $\varpi_2 = 0$. When this happens the family takes the simple form

$$x^2+zy^2-\left(z\sigma_1^2+(z-\sigma_2)^2\right)(z+\varpi_1) = 0. \tag{4.96}$$

The threefold is defined by the following w-dependence of the Casimirs of $U(2)\times SO(4)$:

$$\sigma_1 = -w\,, \qquad \sigma_2 = w\,, \qquad \varpi_1 = -w\,, \qquad \varpi_2 = 0. \tag{4.97}$$

Plugging these into (4.96), one obtains the hypersurface

$$x^2+zy^2-(z-w)\left(zw^2+(z-w)^2\right)=0. \tag{4.98}$$

This threefold was introduced in [92]. It is singular at the origin, where the ALE fiber develops a D_4 singularity. The total space admits a small resolution with a flop of length two. This leads to a $U(1)$ flavor symmetry in 5d.[14] This threefold has Milnor number 11 and, according to formula (4.19), the number of normalizable deformations is 6, and hence we expect a 6-dimensional Higgs branch.

In IIA we start with a stack of 8 D6-branes at the orientifold location $z=0$ and we switch on a background Higgs (which is identically, modulo exchange of rows and columns, to the example we provided in (3.71)):

$$\Phi=\left(\begin{array}{cccc|cccc} 0 & 1 & 0 & 0 & 0 & 0 & 0 & 0\\ -w & -w & 0 & 0 & 0 & 0 & 0 & 0\\ 0 & 0 & 0 & w & 0 & 0 & 0 & 0\\ 0 & 0 & -1 & w & 0 & 0 & 0 & 0\\ \hline 0 & 0 & 0 & 0 & 0 & 1 & 0 & \frac{w}{4}\\ 0 & 0 & 0 & 0 & -\frac{w}{4} & 0 & -\frac{w}{4} & 0\\ 0 & 0 & 0 & 0 & 0 & 1 & 0 & \frac{w}{4}\\ 0 & 0 & 0 & 0 & -1 & 0 & -1 & 0 \end{array}\right). \tag{4.99}$$

If we choose $SO(8)$ as the global form of the 7d gauge group, the group that stabilizes the Higgs field Φ is isomorphic to $U(1)\times\mathbb{Z}_2$:

$$G_{5d}=\left(\begin{array}{cccc|cccc} e^{i\alpha} & 0 & 0 & 0 & 0 & 0 & 0 & 0\\ 0 & e^{i\alpha} & 0 & 0 & 0 & 0 & 0 & 0\\ 0 & 0 & e^{-i\alpha} & 0 & 0 & 0 & 0 & 0\\ 0 & 0 & 0 & e^{-i\alpha} & 0 & 0 & 0 & 0\\ \hline 0 & 0 & 0 & 0 & & & & \\ 0 & 0 & 0 & 0 & & \varrho & & \\ 0 & 0 & 0 & 0 & & & & \\ 0 & 0 & 0 & 0 & & & & \end{array}\right), \tag{4.100}$$

[14] See [160, 166] for an explicit resolution of these geometries by quiver techniques with a focus on the $U(1)$ symmetry and its charges.

where α is a phase and $\boldsymbol{\varrho}$ lives in the $\mathbb{Z}_2 \subset O(4)$ generated by

$$\boldsymbol{\varrho} = \begin{pmatrix} -1 & 0 & 0 & 0 \\ 0 & -1 & 0 & 0 \\ 0 & 0 & -1 & 0 \\ 0 & 0 & 0 & -1 \end{pmatrix}. \tag{4.101}$$

We then have a continuous abelian group, that is seen as a flavor group in the 5d theory, times a discrete gauge group.

On the other hand, if we had started from $SO(8)/\mathbb{Z}_2$ in 7d, namely with the simply connected gauge group associated to the $\mathfrak{so}(8)$ algebra modulo its center, we would have obtained just $U(1)$ as the stabilizer of Φ. This is the same ambiguity we have encountered in the case of Reid's pagodas of Section 4.5.3.

We now compute the Higgs branch. As for the examples in Section 4.5.3, this consists in the deformations φ of the background Higgs, modulo linearized $SO(8)$ gauge transformations:

$$\varphi \sim \varphi + [\Phi, g]. \tag{4.102}$$

The commutator $[\Phi, g]$ can be written in the block form

$$[\Phi, g] = \left(\begin{array}{c|c|c} B_{2\times 2} & A^u_{2\times 2} & C_{2\times 4} \\ \hline A^d_{2\times 2} & -B^t_{2\times 2} & D_{2\times 4} \\ \hline D_{4\times 2} & C_{4\times 2} & -B_{4\times 4} \end{array}\right), \tag{4.103}$$

where $C_{2\times 4}$ is completely determined by $C_{4\times 2}$ (analogously for the D-blocks). Due to the block-diagonal form of the Higgs (4.99), each block of $[\Phi, g]$ depends only on the entries of g in the same block.

Let us proceed now block by block. We start with

$$B_{2\times 2} = \begin{pmatrix} g_{21} + g_{12} w & -g_{11} + g_{22} + g_{12} w \\ -(g_{11} + g_{21} - g_{22}) w & -g_{21} - g_{12} w \end{pmatrix}.$$

Using g_{21} and the combination $g_{11} - g_{22}$ we can fix to zero the corresponding entries φ_{11} and

φ_{12} in the fluctuation of the Higgs. We are then left with:

$$\varphi_{2\times 2} \sim \underbrace{\begin{pmatrix} 0 & 0 \\ \varphi_{21} & \varphi_{22} \end{pmatrix}}_{\varphi_{2\times 2}} + \underbrace{\begin{pmatrix} 0 & 0 \\ -w(\varphi_{12}-\varphi_{11}) & \varphi_{11} \end{pmatrix}}_{B_{2\times 2}}. \tag{4.104}$$

As a result we see that φ_{21} and φ_{22} are not constrained, and so they are not dynamical in 5d.

The other relevant diagonal block

$$B_{4\times 4} = \begin{pmatrix} g_{58}+g_{65}+\frac{1}{4}(g_{56}-g_{76})w & g_{66}-g_{55} & 0 & -\frac{1}{4}(g_{55}+g_{66})w \\ \frac{1}{4}(g_{66}-g_{55})w & g_{58}-g_{65}+\frac{1}{4}(-g_{56}-g_{76})w & \frac{1}{4}(g_{55}+g_{66})w & 0 \\ 0 & g_{55}+g_{66} & -g_{58}-g_{65}+\frac{1}{4}(g_{76}-g_{56})w & \frac{1}{4}(g_{55}-g_{66})w \\ -g_{55}-g_{66} & 0 & g_{55}-g_{66} & -g_{58}+g_{65}+\frac{1}{4}(g_{56}+g_{76})w \end{pmatrix}$$

does not generate localized modes as well. In fact, using the combinations $(g_{66}-g_{55})$, $(g_{66}+g_{55})$, $(g_{58}-g_{65})$ and $(g_{58}+g_{65})$ we can set to zero, for example, the entries φ_{55}, φ_{56}, φ_{66} and φ_{76}, remaining with:

$$\varphi_{4\times 4} \sim \underbrace{\begin{pmatrix} 0 & 0 & 0 & \varphi_{58} \\ \varphi_{65} & 0 & -\varphi_{58} & 0 \\ 0 & 0 & 0 & \varphi_{78} \\ 0 & 0 & 0 & 0 \end{pmatrix}}_{\varphi_{4\times 4}} + \underbrace{\begin{pmatrix} 0 & 0 & 0 & -\frac{w\varphi_{76}}{4} \\ \frac{w\varphi_{56}}{4} & 0 & \frac{w\varphi_{76}}{4} & 0 \\ 0 & 0 & 0 & -\frac{w\varphi_{56}}{4} \\ 0 & 0 & 0 & 0 \end{pmatrix}}_{B_{4\times 4}}. \tag{4.105}$$

The first localized mode comes when we consider $A^u_{2\times 2}$. The gauge equivalence is

$$\varphi^u_{2\times 2} \sim \underbrace{\begin{pmatrix} 0 & \varphi_{14} \\ -\varphi_{14} & 0 \end{pmatrix}}_{\varphi^u_{2\times 2}} + \underbrace{\begin{pmatrix} 0 & -wg_{14} \\ wg_{14} & 0 \end{pmatrix}}_{A^u_{2\times 2}}. \tag{4.106}$$

We immediately see that φ_{14} is localized on the ideal (w), giving:

$$\varphi_{14} \in \mathbb{C}[w]/(w) \cong \mathbb{C} \tag{4.107}$$

and so it corresponds to 1 localized 5d mode. We note that this mode has charge $+2$ with respect to the flavor $U(1)$ in (4.100).

The block $A^d_{2\times 2}$ acts analogously to $A^u_{2\times 2}$ and it yields a localized mode with charge -2 with respect to the flavor $U(1)$.

Let us come to the block $C_{4\times 2}$. The gauge equivalence is:

$$\varphi_{4\times 2}\sim\underbrace{\begin{pmatrix}\varphi_{53} & \varphi_{54}\\ \varphi_{63} & \varphi_{64}\\ \varphi_{73} & \varphi_{74}\\ \varphi_{83} & \varphi_{84}\end{pmatrix}}_{\varphi_{4\times 2}}+\underbrace{\begin{pmatrix}-g_{18}-g_{27}-\frac{g_{16}w}{4} & \left(g_{17}+g_{27}-\frac{g_{26}}{4}\right)w-g_{28}\\ \frac{1}{4}(g_{15}+g_{17})w-g_{28} & \frac{1}{4}(4g_{18}+g_{25}+g_{27}+4g_{28})w\\ -g_{18}-g_{25}-\frac{g_{16}w}{4} & \left(g_{15}+g_{25}-\frac{g_{26}}{4}\right)w-g_{28}\\ g_{15}+g_{17}-g_{26} & g_{25}+g_{27}+(g_{16}+g_{26})w\end{pmatrix}}_{C_{4\times 2}}. \tag{4.108}$$

Almost all the entries in φ corresponding to this block can be gauge-fixed to zero, except φ_{64} and two linear combinations of φ_{54}, φ_{63}, φ_{64}. After having fixed all the other entries to zero, we have:

$$\begin{aligned}
\varphi_{54}&\sim\varphi_{54}+w^2\left(-\frac{g_{16}}{2}-\frac{g_{26}}{2}\right)+w\left(g_{17}-\frac{g_{26}}{4}+\frac{\varphi_{53}}{2}-\frac{\varphi_{73}}{2}-\frac{\varphi_{84}}{2}\right)-g_{28}\\
\varphi_{63}&\sim\varphi_{63}+\frac{1}{4}w(g_{26}-\varphi_{83})-g_{28}\\
\varphi_{64}&\sim\varphi_{64}+\frac{g_{26}w^2}{4}+\frac{1}{4}w(4g_{28}+2\varphi_{53}+2\varphi_{73}+\varphi_{84})\\
\varphi_{74}&\sim\varphi_{74}+w^2\left(-\frac{g_{16}}{2}-\frac{g_{26}}{2}\right)+w\left(-g_{17}+\frac{3g_{26}}{4}-\frac{\varphi_{53}}{2}+\frac{\varphi_{73}}{2}-\varphi_{83}-\frac{\varphi_{84}}{2}\right)-g_{28}
\end{aligned}$$

To make the computation easier and without loss of generality, we redefine φ_{54}, φ_{63} and φ_{74} as

$$\varphi_{54}=\psi_1-\psi_2\,,\qquad \varphi_{63}=\psi_3\,,\qquad \varphi_{74}=\psi_1+\psi_2. \tag{4.109}$$

Using the gauge freedom given by g_{28} we can set ψ_3 to zero, remaining with:[15]

$$\begin{aligned}
\varphi_{64}&\sim\varphi_{64}+\frac{g_{26}w^2}{2}\\
\psi_1&\sim\psi_1+\frac{1}{4}w^2(-2g_{16}-2g_{26})\\
\psi_2&\sim\psi_2+\frac{1}{4}w(2g_{26}-4g_{17})
\end{aligned} \tag{4.110}$$

We immediately see that φ_{64} is localized on the ideal (w^2), yielding:

$$\varphi_{64}\in\mathbb{C}[w]/(w^2)\cong\mathbb{C}^2. \tag{4.111}$$

On the other hand, we see that:

$$\begin{aligned}
\psi_1&\in\mathbb{C}[w]/(w^2)\cong\mathbb{C}^2\\
\psi_2&\in\mathbb{C}[w]/(w)\cong\mathbb{C}
\end{aligned} \tag{4.112}$$

We then have a total of 5 localized modes with charge +1 under the $U(1)$ in (4.100).

[15] And discarding the dependence on the other φ_{ij}, that are not free parameters.

The block $D_{4\times 2}$ works like $C_{4\times 2}$ and gives 5 localized modes with charge -1 with respect to the $U(1)$ in (4.100).

Summing up, we obtain a 5d $\mathcal{N}=1$ theory with six hypermultiplets (the modes with opposite charge pair up into a hyper):

- **1 hyper** of charge 2:[16]

$$\begin{pmatrix} Q_0 \\ \tilde{Q}_0 \end{pmatrix} = \begin{pmatrix} \varphi_{14} \\ \varphi_{41} \end{pmatrix}$$

- **5 hypers** of charge 1:

$$\begin{pmatrix} Q_1 \\ \tilde{Q}_1 \end{pmatrix} = \begin{pmatrix} \varphi_{64}^{(1)} \\ \varphi_{28}^{(1)} \end{pmatrix}, \qquad \begin{pmatrix} Q_2 \\ \tilde{Q}_2 \end{pmatrix} = \begin{pmatrix} \varphi_{64}^{(2)} \\ \varphi_{28}^{(2)} \end{pmatrix},$$

$$\begin{pmatrix} Q_3 \\ \tilde{Q}_3 \end{pmatrix} = \begin{pmatrix} \psi_1^{(1)} \\ \tilde{\psi}_1^{(1)} \end{pmatrix}, \qquad \begin{pmatrix} Q_4 \\ \tilde{Q}_4 \end{pmatrix} = \begin{pmatrix} \psi_1^{(2)} \\ \tilde{\psi}_1^{(2)} \end{pmatrix}, \qquad \begin{pmatrix} Q_5 \\ \tilde{Q}_5 \end{pmatrix} = \begin{pmatrix} \psi_2 \\ \tilde{\psi}_2 \end{pmatrix}.$$

The Higgs branch will then be $\mathbb{H}^6$ modded out by the discrete gauge symmetry $\mathbb{Z}_2$.

Let us analyze the action of the discrete group on the zero modes we have just found.

- The charge-2 hyper $(Q_0, \tilde{Q}_0)$ is unaffected by the $\mathbb{Z}_2$.
- The non-trivial action occurs on the charge-1 hypers. The gauge fixed $\varphi_{4\times 2}$ block is

$$\varphi_{4\times 2} = \begin{pmatrix} 0 & \psi_1 - \psi_2 \\ 0 & \varphi_{64} \\ 0 & \psi_1 + \psi_2 \\ 0 & 0 \end{pmatrix}. \tag{4.113}$$

  The generator $\boldsymbol{\varrho}$ changes sign to all the modes, thus

$$\boldsymbol{\varrho}: \begin{pmatrix} Q_i \\ \tilde{Q}_i \end{pmatrix} \mapsto - \begin{pmatrix} Q_i \\ \tilde{Q}_i \end{pmatrix} \qquad i = 1, ..., 5.$$

We finally claim that M-theory on the threefold (4.98) leads to a 5d theory with Higgs branch[17]

$$\mathcal{M}_{\text{HB}} = \mathbb{H} \times \mathbb{H}^5/\mathbb{Z}_2, \tag{4.114}$$

[16]The existence of a charge-2 state localized at the origin of threefolds admitting flops of length two was already predicted in [160].

[17]Modulo the ambiguity in the choice of the global form of the 7d gauge group, that can erase the discrete gauging.

where the $\mathbb{Z}_2$ inverts the coordinates. The flavor symmetry is the 7d gauge symmetry, i.e.

$$G_{\text{flavor}} = U(1)\,. \tag{4.115}$$

In this case, we do not have to mod the $U(1)$ by the discrete symmetry, since the $\mathbb{Z}_2$ factor acts differently on the $U(1)$-charged zero modes (there is no element of $U(1)$ that acts on all the modes equally to an element of $\mathbb{Z}_2$).

To conclude, notice that our findings are in agreement with the known results that the Brown-Wemyss threefolds have the following GV invariants [92]:

$$n^{g=0}_{d=2} = 1\,, \qquad\qquad n^{g=0}_{d=1} = 5\,, \tag{4.116}$$

and zero for all other classes and genera. In this regard, the relevant point to stress is that the degree 2 GV invariant corresponds to the hypers of charge 2 under the flavor group generated by the resolution, and to the fact that the dual Coxeter label of the central node in the D_4 Dynkin diagram is equal to 2.

We see here a new feature, that did not appear in the deformed A_n cases: the fact that the length of the flop is higher than 1 predicts that the maximal flavor charge is higher than 1, but does not forbid also lower-charge hypers. Indeed, in our case we have found one charge-2 hyper, along with five charge-1 hypers. We will see this phenomenon recur in all higher-length flops, and we notice that the fact that all the allowed charges are realized by some hyper might be suggestive of relationships with some Swampland conjectures, such as the Completeness hypothesis [167], and the related BPS completeness hypothesis[18].

4.6.3 Laufer's threefold

We now generalize the computation done in the previous section to a famous flop of length two, first discovered by Laufer [161]. It is given by the following hypersurface:

$$x^2 + zy^2 - t\left(t^2 + z^{2k+1}\right) = 0 \quad \text{with } k \geq 1\,. \tag{4.117}$$

By making the change of variable $t = w - z$, one can put this threefold in the form of a D_{2k+3} family with[19]

$$\sigma_{2k+1} = w, \qquad \sigma_{2k-1} = 1, \qquad \sigma_{i\neq 2k\pm 1} = 0, \qquad \varpi_1 = -w, \qquad \varpi_2 = 0. \tag{4.118}$$

The form of the Higgs field is like in (4.93) with $n = 2k+3$. The $SO(4)$ block is identical to the one for the Brown-Wemyss threefold (see (4.99)). The $U(2k+1)$ block is given by (4.58) with the Casimirs defined in (4.118) (modulo a relabeling $\hat{\varrho}_i \to \sigma_i$). Notice that for $k = 1$, the Casimir σ_{2k-1} is along the Cartan subalgebra.

The preserved group is again the diagonal $U(1)$ of the $U(2k+1)$ block times the $\mathbb{Z}_2$

[18] We refer to e.g. [168] for a review of these concepts.

[19] The fact that $\sigma_{2k-1} = 1$ makes the singularity of the ALE fiber at the origin be D_{2k+2}.

generated by (4.101).

The computation of the zero modes proceeds analogous to what done in Section 4.6.2. Now the linearized gauge variation of the deformation φ is

$$[\Phi, g] = \left(\begin{array}{c|c|c} B_{(2k+1)\times(2k+1)} & A^u_{(2k+1)\times(2k+1)} & C_{(2k+1)\times 4} \\ \hline A^d_{(2k+1)\times(2k+1)} & -B^t_{(2k+1)\times(2k+1)} & D_{(2k+1)\times 4} \\ \hline D_{4\times(2k+1)} & C_{4\times(2k+1)} & -B_{4\times 4} \end{array}\right). \tag{4.119}$$

For the zero modes, one again checks if the various blocks of $[\Phi, g]$ localize any mode in 5d. We find:

- $B_{(2k+1)\times(2k+1)}$ and $B_{4\times 4}$ do not localize any modes.
- $A^u_{(2k+1)\times(2k+1)}$ localizes one entry φ_2 as:

$$\varphi_2 \in \mathbb{C}[w]/(w^k) \cong \mathbb{C}^k, \tag{4.120}$$

  thus yielding k charge 2 localized modes. The same goes for $A^d_{(2k+1)\times(2k+1)}$, from which we obtain k modes $\tilde{\varphi}_2$ of charge -2.
- $C_{4\times(2k+1)}$ localizes three entries with the same pattern as in the Brown-Wemyss case, namely:

$$\begin{aligned} &\varphi_1 \in \mathbb{C}[w]/(w^{k+1}) \cong \mathbb{C}^{k+1} \\ &\psi_1 \in \mathbb{C}[w]/(w^{k+1}) \cong \mathbb{C}^{k+1}, \\ &\psi_2 \in \mathbb{C}[w]/(w) \cong \mathbb{C} \end{aligned} \tag{4.121}$$

  obtaining a total of $2k+3$ charge 1 localized modes. $D_{4\times(2k+1)}$ gives the same matter content as $C_{4\times(2k+1)}$, but with charge -1.

Summarizing, the spectrum is given as follows:

- ***k* hypers** of charge 2:

$$\begin{pmatrix} Q_i \\ \tilde{Q}_i \end{pmatrix} = \begin{pmatrix} \varphi_2^{(i)} \\ \tilde{\varphi}_2^{(i)} \end{pmatrix} \qquad i = 1, ..., k;$$

- **$2k+3$ hypers** of charge 1:

$$\begin{pmatrix} Q_{i+k} \\ \tilde{Q}_{i+k} \end{pmatrix} = \begin{pmatrix} \varphi_1^{(i)} \\ \tilde{\varphi}_1^{(i)} \end{pmatrix}, \begin{pmatrix} Q_{i+2k+1} \\ \tilde{Q}_{i+2k+1} \end{pmatrix} = \begin{pmatrix} \psi_1^{(i)} \\ \tilde{\psi}_1^{(i)} \end{pmatrix} \quad i = 1, ..., k+1, \text{ and } \begin{pmatrix} Q_{3k+3} \\ \tilde{Q}_{3k+3} \end{pmatrix} = \begin{pmatrix} \psi_2 \\ \tilde{\psi}_2 \end{pmatrix}.$$

Like for the Brown-Wemyss' case the discrete group in (4.101) acts in the following way:

- The charge 2 hypers are unaffected by the $\mathbb{Z}_2$ discrete symmetry.
- The charge 1 hypers transform under $\boldsymbol{\varrho}$ as

$$\boldsymbol{\varrho} : \begin{pmatrix} Q_i \\ \tilde{Q}_i \end{pmatrix} \mapsto - \begin{pmatrix} Q_i \\ \tilde{Q}_i \end{pmatrix} \qquad i = k+1, ..., 3k+3.$$

The Higgs branch of M-theory on Laufer's threefold is then

$$\mathcal{M}_{\mathrm{HB}} = \mathbb{H}^k \times \mathbb{H}^{2k+3}/\mathbb{Z}_2, \tag{4.122}$$

where the $\mathbb{Z}_2$ inverts the coordinates. Like in the previous example, the flavor group is $G_{\text{flavor}} = U(1)$, and the discrete group might disappear with a different choice of the global form of the 7d gauge group.

Finally, the GV invariants corresponding to Laufer's flop read, matching [86, 89]:

$$n_{d=2}^{g=0} = k\,, \qquad n_{d=1}^{g=0} = 2k+3\,, \tag{4.123}$$

and zero for all other classes and genera.

4.7 Interlude: Higgs backgrounds for general simple flops and a new computational algorithm

Until now, we have analyzed "renowned" simple flops already present in the literature, each time writing down the Higgs background corresponding to the singularity. In this section, we invert the perspective, and seek to find a generalized framework to build, *ab initio*, Higgs backgrounds associated to simple flops of all lengths, without recurring to pre-packaged threefold equations.

To this end, we need to build Higgs backgrounds related to the resolution patterns exhibited in Figure 4.2, where only the black nodes are resolved. The corresponding threefolds we are looking for have then the structure of an ALE fibration over the complex plane $\mathbb{C}_w$ and they will be defined by an equation of the kind displayed in (4.21), depending on the partial Casimirs $\varrho_i(w) \in \mathcal{T}/\mathcal{W}'$. Here, we choose the dependence $\varrho_i(w)$ to be linear, in order to avoid creating further singularities in the resulting threefolds. We will restrict on building threefolds X that have isolated singularities, admitting only a small resolution.

In the following we are going to show how to build a threefold family of deformed ADE surfaces by starting from the requirement that the ALE fibration over $\mathbb{C}_w$ presents a specific partial simultaneous resolution, i.e. a choice of a single simple root, say α_c. This will precisely produce a threefold simple flop. As we will see, this method can actually produce in principle the full ADE family over $\mathcal{T}/\mathcal{W}'$.

4.7.1 The Higgs field from the simultaneous resolution

Our objective is to explicitly construct a vev for Φ that allows the (simultaneous) resolution at the origin only of a choice of a unique simple root α_c of $\mathfrak{g}$. From the 7d gauge theory perspective, we are turning on a vev for ϕ_3 along the subalgebra

$$\mathcal{H} = \langle \alpha_c^* \rangle. \tag{4.124}$$

Given that $[\Phi, \phi_3] = 0$, then Φ must live in the commutant of $\mathcal{H}$, which is a Levi subalgebra $\mathcal{L}$, of the form (3.100). As we are choosing to blow up a single simple root, this means that the Higgs background should live in the Levi subalgebra defined by (4.124):

$$\mathcal{L} = \bigoplus_h \mathcal{L}_h \oplus \mathcal{H} \tag{4.125}$$

with $\mathcal{L}_h$ simple Lie algebras. We take Φ to be a generic element of $\mathcal{L}$. This is precisely equivalent to switching on a vev for Φ along the Levi subalgebra that corresponds to the partial Springer resolution of the root α_c, as we have seen in Chapter 2.

The Casimir invariants of the Higgs field Φ tell us how the ALE fiber is deformed. Since at the origin of $\mathbb{C}_w$ the fiber presents the full ADE singularity, we expect that all the Casimir invariants of Φ vanish at $w = 0$. This means that at $w = 0$ the Higgs field should be a non-zero nilpotent element of $\mathcal{L}$. In particular, when restricted on each summand $\mathcal{L}_h$ of the Levi subalgebra, Φ must be in the corresponding principal nilpotent orbit, if we do not want terminal singularities after the simultaneous resolution.

We call the Higgs at the origin X_+. The generic Higgs field has then the following form

$$\Phi = X_+ + w\, Y \tag{4.126}$$

where $Y \in \mathcal{L}$ can in principle depend on w; in this chapter we mainly consider cases with constant Y.

The Higgs field Φ must deform the singularity outside the origin. At least in a neighborhood of $w = 0$, we demand that the ALE fiber does not develop any singularity. This happens when Φ restricted on each summand of $\mathcal{L}$ is a non-zero semisimple element of that summand. For $\mathcal{L}_h = A_{m-1}$, the generic form of Φ, up to gauge transformations is in the form of a *reconstructible Higgs* [94], that we have recalled in (4.58). As we did there, we call $\hat{\varrho}_j$

($j = 2, ..., m$) the Casimirs of $\Phi|_{A_{m-1}}$ (we called them the partial Casimirs of $\mathfrak{g}$). There are analogous canonical forms when the summand is a different Lie algebra: we will explicitly build them in the following, by embedding the form (4.58) into the D and E algebras.

Collecting the Casimirs $\hat{\varrho}_j$'s for each summand $\mathcal{L}_h$ and the coefficient deformations $\hat{\rho}$ along $\mathcal{H}$ one obtains the set of invariant coordinates ϱ_i that span the base of the family with simultaneous partial resolution. The total Casimirs μ_i of Φ (that appear as coefficients of the deforming monomials in the versal deformation of the ADE singularity) can be written as functions of the ϱ_i's. Notice that by formulae like (4.58), we give Φ as a function of the partial Casimirs ϱ_i. The choice of a dependence of ϱ_i on w produces a threefold.

In Section 4.5.2 we followed this road for the A_n singularities, that is in the case $\mu_i = \sigma_i$, reproducing flops of length 1 such as Reid's pagodas. Here, we aim at a more general purpose, wishing to build flops of all lengths.

Summing up, the change of basis from the non-resolved family to the family admitting a simple flop reads:

$$\text{Total Casimirs } \mu_i \quad \longrightarrow \quad \text{partial Casimirs } \varrho_i = (\hat{\varrho}_i, \hat{\rho}) \tag{4.127}$$

We finally notice that the ADE Lie Algebra $\mathfrak{g}$ can be decomposed into representations of the Levi subalgebra:

$$\mathfrak{g} = \mathcal{L} \oplus ... = \bigoplus_p R_p^{\mathcal{L}}, \tag{4.128}$$

where the irreps $R_p^{\mathcal{L}}$ include the terms in the decomposition (4.125). This will turn out useful in the following.

4.7.2 The threefold equation from Φ

We are going to build Higgs backgrounds corresponding to simple flops by switching on a non-trivial vev along the A_n subalgebras corresponding to the white nodes in Figure 4.2. In order to obtain the equations of the threefolds corresponding to these Higgs backgrounds, we recur to the expressions, valid in all the A, D, E_6, E_7, E_8 cases, displayed in Section 3.8. The computation is readily performed: we plug in the explicit expression of the Higgs background, written in term of the partial Casimirs $\varrho_i(w)$, into the formulas (3.91), (3.92) or the expressions in Appendix B, depending on which ADE algebra we are considering. The result gives the explicit threefold equation, as a fibration of an ADE singularity over $\mathbb{C}_w$.

If, instead, we keep the ϱ_i as full-fledged coordinates, we obtain a $(n+2)$-dimensional deformed family admitting a simultaneous resolution of the node α_c. This is no trivial task to perform with the standard methods of [111]. Our technique makes it completely automatic and easily computable.

In the next section, we introduce a new method to compute the localized 5d modes arising from M-theory on these simple flops, and correspondingly the GV invariants of the latter, in an algorithmic fashion.

4.7.3 A new algorithm to compute zero-modes

We have seen in Section 4.5 that the Higgs branch data and the GV invariants related to simple threefold flops can be computed as zero-modes of fluctuations around the Higgs background $\Phi(w)$. Here we show a more efficient and general method to compute these zero-modes in a way that can be easily implemented in a Mathematica code.

Given a vev for Φ, the zero modes are the deformation $\varphi \in \mathfrak{g}$ of the Higgs field up to the (linearized) gauge transformations

$$\delta_g \varphi = [\Phi, g] \qquad \text{with} \qquad g \in \mathfrak{g}. \tag{4.129}$$

We take $\Phi = X_+ + w\,Y$ as explained at page 141, where $X_+ \in \mathcal{L}$ is in the principal nilpotent orbit of each $\mathcal{L}_h$. We need to work out which components of the deformation φ can be set to zero by a gauge transformation (4.129). One then tries to solve the equation

$$\varphi + \delta_g \varphi = 0\,, \qquad \text{with} \qquad \delta_g \varphi = [X_+ + w\,Y, g] \tag{4.130}$$

with unknown $g \in \mathfrak{g}$. As we have seen, at special points in $\mathbb{C}_w$, there can be components of φ that cannot be gauge-fixed to zero: these directions in the Lie algebra $\mathfrak{g}$ support zero modes.

Since the irreducible representations $R^{\mathcal{L}}$ of $\mathcal{L}$ are invariant under the action of Φ, we implement the decomposition (4.128) and we solve the equation (4.130) in each representation $R^{\mathcal{L}}$ at a time, where now $g, \varphi \in R^{\mathcal{L}} \subset \mathfrak{g}$. We can write more explicitly the representation $R^{\mathcal{L}}$ of $\mathcal{L} = \mathcal{H} \oplus \mathcal{L}_1 \oplus \mathcal{L}_2 \oplus ...$ as

$$R^{\mathcal{L}} = \left(\; R^{\mathcal{L}_1}\;,\; R^{\mathcal{L}_2}\;,\; ...\;\right)_{q_1,\ldots,q_f} \tag{4.131}$$

where $R^{\mathcal{L}_h}$ is an irreducible representation of the simple summand $\mathcal{L}_h$ and $(q_1, ..., q_f)$ are the charges under the $U(1)^f$ group generated by $\mathcal{H}$. If there are n 5d modes in the representation $R^{\mathcal{L}}$, there will be other n 5d modes in the conjugate representation $\bar{R}^{\mathcal{L}}$; together these generate n massless hypermultiplets in the 5d theory localized at the singularity. By using the correspondence (4.28), we can then say that the GV invariant with degrees $(q_1, ..., q_f)$ is

$$n^{g=0}_{q_1,\ldots,q_f} = \tfrac{1}{2} \cdot \#\,\text{localized zero-modes from } \; R^{\mathcal{L}} \oplus \bar{R}^{\mathcal{L}} \tag{4.132}$$

with $R^{\mathcal{L}} = \left(R^{\mathcal{L}_1}, R^{\mathcal{L}_2}, ...\right)_{q_1,\ldots,q_f}$.

Let us describe our algorithm to compute the number and the charges of zero modes. For each representation $R^{\mathcal{L}}$ of $\mathcal{L}$ with dimension d_R, we choose a basis $e_1, ..., e_{d_R}$ of $R^{\mathcal{L}}$. In this basis, the equation (4.130) becomes

$$(A+w\,B)\,\boldsymbol{\rho} = -\boldsymbol{\phi} \tag{4.133}$$

where $\boldsymbol{\rho}$ and $\boldsymbol{\phi}$ are the d_R-column vectors of coefficients of g and φ in the given basis and A, B are the constant $d_R \times d_R$ matrices representing the linear operators X_+ and Y respectively.

If $A+w\,B$ is invertible, then there exists a vector $\boldsymbol{\rho}$ (i.e. a $g \in R^{\mathcal{L}}$) that completely gauge fixes $\varphi \in R^{\mathcal{L}}$ to zero at generic w. At the values of w where the rank of $A+w\,B$ decreases, there will be vectors $\boldsymbol{\phi}$ that cannot be set to zero, leaving a zero mode localized at that points.

With the chosen X_+, we immediately see that such a special point is (by construction) the origin $w = 0$. Here the matrix $A+w\,B$ reduces to the nilpotent matrix A, that has non-trivial kernel.[20] In the following we only use the fact that A has rank $r < d_R$; hence, our conclusions are valid also when A is not necessarily nilpotent. What we are going to say of course applies also for a nilpotent A.

We choose the basis $e_1, ..., e_{d_R}$ of $R^{\mathcal{L}}$ such that A is in the Jordan form. If the rank of A is r, we then have $d_R - r$ rows of zeros and $d_R - r$ columns of zeros. We can rearrange rows and columns such that A takes the block diagonal form

$$A = \left(\begin{array}{c|c} A_u & \mathbf{0}_{r\times(d_R-r)} \\ \hline \mathbf{0}_{(d_R-r)\times r} & \mathbf{0}_{(d_R-r)\times(d_R-r)} \end{array}\right), \text{ with } A_u \text{ invertible.} \tag{4.134}$$

Doing the same operations on B, we obtain

$$B = \left(\begin{array}{c|c} B_u & B_r \\ \hline B_l & B_d \end{array}\right). \tag{4.135}$$

The equations (4.133) now read

$$\begin{cases} (A_u + wB_u)\boldsymbol{\rho}_u + wB_r\boldsymbol{\rho}_d &= -\boldsymbol{\phi}_u \\ wB_l\boldsymbol{\rho}_u + wB_d\boldsymbol{\rho}_d &= -\boldsymbol{\phi}_d \end{cases} \tag{4.136}$$

Since $(A_u + wB_u)$ is invertible (at least in the vicinity of $w = 0$), from the first set of equations we see that we can always gauge fix the $\boldsymbol{\phi}_u$ components to zero,[21] by setting

$$\boldsymbol{\rho}_u = -(A_u + w\,B_u)^{-1}\,(\boldsymbol{\phi}_u + w\,B_r\boldsymbol{\rho}_d)\,. \tag{4.137}$$

Substituting in the second set of equations we obtain

$$w\,\left[B_d - w\,B_l(A_u + w\,B_u)^{-1}B_r\right]\boldsymbol{\rho}_d = -\boldsymbol{\phi}_d + w\,B_l(A_u + w\,B_u)^{-1}\boldsymbol{\phi}_u. \tag{4.138}$$

[20]In particular, the kernel is spanned by the vectors $|j, j\rangle$, when writing $R^{\mathcal{L}}$ in terms of $\mathfrak{sl}(2)$ representations, where $\mathfrak{sl}(2)$ is generated by the Jacobson-Morozov standard triple associated with X_+.

[21]These correspond to all states except $|j, -j\rangle$.

We see that the components $\boldsymbol{\phi}_d$ cannot be fixed identically to zero: at $w=0$ there can be a remnant, i.e. a localized mode. Said differently, the best we can do is to cancel from $\boldsymbol{\phi}_d$ its dependence on w, leaving a constant entry (instead of a generic polynomial in w). This is possible for all components of $\boldsymbol{\phi}_d$ only when the matrix B_d has maximal rank, i.e. rank equal to $d_R - r$. In this case, the number of zero modes is

$$\# = d_R - r,$$

because each component of $\boldsymbol{\phi}_d$ has now a constant entry, i.e. one degree of freedom.

If B_d is not invertible, we can iterate what we have done so far, in the following way. Let us define for simplicity $\boldsymbol{\rho}' \equiv \boldsymbol{\rho}_d$, $\boldsymbol{\phi}'_{\text{tot}} \equiv \boldsymbol{\phi}_d - w\, B_l (A_u + w\, B_u)^{-1} \boldsymbol{\phi}_u$, $A' \equiv B_d$ and $B' \equiv -B_l (A_u + w\, B_u)^{-1} B_r$. We can decompose $\boldsymbol{\phi}'_{\text{tot}} = \boldsymbol{\phi}'_0 + w \boldsymbol{\phi}'$, where $\boldsymbol{\phi}'_0$ is $\boldsymbol{\phi}'_{\text{tot}}$ evaluated at $w=0$. We can then rewrite the equation (4.138) as

$$(A' + w\, B')\, \boldsymbol{\rho}' = -\boldsymbol{\phi}' . \tag{4.139}$$

This has the same form as (4.133), so we can again change the basis such that $A' \equiv B_d$ is in the Jordan form and write the equations in this basis. We will obtain a set of equations in the form (4.136) where we have to substitute $(A, B)_{u,l,r,d} \to (A', B')_{u,l,r,d}$ and $(\boldsymbol{\rho}, \boldsymbol{\phi}) \to (\boldsymbol{\rho}', \boldsymbol{\phi}')$.

The matrix A' will now have rank $r' < d_R - r$. There will then be r' components of $\boldsymbol{\phi}'$ that can be gauge fixed to zero; we correspondingly have r' zero modes along the corresponding components of $\boldsymbol{\phi}_d$. If the matrix B'_d has maximal rank (i.e. $d_R - r - r'$), then the other $d_R - r - r'$ components of $\boldsymbol{\phi}_d$ will be of the form $a + bw$ and hence each hosts *two* zero modes. In this case the number of zero modes is

$$\# = r' + 2(d_R - r - r') . \tag{4.140}$$

On the other hand, if B'_d has rank $r'' < d_R - r - r'$, then we have to iterate once more the algorithm above and, provided B''_d has maximal rank (i.e. $d_R - r - r' - r''$) we obtain

$$\# = r' + 2r'' + 3(d_R - r - r' - r'') .$$

We now have the factor "3" because the $d_R - r - r' - r''$ directions of $\boldsymbol{\phi}_d$ are of the form $a + bw + cw^2$, i.e. they host *three* zero modes each.

In conclusion, let us assume that the algorithm stops at the N-th step and let us call $r^{(k)}$ the rank of the matrix A at the step k, then the number of zero modes is

$$\#_{\text{zero modes}} = \sum_{k=0}^{N} k\, r^{(k)} \qquad \text{with} \qquad \sum_{k=0}^{N} r^{(k)} = d_R \tag{4.141}$$

where $r^{(0)} = r$.

If there are other values of w, say $w = w_0$, where the rank of $A + wB$ is not maximal, one can shift $w \mapsto w + w_0$ ending out with the same situation as above, where the new A is now

$A+w_0B$. Applying the algorithm that we have just outlined, one computes the zero modes localized at $w = w_0$. In this case the matrix at $w = w_0$ is not necessarily nilpotent.

Notice that this algorithm could never end. This is the case for example when the $A+wB$ matrix is identically zero at one step. The corresponding directions of φ cannot be gauge fixed at any order in w, leaving a zero mode that lives in 7d.

In conclusion, in this section we have shown that one can reduce the problem of finding the zero modes to a simple exercise in linear algebra. These computations are algorithmic and can be done by a calculator in a reasonable amount of time. In [99] we describe the implementation of the algorithm in Mathematica, that we used for our computations, providing ancillary files containing the code.

4.8 Simple flops of length $l = 1, \dots 6$: general construction

In the following, we apply the method discussed in Section 4.7 to construct threefolds with a simple flop. The threefold will be obtained from a family of deformed ADE singularities in which only the black node in Figure 4.2 is simultaneously resolved. In (4.124), we have called it α_c. The subalgebra $\mathcal{H}$ is then generated by α_c^*, i.e. $\mathcal{H} = \langle \alpha_c^* \rangle$, and the Higgs field will correspondingly be chosen in the commutant $\mathcal{L}$ of $\mathcal{H}$, i.e. the Levi subalgebra corresponding to the chosen partial simultaneous resolution (4.125). From Figure 4.2, we see that the simple summands $\mathcal{L}_h$ of $\mathcal{L}$ are *all* of A-type. The Higgs Φ restricted on these spaces is then of the form (4.58), and collecting the $\hat{\varrho}$'s from each summand $\mathcal{L}_h$ gives the partial Casimirs ϱ_i's that parametrize the base $\mathcal{T}/\mathcal{W}'$. The threefold is obtained by setting $\varrho_i = \varrho_i(w)$.

We will construct threefolds with different values of *length* from 1 to 6, recalling the correspondence of the length with the dual Coxeter label of the resolved node. Thus, building simple flops with resolution patterns as in Figure 4.2, we realize *all* possible lengths.

For each manifold we give the Higgs field Φ that produces the desired simple flop threefold X. This allows us to build the 5d theory realized from reducing M-theory on X. In particular the flavor group will always be the $U(1)$ group generated by α_c^*. The number of hypermultiplets and their charges under the $U(1)$ flavor group, namely the GV invariants of X and their degrees, will be derived by counting the zero modes of Φ.

From a physical perspective, as we have seen profusely in the preceding sections, GV invariants count 5d hypermultiplets arising from M-theory geometrically engineered on the simple threefold flops, and their degree corresponds to the flavor charges of such hypermultiplets: the maximal flavor charge is given by the length of the flop, which is equal to the dual Coxeter label of the node α_c in the corresponding Dynkin diagram.

We will explicitly check these points in our concrete examples.

4.8.1 Simple flop with length 1

With the new algorithm in our hands, we can now tackle the general simple flops of length 1, built as a deformed A singularity, outlined in Section 4.5.2.

We start from the Lie algebra A_{n-1}, and require only the resolution of the simple root α_c. Consequently, we have $\mathcal{H} = \langle \alpha_c^* \rangle$. Its commutant is given by (4.56), that we reproduce here for convenience:

$$\mathcal{L} = A_{c-1} \oplus A_{n-c-1} \oplus \langle \alpha_c^* \rangle . \tag{4.142}$$

The Higgs field at $w = 0$ is (in the principal nilpotent orbit when restricted on the simple summands of $\mathcal{L}$, namely in the reconstructible form):

$$X_+ = E_{\alpha_1} + \cdots + E_{\alpha_{c-1}} + E_{\alpha_{c+1}} + \cdots + E_{\alpha_{n-1}} , \tag{4.143}$$

where the E_{α_i} are the Lie algebra generators defined in Appendix A. We choose the w-dependence of the partial Casimirs such that the Higgs restricted on each block is[22]

$$\Phi|_{A_{c-1}} = \begin{pmatrix} 0 & 1 & 0 & \cdots & 0 \\ 0 & 0 & 1 & 0 & 0 \\ \vdots & 0 & \ddots & \ddots & 0 \\ 0 & 0 & 0 & 0 & 1 \\ w & 0 & \cdots & 0 & 0 \end{pmatrix} \quad \text{and} \quad \Phi|_{A_{n-c-1}} = \begin{pmatrix} 0 & 1 & 0 & \cdots & 0 \\ 0 & 0 & 1 & 0 & 0 \\ \vdots & 0 & \ddots & \ddots & 0 \\ 0 & 0 & 0 & 0 & 1 \\ -w & 0 & \cdots & 0 & 0 \end{pmatrix} . \tag{4.144}$$

This means that

$$Y = E_{-\alpha_1-\alpha_2-\ldots-\alpha_{c-1}} - E_{-\alpha_{c+1}-\alpha_{c+2}-\ldots-\alpha_{2n-1}} . \tag{4.145}$$

The equation of the threefolds is read form (3.91), by using the chosen $\Phi = X_+ + w\, Y$:

$$u\, v = (z^c - w)(z^{n-c} + w) . \tag{4.146}$$

When $n = 2k$ is even and $c = k$, we have the *Reid Pagoda* of degree k analyzed in Section 4.5.3.

For generic n and c, we perform the zero-mode counting by decomposing the A_{n-1} into representations of the Levi subalgebra (4.142). Explicitly, the decomposition reads:

$$A_{n-1} = (\boldsymbol{c^2 - 1}, \mathbf{1})_0 \oplus (\mathbf{1}, \boldsymbol{(n-c)^2 - 1})_0 \oplus (\mathbf{1}, \mathbf{1})_0 \oplus (\boldsymbol{c}, \overline{\boldsymbol{n-c}})_+ \oplus (\bar{\boldsymbol{c}}, \boldsymbol{n-c})_- , \tag{4.147}$$

where the two entries in brackets refer to the A_{c-1} and A_{n-c-1} representations, respectively, and the subscript is the $U(1)$ charge.

The first three representations host 7d modes, but no localized one. Let us concentrate

[22] A different choice would only complicate the equation of the threefold, without changing its salient features.

on the charged representation $(\boldsymbol{c}, \overline{\boldsymbol{n-c}})_+$ of dimension $c(n-c)$. With the choice $c \geq \frac{n}{2}$, we have $c \geq n-c$. The matrix corresponding to X_+ in this representation has kernel with dimension equal to $n-c$, then in our algorithm $r = (c-1)(n-c)$. With a bit of work, one can check that B_d has rank $n-c = d_R - r$, that gives then $n-c$ modes localized at $w = 0$ with charge $+1$ with respect to the flavor $U(1)$. The other charge representation hosts again $n-c$ modes localized at $w = 0$ and with charge -1. In total we then have $n-c$ charged hypermultiplets, i.e. the GV invariant is

$$n_1^{g=0} = n-c. \tag{4.148}$$

When $n = 2k$ and $c = k$, we obtain k hypers, that is the result we have found for the Reid's pagodas in Section 4.5.3, i.e. $n_1^{g=0} = k$.

4.8.2 Simple flop with length 2

In this section we generalize the Brown-Wemyss and Laufer examples examined in Section 4.6, considering a family of flops of length 2 arising from a D_4 singularity deformed over the $\mathbb{C}_w$ plane. The threefold is singular at the origin (where the fiber exhibits a D_4 singularity) and can only be partially resolved inflating a $\mathbb{P}^1$ corresponding to the central root of the D_4 Dynkin diagram. As we can see from Figure 4.2 the central node has dual Coxeter label equal to 2, and thus its resolution yields a flop of length 2. In Figure 4.4 we show our conventions for the labeling of the simple roots.

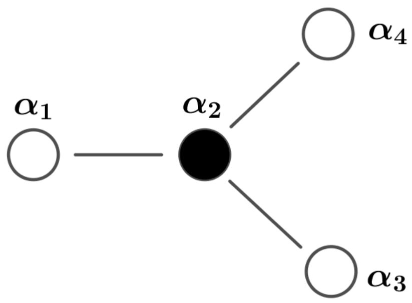

Figure 4.4: *D_4 Dynkin diagram.*

Since we wish to blow up only the central node, we have $\mathcal{H} = \langle \alpha_2^* \rangle$. The Levi subalgebra $\mathcal{L}$ commuting with $\mathcal{H}$ is:

$$\mathcal{L} = A_1^{(1)} \oplus A_1^{(3)} \oplus A_1^{(4)} \oplus \langle \alpha_2^* \rangle, \tag{4.149}$$

where the A_1 algebras correspond to the white "tails" in picture 4.4, generated by the roots α_1, α_3 and α_4 respectively.

Following the prescription (4.58) for each A_1 summand we have

$$\Phi|_{A_1^{(i)}} = \begin{pmatrix} 0 & 1 \\ \varrho_i & 0 \end{pmatrix} = E_{\alpha_i} + \varrho_i E_{-\alpha_i} \qquad i = 1,3,4, \tag{4.150}$$

where ϱ_i ($i = 1,3,4$) is the Casimir of the $\mathfrak{sl}(2)$ algebra $A_1^{(i)}$. Moreover Φ can have a component along α_2^* with coefficient ϱ_2. Although not necessary for the employment of our machinery, we report for the sake of visual clarity the explicit matrix form of the adjoint Higgs field corresponding to the choice (4.149), employing the standard basis of [112]:

$$\Phi = \left(\begin{array}{cccc|cccc} \varrho_2 & 1 & 0 & 0 & 0 & 0 & 0 & 0 \\ \varrho_1 & \varrho_2 & 0 & 0 & 0 & 0 & 0 & 0 \\ 0 & 0 & 0 & 1 & 0 & 0 & 0 & 1 \\ 0 & 0 & \varrho_3 & 0 & 0 & 0 & -1 & 0 \\ \hline 0 & 0 & 0 & 0 & -\varrho_2 & -\varrho_1 & 0 & 0 \\ 0 & 0 & 0 & 0 & -1 & -\varrho_2 & 0 & 0 \\ 0 & 0 & 0 & -\varrho_4 & 0 & 0 & 0 & -\varrho_3 \\ 0 & 0 & \varrho_4 & 0 & 0 & 0 & -1 & 0 \end{array}\right). \tag{4.151}$$

The threefold is found by imposing

$$\varrho_i(w) = w\, c_i(w) \qquad \text{for } i = 1,2,3,4, \tag{4.152}$$

where we take the $c_i(w)$'s such that $c_i(0) \neq 0$. Later we will simply choose the $c_i(w)$'s to be constant in w.

The Higgs at the origin is then

$$X_+ = E_{\alpha_1} + E_{\alpha_3} + E_{\alpha_4}, \tag{4.153}$$

while Y is

$$Y = c_1 E_{-\alpha_1} + c_3 E_{-\alpha_3} + c_4 E_{-\alpha_4} + c_2 \langle \alpha_2^* \rangle. \tag{4.154}$$

The threefold equation is simply obtained by taking the choice (4.152) and the expression of Φ (4.151) and plugging them into the formula (3.92):[23]

$$\begin{aligned} &x^2 + zy^2 - z^3 + w^2 z \left[c_1^2 + c_3^2 + c_4^2 + 4c_1c_3 + 4c_1c_4 - 2c_3c_4 - 2c_2^2 w(c_1 - 2c_3 - 2c_4) + c_2^4 w^2\right] + \\ &-2w^3 \left[c_1\left(c_3^2 + c_4^2 + c_1c_3 + c_1c_4 - 2c_3c_4\right) + c_2^2 w\left(c_3^2 + c_4^2 - 2c_1c_3 - 2c_1c_4 - 2c_3c_4\right) + c_2^4 w^2 (c_3 + c_4)\right] + \\ &-2wz^2\left(c_1 + c_3 + c_4 + c_2^2 w\right) + 2w^2 y (c_3 - c_4)\left(c_1 - c_2^2 w\right) = 0. \end{aligned}$$

[23] Notice that the threefold expression is not invariant under the exchange of c_1, c_3 and c_4, which are the Casimirs of the three A_1 tails: this can be overcome by a change of variables. In any case, the mode localization proceeds in a way that is invariant under the exchange of c_1, c_3, c_4.

Let's consider what happens when one of the c_i's vanishes. If $c_2 = 0$, the preserved gauge group after Higgsing is $SU(2)$ instead of $U(1)$. This says that the ALE fiber has an A_1 singularity for all values of w, i.e. the threefold has a non-isolated singularity. If $c_i = 0$ with $i = 1, 3, 4$, then the preserved group is still $U(1)$. However, the threefold equation has an A_1 singularity for generic $w \in \mathbb{C}_w$: in fact, the threefold equation is the same one would obtain by taking $\Phi|_{A_1^{(i)}}$ identically zero (the equation is insensitive to the "1" in (4.150)). Such a nilpotent vev for the Higgs field is called a T-brane [94].

Since we want to consider isolated singularities (with a simple flop), avoiding T-brane configurations, we will take $c_i \neq 0 \; \forall i$.

Zero modes. We now analyze the 5d zero modes arising from M-theory reduced on the flop of length 2 defined by (4.152). We keep the c_i's as generic constants.

As in the case of the flops of length 1, the first step consists in determining the decomposition of the algebra $\mathfrak{g} = D_4$ into irreps of the Levi subalgebra (4.149), obtaining:

$$D_4 = (\mathbf{3},\mathbf{1},\mathbf{1})_0 \oplus (\mathbf{1},\mathbf{3},\mathbf{1})_0 \oplus (\mathbf{1},\mathbf{1},\mathbf{3})_0 \oplus (\mathbf{2},\mathbf{2},\mathbf{2})_1 \oplus (\mathbf{2},\mathbf{2},\mathbf{2})_{-1} \oplus (\mathbf{1},\mathbf{1},\mathbf{1})_2 \oplus (\mathbf{1},\mathbf{1},\mathbf{1})_{-2}, \tag{4.155}$$

where the numbers in parenthesis refer to representations of the three A_1 factors, and the subscript is the charge w.r.t. the Cartan $\langle \alpha_2^* \rangle$. Let us examine the zero-mode content of the Levi representations in (4.155) one by one:

$(\mathbf{3},\mathbf{1},\mathbf{1})_0$: in this representation, the operator X_+ can be represented in the basis $\{-E_{\alpha_1}, \frac{1}{2}H_1, \frac{1}{2}E_{-\alpha_1}\}$ as:

$$A_{(\mathbf{3},\mathbf{1},\mathbf{1})_0} = \left(\begin{array}{c|cc} 0 & 1 & 0 \\ 0 & 0 & 1 \\ \hline 0 & 0 & 0 \end{array}\right). \tag{4.156}$$

It is easy to show that this representation does not host any localized 5d zero mode. The same holds for the representations $(\mathbf{1},\mathbf{3},\mathbf{1})_0$ and $(\mathbf{1},\mathbf{1},\mathbf{3})_0$.

$(\mathbf{1},\mathbf{1},\mathbf{1})_2$: X_+ is represented by a 1-dimensional matrix that, in the basis $E_{\alpha_1+2\alpha_2+\alpha_3+\alpha_4}$, reads

$$A_{(\mathbf{1},\mathbf{1},\mathbf{1})_2} = (0)\,. \tag{4.157}$$

We also have:

$$B_{(\mathbf{1},\mathbf{1},\mathbf{1})_2} = 2c_2. \tag{4.158}$$

As a result we find that B has maximal rank, i.e. 1, and so we obtain *one* localized 5d zero-mode with $U(1)$ charge 2. Analogously, the representation $(\mathbf{1},\mathbf{1},\mathbf{1})_{-2}$ yields one 5d zero-mode of $U(1)$ charge -2.

$(\mathbf{2},\mathbf{2},\mathbf{2})_1$: X_+, once put in Jordan form in an appropriate basis[24], is represented as the

[24] The basis explicitly reads: $\{-E_{\alpha_1+\alpha_2} - E_{\alpha_2+\alpha_3}, E_{\alpha_1+\alpha_2+\alpha_4} - E_{\alpha_2+\alpha_3+\alpha_4}, \frac{2E_{\alpha_1+\alpha_2}}{3} + \frac{E_{\alpha_2+\alpha_3}}{3} + \frac{E_{\alpha_2+\alpha_4}}{3}, -\frac{1}{3}E_{\alpha_1+\alpha_2+\alpha_3} - \frac{1}{3}E_{\alpha_1+\alpha_2+\alpha_4} + \frac{2}{3}E_{\alpha_2+\alpha_3+\alpha_4}, -6E_{\alpha_2}, -2E_{\alpha_1+\alpha_2} + 2E_{\alpha_2+\alpha_3} + 2E_{\alpha_2+\alpha_4}, E_{\alpha_1+\alpha_2+\alpha_3} +$

8-dimensional matrix

$$A_{(\mathbf{2},\mathbf{2},\mathbf{2})_1} = \begin{pmatrix} 0&1&0&0&0&0&0&0 \\ 0&0&0&0&0&0&0&0 \\ 0&0&0&1&0&0&0&0 \\ 0&0&0&0&0&0&0&0 \\ 0&0&0&0&0&1&0&0 \\ 0&0&0&0&0&0&1&0 \\ 0&0&0&0&0&0&0&1 \\ 0&0&0&0&0&0&0&0 \end{pmatrix}, \tag{4.159}$$

which has rank $r = 5$. Using the same basis for Y we get:

$$B_{(\mathbf{2},\mathbf{2},\mathbf{2})_1} = \begin{pmatrix} c_2 & 0 & 0 & 0 & 6c_4-6c_3 & 0 & 0 & 0 \\ c_1-c_3+c_4 & c_2 & \frac{2(c_3-c_4)}{3} & 0 & 0 & 2c_4-2c_3 & 0 & 0 \\ 0 & 0 & c_2 & 0 & -6(c_1+c_3-2c_4) & 0 & 0 & 0 \\ 2(c_1-c_3) & 0 & \frac{-c_1+5c_3-c_4}{3} & c_2 & 0 & -2(c_1+c_3-2c_4) & 0 & 0 \\ 0 & 0 & 0 & 0 & \rho & 0 & 0 & 0 \\ 0 & 0 & 0 & 0 & c_1+c_3+c_4 & c_2 & 0 & 0 \\ \frac{c_3-c_1}{3} & 0 & \frac{2c_1-c_3-c_4}{9} & 0 & 0 & \frac{4(c_1+c_3+c_4)}{3} & c_2 & 0 \\ 0 & c_3-c_1 & 0 & \frac{2c_1-c_3-c_4}{3} & 0 & 0 & c_1+c_3+c_4 & c_2 \end{pmatrix}. \tag{4.160}$$

Let us pause for a moment and use the results just found to prove that there are other isolated singularities in the threefold. In fact, these correspond to values of w where 5d localized modes appear. This happens in the representation under study when the rank of $A_{(\mathbf{2},\mathbf{2},\mathbf{2})_1}+wB_{(\mathbf{2},\mathbf{2},\mathbf{2})_1}$ drops. Its determinant explicitly reads:

$$\begin{aligned} \det(A_{(\mathbf{2},\mathbf{2},\mathbf{2})_1}+wB_{(\mathbf{2},\mathbf{2},\mathbf{2})_1}) = w^4 \big[& (c_1^2+c_3^2+c_4^2-2c_1c_3-2c_1c_4-2c_3c_4)^2+ \\ & -4c_2^2w(c_1^3+c_3^3+c_4^3-c_1^2c_3-c_1^2c_4-c_3^2c_1-c_3^2c_4-c_4^2c_1-c_4^2c_3+10c_1c_3c_4)+ \\ & +2c_2^4w^2(3c_1^2+3c_3^2+3c_4^2+2c_1c_3+2c_1c_4+2c_3c_4)-4c_2^6w^3(c_1+c_3+c_4)+c_2^8w^4 \big] . \end{aligned} \tag{4.161}$$

It turns out that for generic c_i's the rank of $A_{(\mathbf{2},\mathbf{2},\mathbf{2})_1}+wB_{(\mathbf{2},\mathbf{2},\mathbf{2})_1}$ drops on top of $w = 0$, as well as on further *four* distinct points with non-zero w. It can be checked that these additional points correspond to conifold singularities far from the origin. In addition, if the condition

$$c_1^2+c_3^2+c_4^2-2c_1c_3-2c_1c_4-2c_3c_4 = 0 \tag{4.162}$$

is satisfied, one of the additional singularities collides onto the origin: in this case, the rank of $A_{(\mathbf{2},\mathbf{2},\mathbf{2})_1}+wB_{(\mathbf{2},\mathbf{2},\mathbf{2})_1}$ drops on $w = 0$ as well as on *three* additional points outside the origin. This signals the appearance of further localized modes at $w = 0$, coming from the conifold singularity that has collided onto the origin. We will explicitly check this claim momentarily, deriving again condition (4.162).

$E_{\alpha_1+\alpha_2+\alpha_4}+E_{\alpha_2+\alpha_3+\alpha_4}, E_{\alpha_1+\alpha_2+\alpha_3+\alpha_4}\}$.

Rearranging rows and columns to get to the form (4.134) we obtain:

$$B_u = \begin{pmatrix} 0 & 0 & 0 & 0 & 0 \\ 0 & 0 & 0 & 0 & 0 \\ 0 & 0 & 0 & 0 & 0 \\ 0 & 0 & c_2 & 0 & 0 \\ 0 & 0 & \frac{4(c_1+c_3+c_4)}{3} & c_2 & 0 \end{pmatrix}$$

$$B_r = \begin{pmatrix} c_2 & 0 & 6c_4-6c_3 \\ 0 & c_2 & -6(c_1+c_3-2c_4) \\ 0 & 0 & c_2 \\ 0 & 0 & c_1+c_3+c_4 \\ \frac{c_3-c_1}{3} & \frac{2c_1-c_3-c_4}{9} & 0 \end{pmatrix} \tag{4.163}$$

$$B_l = \begin{pmatrix} c_2 & 0 & 2c_4-2c_3 & 0 & 0 \\ 0 & c_2 & -2(c_1+c_3-2c_4) & 0 & 0 \\ c_3-c_1 & \frac{2c_1-c_3-c_4}{3} & 0 & c_1+c_3+c_4 & c_2 \end{pmatrix}$$

$$B_d = \begin{pmatrix} c_1-c_3+c_4 & \frac{2(c_3-c_4)}{3} & 0 \\ 2(c_1-c_3) & \frac{-c_1+5c_3-c_4}{3} & 0 \\ 0 & 0 & 0 \end{pmatrix}$$

Notice that the rank of B_d, which is surely non-maximal, depends on the precise choice of the partial Casimirs. It drops to one when its determinant is equal to zero. This happens when

$$c_1^2+c_3^2+c_4^2-2c_1c_3-2c_1c_4-2c_3c_4 = 0. \tag{4.164}$$

Let us first examine the case in which the c_i's are generic constants, i.e. B_d has rank 2. Afterwards we take a look at the case where B_d has rank 1. Notice that B_d cannot have rank zero, otherwise $c_1 = c_3 = c_4 = 0$, that we excluded.

- Let's take generic c_i's such that $c_1^2+c_3^2+c_4^2-2c_1c_3-2c_1c_4-2c_3c_4 \neq 0$. Renaming $A' \equiv B_d$ and $B' \equiv -B_l(A_u+wB_u)^{-1}B_r$ we can use equation (4.139) to rerun the algorithm. A' is already in a form with a 2×2 invertible block and all other elements equal to zero, i.e. $r' = 2$. We can then immediately read B'_d by computing the (33) element of B'. It is

$$B'_d = 3\left(c_1^2+c_3^2+c_4^2-2c_1c_3-2c_1c_4-2c_3c_4\right)+\frac{10}{3}wc_2^2(c_1+c_3+c_4)-c_2^4w^2, \tag{4.165}$$

  that has rank 1. As a result, according to (4.140), we find that the total number of zero modes is:

$$\# = r'+2(d_R-r-r') = 2+2(8-5-2) = 4, \tag{4.166}$$

  where we recall that d_R is the dimension of the representation, r is the rank of

(4.159) and r' is the rank of A'. The zero-modes have charge $+1$ with respect to the $U(1)$ generator.
Analogously, we find 4 localized zero-modes with charge -1 in the $(\mathbf{2},\mathbf{2},\mathbf{2})_{-1}$ representation.

- When the c_i's fulfill (4.164), the rank of B_d drops to 1. This produces a change in the zero-mode counting. We can parametrize a solution of (4.164) in terms of two parameters q_1, q_4 as:

$$c_1 = q_1^2, \qquad c_3 = (q_1+\varepsilon q_4)^2, \qquad c_4 = q_4^2 \tag{4.167}$$

where ε can take the values ± 1. Now we have

$$A' = \begin{pmatrix} 2q_1q_4 & \frac{2}{3}q_1(q_1+2\varepsilon q_4) & 0 \\ -2q_4(q_4+2\varepsilon q_1) & \frac{2}{3}(2q_1^2+5\varepsilon q_1q_4+2q_4^2) & 0 \\ 0 & 0 & 0 \end{pmatrix}, \tag{4.168}$$

When $q_1^2+\varepsilon q_1 q_4+q_4^2 \neq 0$, the 2×2 matrix is diagonalizable with the non-zero eigenvalue equal to $\frac{4}{3}\,(q_1^2+\varepsilon q_1q_4+q_4^2)$. The corresponding B'_d is

$$B'_d = \begin{pmatrix} c_2^2 & -\frac{12c_2q_1q_4(q_1+\varepsilon q_4)}{q_1^2+\varepsilon q_1q_4+q_4^2} \\ 4c_2q_1q_4(q_1+\varepsilon q_4) & 0 \end{pmatrix}. \tag{4.169}$$

This matrix has rank less than two only when one of the c_i's vanishes (and consequently the other two are equal to each other), that we excluded.
When $q_1^2+\varepsilon q_1q_4+q_4^2 = 0$ (i.e. all the eigenvalues vanish) the 2×2 matrix has still rank 1 and the corresponding B'_d is also forced to have rank 2 (for non-vanishing c_i's).
We can finally count the localized zero-modes using formula (4.140), finding:

$$\# = r'+2(d_R-r-r') = 1+2(8-5-1) = 5. \tag{4.170}$$

Notice that, with respect to the case (4.166) in which the Casimirs were totally generic, we have found an enhancement in the number of modes on a specific locus in the space of the partial Casimirs. This is the same locus where one conifold singularity that was at $w\neq 0$ collides onto the origin.
The representation $(\mathbf{2},\mathbf{2},\mathbf{2})_{-1}$ gives us further 5 zero-modes of charge -1.

Let us summarize our findings for the modes localized at $w=0$ for the simple flop of length 2 and partial Casimirs given by $\varrho_i(w) = w\,c_i$, with c_i constants.

- For generic values of c_i's, we get:
  - 8 modes with charge ± 1,

- 2 modes with charge ± 2.

In terms of the GV invariants, this means

$$n_1^{g=0} = 4 \qquad \text{and} \qquad n_2^{g=0} = 1\,. \tag{4.171}$$

- For c_i's satisfying the constraint (4.164), we get:
  - 10 modes with charge ± 1,
  - 2 modes with charge ± 2.

  In terms of the GV invariants, this means

$$n_1^{g=0} = 5 \qquad \text{and} \qquad n_2^{g=0} = 1\,. \tag{4.172}$$

For the other (non-zero) values of w where there are localized modes, we have conifold singularities and the flop is therefore not of length two: in fact, at these values of w the D_4 is still deformed to a smaller singularity of A-type.

As usual, we can translate from the GV language to the Higgs branch data, noticing that (4.171) predicts that M-theory on this flop of length 2 geometrically engineers a rank-0 5d $\mathcal{N}=1$ SCFT with a $U(1)$ flavor group, 4 hypers of charge 1 and 1 hyper of charge 2 under this group. The enhancement (4.172) simply adds a hyper of charge 1 to the Higgs branch. If we pick the choice $SO(8)/\mathbb{Z}_2$ for the global form of the 7d gauge group, we find no discrete group in 5d.

Non-constant c_i's. For simplicity, we have analyzed cases when the partial Casimirs ϱ_i are just a constant c_i multiplied by w. Of course, one can also let c_i depend on w and rerun the algorithm.

One can in particular find the dependence of the $c_i(w)$'s such that the threefold X has only one isolated singularity at the origin. An easy solution is when

$$c_1 = 4a + b^2\, w\,, \qquad c_2 = b\,, \qquad c_3 = c_4 = a\,. \tag{4.173}$$

One can check that for this choice the determinant (4.161) is equal to $-256a^3b^2w^5$, i.e. it vanishes only at $w=0$. The corresponding threefold has $n_1^{g=0} = 5$ and $n_2^{g=0} = 1$. For $a = -1/4$ and $b = 1/2$ one actually recovers the Brown-Wemyss threefold [92] in the form that appeared in Section 4.6.2 (that has the expected GV invariants). Notice, moreover, that the GV invariants match the one of the Laufer singularity of Section 6.3.2, that is also a flop of length[25] 2.

[25] As argued in [92], the Brown-Wemyss and the Laufer singularity possess the same GV invariants, but are distinguished by their contraction algebra.

4.8.3 Simple flop with length 3

In this section we engineer a threefold X with a simple flop of length three. Analogously to the previous sections, we are going to define a suitable Higgs field, valued in the E_6 Lie algebra, that generates a family of deformed E_6 surfaces with an E_6 singularity at $w = 0$. The resolution of the isolated singularity in the threefold X will blow-up only the trivalent node of the E_6 Dynkin diagram (see Figure 4.2). To achieve this result, we pick the following Levi subalgebra

$$\mathcal{L} = A_2^{(1,2)} \oplus A_2^{(4,5)} \oplus A_1^{(6)} \oplus \langle \alpha_3^* \rangle, \tag{4.174}$$

where the factors $A_2^{(i,j)}$ are associated, as subalgebras, to the roots α_i, α_j of the E_6 Dynkin diagram (we follow the labels in Figure 4.5) and $A_1^{(6)}$ is the algebra associated to the root α_6.

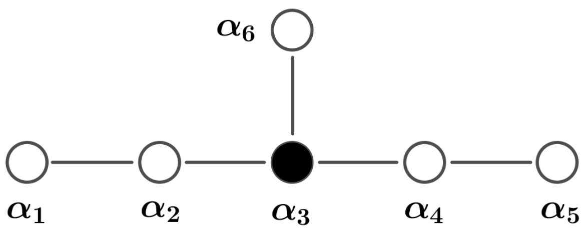

Figure 4.5: *E_6 Dynkin diagram, with the root blown up in the length three flop colored in black.*

Again, we pick $X_+ \equiv \Phi|_{w=0}$ to be an element of the principal nilpotent orbit of each simple factor of $\mathcal{L}$. The partial Casimirs relative to $\mathcal{L}$ are the total Casimirs of each simple factor of (4.174), plus the coefficient along the Cartan element $\langle \alpha_3^* \rangle$. I.e. the generic Φ will be such that[26]

$$\Phi|_{A_2^{(i,j)}} = \begin{pmatrix} 0 & 1 & 0 \\ 0 & 0 & 1 \\ \varrho_3^{(i,j)} & \varrho_2^{(i,j)} & 0 \end{pmatrix} = E_{\alpha_i} + E_{\alpha_j} + \varrho_2^{(i,j)} E_{-\alpha_j} + \varrho_3^{(i,j)} [E_{-\alpha_j}, E_{-\alpha_i}], \qquad i < j, \tag{4.175}$$

$$\Phi|_{A_1^{(6)}} = \begin{pmatrix} 0 & 1 \\ \varrho_2^{(6)} & 0 \end{pmatrix} = E_{\alpha_6} + \varrho_2^{(6)} E_{-\alpha_6} \qquad \text{and} \qquad \Phi|_{\langle \alpha_3^* \rangle} = \varrho_1^{(3)} \langle \alpha_3^* \rangle .$$

[26]To match the conventions of Section 1.3.4, one takes $\{\varrho_i |\ i = 1, ..., 6\} = \{\varrho_1^{(3)}, \varrho_2^{(6)}\} \cup \{\varrho_3^{(i,j)}, \varrho_2^{(i,j)} |\ (i,j) = (1,2), (4,5)\}$.

We now explicitly construct a threefold, by making the choice

$$\begin{aligned}
\varrho_1^{(3)} &= w\, c_3 \\
\varrho_2^{(6)} &= w\, c_6 \\
\varrho_2^{(1,2)} &= 0 \\
\varrho_2^{(4,5)} &= 0 \\
\varrho_3^{(1,2)} &= w\, c_{12} \\
\varrho_3^{(4,5)} &= w\, c_{45}
\end{aligned} \tag{4.176}$$

with c_3, c_6, c_{12}, c_{45} constant numbers.

By plugging this choice into the Higgs field vev Φ, and following the procedure described in Section 4.7.2, one obtains the threefold as an hypersurface of $(x, y, z, w) \in \mathbb{C}^4$.

As an example, if we pick $c_3 = 0, c_6 = -3, c_{12} = 1, c_{45} = -1$, one gets the following threefold, which is singular at the origin (as well as at other three points with non-zero w):

$$x^2+y^3+z^4+\frac{27w^6}{32}+18w^5+\left(12w^3-\frac{27w^4}{16}\right)y+2\left(w^2-\frac{9w^3}{8}\right)z^2+3wyz^2=0. \tag{4.177}$$

Via a change of coordinates, this exactly coincides with the length 3 threefold explicitly presented by [91].

Zero modes. We now proceed (with the same procedure of the previous sections) to the mode counting. The branching of the adjoint representation **78** of E_6 w.r.t $\mathcal{L}$ in (4.174) is given by[27]

$$\begin{aligned}
\mathbf{78} \;=\; & (\mathbf{8,1,1})_0 \oplus (\mathbf{1,8,1})_0 \oplus (\mathbf{1,1,3})_0 \oplus (\mathbf{1,1,2})_3 \oplus (\mathbf{1,1,2})_{-3} \oplus (\mathbf{1,1,1})_0 \oplus \\
& \oplus (\mathbf{3},\overline{\mathbf{3}},\mathbf{2})_1 \oplus (\mathbf{3},\overline{\mathbf{3}},\mathbf{1})_{-2} \oplus (\overline{\mathbf{3}},\mathbf{3},\mathbf{2})_{-1} \oplus (\overline{\mathbf{3}},\mathbf{3},\mathbf{1})_2 ,
\end{aligned} \tag{4.178}$$

where the subscripts denote the charges under $\langle \alpha_3^* \rangle$.

For the E-cases the explicit computations done for length one and two become convoluted. We present here only the results. A Mathematica routine, presented in [99], that implements the algorithm described in Section 4.7.3, can be used to check the results. Running this code for a generic choice of the parameters c_6, c_3, c_{12}, c_{45}, we obtained, for each irreducible representation appearing in (4.178), the 5d modes shown in Table 4.1. In the table, we also write how many elements of the given representation support a mode localized in $\mathbb{C}[w]/(w^k)$, for each k; we find that $k \leq 2$. We get a total of 20 5d modes:

- one hyper with charge three, inside $(\mathbf{1},\mathbf{1},\mathbf{2})_3 \oplus (\mathbf{1},\mathbf{1},\mathbf{2})_{-3}$;
- three hypers with charge two inside $(\overline{\mathbf{3}},\mathbf{3},\mathbf{1})_2 \oplus (\mathbf{3},\overline{\mathbf{3}},\mathbf{1})_{-2}$;

[27] It can be better understood starting from the one of the maximal subalgebra $A_2^{(1,2)} \oplus A_2^{(4,5)} \oplus A_2'$ (with A_2' containing E_{α_6}): $\mathbf{78} = (\mathbf{8,1,1}) \oplus (\mathbf{1,8,1}) \oplus (\mathbf{1,1,8}) \oplus (\mathbf{3},\overline{\mathbf{3}},\mathbf{3}) \oplus (\overline{\mathbf{3}},\mathbf{3},\overline{\mathbf{3}})$. One then selects the subalgebra $A_1^{(6)} \subset A_2'$, and correspondingly branches each term of the sum.

$R^{\mathcal{L}}$	$\mathbb{C}[w]/(w)$	$\mathbb{C}[w]/(w^2)$	$\#_{\text{zero modes}}$
$(\mathbf{8},\mathbf{1},\mathbf{1})_0$	0	0	0
$(\mathbf{1},\mathbf{8},\mathbf{1})_0$	0	0	0
$(\mathbf{1},\mathbf{1},\mathbf{3})_0$	0	0	0
$(\mathbf{1},\mathbf{1},\mathbf{1})_0$	0	0	0
$(\mathbf{3},\overline{\mathbf{3}},\mathbf{2})_1$	4	1	6
$(\overline{\mathbf{3}},\mathbf{3},\mathbf{2})_{-1}$	4	1	6
$(\overline{\mathbf{3}},\mathbf{3},\mathbf{1})_2$	3	0	3
$(\mathbf{3},\overline{\mathbf{3}},\mathbf{1})_{-2}$	3	0	3
$(\mathbf{1},\mathbf{1},\mathbf{2})_3$	1	0	1
$(\mathbf{1},\mathbf{1},\mathbf{2})_{-3}$	1	0	1

Table 4.1: *5d modes for E_6 length three simple flop.*

- six hypers with charge one inside $(\mathbf{3},\overline{\mathbf{3}},\mathbf{2})_1 \oplus (\overline{\mathbf{3}},\mathbf{3},\mathbf{2})_{-1}$.

In terms of the GV invariants, one then reads

$$n_1^{g=0} = 6\,, \qquad n_2^{g=0} = 3 \qquad \text{and} \qquad n_3^{g=0} = 1\,, \tag{4.179}$$

which perfectly coincides with the results of [91]. Notice that the maximal flavor charge is equal to the length of the flop and to the dual Coxeter label of the resolved node.

In addition, M-theory on this simple flop of length 3 geometrically engineers a rank-0 5d $\mathcal{N}=1$ SCFT with Higgs branch data encoded in (4.179), with the usual correspondences. No discrete group is present if we pick the simply connected form of the E_6 group, modded by its center $\mathbb{Z}_3$. Notice that all the charges from 1 to 3 are realized.

We can finally check whether there are special choices of the parameters c_{12}, c_{45}, c_6, c_3 for which the number of 5d modes localized at $w=0$ enhances. A necessary condition for the enhancement of the number of modes is that the rank of the matrix B_d drops for a special choice of the partial Casimirs. By explicit computation, we find that the rank drops when $c_{12}=c_{45}$ or $c_6=0$. However, these choices would create a non-isolated singularity.

4.8.4 Simple flop with length 4

In the following section we engineer, by means of a Higgs field Φ valued in the E_7 Lie algebra, a flop of length four. By looking at the dual Coxeter labels of the E_7 Dynkin diagram in Figure 4.2, we see that the simultaneous resolution should involve the trivalent node. Analogously to the previous examples, this means that we have to pick the Higgs field in the Levi subalgebra

$$\mathcal{L} \equiv A_3^{(4,5,6)} \oplus A_2^{(1,2)} \oplus A_1^{(7)} \oplus \langle \alpha_3^* \rangle, \tag{4.180}$$

where the superscripts refer to the roots of the E_7 Dynkin diagram numbered as in the Figure 4.6, and α_3 is the trivalent root of E_7.

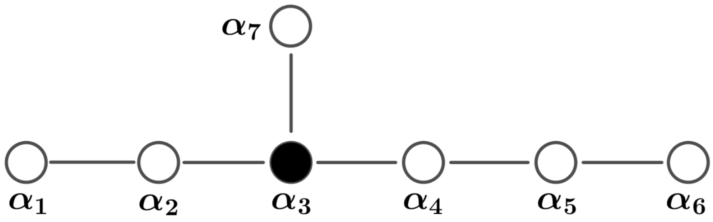

Figure 4.6: *E_7 Dynkin diagram, with the root blown up in the length four flop colored in black.*

Analogously to the E_6 case, we choose the Higgs field as follows:

$$\Phi|_{\langle \alpha_3^* \rangle} = c_3 w \langle \alpha_3^* \rangle \tag{4.181}$$

and

$$\Phi|_{A_1^{(7)}} = \begin{pmatrix} 0 & 1 \\ c_7 w & 0 \end{pmatrix} = E_{\alpha_7} + c_7 w \, E_{-\alpha_7},$$

$$\Phi|_{A_2^{(1,2)}} = \begin{pmatrix} 0 & 1 & 0 \\ 0 & 0 & 1 \\ c_{12} w & 0 & 0 \end{pmatrix} = E_{\alpha_1} + E_{\alpha_2} + c_{12} w \, [E_{-\alpha_1}, E_{-\alpha_2}],$$

$$\Phi|_{A_3^{(4,5,6)}} = \begin{pmatrix} 0 & 1 & 0 & 0 \\ 0 & 0 & 1 & 0 \\ 0 & 0 & 0 & 1 \\ c_{456} w & 0 & 0 & 0 \end{pmatrix} = E_{\alpha_4} + E_{\alpha_5} + E_{\alpha_6} + c_{456} w \Big[[E_{-\alpha_4}, E_{-\alpha_5}], E_{-\alpha_6} \Big].$$

The corresponding threefold is a hypersurface in $\mathbb{C}^4$, that is a family of deformed E_7 singularities over $\mathbb{C}_w$. To make the equation of the threefold more readable, we set the parameters to specific values, picking $c_3 = 0, c_7 = 3, c_{12} = \frac{1}{2}, c_{456} = -\frac{1}{2}$, obtaining

$$x^2 - y^3 + yz^3 + 3wy^2 z + y^2 \frac{81 w^2}{16} - yz \frac{w^2}{12} + z^2 \frac{5w^3}{8} - y \frac{w^3}{108} + z \frac{w^4}{3} + \frac{w^5}{144} = 0. \tag{4.182}$$

where we neglected terms of high degree, irrelevant for the singularity at $w = 0$.

Zero modes. We now proceed with the modes counting. We will again perform the gauge-fixing separately in each irreducible representation of the branching of the adjoint representation **133** of E_7 under the subalgebra $\mathcal{L}$:[28]

$$\begin{aligned}\mathbf{133} \;=\; & (\mathbf{15},\mathbf{1},\mathbf{1})_0 \oplus (\mathbf{1},\mathbf{8},\mathbf{1})_0 \oplus (\mathbf{1},\mathbf{1},\mathbf{3})_0 \oplus (\mathbf{1},\mathbf{1},\mathbf{1})_0 \oplus \\ & (\overline{\mathbf{4}},\mathbf{3},\mathbf{2})_{-1} \oplus (\mathbf{4},\overline{\mathbf{3}},\mathbf{2})_1 \oplus (\mathbf{6},\overline{\mathbf{3}},\mathbf{1})_{-2} \oplus (\mathbf{6},\mathbf{3},\mathbf{1})_2 \oplus \\ & (\mathbf{4},\mathbf{1},\mathbf{2})_{-3} \oplus (\overline{\mathbf{4}},\mathbf{1},\mathbf{2})_3 \oplus (\mathbf{1},\mathbf{3},\mathbf{1})_{-4} \oplus (\mathbf{1},\overline{\mathbf{3}},\mathbf{1})_4 .\end{aligned} \tag{4.183}$$

Running the Mathematica routine described in [99], we find the results displayed in table 4.2. As in the E_6 case, there are no five-dimensional modes localized in $\mathbb{C}[w]/(w^k)$, with $k > 2$. In total, we find 28 modes localized at $w = 0$:

$R^{\mathcal{L}}$	$\mathbb{C}[w]/(w)$	$\mathbb{C}[w]/(w^2)$	$\#_{\text{zero modes}}$
$(\mathbf{15},\mathbf{1},\mathbf{1})_0$	0	0	0
$(\mathbf{1},\mathbf{8},\mathbf{1})_0$	0	0	0
$(\mathbf{1},\mathbf{1},\mathbf{3})_0$	0	0	0
$(\mathbf{1},\mathbf{1},\mathbf{1})_0$	0	0	0
$(\overline{\mathbf{4}},\mathbf{3},\mathbf{2})_{-1}$	6	0	6
$(\mathbf{4},\overline{\mathbf{3}},\mathbf{2})_1$	6	0	6
$(\mathbf{6},\overline{\mathbf{3}},\mathbf{1})_{-2}$	3	1	5
$(\mathbf{6},\mathbf{3},\mathbf{1})_2$	3	1	5
$(\mathbf{4},\mathbf{1},\mathbf{2})_{-3}$	2	0	2
$(\overline{\mathbf{4}},\mathbf{1},\mathbf{2})_3$	2	0	2
$(\mathbf{1},\mathbf{3},\mathbf{1})_{-4}$	1	0	1
$(\mathbf{1},\overline{\mathbf{3}},\mathbf{1})_4$	1	0	1

Table 4.2: *five-dimensional modes for E_7 length four simple flop.*

- one hyper with charge four, inside $(\mathbf{1},\mathbf{3},\mathbf{1})_{-4} \oplus (\mathbf{1},\overline{\mathbf{3}},\mathbf{1})_4$;
- two hypers with charge three inside $(\mathbf{4},\mathbf{1},\mathbf{2})_{-3} \oplus (\overline{\mathbf{4}},\mathbf{1},\mathbf{2})_3$;
- five hypers with charge two inside $(\mathbf{6},\overline{\mathbf{3}},\mathbf{1})_{-2} \oplus (\mathbf{6},\mathbf{3},\mathbf{1})_2$.
- six hypers with charge one inside $(\overline{\mathbf{4}},\mathbf{3},\mathbf{2})_{-1} \oplus (\mathbf{4},\overline{\mathbf{3}},\mathbf{2})_1$.

[28] The first entry of each summand is a representation of $A_3^{(4,5,6)}$, the second one is a representation of $A_2^{(1,2)}$, and the third on a representation of $A_1^{(7)}$. The subscript is the charge under $\langle \alpha_3^* \rangle$.

In terms of the GV invariants, one then reads

$$n_1^{g=0} = 6\,, \qquad n_2^{g=0} = 5\,, \qquad n_3^{g=0} = 2 \qquad \text{and} \qquad n_4^{g=0} = 1\,, \tag{4.184}$$

where again we notice the correspondence between the maximal degree of the GV invariants and the length of the flop.

The Higgs branch data of the 5d SCFT engineered by M-theory on the simple flop of length 4 can be read directly from (4.184). As in all the preceding cases, no discrete group is present when we take as global form E_7 modded by its center $\mathbb{Z}_2$, and all the charges from 1 to 4 are realized by some hypermultiplet.

Finally, we find (as in the E_6 case) that no particular choice of the constants c_i can enhance the number of zero modes at $w = 0$ (without generating non-isolated singularities).

4.8.5 Simple flop with length 5

A flop with length 5 is obtained from an E_8 family over $\mathbb{C}_w$. The node that should be simultaneously resolved at $w = 0$ is depicted in Figure 4.7.

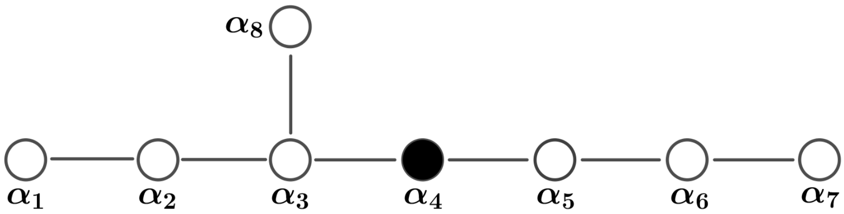

Figure 4.7: *E_8 Dynkin diagram, with the root blown up in the length five flop colored in black.*

We then have $\mathcal{H} = \langle \alpha_4^* \rangle$ and

$$\mathcal{L} = A_3^{(5,6,7)} \oplus A_4^{(1,2,3,8)} \oplus \langle \alpha_4^* \rangle. \tag{4.185}$$

We make the simple choice

$$\begin{aligned}
\Phi|_{\langle \alpha_4^* \rangle} &= c_4 w \, \langle \alpha_4^* \rangle \\
\Phi|_{A_3^{(5,6,7)}} &= \begin{pmatrix} 0 & 1 & 0 & 0 \\ 0 & 0 & 1 & 0 \\ 0 & 0 & 0 & 1 \\ c_{567}w & 0 & 0 & 0 \end{pmatrix} = E_{\alpha_5} + E_{\alpha_6} + E_{\alpha_7} + c_{567} w \, [[E_{-\alpha_5}, E_{-\alpha_6}], E_{-\alpha_7}] \\
\Phi|_{A_4^{(1,2,3,8)}} &= \begin{pmatrix} 0 & 1 & 0 & 0 & 0 \\ 0 & 0 & 1 & 0 & 0 \\ 0 & 0 & 0 & 1 & 0 \\ 0 & 0 & 0 & 0 & 1 \\ c_{1238}w & 0 & 0 & 0 & 0 \end{pmatrix} = E_{\alpha_1} + E_{\alpha_2} + E_{\alpha_3} + E_{\alpha_8} - c_{1238} w \left[\left[[E_{-\alpha_1}, E_{-\alpha_2}], E_{-\alpha_3} \right], E_{-\alpha_8} \right]
\end{aligned}$$

with constant c's. We obtain our threefold as a hypersurface in $\mathbb{C}^4$. To make the equation

$R^{\mathcal{L}}$	$\mathbb{C}[w]/(w)$	$\mathbb{C}[w]/(w^2)$	$\#_{\text{zero modes}}$
$(\mathbf{1},\mathbf{24})_0$	0	0	0
$(\mathbf{15},\mathbf{1})_0$	0	0	0
$(\mathbf{1},\mathbf{1})_0$	0	0	0
$(\mathbf{4},\overline{\mathbf{10}})_1$	6	1	8
$(\overline{\mathbf{4}},\mathbf{10})_{-1}$	6	1	8
$(\mathbf{6},\mathbf{5})_2$	6	0	6
$(\mathbf{6},\overline{\mathbf{5}})_{-2}$	6	0	6
$(\overline{\mathbf{4}},\overline{\mathbf{5}})_3$	4	0	4
$(\mathbf{4},\mathbf{5})_{-3}$	4	0	4
$(\mathbf{1},\mathbf{10})_4$	2	0	2
$(\mathbf{1},\overline{\mathbf{10}})_{-4}$	2	0	2
$(\mathbf{4},\mathbf{1})_5$	1	0	1
$(\overline{\mathbf{4}},\mathbf{1})_{-5}$	1	0	1

Table 4.3: *five-dimensional modes for E_8 length five simple flop.*

more readable, we pick explicit values for the parameters, setting $c_4 = 0, c_{567} = 1, c_{1238} = -1$:

$$x^2+y^3+z^5+w^7+\frac{w^6}{864}-\frac{23w^5z}{36}-\frac{w^4y}{48}-\frac{187w^4z^2}{36}-\frac{13}{3}w^3yz-\frac{2w^3z^3}{27}-\frac{1}{3}w^2yz^2=0. \quad (4.186)$$

Zero modes. We can explicitly perform the branching of the adjoint representation **248** of E_8 under the chosen $\mathcal{L}$:[29]

$$\begin{aligned}\mathbf{248} \;=\; & (\mathbf{1},\mathbf{24})_0\oplus(\mathbf{15},\mathbf{1})_0\oplus(\mathbf{1},\mathbf{1})_0\oplus \\ & (\mathbf{4},\overline{\mathbf{10}})_1\oplus(\overline{\mathbf{4}},\mathbf{10})_{-1}\oplus(\mathbf{6},\mathbf{5})_2\oplus(\mathbf{6},\overline{\mathbf{5}})_{-2}\oplus \\ & (\overline{\mathbf{4}},\overline{\mathbf{5}})_3\oplus(\mathbf{4},\mathbf{5})_{-3}\oplus(\mathbf{1},\mathbf{10})_4\oplus(\mathbf{1},\overline{\mathbf{10}})_{-4}\oplus \\ & (\mathbf{4},\mathbf{1})_5\oplus(\overline{\mathbf{4}},\mathbf{1})_{-5}. \end{aligned} \quad (4.187)$$

The result of the zero mode counting is displayed in Table 4.3. There are no modes localized in $\mathbb{C}[w]/(w^k)$, with $k > 2$. We find 48 modes localized at $w = 0$:

- one hyper with charge five, inside $(\mathbf{4},\mathbf{1})_5\oplus(\overline{\mathbf{4}},\mathbf{1})_{-5}$;
- two hyper with charge four, inside $(\mathbf{1},\mathbf{10})_4\oplus(\mathbf{1},\overline{\mathbf{10}})_{-4}$;

[29]The first number denotes the dimension of the representation of $A_3^{(5,6,7)}$, the second under $A_4^{(1,2,3,8)}$ and the subscript is the charge under the Cartan α_4^*.

- four hypers with charge three inside $(\overline{\mathbf{4}},\overline{\mathbf{5}})_3 \oplus (\mathbf{4},\mathbf{5})_{-3}$;
- six hypers with charge two inside $(\mathbf{6},\mathbf{5})_2 \oplus (\mathbf{6},\overline{\mathbf{5}})_{-2}$;
- eight hypers with charge one inside $(\mathbf{4},\overline{\mathbf{10}})_1 \oplus (\overline{\mathbf{4}},\mathbf{10})_{-1}$.

In terms of the GV invariants, one obtains

$$n_1^{g=0} = 8\,, \qquad n_2^{g=0} = 6\,, \qquad n_3^{g=0} = 4\,, \qquad n_4^{g=0} = 2 \qquad \text{and} \qquad n_5^{g=0} = 1\,. \tag{4.188}$$

Suitably translating the GV invariants into the Higgs branch data of M-theory on the simple flop of length 5, we find hypers with charges defined by (4.188). Taking the simply connected E_8 group modded by its (trivial) center we obtain no discrete group. All the charges from 1 to 5 are realized.

Again, we notice that we can not enhance the number of zero-modes at $w = 0$ without generating a non-isolated singularity.

4.8.6 Simple flop with length 6

In this section we conclude our analysis of simple flops by dealing with the highest length case, i.e. a flop of length 6 arising from a E_8 singularity deformed over the plane $\mathbb{C}_w$. We choose the Higgs $\Phi \in E_8$ in such a way to resolve only the central node of the E_8 Dynkin diagram as depicted in Figure 4.8.

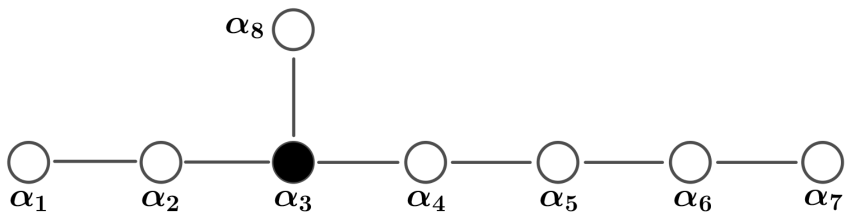

Figure 4.8: *E_8 Dynkin diagram, with the root blown up in the length six flop colored in black.*

According to the principles outlined in previous sections, the Higgs field resolving the central node must lie in the Levi subalgebra defined by:

$$\mathcal{L} = A_4^{(4,5,6,7)} \oplus A_2^{(1,2)} \oplus A_1^{(8)} \oplus \langle \alpha_3^* \rangle, \tag{4.189}$$

where as usual the upper indices label the simple roots. Again we choose Φ of the following form:

$$
\begin{aligned}
\Phi|_{A_4^{(4,5,6,7)}} &= \begin{pmatrix} 0 & 1 & 0 & 0 & 0 \\ 0 & 0 & 1 & 0 & 0 \\ 0 & 0 & 0 & 1 & 0 \\ 0 & 0 & 0 & 0 & 1 \\ c_{4567}w & 0 & 0 & 0 & 0 \end{pmatrix} = E_{\alpha_4}+E_{\alpha_5}+E_{\alpha_6}+E_{\alpha_7}-c_{4567}w\,[[[E_{-\alpha_1},E_{-\alpha_2}],E_{-\alpha_3}],E_{-\alpha_4}]\,, \\
\Phi|_{A_2^{(1,2)}} &= \begin{pmatrix} 0 & 1 & 0 \\ 0 & 0 & 1 \\ c_{12}w & 0 & 0 \end{pmatrix} = E_{\alpha_1}+E_{\alpha_2}+c_{12}w\,[E_{-\alpha_1},E_{-\alpha_2}]\,, \\
\Phi|_{A_1^{(8)}} &= \begin{pmatrix} 0 & 1 \\ c_8 w & 0 \end{pmatrix} = E_{\alpha_8}+c_8 w\,E_{-\alpha_8}, \\
\Phi|_{\langle\alpha_3^*\rangle} &= c_3 w\,\langle\alpha_3^*\rangle.
\end{aligned}
\tag{4.190}
$$

To make the equation more readily understandable, we set the parameters to a specific value $c_3=0, c_8=1, c_{12}=-1, c_{4567}=1$. In this way we obtain the threefold

$$
x^2+y^3+z^5-wyz^3-\frac{w^4}{48}y+\frac{w^6}{864}-\frac{7w^2}{2}yz^2-\frac{23w^4}{20}yz-\frac{11w^3}{12}z^3-\frac{17w^4}{24}z^2+\frac{47w^6}{240}z=0, \tag{4.191}
$$

where we neglected terms of high degree, irrelevant for the singularity at $w=0$.

Zero modes. We perform the mode counting explicitly, independently for each irreducible representation arising from the adjoint **248** of E_8, branched under the Levi subalgebra (4.189). The decomposition reads:

$$
\begin{aligned}
\mathbf{248} \;=\;& (\mathbf{24},\mathbf{1},\mathbf{1})_0\oplus(\mathbf{1},\mathbf{8},\mathbf{1})_0\oplus(\mathbf{1},\mathbf{1},\mathbf{3})_0\oplus(\mathbf{1},\mathbf{1},\mathbf{1})_0\oplus \\
& (\mathbf{5},\overline{\mathbf{3}},\mathbf{2})_1\oplus(\overline{\mathbf{5}},\mathbf{3},\mathbf{2})_{-1}\oplus(\mathbf{10},\mathbf{3},\mathbf{1})_2\oplus(\overline{\mathbf{10}},\overline{\mathbf{3}},\mathbf{1})_{-2}\oplus \\
& (\overline{\mathbf{10}},\mathbf{1},\mathbf{2})_3\oplus(\mathbf{10},\mathbf{1},\mathbf{2})_{-3}\oplus(\overline{\mathbf{5}},\overline{\mathbf{3}},\mathbf{1})_4\oplus(\mathbf{5},\mathbf{3},\mathbf{1})_{-4}\oplus \\
& (\mathbf{1},\mathbf{3},\mathbf{2})_5\oplus(\mathbf{1},\overline{\mathbf{3}},\mathbf{2})_{-5}\oplus(\mathbf{5},\mathbf{1},\mathbf{1})_6\oplus(\overline{\mathbf{5}},\mathbf{1},\mathbf{1})_{-6}
\end{aligned}
\tag{4.192}
$$

Applying the Mathematica routine presented in [99], we find the zero modes in Table 4.4. We find a total of 44 localized modes:

- one hyper with charge six, inside $(\mathbf{5},\mathbf{1},\mathbf{1})_6\oplus(\overline{\mathbf{5}},\mathbf{1},\mathbf{1})_{-6}$;
- two hypers with charge five, inside $(\mathbf{1},\mathbf{3},\mathbf{2})_5\oplus(\mathbf{1},\overline{\mathbf{3}},\mathbf{2})_{-5}$;
- three hypers with charge four, inside $(\overline{\mathbf{5}},\overline{\mathbf{3}},\mathbf{1})_4\oplus(\mathbf{5},\mathbf{3},\mathbf{1})_{-4}$;
- four hypers with charge three inside $(\overline{\mathbf{10}},\mathbf{1},\mathbf{2})_3\oplus(\mathbf{10},\mathbf{1},\mathbf{2})_{-3}$;

$R^{\mathcal{L}}$	$\mathbb{C}[w]/(w)$	$\mathbb{C}[w]/(w^2)$	$\#_{\text{zero modes}}$
$(\mathbf{24},\mathbf{1},\mathbf{1})_0$	0	0	0
$(\mathbf{1},\mathbf{8},\mathbf{1})_0$	0	0	0
$(\mathbf{1},\mathbf{1},\mathbf{3})_0$	0	0	0
$(\mathbf{1},\mathbf{1},\mathbf{1})_0$	0	0	0
$(\mathbf{5},\overline{\mathbf{3}},\mathbf{2})_1$	6	0	6
$(\overline{\mathbf{5}},\mathbf{3},\mathbf{2})_{-1}$	6	0	6
$(\mathbf{10},\mathbf{3},\mathbf{1})_2$	6	0	6
$(\overline{\mathbf{10}},\overline{\mathbf{3}},\mathbf{1})_{-2}$	6	0	6
$(\overline{\mathbf{10}},\mathbf{1},\mathbf{2})_3$	4	0	4
$(\mathbf{10},\mathbf{1},\mathbf{2})_{-3}$	4	0	4
$(\overline{\mathbf{5}},\overline{\mathbf{3}},\mathbf{1})_4$	3	0	3
$(\mathbf{5},\mathbf{3},\mathbf{1})_{-4}$	3	0	3
$(\mathbf{1},\mathbf{3},\mathbf{2})_5$	2	0	2
$(\mathbf{1},\overline{\mathbf{3}},\mathbf{2})_{-5}$	2	0	2
$(\mathbf{5},\mathbf{1},\mathbf{1})_6$	1	0	1
$(\overline{\mathbf{5}},\mathbf{1},\mathbf{1})_{-6}$	1	0	1

Table 4.4: *Five-dimensional modes for E_8 length six simple flop.*

- six hypers with charge two inside $(\mathbf{10},\mathbf{3},\mathbf{1})_2\oplus(\overline{\mathbf{10}},\overline{\mathbf{3}},\mathbf{1})_{-2}$;
- six hypers with charge one inside $(\mathbf{5},\overline{\mathbf{3}},\mathbf{2})_1\oplus(\overline{\mathbf{5}},\mathbf{3},\mathbf{2})_{-1}$.

In terms of the GV invariants, one then reads

$$n_1^{g=0}=6, \qquad n_2^{g=0}=6, \qquad n_3^{g=0}=4, \qquad n_4^{g=0}=3, \qquad n_5^{g=0}=2 \quad \text{and} \quad n_6^{g=0}=1.$$

The Higgs branch data corresponding to M-theory on the simple flop of length 6 is immediately deduced from (4.193). Analogously to the lower-length cases, we see no discrete group, and all the charges from 1 to 6 are realized.

Finally, analyzing the rank of the matrix B_d, we find that no enhancement in the number of localized modes at $w=0$ is feasible without generating a non-isolated singularity.

4.9 Beyond simple flops

In light of the applications of the next chapter, in this last section we start going outside of the environment provided by simple threefold flops. Namely, we start considering singular threefolds that can be expressed as deformed ADE singularities admitting more than one inflated $\mathbb{P}^1$ (also called *non-simple flops*), or no crepant resolution at all.

Given the simplicity of the setups[30], we compute zero-modes in the standard way introduced in (4.5), making the exposition more transparent.

4.9.1 Generalized conifold

In this section we present an easy example of non-simple flop, i.e. an isolated singularity whose exceptional locus is a collection of $\mathbb{P}^1$'s. This threefold is a deformation of A_2 and is given by the equation

$$x^2+y^2 = z^3-w^2z, \tag{4.193}$$

and was dubbed "generalized conifold" in [158]. Since it is a A_2-family, the corresponding IIA Higgs field lives in the adjoint of $SU(3)$. It is given by

$$\Phi = \begin{pmatrix} 0 & 0 & 0 \\ 0 & -w & 0 \\ 0 & 0 & w \end{pmatrix}. \tag{4.194}$$

Notice that this equals switching on a vev for ϕ_3 along:

$$\mathcal{H} = \langle \alpha_1^*, \alpha_2^* \rangle, \tag{4.195}$$

where α_1 and α_2 are the two simple roots of A_2. Geometrically, this amounts to the simultaneous resolution of both the nodes of the A_2 Dynkin diagram.

As for the Reid's pagodas (that were also A_n-families) we recover the hypersurface (4.193) computing:

$$uv = \det(z\mathbb{1}-\Phi) = z^3-w^2z. \tag{4.196}$$

The group preserving the above Higgs is:

$$G_{5d} = \begin{pmatrix} e^{i\alpha} & 0 & 0 \\ 0 & e^{i\beta} & 0 \\ 0 & 0 & e^{i\gamma} \end{pmatrix} \qquad \text{with } \alpha+\beta+\gamma = 0 \bmod 2\pi, \tag{4.197}$$

where we have decoupled the diagonal center of mass $U(1)$.

In order to find the possible zero modes we must mod the fluctuations φ of the Higgs by:

$$\varphi \sim \varphi+[\Phi, g], \tag{4.198}$$

[30]These are all special subcases of the singularities we will treat more systematically in Chapter 5.

with g a generic element of $\mathfrak{sl}(3)$.

A direct computation shows that:

$$\varphi \sim \underbrace{\begin{pmatrix} \varphi_{11} & \varphi_{12} & \varphi_{13} \\ \varphi_{21} & \varphi_{22} & \varphi_{23} \\ \varphi_{31} & \varphi_{32} & \varphi_{33} \end{pmatrix}}_{\varphi} + \underbrace{\begin{pmatrix} 0 & g_{12}w & -g_{13}w \\ -g_{21}w & 0 & -2g_{23}w \\ g_{31}w & 2g_{32}w & 0 \end{pmatrix}}_{[\Phi,g]} . \tag{4.199}$$

We then see that φ_{11}, φ_{22} and φ_{33} cannot be fixed, and so do not give rise to localized modes in 5d. On the other hand, note that using the gauge freedom we can set:

$$\varphi_{12}, \varphi_{13}, \varphi_{23} \in \mathbb{C}[w]/(w) \cong \mathbb{C} \tag{4.200}$$

so that we obtain 3 localized modes. The same goes for $\varphi_{21}, \varphi_{31}$ and φ_{32}, that give rise to other 3 modes.

It is immediate to obtain the charges of the modes under the three dependent $U(1)$'s in (4.197):

$$U\varphi U^{-1} = \begin{pmatrix} 0 & e^{i(\alpha-\beta)}\varphi_{12} & e^{i(\alpha-\gamma)}\varphi_{13} \\ e^{-i(\alpha-\beta)}\varphi_{21} & 0 & e^{i(\beta-\gamma)}\varphi_{23} \\ e^{-i(\alpha-\gamma)}\varphi_{31} & e^{-i(\beta-\gamma)}\varphi_{32} & 0 \end{pmatrix} . \tag{4.201}$$

There is no discrete gauge symmetry and then the Higgs branch is simply given by **three free hypermultiplets**. Hence, the Higgs branch is simply:

$$\mathcal{M}_{\text{HB}} = \mathbb{H}^3 , \tag{4.202}$$

with flavor symmetry

$$G_{\text{flavor}} = U(1)^2 . \tag{4.203}$$

Finally, the GV invariants of (4.193) read:

$$n_{d=1}^{g=0} = 3. \tag{4.204}$$

4.9.2 Non-resolvable threefolds and T-branes

In this section, we analyze threefolds that admit *no crepant simultaneous resolution.*

We start with the class of threefolds given by the equation

$$x^2+y^2 = z^{2k+1}-w^2. \tag{4.205}$$

These are A_{2k}-families and then admit a description in IIA in terms of a non-zero vev for a Higgs field living on a $SU(2k+1)$ stack of D6-branes.

Let us describe in more detail the simplest case, i.e. $k = 1$:

$$x^2+y^2 = z^3-w^2. \tag{4.206}$$

This manifold was studied in [169] in the context of F-theory, where the authors showed that there is matter localized at the singularity, even though such isolated singularity does not admit a crepant small resolution. It admits however a non-Kähler resolution, as anticipated in [170].

Here we confirm the existence of one localized hyper. The characteristic polynomial is now singular, hence the field Φ does not take the form (4.58) of a reconstructible Higgs. However we can work out the form of Φ that deforms the $SU(3)$ stack to (4.206):

$$\Phi = \begin{pmatrix} 0 & w & 0 \\ 0 & 0 & w \\ 1 & 0 & 0 \end{pmatrix}. \tag{4.207}$$

In order to find the zero-modes in the fluctuation matrix φ we have to mod out by gauge equivalences:

$$\varphi \sim \varphi + [\Phi, g] \tag{4.208}$$

where $g \in \mathfrak{sl}(3)$.

Doing so, we find that all the entries in φ can be fixed to zero or are not localized on any ideal, except for:

$$\begin{aligned} \varphi_{12} &\sim \varphi_{12} + w(g_{22} - g_{33}) \qquad & \varphi_{23} &\sim \varphi_{23} - w(g_{22} - g_{33}) \\ \varphi_{22} &\sim \varphi_{22} + w(g_{32} - g_{21}) \qquad & \varphi_{33} &\sim \varphi_{33} - w(g_{32} - g_{21}) \end{aligned} \tag{4.209}$$

We note that φ_{12} and φ_{23} depend on the same parameter, as φ_{22} and φ_{33} do. As a consequence, we can choose to localize the first two (say φ_{12} and φ_{22}) in 5d, while the other stay non-dynamical. Acting in this way we get:

$$\varphi_{12}, \varphi_{22} \in \mathbb{C}[w]/(w) \cong \mathbb{C} \tag{4.210}$$

thus giving us $1+1 = 2$ modes in total. Since there is no discrete gauge symmetry left by the Higgs vev, the Higgs branch is given by **one free hypermultiplet**.

This computation is easily generalized to a generic k. The Higgs field is now

$$\Phi = \begin{pmatrix} & w & 0 \\ & 0 & w \\ \mathbb{1}_{2k-1} & & \end{pmatrix}. \tag{4.211}$$

The computation of the localized zero modes proceeds with the same steps done with $k = 1$. The Higgs branch is now given by **k free hypermultiplets**. This result confirms what found with different method in [59].

$$\boxed{x^2 + y^2 = z^{2k+1} - w^2 \qquad \longleftrightarrow \qquad \text{k free hypers}} \tag{4.212}$$

The corresponding GV invariant can hence be read off as:

$$n_{d=0}^{g=0} = k. \tag{4.213}$$

Note that we are in this way *defining* Gopakumar-Vafa invariants for singular varieties without any reference to a small resolution, since the variety is not small-resolvable in Kähler way. In this perspective, we can dub them "degree 0" GV invariants, as they do *not* correspond in 5d to hypers charged under any $U(1)$, simply because there is no such group.

As we have previously mentioned, different choices of the Higgs field can be made, corresponding to inequivalent T-brane backgrounds (putting the 1's and w's in different entries) that would generate a smaller spectrum, and therefore a lower-dimensional Higgs branch.

In this regard, let us examine a simple example of a geometry that admits three possible Higgs branches, depending on the choice of T-brane data. Take the hypersurface given by

$$x^2+y^2 = z^5-w^2\,. \tag{4.214}$$

Again, this is a singular hypersurface that does not admit a crepant Kähler resolution. Nevertheless, it does admit a fiberwise reduction to IIA string theory with D6-branes, albeit with D6-branes that wrap singular Riemann surfaces. For the Higgs background, we see the following three possible choices, each giving rise to a different hypermultiplet spectrum:

$$\Phi_2 = \begin{pmatrix} 0 & w & 0 & 0 & 0 \\ 0 & 0 & 1 & 0 & 0 \\ 0 & 0 & 0 & 1 & 0 \\ 0 & 0 & 0 & 0 & w \\ 1 & 0 & 0 & 0 & 0 \end{pmatrix} \;\Rightarrow\; 2 \text{ free hypers}$$

$$\Phi_1 = \begin{pmatrix} 0 & w & 0 & 0 & 0 \\ 0 & 0 & w & 0 & 0 \\ 0 & 0 & 0 & 1 & 0 \\ 0 & 0 & 0 & 0 & 1 \\ 1 & 0 & 0 & 0 & 0 \end{pmatrix} \;\Rightarrow\; 1 \text{ free hyper}$$

$$\Phi_0 = \begin{pmatrix} 0 & 1 & 0 & 0 & 0 \\ 0 & 0 & 1 & 0 & 0 \\ 0 & 0 & 0 & 1 & 0 \\ 0 & 0 & 0 & 0 & 1 \\ w^2 & 0 & 0 & 0 & 0 \end{pmatrix} \;\Rightarrow\; 0 \text{ free hypers}$$

In all three cases, there is no discrete gauging, so we just have free hypermultiplets. We refer to these different choices as T-brane data, as they consist in inherently non-abelian information that does not alter the M-theory geometry, but nevertheless has a severe impact on the effective physics.

T-brane phenomena are not restricted to non-resolvable threefolds, but invest all the deformed ADE singularities we have studied so far: we will have much more to say on the impact of T-branes on Higgs branch spectra in the following chapter.

4.9.3 Partially resolvable singularities

We finally consider a class of threefolds that are a straightforward generalization of (4.206):

$$x^2+y^2 = z(z^{2k+1}-w^2). \tag{4.215}$$

These spaces can be *partially* resolved by taking

$$\begin{pmatrix} u & z \\ z^{2k+1}-w^2 & v \end{pmatrix} \cdot \begin{pmatrix} s \\ t \end{pmatrix} = 0\,, \tag{4.216}$$

where $[s:t]$ are the homogeneous coordinates of the exceptional $\mathbb{P}^1$. However, the resolution still possesses a terminal singularity. Hence one expects hypers coming from M2-branes wrapping the exceptional $\mathbb{P}^1$ and hypers coming from the terminal singularity. Moreover, we expect a continuous $U(1)$ flavor symmetry from the non-Cartier divisor related to the small resolution (like in all the previous cases where a small resolution was possible).

Again we study in detail only the case $k = 1$. The Higgs field whose characteristic polynomial reproduces (4.215) is

$$\Phi = \left(\begin{array}{c|ccc} 0 & 0 & 0 & 0 \\ \hline 0 & 0 & w & 0 \\ 0 & 0 & 0 & w \\ 0 & 1 & 0 & 0 \end{array}\right). \tag{4.217}$$

where notice that the theory of Springer resolutions correctly predicts a resolution of a single node (the first of the A_3 chain). The Higgs field fluctuations φ are given modulo linearized gauge transformation:

$$\varphi \sim \varphi+[\Phi, g] \qquad \text{with} \qquad g \in \mathfrak{sl}(4). \tag{4.218}$$

Explicitly we get:

$$\varphi \sim \underbrace{\begin{pmatrix} \varphi_{11} & \varphi_{12} & \varphi_{13} & \varphi_{14} \\ \varphi_{21} & \varphi_{22} & \varphi_{23} & \varphi_{24} \\ \varphi_{31} & \varphi_{32} & \varphi_{33} & \varphi_{34} \\ \varphi_{41} & \varphi_{42} & \varphi_{43} & \varphi_{44} \end{pmatrix}}_{\varphi} + \underbrace{\begin{pmatrix} 0 & g_{14} & g_{12}w & g_{13}w \\ -g_{31}w & g_{24}-g_{32}w & (g_{22}-g_{33})w & (g_{23}-g_{34})w \\ -g_{41}w & g_{34}-g_{42}w & (g_{32}-g_{43})w & (g_{33}-g_{44})w \\ -g_{21} & g_{44}-g_{22} & g_{42}w-g_{23} & g_{43}w-g_{24} \end{pmatrix}}_{[\Phi,g]}.$$

Using the gauge redundancy we can set φ_{12}, φ_{41}, φ_{42}, φ_{43}, φ_{44} and φ_{32} to zero.

We are then left with:

$$\varphi \sim \underbrace{\begin{pmatrix} \varphi_{11} & 0 & \varphi_{13} & \varphi_{14} \\ \varphi_{21} & \varphi_{22} & \varphi_{23} & \varphi_{24} \\ \varphi_{31} & 0 & \varphi_{33} & \varphi_{34} \\ 0 & 0 & 0 & 0 \end{pmatrix}}_{\varphi} + \underbrace{\begin{pmatrix} 0 & 0 & g_{12}w & g_{13}w \\ -g_{31}w & (g_{43}-g_{32})w & (g_{44}-g_{33})w & 0 \\ -g_{41}w & 0 & -(g_{43}-g_{32})w & -(g_{44}-g_{33})w \\ 0 & 0 & 0 & 0 \end{pmatrix}}_{[\Phi,g]}.$$

We see that φ_{11} and φ_{24} are unconstrained, and that the pairs $(\varphi_{22}, \varphi_{33})$ and $(\varphi_{23}, \varphi_{34})$ depend on the same parameters, so that we can gauge-fix only a linear combination for each pair. As a result (making a choice for the gauge-fixing), in total we get **6 modes**, or equivalently **3 hypers**:

$$\varphi_{13}, \varphi_{14}, \varphi_{21}, \varphi_{31} \in \mathbb{C}[w]/(w) \cong \mathbb{C} \qquad \text{and} \qquad \varphi_{22}, \varphi_{23} \in \mathbb{C}[w]/(w) \cong \mathbb{C}. \tag{4.219}$$

The subgroup of $SU(4)$ preserving Φ as in (4.217) is given by matrices

$$G_{5d} = \begin{pmatrix} e^{-3i\alpha} & 0 \\ 0 & e^{i\alpha}\mathbb{1}_3 \end{pmatrix}. \tag{4.220}$$

A direct computation shows that the modes $\varphi_{13}, \varphi_{14}, \varphi_{21}, \varphi_{31}$ are charged under the $U(1)$, whereas $\varphi_{22}, \varphi_{23}$ are not. Summing up, we get **2 charged hypers** and **1 uncharged hyper.**

In the generic k case we still have a $U(1)$ flavor and the modes are organized (as in the $k = 1$ case) as follows:

$$\left(\begin{array}{c|c} 0 & \text{charged}_{1\times(2k+1)} \\ \hline \text{charged}_{(2k+1)\times 1} & \text{uncharged}_{(2k+1)\times(2k+1)} \end{array}\right) \tag{4.221}$$

We obtain **2 charged hypers** along with ***k* uncharged hypers**. Since there is no discrete gauge symmetry, the Higgs branch is given by $k+2$ free hypermultiplets.

$$\boxed{x^2+y^2 = z(z^{2k+1}-w^2). \qquad \longleftrightarrow \qquad \text{2 charged hypers} + k \text{ uncharged hypers}} \tag{4.222}$$

The corresponding GV invariants are (stressing again that the "degree 0" GV invariants are so far only formally defined, as they have no known mathematical counterpart):

$$n^{g=0}_{d=0} = k, \qquad n^{g=0}_{d=1} = 2. \tag{4.223}$$

CHAPTER 5

M-theory on quasi-homogeneous cDV singularities

In this chapter, we proceed with the systematic application of the techniques we have developed so far, with a clear-cut objective in mind: we wish to analyze the 5d effective theories arising from M-theory on *quasi-homogeneous compound Du Val (cDV) singularities*, in *all* cases. In turn, in light of the correspondence between Higgs branch data and the GV invariant theory, this is equivalent to classifying the GV invariants of all quasi-homogeneous cDV singular threefolds[1].

This prospect will bring us way beyond the realm of simple flops we have explored so far, as quasi-homogeneous cDV singularities can exhibit a wide variety of crepant resolution patterns, admitting none, one, or more than one inflated $\mathbb{P}^1$'s[2]. Namely, following Section 4.2, we have:

$$r = 0, \qquad f \geq 0. \tag{5.1}$$

Hence, quasi-homogeneous cDV singularities engineer *rank-0* 5d $\mathcal{N} = 1$ SCFTs.

We start by recapping the properties of the Higgs background Φ in Section 5.1, with specific attention devoted to the preserved discrete symmetries; we go along introducing a systematic method to extract the Higgs background associated to a given quasi-homogeneous cDV singularity in Section 5.2, and we finally employ this knowledge in Section 5.3 to write down the Higgs branches of all the 5d SCFTs coming from M-theory on quasi-homogeneous cDV singularities. As always, the number of hypermultiplets and their flavor charges intrinsically encode the GV invariants of the corresponding cDV singularities.

Before this, we briefly review the classification of the singularities that we are interested in.

[1]As a consequence, in order to simplify the exposition, we will not repeat the correspondence each time. The GV invariants can always be recovered from the Higgs branch data in the standard way outlined in Chapter 4.

[2]Still, we will see that the exceptional $\mathbb{P}^1$'s never intersect each other, thus giving rise only to $U(1)^f$ flavor groups in five dimensions.

In Chapter 1 we have introduced cDV singularities as hypersurfaces in $\mathbb{C}^4$ of the form:

$$F(x,y,z,w): \qquad x^2+P_{\mathfrak{g}}(y,z)+wg(x,y,z,w)=0 \tag{5.2}$$

where $P_{\mathfrak{g}}$ classifies ADE singularities as in (1.32). In this chapter, we focus on *quasi-homogeneous* cDV singularities, i.e. hypersurfaces of the form (5.2) admitting a specific $\mathbb{C}^*$-action. This means that there exists a choice of weights q_i for the coordinates (x,y,z,w), where $i=x,y,z,w$, such that:

$$F(\lambda^{q_x}x,\lambda^{q_y}y,\lambda^{q_z}z,\lambda^{q_w}w)=\lambda F(x,y,z,w), \quad \text{with } q_i\neq 0. \tag{5.3}$$

Now, let us consider as an example the following hypersurfaces:

$$P_{\mathfrak{g}'}(x,w)+P_{\mathfrak{g}}(y,z)=0 \tag{5.4}$$

with $\mathfrak{g}',\mathfrak{g}$ two ADE algebras. It is known that reducing type IIB string theory on such threefolds, one obtains Argyres-Douglas theory of type $(\mathfrak{g}',\mathfrak{g})$ [171].

If one restricts to the case $\mathfrak{g}'=A_n$, one obtains a notable subclass of cDV singularities, known as $(A,\mathfrak{g})$ hypersurfaces[3]:

$$x^2+P_{\mathfrak{g}}(y,z)+w^{n+1}=0. \tag{5.5}$$

We notice that the first two terms reconstruct the ADE singularity of type $\mathfrak{g}$ in (1.2), while the last term can be interpreted as a deformation of this singularity. Hence the equation (5.5) describes a family of deformed $\mathfrak{g}$-singularities, fibered over a complex plane $\mathbb{C}_w$. This is precisely the setting in which our techniques can be applied.

The threefolds (5.5) belong to the class of quasi-homogeneous compound Du Val threefold singularities. There exists an exhaustive classification of quasi-homogeneous cDV singularities, computed in [131], that we recall in Table (5.1), where we also make explicit the algebra $\mathfrak{g}$ for the $(A,\mathfrak{g})$ threefolds. Notice that also the threefolds that are not of $(A,\mathfrak{g})$ type are one-parameter families of deformed ADE singularities, which is precisely the requirement we need to employ our machinery.

We aim at completely classifying the Higgs branches of M-theory on the cDV singularities (5.1), proceeding as in the previous chapters. We will see, though, that each class in the ADE classification presents different obstacles, and we will introduce suitable refinements of our techniques whenever necessary.

For the explicit computations regarding the Higgs branches, we will recur to the algorithm presented in Chapter 4. In the next section, we refine our strategy to explicitly compute Higgs backgrounds, showing how to extract them directly from the quasi-homogeneous cDV singularity equation.

[3]These give rise, upon compactification of Type IIB on them, to the $(A,\mathfrak{g})$ Argyres-Douglas theories.

ADE	Label	Singularity	Non-vanishing deformation parameter
A	(A_{k-1}, A_{N-1})	$x^2+y^2+z^k+w^N=0$	$\mu_k = w^N$
	$A_{k-1}^{(k-1)}[N]$	$x^2+y^2+z^k+w^N z=0$	$\mu_{k-1} = w^N$
D	(A_{N-1}, D_k)	$x^2+zy^2+z^{k-1}+w^N=0$	$\mu_{2k-2} = w^N$
	$D_k^{(k)}[N]$	$x^2+zy^2+z^{k-1}+w^N y=0$	$\tilde{\mu}_k = w^N$
E_6	(A_{N-1}, E_6)	$x^2+y^3+z^4+w^N=0$	$\mu_{12} = w^N$
	$E_6^{(9)}[N]$	$x^2+y^3+z^4+w^N z=0$	$\mu_9 = w^N$
	$E_6^{(8)}[N]$	$x^2+y^3+z^4+w^N y=0$	$\mu_8 = w^N$
E_7	(A_{N-1}, E_7)	$x^2+y^3+yz^3+w^N=0$	$\mu_{18} = w^N$
	$E_7^{(14)}[N]$	$x^2+y^3+yz^3+w^N z=0$	$\mu_{14} = w^N$
E_8	(A_{N-1}, E_8)	$x^2+y^3+z^5+w^N=0$	$\mu_{30} = w^N$
	$E_8^{(24)}[N]$	$x^2+y^3+z^5+w^N z=0$	$\mu_{24} = w^N$
	$E_8^{(20)}[N]$	$x^2+y^3+z^5+w^N y=0$	$\mu_{20} = w^N$

Table 5.1: *Quasi-homogeneous cDV singularities as ADE families.*

5.1 The Higgs background Φ

5.1.1 Maximal subalgebras

In Section 3.9, we have recapped how a Higgs background $\Phi(w)$ for a one-parameter deformed singular ADE family living in a Levi subalgebra of an ADE algebra $\mathfrak{g}$

$$\mathcal{L} = \bigoplus_h \mathcal{L}_h \oplus \mathcal{H}, \tag{5.6}$$

yields a resolution of the corresponding singularity that is dictated by the commutant $\mathcal{H}$ of $\Phi(w)$:

$$\mathcal{H} = \langle \alpha_1^*, \ldots, \alpha_f^* \rangle. \tag{5.7}$$

In this chapter we introduce a refinement to this statement, that will prove essential to correctly deal with the five-dimensional discrete symmetries of the SCFTs arising from M-theory on quasi-homogeneous compound Du Val singularities.

Recall that $\mathcal{L}$ in (5.6) is a direct sum of $\mathcal{H}$ with a semi-simple Lie algebra, i.e. $\mathcal{L} = \mathcal{L}^{\text{semi-simp}} \oplus \mathcal{H}$. In order for a Higgs background to break to $\mathcal{H}$, it is enough that $\Phi(w)$

belongs to $\mathcal{M} = \mathcal{M}^{\text{semi-simp}} \oplus \mathcal{H}$, where $\mathcal{M}^{\text{semi-simp}}$ is a maximal subalgebra of $\mathcal{L}^{\text{semi-simp}}$ of maximal rank[4]. We can then write

$$\Phi \in \mathcal{M} \equiv \bigoplus_h \mathcal{M}_h \oplus \mathcal{H}, \tag{5.8}$$

where $\mathcal{M}_h$ are simple Lie algebras.

In the preceding chapters we have neglected this subtlety, as it was not needed to deal with the examples examined up to this point[5].

To sum up, we have the relations

$$\text{simult.resol. : } \alpha_1, ..., \alpha_f \quad \leftrightarrow \quad \mathcal{H} = \langle \alpha_1^*, ... \alpha_f^* \rangle \quad \leftrightarrow \quad \mathcal{L}. \tag{5.9}$$

We can summarize these data in the Dynkin diagram of $\mathfrak{g}$: we color in black the nodes corresponding to roots belonging to $\mathcal{H}$ (namely, they are the nodes that get blown-up by the simultaneous resolution). Then the semi-simple part $\mathcal{L}^{\text{semi-simp}}$ of the corresponding Levi subalgebra is given by the Dynkin diagram colored in white. Hence, a coloring of the nodes of the Dynkin diagram completely and univocally fixes a Levi subalgebra $\mathcal{L} = \mathcal{L}^{\text{semi-simp}} \oplus \mathcal{H}$. Given the Levi $\mathcal{L}$, one can look for maximal subalgebras of the form (5.8), employing the usual technique based on extended Dynkin diagrams. A $\Phi(w)$ producing a fibration with the given simultaneous resolution must belong to one of these maximal subalgebras.

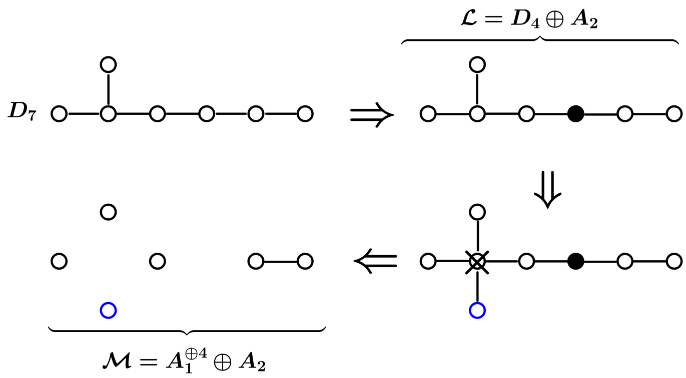

Figure 5.1: $A_1^4 \oplus A_2$ *subalgebra of* D_7.

Let us see a simple example of this framework: take the Dynkin diagram of the Lie algebra D_7 and color one node α_c in black as in Figure 5.1. We immediately read $\mathcal{L} = D_4 \oplus A_2 \oplus \langle \alpha_c^* \rangle$ from the white nodes. D_4 has a maximal subalgebra $A_1^{\oplus 4}$, that we can extract pictorially as in Figure 5.1. If we want Φ to produce a threefold with a simultaneous resolution of only the root α_c, then either $\Phi \in \mathcal{M} = \mathcal{L}$ or $\Phi \in \mathcal{M} = A_1^4 \oplus A_2 \oplus \langle \alpha_c^* \rangle$.

[4]This is true because the Cartan subalgebra of $\mathcal{L}^{\text{semi-simp}}$ coincides with the Cartan subalgebra of $\mathcal{M}^{\text{semi-simp}}$, as it is a maximal subalgebra of maximal rank.

[5]Moreover, notice that the fact that Φ can reside in a maximal subalgebra (5.8) of $\mathcal{L}$ is a fact that is *not* captured by the Springer resolution formalism that we have employed so far, as it exclusively deals with Levi subalgebras related to partial or complete flags.

5.1.2 The threefold equation and 5d modes from the Higgs background

As we have declared at the beginning of the chapter, we aim at studying the 5d Higgs branches from M-theory on all the compound Du Val singularities: to this end, we must associate to every geometry a corresponding Higgs background. In order to carry out this task, we recur to the tools we have introduced in the preceding chapters, namely:

1. We connect Higgs backgrounds and threefold equations via the explicit relations presented in Section 3.8, that relate the Casimirs of $\Phi(w)$ to the deformation parameters of the ADE singularities.

2. We compute the localized 5d modes via the algorithm devised in Section 4.7.3, which lends itself to an efficient computer-based implementation. In order to apply the algorithm in light of the refinements of the preceding section, we slightly modify the decomposition (4.128), branching the algebra $\mathfrak{g}$ with respect to the maximal subalgebra $\mathcal{M}$ containing Φ:
$$\mathfrak{g} = \bigoplus_p R_p^{\mathcal{M}}. \tag{5.10}$$

As regards the mode-counting, we add here some details about a case that we will recurrently encounter in the following. Consider two Higgs fields Φ and $\hat{\Phi}$ related as

$$\hat{\Phi} = w^j \Phi, \tag{5.11}$$

and with $\Phi(0) \neq 0$, while $\hat{\Phi}$ has a zero of order j at $w = 0$.

We can compute the zero modes of $\hat{\Phi}$, knowing the zero modes of Φ: the components of the deformation φ that were gauge fixed to zero by Φ, now host zero modes in $\mathbb{C}[w]/(w^j)$. Components that hosted localized modes in $\mathbb{C}[w]/(w^k)$, now support zero modes in $\mathbb{C}[w]/(w^{j+k})$. We further note that the Casimir invariants of Φ and $\hat{\Phi}$ are related by $\mathrm{Tr}\left((\hat{\Phi})^i\right) = \mathrm{Tr}\left((w^j\Phi)^i\right) = w^{i \cdot j}\mathrm{Tr}\left((\Phi)^i\right)$.

These simple facts will permit us to reproduce the Higgs fields of all the quasi-homogeneous cDV, first identifying a finite set of Higgs field profiles, and then producing all the other Higgs fields multiplying them by an appropriate power of w.

In the next sections, we will exhibit a way to automatically perform point 1, namely associate a Higgs background to a given threefold equation, which in general is quite tricky, as we have mentioned in Section 3.9.

Before that, we devote the next few lines to fleshing out how the symmetry group of the 5d SCFT can be extracted from the Higgs background, with particular attention focused on the discrete symmetries.

5.1.3 The symmetry group

The 7d theory before the Higgsing has gauge group G, whose Lie algebra is $\mathfrak{g}$. Since all fields are in the adjoint representation of $\mathfrak{g}$, the non-trivial acting group is the quotient of the simply connected group associated to $\mathfrak{g}$ modulo its center[6]. We take such a quotient as our 7d group G.

Switching on the vev for $\Phi(w)$ on one side breaks G and on the other side generates zero modes localized at $w = 0$, that are charged under the preserved symmetry group. Such a symmetry group is $\text{Stab}_G(\Phi) \subset G$, with

$$\text{Stab}_G(\Phi) \equiv \left\{ U \in G \text{ s.t. } U\Phi U^{-1} = \Phi \right\} . \tag{5.12}$$

Our Higgs field Φ engineers a threefold family that (simultaneously) resolves the roots $\alpha_1, ..., \alpha_f$. This is realized by letting $\mathcal{H}$ (defined in (5.7)) commute with Φ. The commutant of $\mathcal{H}$ is the Levi subalgebra $\mathcal{L}$ associated with the choice of the roots $\alpha_1, ..., \alpha_f$. If the Higgs field Φ is a generic element of $\mathcal{L}$, then $\text{Stab}_G(\Phi) = U(1)^f$ (generated by $\mathcal{H}$).

Such $U(1)^f$ group, namely the symmetry preserved by $\Phi \in \mathcal{L}$, is nothing but the five-dimensional flavor group, acting via its adjoint representation on the hypermultiplets coming from the deformation φ. The explicit flavor charges of the hypermultiplets can be readily computed employing the irrep decomposition (4.128), that naturally regroups hypers of the same charge into the same irrep. In general, if we only have one $U(1)$ factor, associated to a simple root α_i, then the flavor charges can acquire values only up to the dual Coxeter label of the node α_i in the Dynkin diagram of the considered 7d algebra, as we have seen in Chapter 4. If, instead, $\text{Stab}_G(\Phi) = U(1)^f$ with $f > 1$, this is not valid anymore.

As we have said, generically we have

$$\Phi \in \mathcal{M}, \qquad \text{with} \qquad \mathcal{M} = \bigoplus_h \mathcal{M}_h \oplus \mathcal{H} \tag{5.13}$$

where $\mathcal{M}$ is a maximal subalgebra of $\mathcal{L}$. If $\mathcal{M} \subset \mathcal{L}$, the preserved group will be bigger than $U(1)^f$ and it will develop a discrete group part.

To explain how this works, we consider a simple example (that will appear often in the threefolds studied in the following). We take

$$\mathcal{L} = D_4 \quad \text{and} \quad \mathcal{M} = A_1^{\oplus 4}.$$

The Dynkin diagram of D_4 with its dual Coxeter labels, along with its $A_1^{\oplus 4}$ subalgebra, is depicted in Figure 5.2. The $A_1^{\oplus 4}$ maximal subalgebra is generated by adding the external node of the extended D_4 Dynkin diagram and removing the central one.

[6] As we have previously recalled, there actually is an ambiguity in choosing the global group of the 7d theory [76, 149, 164, 165]. Taking the minimal choice, as we are doing, one captures the non-trivial discrete symmetries that come solely from Higgsing. Different choices would enlarge the discrete symmetries with elements of the center of the group.

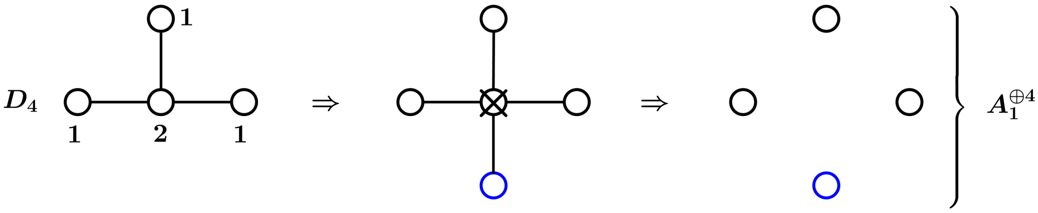

Figure 5.2: $A_1^{\oplus 4}$ *subalgebra of* D_4.

There are transformations of[7] $G_{\mathcal{L}}$ that preserve all the elements of $\mathcal{M} = A_1^{\oplus 4}$ (while they break $\mathcal{L} = D_4$). In this case there is one such element: it is generated by the Cartan α_2^*, i.e. the dual of the root that should be removed from the D_4 extended Dynkin diagram to obtain the Dynkin diagram of $A_1^{\oplus 4}$.[8] The element that is in the stabilizer of $\Phi \in \mathcal{M} = A_1^{\oplus 4}$ is

$$\gamma = \exp\left[\frac{2\pi i}{\mathfrak{q}_{\alpha_2}}\alpha_2^*\right], \tag{5.14}$$

where $\mathfrak{q}_{\alpha_i}$ is the dual Coxeter label of the simple root α_i, and where $\gamma \in G$ acts on the adjoint representation. In our case, we read $\mathfrak{q}_{\alpha_2} = 2$ (see Figure 5.2). In particular, we have

$$\gamma \cdot E_{\alpha_i} = \mathsf{e}^{\frac{2\pi i}{2}0} E_{\alpha_i} = E_{\alpha_i} \quad \text{for } i = 1,3,4, \qquad \gamma \cdot E_{\alpha_2} = \mathsf{e}^{\frac{2\pi i}{2}1} E_{\alpha_2} = -E_{\alpha_2}\,, \tag{5.15}$$

and

$$\gamma \cdot E_{\alpha_\theta} = \mathsf{e}^{\frac{2\pi i}{2}(-2)} E_{\alpha_\theta} = E_{\alpha_\theta}\,, \tag{5.16}$$

where α_θ is the (minus the) highest root corresponding to the extended node. Note that the Lie algebra element E_{α_2} is not preserved by γ.

We see that it is crucial for preserving a maximal subalgebra that the coefficient in front of α_2^* in γ is $\frac{2\pi i}{\mathfrak{q}_{\alpha_2}}$ and not any other number. The discrete group generated by γ in (5.14) is isomorphic to $\mathbb{Z}_2$.

Let us generalize this to an example that is a bit more involved, i.e.

$$\mathcal{L} = D_6 \quad \text{and} \quad \mathcal{M} = A_1^{\oplus 6}.$$

In this case we proceed by steps, following the inclusions $D_6 \supset D_4 \oplus A_1^{\oplus 2} \supset A_1^{\oplus 4} \oplus A_1^{\oplus 2} = A_1^{\oplus 6}$, depicted in Figure 5.3. In the first step, we remove a node with dual Coxeter label equal to 2. We are then left with the final step in which we embed $A_1^{\oplus 4}$ into D_4: again we remove a node of D_4 Dynkin diagram with label equal to 2. We conclude that the discrete group is $\mathbb{Z}_2^2$.

[7] Given a subalgebra $\mathcal{L} \subset \mathfrak{g}$, we call $G_{\mathcal{L}}$ the subgroup of G, whose Lie algebra is $\mathcal{L}$.

[8] In Heterotic string theory on T^3, this element is known as a discrete Wilson line.

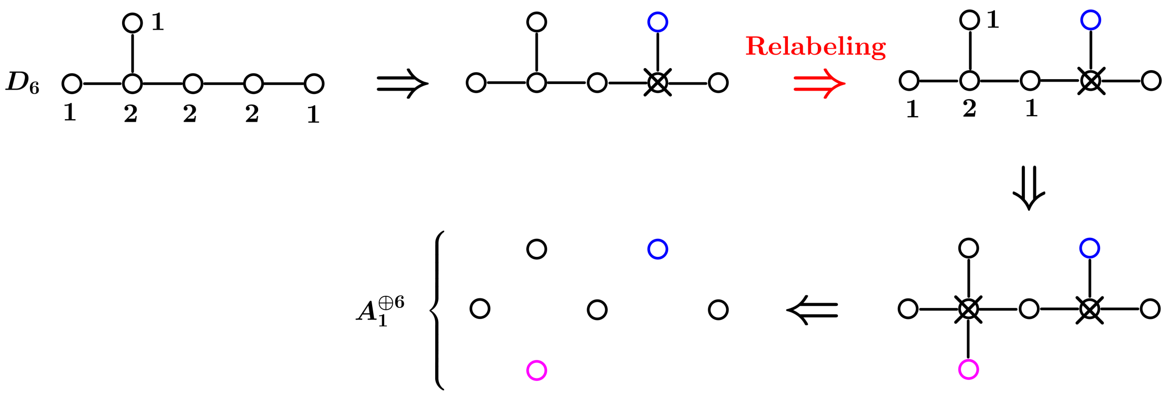

Figure 5.3: *$A_1^{\oplus 6}$ subalgebra of D_6.*

It is then easy to generalize to a generic case. Say that a simple summand of $\mathcal{L}$ has a maximal subalgebra, obtained by subsequently removing nodes with dual Coxeter labels $\mathfrak{q}_{\alpha_{i_1}}, \ldots, \mathfrak{q}_{\alpha_{i_k}}$. Then the stabilizer of Φ will include the discrete group

$$\mathbb{Z}_{\mathfrak{q}_{\alpha_{i_1}}} \times \ldots \times \mathbb{Z}_{\mathfrak{q}_{\alpha_{i_k}}}.$$

Doing this for all simple summands of $\mathcal{L}$, we obtain the full discrete symmetry Γ_Φ. The full symmetry group is then

$$\mathrm{Stab}_G(\Phi) = U(1)^f \times \Gamma_\Phi. \tag{5.17}$$

Since we know how the generators of this group act on the Lie algebra $\mathfrak{g}$, we can easily derive the charges under $\mathrm{Stab}_G(\Phi)$ of the deformations φ in $R^{\mathcal{M}}$, i.e. of the 5d hypermultiplets.

The symmetry group (5.17) is the 7d gauge group that survives the Higgsing. In order to deduce the 5d flavor and gauge symmetries we can proceed as in Chapter 4: we consider the 7d space as a decompactification limit from 5d times a 2-torus. Before the limit, (5.17) is a 5d gauge group; the decompactification limit will ungauge the continuous factor as its gauge coupling vanishes. The discrete part, having no gauge coupling, remains gauged in 5d.

Explicit example: (A_2, D_4) singularity and discrete groups

Let us visualize how it works in an explicit example. We can consider the (A_2, D_4) singularity:

$$x^2 + zy^2 + z^3 + w^3 = 0, \quad (x, y, w, z) \in \mathbb{C}^4. \tag{5.18}$$

The threefold can be described as a family of D_4 ADE singularities deformed by the parameter w. The Higgs field is taken in the maximal subalgebra of D_4, i.e. $\mathcal{M} = D_2 \oplus D_2 \cong A_1^4$.

From what we said above, it is immediate to find out

$$\mathrm{Stab}(\Phi)_G = \mathbb{Z}_2. \tag{5.19}$$

We now see how this discrete group acts on the 5d hypermultiplets. We first branch $\mathfrak{g} = D_4$

under $\mathcal{M}$:

$$D_4 = A_1^{(I)} \oplus A_1^{(II)} \oplus A_1^{(III)} \oplus A_1^{(IV)} \oplus (\mathbf{2},\mathbf{2},\mathbf{2},\mathbf{2}) = \mathcal{M} \oplus (\mathbf{2},\mathbf{2},\mathbf{2},\mathbf{2}). \tag{5.20}$$

We then see how γ in (5.14) acts on the elements of $(\mathbf{2},\mathbf{2},\mathbf{2},\mathbf{2})$. The generators of D_4 appearing in this representation of $\mathcal{M}$ are related to roots that are linear combination of the simple roots where α_2 appears with coefficient 1. This immediately tells us that all elements of $(\mathbf{2},\mathbf{2},\mathbf{2},\mathbf{2})$ get a -1 factor when we act with γ.

This can be easily generalized to any choice of $\Phi \in \mathcal{M} \subset \mathfrak{g}$ with $\mathfrak{g} = A, D, E$.

5.2 The Higgs vev from the threefold equation

Our question is now: given a CY equation like (5.5), what is the Higgs field that can generate it? The answer to this question is crucial in order to tackle the dynamics of M-theory on the quasi-homogeneous cDV singularities in Table 5.1.

With this objective in mind, we proceed as follows: given a cDV singularity, built as an ADE singularity with some deformation parameters $\mu_i(w) \in \mathcal{T}/\mathcal{W}$ switched on, we wish to perform a change of basis and rewrite the deformation terms with respect to a set of partial Casimirs $\varrho_i(w) \in \mathcal{T}/\mathcal{W}'$, as we have explained in full generality in Section 1.3.4. This will allow us to build a Higgs background encoding the physics of the 5d SCFT in an explicit manner.

We can hence describe the base change in the following way:

1. we first go from $\mathcal{T}/\mathcal{W}$ to $\mathcal{T}/\mathcal{W}'$, by putting $\mu_i = \mu_i(\varrho_1, ..., \varrho_n)$ (where n is the rank of the considered Lie algebra);

2. we then allow a holomorphic dependence $\varrho_i = \varrho_i(w)$ that makes all $\mu_i = 0$, except the constant deformation that must take the form $\mu(\varrho_i(w)) = w^N$.

Of course this is not unique: several choices of $\mathcal{W}' \subset \mathcal{W}$ produce the same threefold (5.5), by taking the proper expressions for $\varrho_i(w)$. As we will see in detail below, the different choices of $\mathcal{W}'$ correspond to different T-brane backgrounds associated with the same singular threefold in M-theory. The presence of a T-brane can obstruct the resolution of some roots [94, 133], enlarging the subgroup $\mathcal{W}'$. In order to have a geometry without T-branes, we will make the following choice: we consider the smallest choice of $\mathcal{W}'$ that reproduces the equation (5.5) (that is not necessarily the trivial subgroup). This corresponds to a family over $\mathcal{T}/\mathcal{W}'$ with the biggest possible number of resolved simple roots in the simultaneous resolution. From this perspective, the threefold is naturally embedded into the family over $\mathcal{T}/\mathcal{W}'$ by choosing a one-dimensional subspace parametrized by $\mathbb{C}_w$. This means that the threefold will inherit the partial simultaneous resolution associated to $\mathcal{W}'$: both in the family and in the threefold the blown up roots will be, say $\alpha_1, ..., \alpha_f$. This immediately tells us that the commutant of Φ is $\mathcal{H}$ in (5.7). The choice of $\mathcal{W}'$ selects a maximal subalgebra $\mathcal{M}$ of the commutant $\mathcal{L}$ of $\mathcal{H}$

(see (5.8)), whose Casimirs are invariant under $\mathcal{W}'$ and are then good coordinates on $\mathcal{T}/\mathcal{W}'$. An element $\Phi \in \mathcal{M} \subseteq \mathcal{L}$ can be written as

$$\Phi = \sum_h \Phi_h + \sum_{a=1}^{f} \varrho_1^a \alpha_a^* \tag{5.21}$$

where Φ_h is an element of $\mathcal{M}_h$. Collecting the degree-j Casimir invariants ϱ_j^h of Φ_h in $\mathcal{M}_h$, together with the coefficients ϱ_1^a , one obtains the invariant coordinates ϱ_i on the base $\mathcal{T}/\mathcal{W}'$.

5.2.1 From the threefold equation to the partial Casimirs $\varrho_i(w)$

Now, we proceed as follows: we start from the equation of a threefold in Table 5.1. We derive what is the minimal $\mathcal{W}'$ such that the partial Casimirs ϱ_i can be taken as holomorphic (homogeneous) functions of w, in a way that produces the CY equation by taking $\mu_i = \mu_i(\varrho(w))$. This will tell us what is the w-dependence of the Casimirs ϱ_j^h of each Φ_h and the w-dependence of the coefficients ϱ_a. Finally, we will look for Higgs fields $\Phi(w) \in \mathcal{M}$, holomorphic in w, that have the given w-dependence for their partial Casimirs.[9]

In particular, to reproduce the threefolds in Table 5.1, we want to determine which holomorphic functions $\varrho_j^I(w)$, with $I = (h, a)$ make all deformation parameters vanish except one of degree M, that is

$$\mu_M(\varrho(w)) = w^N. \tag{5.22}$$

We stress that $\mu_M(\varrho(w))$ is a *homogeneous* polynomial in w of degree N.

Both the μ_M and the ϱ_j^I can be written as homogeneous polynomials in the $t_i \in \mathcal{T}$ of degree, respectively, M and j. This implies that $\mu_M(\varrho)$ will be a weighted *homogeneous* polynomial in the coordinates ϱ_j^I's of degree M, where the coordinate ϱ_j^I has weight j. This, together with (5.22), implies that $\varrho_j^I(w)$ is a homogeneous function of w with degree $\frac{jN}{M}$, i.e.

$$\varrho_j^I(w) = c_j^I\, w^{\frac{jN}{M}}. \tag{5.23}$$

Now:

- Since we require that $\varrho_j^I(w)$ is holomorphic, the partial Casimirs that give a non-zero contribution (i.e. $c_j^I \neq 0$) are those with j such that

$$\frac{j\,N}{M} \in \mathbb{Z}^{>0}. \tag{5.24}$$

- Moreover, we want to pick the smallest $\mathcal{W}'$ that allows holomorphic functions $\varrho_j^I(w)$ compatible with (5.22). Small $\mathcal{W}'$ correspond to subalgebras $\mathcal{M}$ with several simple summands with small rank. This subalgebra then yields the smallest degree partial Casimirs that realize (5.24), for given M, N.

[9]Fixing the w-dependence of the partial Casimir invariants does not give a unique choice for a holomorphic element of $\mathcal{M}$.

Choosing the threefold in Table 5.1 determines M (see the last column of the table). For each value of N, we look for the minimal value of j that satisfies (5.24). Say that M has n_M divisors $q_1, ..., q_{n_M}$, where $q_1 = 1$ and $q_{n_M} = M$. Then N can always be written in a unique way as

$$N = \frac{p}{q_\alpha} M \mod M \,, \tag{5.25}$$

with q_α a divisor of M, $p < q_\alpha$ and (p, q_α) coprime. The condition (5.24) becomes then

$$\frac{j\,p}{q_\alpha} \in \mathbb{Z}^{>0}, \tag{5.26}$$

and the minimal value of j fulfilling it is $j = q_\alpha$.

Given N, only ϱ^I_j with j a multiple of q_α can be non zero. In other words, $c^I_j = 0$ when $j \neq m\,q_\alpha$ with $m \in \mathbb{Z}$. Because of homogeneity, this implies also that $\mu_i(\varrho) = 0$ with $i \neq m\,q_\alpha$. We are then left with the following equations with unknown c^I_j $(j = mq_\alpha)$:

$$\begin{cases} \mu_{m\,q_\alpha}(c) = 0 & m\,q_\alpha < M \\ \mu_M(c) = 1 & \end{cases} \tag{5.27}$$

(where we have factored out the powers in w). In order to have a non-trivial solution, one requires that all c^I_j with $j = m\,q_\alpha$ be non-zero[10].

Let us see how we can use this information to extract the subalgebra $\mathcal{M}$ corresponding to a given choice of $(A_{N-1}, \mathfrak{g})$. We describe this in a simple example, i.e. (A_{N-1}, D_4). The D_4 algebra has four Casimirs: μ_2, μ_4, $\tilde{\mu}_4$ and μ_6. Hence $M = 6$. There are four divisors of 6:

$$q_\alpha \in \{1, 2, 3, 6\}.$$

We now see which (minimal) degree can take the partial Casimirs and then what is the choice of the minimal subalgebra $\mathcal{M}$ (minimal $\mathcal{W}'$). Let us vary N:

For $N = 0$ **mod** 6 $(q_\alpha = 1)$, the minimal degree is $j = 1$. We look for a subalgebra $\mathcal{M}$ with all four partial Casimirs of degree 1. This is the smallest possible choice, i.e. the Cartan subalgebra of D_4. In this case, all four roots of D_4 are blown up in the simultaneous resolution.

For $N = 3$ **mod** 6 $(q_\alpha = 2)$, the minimal degree is $j = 2$. There is actually a subalgebra of D_4 with four partial Casimirs of degree 2, i.e. $\mathcal{M} = A_1^{\oplus 4}$.[11] $\mathcal{M}$ is now a maximal

[10]Otherwise the system of homogeneous equations in the first row of (5.27) will force all c^I_j's to vanish. We notice that the number of holomorphic ρ^I_j has to be equal to the number of all the $\mu_{m\,q_\alpha}$, μ_M. If that was not the case, the system (5.27) would be overconstrained, and a solution would not be guaranteed to exist.

[11]Notice that all c^I_2's must be non-zero; otherwise, if one vanished, the equations $\mu_2 = \mu_4 = \tilde{\mu}_4 = 0$ would force all the others c^I_2's to be zero as well as μ_6.

subalgebra of D_4; correspondingly, there is no resolution at the origin of the family, hence the singularity is terminal.

For $N = 2, 4$ **mod** 6 ($q_\alpha = 3$), the minimal degree for the non-zero partial Casimir is $j = 3$. Due to the rank of D_4, we can have at most one partial Casimir of degree 3. Moreover, μ_2 must depend on partial Casimirs of degree lower than 3, that must vanish identically (otherwise they would be non-holomorphic, due to (5.24)). We have $\mathcal{M} = A_2 \oplus \langle \alpha_3^*, \alpha_4^* \rangle$. Only the partial Casimirs of the semi-simple part of $\mathcal{M}$, that is A_2, are non-vanishing. In this case, the roots α_3 and α_4 of D_4 are blown up in the partial simultaneous resolution.

For $N = 1, 5$ **mod** 6 ($q_\alpha = 6$), the minimal degree for a non-vanishing partial Casimir is $j = 6$, hence in this case $\mathcal{M} = D_4$ with all Casimirs equal to zero, except the maximal degree one. For $N = 1$ the manifold is non-singular, while for $N = 5$ there is a terminal singularity at the origin of the family.

As one can note in the presented example, the simple algebras $\mathcal{M}_h$ in $\mathcal{M}$ are all of the same type for a given value of N. This actually happens for all the cases we study in this chapter. The reason is the following: we look for partial Casimirs with the lowest possible degree, realizing $\mu_M = w^N$. If one degree is allowed, we take as many partial Casimirs with that degree as we are allowed. Small degree partial Casimirs correspond to small subalgebras $\mathcal{M}_h$, hence we finish with as many summands of a given small algebra as we can.

5.2.2 From the partial Casimirs $\varrho_i(w)$ to the Higgs field $\Phi(w)$

Now that we have the w-dependence of the ϱ_j^I's, we need to take a Higgs field in $\mathcal{M}$, whose partial Casimirs have that dependence. In general, there are several choices for $\Phi_h(w)$ (see (5.21)) with given $\varrho_j^h(w)$. Each choice produces a different number of zero modes. We decide to look for the Higgs field Φ that localizes the maximal number of zero modes and breaks the 7d gauge symmetry in the least disruptive way, and we interpret the others as T-brane deformations of Φ, i.e. deformations that kill a number of modes, or destroy a preserved symmetry, without touching the threefold singularity (we come to this point in Section 5.5). With this choice, we pick up the Higgs field that leads to the same number of zero modes that are counted by the normalized complex structure deformations of the CY, as reviewed in Section 4.2.

Let us first describe what is the structure of the Higgs field. At $w = 0$ the fiber of the one-parameter $\mathfrak{g}$-family must develop a full $\mathfrak{g}$-type singularity. This means that $\Phi(0)$ must be a nilpotent element of $\mathcal{M}$ (as all its Casimirs should vanish), that we take in its canonical form (recapped in Section 2.1.2 for the A and D algebras; for the E algebras, we will give a few details momentarily). Now, $\Phi(w)$ must be a deformation of the nilpotent element $\Phi(0)$, with deformation proportional to w and belonging to $\mathcal{M}$. The way to do it in a way that goes into a transverse direction to the nilpotent orbit (that includes $\Phi(0)$) is dictated by taking Φ_h in the Slodowy slice in $\mathcal{M}_h$ passing through $\Phi_h(0)$. We have reviewed Slodowy slices in Section 2.1.5. What is important here is that this allows to have canonical forms for the Higgs field in $\mathcal{M}$, that are not equivalent by gauge transformations. The Higgs field will then be given as the sum of some simple root generators of $\mathfrak{g}$ multiplied by 1 and of other generators (in $\mathcal{M}$) multiplied by powers of w.

Here, a remark on the exceptional singularities is required: in Chapter 2 we have seen how to explicitly construct nilpotent orbits (and, consequently, Slodowy slices through them) for the singularities in the A and D series. For the E_6, E_7, E_8 cases, the classification of nilpotent orbits (which can be found e.g. in [112]) has been derived in the work of Bala and Carter [172, 173], and does *not* rely on partitions. Nevertheless, representatives corresponding to each nilpotent orbit can be explicitly constructed, as displayed in [174]. In order to construct our Higgs backgrounds as elements in the Slodowy slice through some nilpotent orbit of E_6, E_7, E_8, we make vast use of these tools.

Let us consider now $\Phi, \Phi' \in \mathcal{M}$ with the same expressions for ϱ^I_j, but such that $\Phi(0)$ and $\Phi'(0)$ belong to two different nilpotent orbits. Then, they produce a different number of zero modes: the one whose nilpotent orbit at the origin is smaller has a bigger number of zero modes. Roughly speaking, if at the origin the orbit is bigger, one has a larger number of '1's in the canonical form of the Higgs; these gauge fix to zero a bigger number of Lie algebra components in the deformation φ. We put this observation on more rigorous grounds in Appendix C and Appendix D.

If the power of w in the partial Casimirs ϱ^I_j is high, the minimal orbit at the origin reproducing the required w-dependence will be the trivial one. In these cases, the Higgs field that leads to the maximum number of zero modes is such that

$$\Phi = w^k \hat{\Phi} \,, \tag{5.28}$$

with $\hat{\Phi}(0)$ a non-trivial nilpotent element of $\mathcal{M}$. Knowing the zero modes of $\hat{\Phi}$, one is able to find the zero modes of Φ.

Let us explain how we pick the right choice of Φ with given $\varrho^I_j(w)$, by using the (A_{N-1}, D_4) example.

For $N = 1$, $\mathcal{M} = D_4$, $\varrho_6 = \mu_6 = w$. $\Phi(0)$ is in the maximal nilpotent orbit of D_4 and its expression at generic w is dictated by the w-dependence of the Casimir:

$$\Phi = E_{\alpha_1} + E_{\alpha_2} + E_{\alpha_3} + E_{\alpha_4} + \frac{w}{4} E_{-\alpha_1-2\alpha_2-\alpha_3-\alpha_4} \,. \tag{5.29}$$

For $N = 2$, $\mathcal{M} = A_2 \oplus \langle \alpha_3^*, \alpha_4^* \rangle$. The only non-zero partial Casimir is the degree 3 Casimir of A_2: $\varrho_3 = w$. The Higgs field is now

$$\Phi = \Phi_{A_2} \quad \text{with} \quad \Phi_{A_2} = \begin{pmatrix} 0 & 1 & 0 \\ 0 & 0 & 1 \\ w & 0 & 0 \end{pmatrix} = E_{\alpha_1} + E_{\alpha_2} + w\, E_{-\alpha_1-\alpha_2} \,. \tag{5.30}$$

For $N=3$, $\mathcal{M}=A_1^{\oplus 4}$, $\varrho_2^h = c^h w$ $(h=1,...,4)$, with c^h solving (5.27). The form of the Higgs field with these partial Casimirs is unique:

$$\Phi = \sum_{h=1}^{4} \Phi_h \quad \text{with} \quad \Phi_h = \begin{pmatrix} 0 & 1 \\ c^h\, w & 0 \end{pmatrix} = E_{\alpha^h} + c^h w\, E_{-\alpha^h}\,, \tag{5.31}$$

where α^h is the root of the subalgebra A_1^h.

For $N=4$, $\mathcal{M}=A_2\oplus\langle\alpha_3^*,\alpha_4^*\rangle$. Now, differently from the $N=2$ case, the only non-zero partial Casimir of degree 3 is quadratic in w: $\varrho_3 = w^2$. In this case we have two possible Higgs fields that are consistent with this, i.e. $\Phi = \Phi_{A_2}$ with

$$\text{either} \quad \Phi_{A_2} = \begin{pmatrix} 0 & 1 & 0 \\ 0 & 0 & 1 \\ w^2 & 0 & 0 \end{pmatrix} \quad \text{or} \quad \Phi_{A_2} = \begin{pmatrix} 0 & 1 & 0 \\ 0 & 0 & w \\ w & 0 & 0 \end{pmatrix}. \tag{5.32}$$

At the origin $w=0$, the left one is in the maximal nilpotent orbit while the right one is in the minimal one. Hence we expect that choosing the right one will give us the bigger number of zero modes. Indeed this happens, as it can be easily verified by an explicit computation.

For $N=5$, $\mathcal{M}=D_4$, $\varrho_6=\mu_6=w^5$, the Higgs field is of the same shape as the $N=1$ case, with some coefficients proportional to w:

$$\Phi = E_{\alpha_1} + w\left(E_{\alpha_2} + E_{\alpha_3} + E_{\alpha_4} + \frac{1}{4} E_{-\alpha_1-2\alpha_2-\alpha_3-\alpha_4} \right). \tag{5.33}$$

For $N=6$, $\mathcal{M}=\mathcal{H}$, $\varrho_1^a = c^a w$ $(a=1,...,4)$. Φ is forced to be of the form

$$\Phi = c^1 w\, \alpha_1^* + c^2 w\, \alpha_2^* + c^3 w\, \alpha_3^* + c^4 w\, \alpha_4^*. \tag{5.34}$$

Let us see some cases where we go up with the power N of w in μ_6:

For $N=8$, we obtain the same algebra as for $N=2$, i.e. $\mathcal{M}=A_2\oplus\langle\alpha_3^*,\alpha_4^*\rangle$. Now, the only non-zero partial Casimir of degree 3 of A_2 takes the following w-dependence $\varrho_3 = w^4$. The minimal nilpotent orbit at the origin compatible with this partial Casimir is now the trivial one. The Higgs field giving the maximal number of zero modes is

$$\Phi = \Phi_{A_2} \quad \text{with} \quad \Phi_{A_2} = w \begin{pmatrix} 0 & 1 & 0 \\ 0 & 0 & 1 \\ w & 0 & 0 \end{pmatrix} = w\, E_{\alpha_1} + w\, E_{\alpha_2} + w^2\, E_{-\alpha_1-\alpha_2}\,. \tag{5.35}$$

For $N=9$, we obtain the same algebra as for $N=3$, i.e. $\mathcal{M}=A_1^{\oplus 4}$. The Higgs field giving the maximal number of zero modes is

$$\Phi = \sum_{h=1}^{4} \Phi_h \quad \text{with} \quad \Phi_h = w \begin{pmatrix} 0 & 1 \\ c^h w & 0 \end{pmatrix} = w\, E_{\alpha^h} + c^h w^2\, E_{-\alpha^h}\,. \tag{5.36}$$

The same can be done for the cases $N = 7, 10, 11, 12$, where the Higgs contributing most to the zero modes is the one with $N-6$ multiplied by w. In general, the Higgs fields given above for $N = 1, ..., 6$ are enough to write the Higgs field for any N: If $N = n+6k$, with $n \in \{1, ..., 6\}$, the Higgs field is $\Phi = w^k \Phi^{(n)}$, where $\Phi^{(n)}$ is the Higgs field for $N = n$.

This is actually true for all the cDV singularities in Table 5.1:

Given M and N as above, one needs to find the Higgs fields $\Phi^{(n)}$ for $N = n$, with $n \in \{1, ..., M\}$. The Higgs field for $N = n+kM$ is then $\Phi = w^k \Phi^{(n)}$.

This is remarkably convenient also from the physical point of view, as the Higgs background Φ encodes all the 5d physics, meaning the localized hypers and their charges under the flavor and discrete symmetries. What the statement in italics is telling us is that, given a quasi-homogeneous cDV singularity built as an ADE singularity with a $\mu_M = w^N$ deformation term, we need to know only the Higgs backgrounds for N up to M: all the rest can be obtained simply by multiplying these Higgs backgrounds by some power of w. The 5d mode counting changes as explained at the end of Section 5.1.2, the symmetries act in the same way on the (now possibly increased) modes, and the Higgs branch content varies accordingly, so that no new computation must be performed.

5.3 5d Higgs branches from quasi-homogeneous cDV singularities

In this section we exhibit the complete classification of the 5d theories arising from M-theory on quasi-homogeneous cDV singularities.

First, given a quasi-homogeneous cDV singularity, we must find the minimal subalgebra $\mathcal{M}$ in which a Higgs background Φ can reside, compatibly with the threefold equation (see Section 5.2.1). Then, we find the Higgs field that produces the maximal number of modes following Section 5.2.2 (checking that it is consistent with the Higgs branch dimension given by the normalizable complex structure deformations, as in formula (4.19)). Once we have the Higgs field Φ, we can compute the 5d continuous flavor group, the discrete gauge group and the charges of the hypermultiplets under these groups.

We proceed metodically through all the cases in Table 5.1, adding some details on an alternative method to analyze the A-cases in Appendix C.

5.3.1 Quasi-homogeneous cDV singularities of A type

Two quasi-homogeneous cDV singularities of A type exist: the (A_{N-1}, A_{M-1}) and the $A_M^{(M)}[N]$. Their defining equations are

$$\boldsymbol{(A_{M-1}, A_{N-1})}: \qquad x^2+y^2+z^M+w^N = 0, \tag{5.37}$$

$$\boldsymbol{A_M^{(M)}[N]}: \qquad x^2+y^2+z\cdot(z^M+w^N) = 0. \tag{5.38}$$

The non-vanishing deformation parameters are, in both cases, $\mu_M(w) = w^N$. The equation (5.37) is a A_{M-1} family, while (5.38) is a A_M family. In Appendix C we analyze the (A_{M-1}, A_{N-1}) singularities fleshing out all the details.

Employing the results from the Appendix, or equivalently the technique adopted in Section 5.2, it is easy to see that the analysis of the $A_M^{(M)}[N]$ singularities can be fully traced back to the (A_{M-1}, A_{N-1}) singularities: in particular one can see that the Higgs field in the A_M family is living in a A_{M-1} subalgebra and that both spaces are produced by the same choice of $\Phi \in A_{M-1}$. The Higgs fields for the (A, A) threefolds are exhibited in Appendix C and can be used also for the $A_M^{(M)}[N]$ singularities. In general (and for some suitable choice of basis for the Cartan subalgebra), we find hypers of charge at most 1, as the dual Coxeter labels of the nodes of the A Dynkin diagrams are all equal to 1, see Figure 5.4.

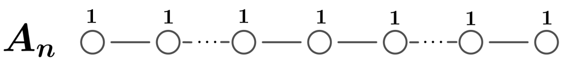

Figure 5.4: *Dual Coxeter labels for the A series.*

In Table 5.2, we report the results for both the (A_{k-1}, A_{N-1}) and the $A_k^{(k)}[N]$ singularities, rewriting them in full generality as (A_{mp-1}, A_{mq-1}) and $A_{mp}^{(mp)}[mq]$ singularities, respectively, and with p and q coprime, $p \geq q$. We give the resolution pattern, the corresponding flavor group, the number of charged hypers and the number of uncharged ones. The latter are a signal of a leftover non-resolvable singularity. The flavor groups are respectively $U(1)^{m-1}$ and $U(1)^m = U(1) \times U(1)^{m-1}$, where in the latter case the factor $U(1)^{m-1}$ is contained in a A_{mp-1} subalgebra, as we have mentioned above. The flavor charges can be succintly understood as follows, in some basis of the Cartan subalgebra[12]: for the (A_{mp-1}, A_{mq-1}) cases, there are pq hypers charged in the bifundamental of every possible pair of $U(1)$'s, as well as $m\frac{(p-1)(q-1)}{2}$ uncharged hypers. For the $A_{mp}^{(mp)}[mq]$ cases, there are pq hypers charged in the bifundamental of every possible pair of $U(1)$'s in the $U(1)^{m-1}$ factor contained in the A_{mp-1} subalgebra, q hypers charged bifundamentally under every possible pair formed by the $U(1)$ *outside* the A_{mp-1} subalgebra and a $U(1) \in U(1)^{m-1}$, and finally there are $m\frac{(p-1)(q-1)}{2}$ uncharged hypers.

[12]For further details, we refer to the much more in-depth analysis of Appendix C.

Singularity	Resolution pattern	Flavor group	Hypers	Total hypers
(A_{mp-1}, A_{mq-1})	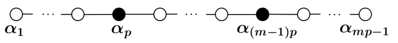	$U(1)^{m-1}$	Charged: $pq\frac{m(m-1)}{2}$ Uncharged: $m\frac{(p-1)(q-1)}{2}$	$\frac{1}{2}m(p(mq-1)-q+1)$
$A_{mp}^{(mp)}[mq]$	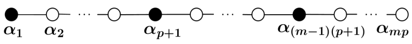	$U(1)^m$	Charged: $pq\frac{m(m-1)}{2}+\boldsymbol{mq}$ Uncharged: $m\frac{(p-1)(q-1)}{2}$	$\frac{1}{2}m(p(mq-1)-q+1)+\boldsymbol{mq}$

Table 5.2: *Higgs branch data for quasi-homogeneous cDV singularities of A type.*

5.3.2 Quasi-homogeneous cDV singularities of D type

There exist two quasi-homogeneous cDV singularities arising from one-parameter deformations of D singularities: the (A_{N-1}, D_{m+1}) and the $D_m^{(m)}[N]$. Their defining equations read

$$\boldsymbol{(A_{N-1}, D_{m+1})}: \qquad x^2+zy^2+z^m+w^N=0, \tag{5.39}$$

$$\boldsymbol{D_m^{(m)}[N]}: \qquad x^2+zy^2+z^{m-1}+yw^N=0. \tag{5.40}$$

In the two cases, the non-vanishing deformation parameter is $\mu_M = w^N$, that is the maximal degree one for the first case ($M = 2m$), while for the second case it is the always present n-degree deformation parameter of D_n ($M = m$).

Employing the methods of the preceding sections, we can work out the Higgs branch of all the (A, D) and the $D_m^{(m)}[N]$ singularities.

As they are useful to identify the flavor charges of the hypermultiplets whenever a single node is resolved, in Figure 5.5 we report the dual Coxeter labels of the nodes of the Dynkin diagrams in the D series.

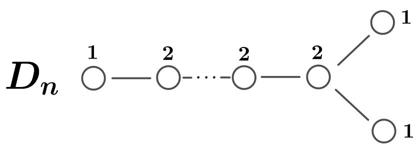

Figure 5.5: *Dual Coxeter labels for the D series.*

We notice that, in full generality, all the (A_{2km-1}, D_{m+1}) and the $D_m^{(m)}[km]$ are completely resolvable, because in that case $N = kM$; this means, following Section 5.2, that $q_\alpha = 1$ and the minimal degree for the partial Casimirs is $j = 1$, i.e. $\mathcal{M}$ is the Cartan subalgebra of $\mathfrak{g}$.

In Table 5.3 and Table 5.4 we report the results for the Higgs branch data, respectively, of the (A_{N-1}, D_4), (A_{N-1}, D_7) and $D_4^{(4)}[N], D_5^{(5)}[N], D_6^{(6)}[N]$ cases, specifying the flavor and discrete charges of the hypermultiplets. Other deformed D_n examples can be treated analogously. For a slightly different approach, employing the Type IIA picture and the explicit D6-brane locus, and producing extended Tables of Higgs branches, we refer to [98].

Singularity	Resolution pattern	$\mathcal{M}$	Symmetry group	Hypers	Total hypers
(A_{N-1}, D_4)	$N = 6n$: 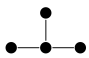	$\mathcal{T}$	$U(1)^4$	$12n$ Charges: **root system** of D_4	$12n$
	$N = 2n$ $n \neq 3j$: 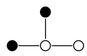	A_2	$U(1)_a \times U(1)_b$	$(q_a, q_b) = (2, 0)$: $\boldsymbol{n}$ $(q_a, q_b) = (1, 1)$: $\boldsymbol{2n}$ $(q_a, q_b) = (0, 0)$: $\boldsymbol{n-1}$	$4n-1$
	$N = 3n$ $n \neq 2j$: 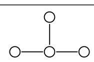	$A_1^{\oplus 4}$	$\mathbb{Z}_2$	$q_{\mathbb{Z}_2} \neq 0$: $\boldsymbol{4n}$ $q_{\mathbb{Z}_2} = 0$: $\boldsymbol{2(n-1)}$	$2(3n-1)$
	$N \neq 2n, 3n$: 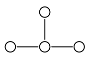	D_4	$\emptyset$	$2(N-1)$	$2(N-1)$
(A_{N-1}, D_7)	$N = 12n$: 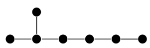	$\mathcal{T}$	$U(1)^7$	$42n$ Charges: **root system** of D_7	$42n$
	$N = 6n$ $n \neq 2j$: 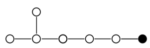	$A_1^{\oplus 6}$	$U(1)_a \times \mathbb{Z}_2^{(b)} \times \mathbb{Z}_2^{(c)}$	$(q_a, q_b, q_c) = (1, 0, 0)$: $\boldsymbol{2n}$ $(q_a, q_b, q_c) = (1, 0, 1)$: $\boldsymbol{2n}$ $(q_a, q_b, q_c) = (1, 1, 0)$: $\boldsymbol{2n}$ $(q_a, q_b, q_c) = (0, 1, 1)$: $\boldsymbol{n-1}$ $(q_a, q_b, q_c) = (0, 1, 0)$: $\boldsymbol{n-1}$ $(q_a, q_b, q_c) = (0, 0, 1)$: $\boldsymbol{n-1}$ $(q_a, q_b, q_c) = (0, 0, 0)$: $\boldsymbol{12n}$	$3(7n-1)$
	$N = 3n$ $n \neq 2j$: 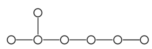	$D_4 \oplus A_3$	$\mathbb{Z}_2$	$q_{\mathbb{Z}_2} \neq 0$: $\boldsymbol{6n}$ $q_{\mathbb{Z}_2} = 0$: $\boldsymbol{\frac{9n-7}{2}}$	$\frac{21n-7}{2}$
	$N = 4n$ $n \neq 3j$: 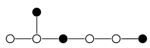	$A_2 \oplus A_2$	$U(1)_a \times U(1)_b \times U(1)_c$	$(q_a, q_b, q_c) = (0, 2, 0)$: $\boldsymbol{n}$ $(q_a, q_b, q_c) = (0, 0, 2)$: $\boldsymbol{n}$ $(q_a, q_b, q_c) = (0, 1, 1)$: $\boldsymbol{6n}$ $(q_a, q_b, q_c) = (1, 1, 0)$: $\boldsymbol{2n}$ $(q_a, q_b, q_c) = (1, 0, 1)$: $\boldsymbol{2n}$ $(q_a, q_b, q_c) = (0, 0, 0)$: $\boldsymbol{2(n-1)}$	$2(7n-1)$
	$N = 2n$ $n \neq 2j, 3j$: 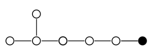	D_6	$U(1)$	$q = 1$: $\boldsymbol{5n-3}$ $q = 0$: $\boldsymbol{2n}$	$7n-3$
	$N \neq 2n, 3n$: 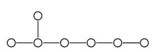	D_7	$\emptyset$	$\frac{7(N-1)}{2}$	$\frac{7(N-1)}{2}$

Table 5.3: *Higgs branch data for quasi-homogeneous cDV singularities of* (A_{N-1}, D_4) *and* (A_{N-1}, D_7) *type.*

Singularity	Resolution pattern	$\mathcal{M}$	Symmetry group	Hypers	Total hypers
$D_4^{(4)}[N]$	$N=4n$: 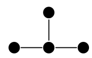	$\mathcal{T}$	$U(1)^4$	$12n$ Charges: **root system** of D_4	$12n$
	$N=2(2n-1)$: 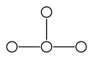	$A_1^{\oplus 4}$	$\mathbb{Z}_2$	$q_{\mathbb{Z}_2}\neq 0$: $\boldsymbol{4(2n-1)}$ $q_{\mathbb{Z}_2}=0$: $\boldsymbol{4(n-1)}$	$4(3n-2)$
	$N\neq 4n, 4n-2$: 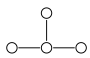	D_4	$\emptyset$	$3N-2$	$3N-2$
$D_5^{(5)}[N]$	$N=5n$: 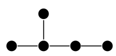	$\mathcal{T}$	$U(1)^5$	$20n$ Charges: **root system** of D_5	$20n$
	$N\neq 5n$: 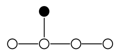	A_4	$U(1)$	$q=1$: $\boldsymbol{2N}$ $q=0$: $\boldsymbol{2(N-1)}$	$2(2N-1)$
$D_6^{(6)}[N]$	$N=6n$: 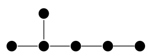	$\mathcal{T}$	$U(1)^6$	$30n$ Charges: **root system** of D_6	$30n$
	$N=2n$, $n\neq 3j$: 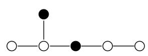	$A_2\oplus A_2$	$U(1)_a\times U(1)_b$	$(q_a,q_b)=(2,0)$: $\boldsymbol{n}$ $(q_a,q_b)=(0,2)$: $\boldsymbol{n}$ $(q_a,q_b)=(1,1)$: $\boldsymbol{6n}$ $(q_a,q_b)=(0,0)$: $\boldsymbol{2(n-1)}$	$2(5n-1)$
	$N=6n-3$: 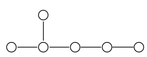	$A_1^{\oplus 6}$	$\mathbb{Z}_2^2$	$q_{\mathbb{Z}_2}\neq 0$: $\boldsymbol{12(2n-1)}$ $q_{\mathbb{Z}_2}=0$: $\boldsymbol{6(n-1)}$	$6(5n-3)$
	$N\neq 2n, 6n-3$: 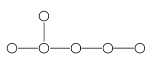	D_6	$\emptyset$	$5N-3$	$5N-3$

Table 5.4: *Higgs branch data for quasi-homogeneous cDV singularities of* $D_4^{(4)}[N], D_5^{(5)}[N], D_6^{(6)}[N]$ *type.*

5.3.3 Quasi-homogeneous cDV singularities of E_6, E_7, E_8 type

In this section, we focus on the deformed E_6, E_7, E_8 cases, looking for the minimal subalgebras containing the Higgs backgrounds reproducing a given quasi-homogeneous cDV singularity of E_6, E_7, E_8 type.

As they are useful to identify the flavor charges, we report the dual Coxeter labels for the E_6, E_7, E_8 Dynkin diagrams in Figure 5.6.

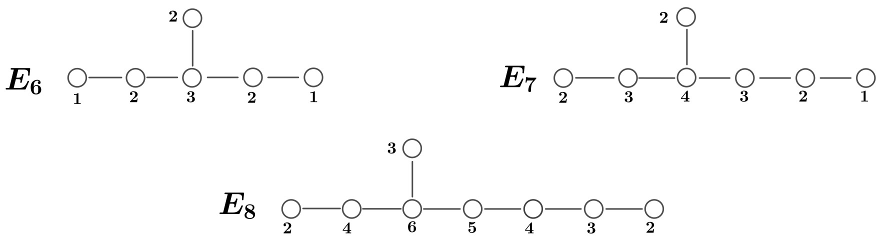

Figure 5.6: *Dual Coxeter labels for the E series.*

To illustrate how we get our results, we explicitly go through the (A_{N-1}, E_6) and the $E_7^{(14)}[N]$ cases. We sum up the results for all the cases in Tables 5.5, 5.6, 5.7, 5.8, 5.9, 5.10.

(A, E_6) singularities

Let us start by showing how this works in the (A_{N-1}, E_6) class, employing the techniques of Section 5.2. The (A_{N-1}, E_6) threefolds are expressed as:

$$\underbrace{x^2+y^3+z^4}_{E_6 \text{ sing}} + \underbrace{w^N}_{\text{def}} = 0. \tag{5.41}$$

Notice that the only non-vanishing deformation parameter is:

$$\mu_{12}(w) = w^N. \tag{5.42}$$

The other (vanishing) deformation parameters are $\mu_2, \mu_5, \mu_6, \mu_8, \mu_9$. Eq. (5.42) tells us that $M = 12$, according to the notation of Section 5.2. There are six divisors of 12:

$$q_\alpha \in \{1, 2, 3, 4, 6, 12\}. \tag{5.43}$$

Now, we must look for the minimal degrees that the candidate partial Casimirs can acquire, thus forecasting the minimal subalgebra in which Φ can be contained. As $M = 12$, the minimal subalgebras will recur with periodicity 12, namely the minimal subalgebra corresponding to the Higgs describing the (A_k, E_6) singularity coincides with the one of (A_{k+12}, E_6). Let us proceed case by case:

For $N = 5, 7, 10, 11$ **mod** 12 ($q_\alpha = 12$), the minimal degree is $j = 12$. This means that $\mathcal{M} = E_6$, with all Casimirs equal to zero, except the maximal degree one. This implies that no resolution is possible.

For $N = 2$ **mod** 12 ($q_\alpha = 6$), the candidate minimal degree is $j = 6$. This tells us that the only c's that can be non-vanishing are c_6^I and c_{12}^I, according to the notation of Section 5.2. To solve the system (5.27) where only μ_6, μ_{12} appear, we need at least two Casimirs of degree 6, but this is not possible because of the rank of E_6[13]. This implies that no resolution is possible, and that the correct minimal subalgebra is $\mathcal{M} = E_6$ with all Casimirs equal to zero, except the maximal degree one.

For $N = 3, 9$ **mod** 12 ($q_\alpha = 4$), the minimal degree for the non-vanishing partial Casimirs is $j = 4$. To solve system (5.27), we have to set two parameters (μ_8 and μ_{12}), and thus we need at least two partial Casimirs of degree 4. They are provided by $\mathcal{M} = D_4$. This implies that the two external nodes of the E_6 Dynkin diagram get inflated, as can be seen in Figure 5.7.

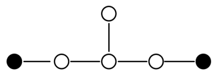

Figure 5.7: *D_4 subalgebra in the $N = 3, 9$ case.*

This yields 5d hypers with charge 1 under the flavor groups corresponding to the resolved nodes, as they have dual Coxeter label equal to 1, as well as uncharged hypers.

For $N = 4, 8$ **mod** 12 ($q_\alpha = 3$), the minimal degree for the non-zero partial Casimirs is $j = 3$. System (5.27) tells us that we need at least three Casimirs of degree 3 to extract a solution and fix the deformation parameters μ_6, μ_9, μ_{12}. Indeed, the subalgebra $\mathcal{M} = A_2 \oplus A_2 \oplus A_2$ gives us the correct partial Casimirs. This choice produces no simultaneous resolution of the deformed family. Furthermore, the fact that $\Phi \in \mathcal{M} = A_2 \oplus A_2 \oplus A_2$ signals that in this case we have a non trivial $\mathrm{Stab}_G(\Phi) = \mathbb{Z}_3$, that reflects in a discrete-gauging of the hypermultiplets of the five-dimensional SCFT. The actual discrete group $\mathbb{Z}_3$ comes because the maximal subalgebra $A_2^{\oplus 3}$ of E_6 is obtained removing the trivalent node from the extended Dynkin diagram of E_6, that has dual Coxeter number equal to 3 (see Section 5.1.3), as depicted in Figure 5.8.

[13]For example, one could have two degree 6 Casimirs using $\mathcal{M} = A_5 \oplus A_5$, or $\mathcal{M} = D_6$, but these cannot be embedded into E_6.

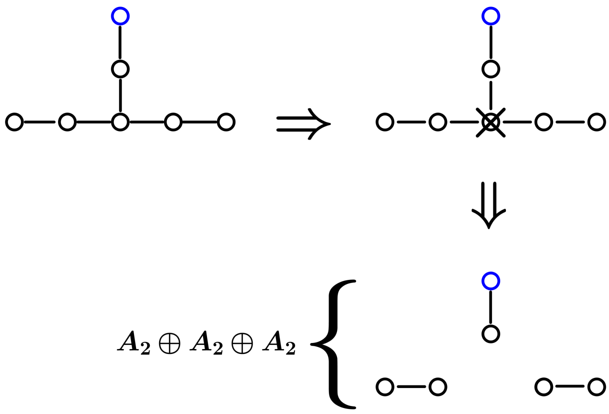

Figure 5.8: *$A_2^{\oplus 3}$ subalgebra in the $N = 4, 8$ case.*

For $N = 6$ **mod** 12 ($q_\alpha = 2$), the minimal degree for the non-zero partial Casimirs is $j = 2$. According to the system (5.27), we have to set the μ_2, μ_6, μ_8 parameters to zero, as well as $\mu_{12} = w^6$. This requires four partial Casimirs of minimal degree 2. It turns out that there exists a unique subalgebra of E_6 doing the work, i.e. $A_1 \oplus A_1 \oplus A_1 \oplus A_1$. We then have $\mathcal{M} = A_1^{\oplus 4} \oplus \mathcal{H}$, with $\mathcal{H}$ generated by the two external nodes in the Dynkin diagram of E_6. The Higgs field take values in the semi-simple part of $\mathcal{M}$. This choice yields the resolution of the two external nodes with Coxeter label 1 of the E_6 Dynkin diagram, and produces a $\mathbb{Z}_2$ discrete group in 5d (since $\mathcal{L} = D_4$ and $A_1^{\oplus 4}$ is its maximal subalgebra, see Section 5.1.3), as depicted in Figure 5.9.

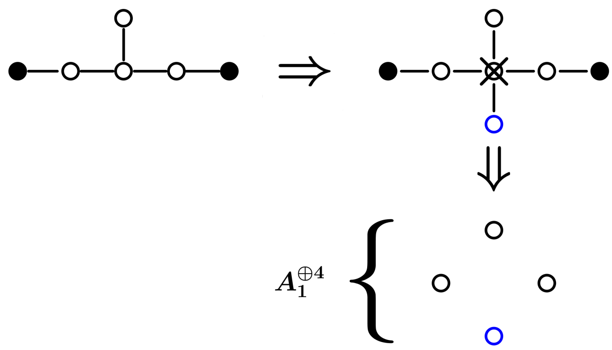

Figure 5.9: *$A_1^{\oplus 4}$ subalgebra in the $N = 6$ case.*

For $N = 12$ **mod** 12 ($q_\alpha = 1$), the minimal degree for the non-zero partial Casimirs is $j = 1$. Then $\mathcal{M}$ is the Cartan subalgebra of E_6. As a result, all the simple roots of E_6 are blown up in the simultaneous resolution. The flavor charges of the 5d hypermultiplets are given, in some basis, by the root system of the E_6 algebra[14].

[14]In general, for all the completely resolvable cases of Tables (5.5) and (5.6), the flavor charges are given by the roots of the corresponding algebra.

$E_7^{(14)}[N]$ singularities

The $E_7^{(14)}[N]$ singularities are expressed as deformed Du Val E_7 singularities:

$$x^2 + y^3 + yz^3 + zw^N = 0. \tag{5.44}$$

Notice that the only non-zero deformation parameter is

$$\mu_{14}(w) = w^N. \tag{5.45}$$

The other (vanishing) deformation parameters are $\mu_2, \mu_6, \mu_8, \mu_{10}, \mu_{12}, \mu_{18}$. From (5.45), we read $M = 14$. Its divisors are:

$$q_\alpha \in \{1, 2, 7, 14\}. \tag{5.46}$$

With this in hand, we can start looking for the minimal degrees of candidate partial Casimirs, pinpointing the minimal subalgebra of E_7 containing Φ for a given $E_7^{(14)}[N]$. As in the previous section, we expect that the subalgebra corresponding to $E_7^{(14)}[N]$ is equal to the one of $E_7^{(14)}[N+14]$, given the degree 14 deformation parameter that is switched on.

For $N = 1, 3, 5, 9, 11, 13$ **mod** 14 ($q_\alpha = 14$), the minimal degree is $j = 14$. Consequently, $\mathcal{M} = E_7$, with all Casimirs equal to zero except the maximal degree one. This entails that no resolution is possible.

For $N = 2, 4, 6, 8, 10, 12$ **mod** 14 ($q_\alpha = 7$), the minimal degree for the partial Casimirs is 7. In order to solve system (5.27), namely to fix μ_{14}, we need only one partial Casimir. A degree 7 partial Casimir can be provided choosing $\mathcal{M} = A_6 \oplus \langle \alpha_7^* \rangle$, which naturally lies inside E_7. This implies that a single node of E_7, with Coxeter label 2, gets inflated by the allowed resolution (see Figure 5.10). This yields 5d hypers with charge 1 and 2, as well as uncharged hypers. The Higgs field Φ lives only in the semi-simple part of $\mathcal{M}$. See Figure 5.10.

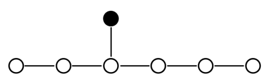

Figure 5.10: *A_6 subalgebra in the $N = 2, 4, 6, 8, 10, 12$ case.*

For $N = 7$ **mod** 14 ($q_\alpha = 2$), the minimal degree for the partial Casimirs is 2. According to (5.27), we need seven distinct such Casimirs. It can be shown that indeed there exists a choice $\mathcal{M} = A_1^{\oplus 7} \in E_7$, that yields seven partial Casimirs of degree 2. This maximal subalgebra can be found noticing the chain of maximal subalgebras $E_7 \supset A_1 \oplus D_6 \supset A_1 \oplus A_1^{\oplus 2} \oplus D_4 \supset A_1^7$, that is depicted in Figure 5.11.

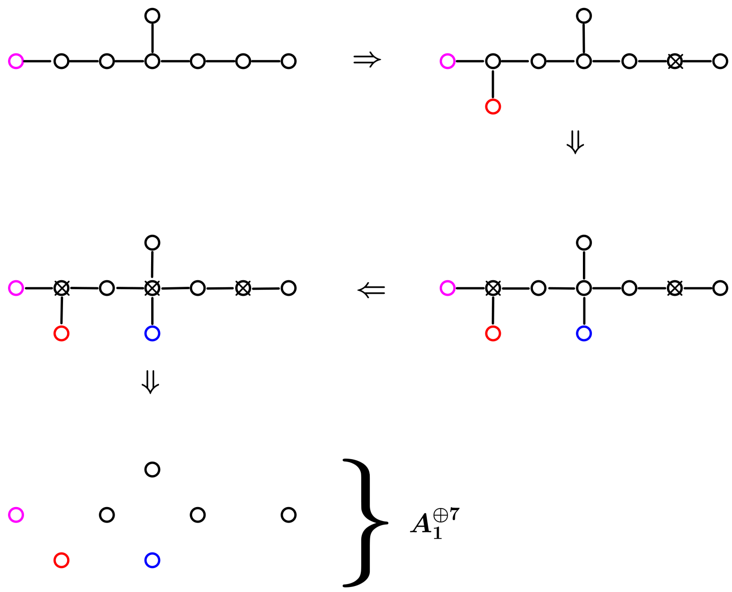

Figure 5.11: *Maximal subalgebra in the $N = 7$ case.*

The three steps in obtaining the maximal subalgebra $A_1^{\oplus 7}$ of E_7, where nodes with Coxeter number equal to two are removed, tells us that we have the non trivial discrete $\mathrm{Stab}_G(\Phi) = \mathbb{Z}_2^3$.

For $N = 14$ **mod** 14 ($q_\alpha = 1$), the minimal degree for the non-vanishing partial Casimirs is $j = 1$. We need at least seven partial Casimirs to fix all the deformation parameters, and hence we can pick as partial Casimirs the Casimirs of the Cartan subalgebra of E_7. In this way, we see that all the simple roots of E_7 are blown-up in the simultaneous resolution. The flavor charges of the 5d hypers can be written as the root system of E_7.

Other quasi-homogeneous cDV singularities of type E

Proceeding along the same path as the previous sections, we can readily find the minimal subalgebras containing the appropriate Higgs background Φ for each class of quasi-homogeneous cDV singularities arising from deformed E_6, E_7, E_8 singularities.

We sum up our results in Table 5.5, 5.6 and 5.7. In particular, we list:

- In the first column, the cDV singularity.
- In the second column, the maximal allowed simultaneous resolution (resolved nodes are in black). This fixes the Levi subalgebra.
- In the third column, the flavor group of the 5d theory.
- In the fourth column, the number of five-dimensional hypers localized in 5d, and their charges under the flavor symmetries.

- In the fifth column, the total number of hypers, to be compared with the number of normalizable complex structure deformations of the corresponding cDV singularity, that can be computed with the tools reviewed in Section 4.2.

In Tables 5.8, 5.9, 5.10, we further classify the discrete symmetries preserved by the Higgs background for all the quasi-homogeneous cDV singularities of E_6, E_7, E_8 type, computed in the same fashion as the explicit examples of the preceding sections. The content of the columns reads:

- In the first column, the cDV singularity.
- In the second column, the maximal allowed simultaneous resolution (resolved nodes are in black) corresponding to each sub-case. This fixes the Levi subalgebra $\mathcal{L}$ containing Φ.
- In the third column, the minimal subalgebra $\mathcal{M} \subseteq \mathcal{L}$ containing Φ. If it is non-trivial, this yields a discrete group in 5d.
- The discrete group preserved by Φ.

Singularity	Resolution pattern	Flavor group	Hypers	Total hypers
Deformed E_6				
(A_{N-1}, E_6)	$N = 12n$: 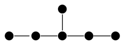	$U(1)^6$	$36n$ Charges: **root system** of E_6	$36n$
	$N = 3n$, $n \neq 4j$: 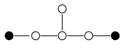	$U(1)_a \times U(1)_b$	$(q_a, q_b) = (1, 0)$: $\boldsymbol{2n}$ $(q_a, q_b) = (0, 1)$: $\boldsymbol{2n}$ $(q_a, q_b) = (1, 1)$: $\boldsymbol{2n}$ $(q_a, q_b) = (0, 0)$: $\boldsymbol{3n-2}$	$9n-2$
	$N \neq 3n$: 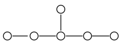	$\emptyset$	$3N$	$3N$
$E_6^{(8)}[N]$	$N = 8n$: 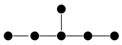	$U(1)^6$	$36n$ Charges: **root system** of E_6	$36n$
	$N = 2n$, $n \neq 4j$: 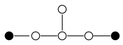	$U(1)_a \times U(1)_b$	$(q_a, q_b) = (1, 0)$: $\boldsymbol{2n}$ $(q_a, q_b) = (0, 1)$: $\boldsymbol{2n}$ $(q_a, q_b) = (1, 1)$: $\boldsymbol{2n}$ $(q_a, q_b) = (0, 0)$: $\boldsymbol{3n-2}$	$9n-2$
	$N = 2n+1$: 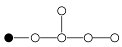	$U(1)$	$q = 1$: $\boldsymbol{4n+2}$ $q = 0$: $\boldsymbol{5n}$	$9n+2$
$E_6^{(9)}[N]$	$N = 9n$: 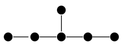	$36n$	0	$36n$
	$N \neq 9n$: 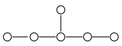	$\emptyset$	$4N-3$	$4N-3$

Table 5.5: *Higgs branch data for quasi-homogeneous cDV singularities of E_6 type.*

Singularity	Resolution pattern	Flavor group	Hypers	Total hypers
Deformed E_7				
(A_{N-1}, E_7)	$N = 18n$: 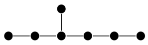	$U(1)^7$	$63n$ Charges: **root system** of E_7	$63n$
	$N = 2n$ $n \neq 9j$: 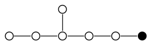	$U(1)$	$q = 1 : \mathbf{3n}$ $q = 0 : \mathbf{4n-3}$	$7n-3$
	$N \neq 2n$: 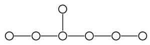	0	$\frac{7N}{2}$	$\frac{7N}{2}$
$E_7^{(14)}[N]$	$N = 14n$: 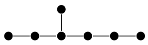	$U(1)^7$	$63n$ Charges: **root system** of E_7	$63n$
	$N = 2n$ $n \neq 7j$: 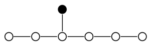	$U(1)$	$q = 2 : \boldsymbol{n}$ $q = 1 : \mathbf{5n}$ $q = 0 : \mathbf{3n-3}$	$9n-3$
	$N \neq 2n$: 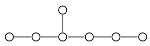	0	$\frac{9N-7}{2}$	$\frac{9N-7}{2}$

Table 5.6: *Higgs branch data for quasi-homogeneous cDV singularities of E_7 type.*

Singularity	Resolution pattern	Flavor group	Hypers	Total hypers
Deformed E_8				
(A_{N-1}, E_8)	$N = 30n$: 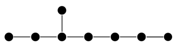	$U(1)^8$	$120n$ Charges: **root system** of E_8	$120n$
	$N \neq 30n$: 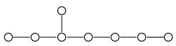	0	$4N$	$4N$
$E_8^{(24)}[N]$	$N = 24n$: 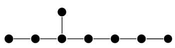	$U(1)^8$	$120n$ Charges: **root system** of E_8	$120n$
	$N \neq 24n$: 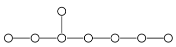	0	$5N-4$	$5N-4$
$E_8^{(20)}[N]$	$N = 20n$: 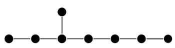	$U(1)^8$	$120n$ Charges: **root system** of E_8	$120n$
	$N \neq 20n$: 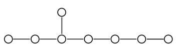	0	$6N-4$	$6N-4$

Table 5.7: *Higgs branch data for quasi-homogeneous cDV singularities of E_8 type.*

Singularity	**Resolution pattern**	$\mathcal{M}$	**Discrete group**
Deformed $\boldsymbol{E_6}$			
(A_{N-1}, E_6)	$N = 12n$: 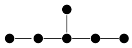	$\mathcal{T}$	$\emptyset$
	$N = 6n$, $n \neq 2j$: 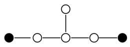	$A_1^{\oplus 4}$	$\mathbb{Z}_2$
	$N = 3n$, $n \neq 2j$: 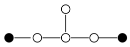	D_4	$\emptyset$
	$N = 4n$, $n \neq 3j$: 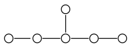	$A_2^{\oplus 3}$	$\mathbb{Z}_3$
	$N \neq 3n, 4n$: 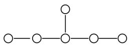	E_6	$\emptyset$
$E_6^{(8)}[N]$	$N = 8n$: 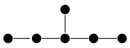	$\mathcal{T}$	$\emptyset$
	$N = 4n$, $n \neq 2j$: 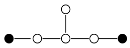	$A_1^{\oplus 4}$	$\mathbb{Z}_2$
	$N = 2n$, $n \neq 2j$: 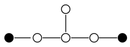	D_4	$\emptyset$
	$N = 2n+1$: 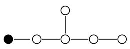	D_5	$\emptyset$
$E_6^{(9)}[N]$	$N = 9n$: 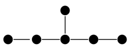	$\mathcal{T}$	$\emptyset$
	$N = 3n$, $n \neq 3j$: 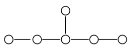	$A_2^{\oplus 3}$	$\mathbb{Z}_3$
	$N \neq 3n$: 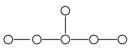	E_6	$\emptyset$

Table 5.8: *Minimal subalgebra $\mathcal{M}$ and discrete group for quasi-homogeneous cDV singularities of E_6 type.*

Singularity	**Resolution pattern**	$\boldsymbol{\mathcal{M}}$	**Discrete group**
Deformed $\boldsymbol{E_7}$			
(A_{N-1}, E_7)	$N = 18n$: 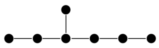	$\mathcal{T}$	$\emptyset$
	$N = 9n$, $n \neq 2j$: 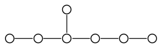	$A_1^{\oplus 7}$	$\mathbb{Z}_2^3$
	$N = 6n$, $n \neq 3j$ 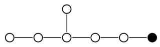	$A_2^{\oplus 3}$	$\mathbb{Z}_3$
	$N = 2n+1$, $2n \neq 9j-1$: 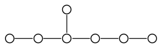	E_7	$\emptyset$
	$N = 2n$, $n \neq 3j$: 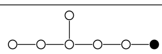	E_6	$\emptyset$
$E_7^{(14)}[N]$	$N = 14n$: 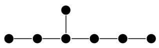	$\mathcal{T}$	$\emptyset$
	$N = 7n$, $n \neq 2j$: 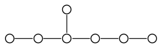	$A_1^{\oplus 7}$	$\mathbb{Z}_2^3$
	$N = 2n+1$, $2n \neq 7j-1$: 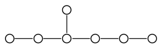	E_7	$\emptyset$
	$N = 2n$, $n \neq 7j$: 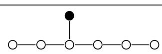	A_6	$\emptyset$

Table 5.9: *Minimal subalgebra $\mathcal{M}$ and discrete group for quasi-homogeneous cDV singularities of E_7 type.*

Singularity	Resolution pattern	$\mathcal{M}$	Discrete group
Deformed E_8			
(A_{N-1}, E_8)	$N = 30n$: 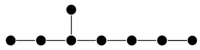	$\mathcal{T}$	$\emptyset$
	$N = 6n$, $n \neq 5j$: 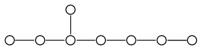	$A_4 \oplus A_4$	$\mathbb{Z}_5$
	$N = 10n$, $n \neq 3j$: 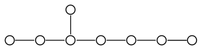	$A_2^{\oplus 4}$	$\mathbb{Z}_3^2$
	$N = 15n$, $n \neq 2j$: 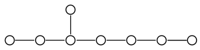	$A_1^{\oplus 8}$	$\mathbb{Z}_2^4$
	$N \neq 6n, 10n, 15n$: 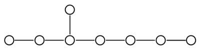	E_8	$\emptyset$
$E_8^{(24)}[n]$	$N = 24n$: 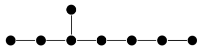	$\mathcal{T}$	$\emptyset$
	$N = 12n$, $n \neq 2j$: 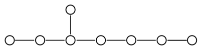	$A_1^{\oplus 8}$	$\mathbb{Z}_2^4$
	$N = 6n$, $n \neq 2j$: 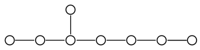	$D_4 \oplus D_4$	$\mathbb{Z}_2^2$
	$N = 3n$, $n \neq 2j$: 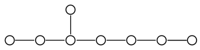	D_8	$\mathbb{Z}_2$
	$N = 8n$, $n \neq 3j$: 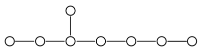	$A_2^{\oplus 4}$	$\mathbb{Z}_3^2$
	$N \neq 3n, 8n$: 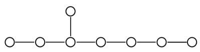	E_8	$\emptyset$
$E_8^{(20)}[N]$	$N = 20n$: 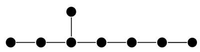	$\mathcal{T}$	$\emptyset$
	$N = 10n$, $n \neq 2j$: 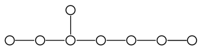	$A_1^{\oplus 8}$	$\mathbb{Z}_2^4$
	$N = 5n$, $n \neq 2j$: 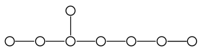	$D_4 \oplus D_4$	$\mathbb{Z}_2^2$
	$N = 4n$, $n \neq 5j$: 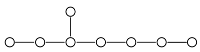	$A_4 \oplus A_4$	$\mathbb{Z}_5$
	$N \neq 4n, 5n$: 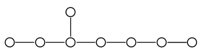	E_8	$\emptyset$

Table 5.10: *Minimal subalgebra $\mathcal{M}$ and discrete group for quasi-homogeneous cDV singularities of E_8 type.*

5.4 0-form discrete symmetries

Having completed the classification of the Higgs branches of M-theory reduced on all the quasi-homogeneous cDV singularities, an observation is in order: consider a cDV singularity obtained as a deformation of an ADE singularity of Type $\mathfrak{g}$. We have chosen as global form of the 7d gauge group the simply connected group containing $\mathfrak{g}$ modulo its center. With this choice, one obtains a discrete group in 5d, arising from the stabilizer of the Higgs background $\Phi(w)$, as we have displayed in the Tables.

Let us add some results for the (A_k, D_n) singularities: proceeding as in Section 5.1.3, or as in [98], one promptly computes the discrete group in 5d, that for $k = 1, \ldots, 8$ and $n = 4, \ldots, 15$ reads:

G_{discrete}	D_4	D_5	D_6	D_7	D_8	D_9	D_{10}	D_{11}	D_{12}	D_{13}	D_{14}	D_{15}
A_1	0	0	0	0	0	0	0	0	0	0	0	0
A_2	$\mathbb{Z}_2$	0	0	$\mathbb{Z}_2$	0	0	$\mathbb{Z}_2$	0	0	$\mathbb{Z}_2$	0	0
A_3	0	$\mathbb{Z}_2$	0	0	0	$\mathbb{Z}_2$	0	0	0	$\mathbb{Z}_2$	0	0
A_4	0	0	$\mathbb{Z}_2^2$	0	0	0	0	$\mathbb{Z}_2^2$	0	0	0	0
A_5	0	0	0	$\mathbb{Z}_2^2$	0	0	0	0	0	$\mathbb{Z}_2^2$	0	0
A_6	0	0	0	0	$\mathbb{Z}_2^3$	0	0	0	0	0	0	$\mathbb{Z}_2^3$
A_7	0	0	0	0	0	$\mathbb{Z}_2^3$	0	0	0	0	0	0
A_8	$\mathbb{Z}_2$	0	0	$\mathbb{Z}_2$	0	0	$\mathbb{Z}_2^4$	0	0	$\mathbb{Z}_2$	0	0

Table 5.11: *Discrete gauge groups of (A_k, D_n) theories.*

Here we notice the striking correspondence between Table 5.11 and the Table presented in [59] for the 1-form symmetries of the 4d $\mathcal{N} = 2$ theories arising from Type IIB on the (A_k, D_n) singularities. This equality holds for all the quasi-homogeneous cDV singularities that have been analyzed via magnetic quiver methods in Type IIB setups, i.e. the (A, A), (A, D) and (A, E) cases [59, 175, 176].

Namely, we observe a one-to-one correspondence between the discrete 0-form symmetries enjoyed by the 5d SCFTs from M-theory on quasi-homogeneous cDV singularities (that are nothing but the discrete symmetries preserved by our Higgs backgrounds), and the discrete 1-form symmetries of Type IIB on the same singularities (that can be extracted e.g. computing the torsion of the singular threefolds at infinity). This is consistent with the analysis of [59–61]: compactifying the 4d SCFT on a circle, the line operators charged under the 1-form symmetry and wrapping the circle become point-like operators in 3d and, correspondingly, the 1-form symmetry becomes a 0-form symmetry acting on the magnetic quiver Coulomb branch; one then ends up with a 0-form symmetry acting on the 5d Higgs branch.

5.5 T-branes

The analysis performed in this chapter, other than allowing the classification of 5d theories from M-theory on quasi-homogeneous cDV singularities, further elucidates the pivotal role of T-branes for the physical description of such theories. In fact, in the preceding sections we have always searched for a Higgs background in some ADE Lie algebra $\mathfrak{g}$, that *maximizes* the number of hypermultiplets of the 5d theory, namely the dimension of the Higgs branch, at the same time breaking the 7d gauge group in the *least* brutal way. These requirements translate into imposing that the Higgs background $\Phi(w)$ lives in the *minimal* subalgebra $\mathcal{M}$ of $\mathfrak{g}$ that allows for a holomorphic dependence of its Casimir invariants on the deformation parameter w. In Section 5.2, we have developed the machinery to satisfy this constraint for all the quasi-homogeneous cDV singularities.

It must be stressed, though, that looking for the minimal subalgebra is a mere choice, enabling comparisons and checks with other existing methods to extract the 5d Higgs branch, but that it is by no means unique, nor necessary from a M-theory point of view. Indeed, in general the Higgs background can be embedded into some larger subalgebra $\mathcal{M}_{\text{T-brane}} \supset \mathcal{M}$, while generating the same threefold equation. This may yield:

1. Less localized modes and a smaller unbroken continuous symmetry in 5d.[15]

2. A smaller unbroken discrete symmetry in 5d.

3. A combination of 1 and 2.

In this regard, the most trivial choice one can pick is:

$$\Phi \in \mathcal{M}_{\text{T-brane}} = \mathfrak{g}, \tag{5.47}$$

namely embedding the Higgs field in the whole algebra.[16] This completely breaks the 7d gauge group and does not produce any hypermultiplet in 5d.

Let us consider a trivial example for the (A_1, A_3) singularity, also called Reid's pagoda with $k = 2$, analyzed in 4.5.3. The Higgs background producing the maximal amount of modes, as well as the expected $U(1)$ flavor symmetry, lies in the algebra $\mathcal{M} = A_1 \oplus A_1 \oplus \langle \alpha_2^* \rangle \subset A_3$, and reads:

$$\Phi = \begin{pmatrix} 0 & 1 & 0 & 0 \\ w & 0 & 0 & 0 \\ 0 & 0 & 0 & 1 \\ 0 & 0 & -w & 0 \end{pmatrix}. \tag{5.48}$$

[15] In this case part of the resolution is obstructed, even though it would appear possible from the geometry.

[16] This can be naturally achieved recalling a theorem by Slodowy [177], that establishes a one-to-one correspondence between the Slodowy slice through the principal nilpotent orbit of $\mathfrak{g}$ and the coordinates on $\mathcal{T}/\mathcal{W}$. Employing this fact one can, for *all* the quasi-homogeneous cDV singularities, pick as Higgs background an element in the Slodowy slice through the principal nilpotent orbit of the corresponding $\mathfrak{g}$, with appropriate coefficients. We will come back to this point momentarily.

In this case, we could have also chosen the following Higgs background:

$$\Phi_{\text{T-brane}} = \begin{pmatrix} 0 & 1 & 0 & 0 \\ 0 & 0 & 1 & 0 \\ 0 & 0 & 0 & 1 \\ w^2 & 0 & 0 & 0 \end{pmatrix}. \tag{5.49}$$

This background obviously reproduces the defining equation of the (A_1, A_3) singularity, via (3.48), but breaks *all* the 7d gauge group (in contrast with a preserved $U(1)$ in the case of Φ in the minimal allowed subalgebra $\mathcal{M}$), and does *not* localize any mode in 5d. This is an example of phenomenon 1.

Furthermore, there can be T-brane cases preserving a smaller discrete group in 5d with respect to their counterpart obtained from Φ in the minimal allowed subalgebra $\mathcal{M}$. Let us take a look again at the (A_2, D_4) example examined in Section 5.1.3, with Higgs background living in the minimal allowed subalgebra:

$$\Phi \in \mathcal{M} = A_1^{\oplus 4}. \tag{5.50}$$

This choice yields:

- 4 hypers in 5d.
- A preserved $\mathbb{Z}_2$ discrete symmetry in 5d.

On the other hand, one could have also made the choice:

$$\Phi \in \mathcal{M}_{\text{T-brane}} = D_4 = \mathfrak{g}, \tag{5.51}$$

that explicitly reads:

$$\Phi_{\text{T-brane}} = \left(\begin{array}{cccc|cccc} 0 & 1 & 0 & 0 & 0 & 0 & 0 & 0 \\ 0 & 0 & w & 0 & 0 & 0 & 0 & 0 \\ 0 & 0 & 0 & 1 & 0 & 0 & 0 & 1 \\ 0 & 0 & 0 & 0 & 0 & 0 & -1 & 0 \\ \hline 0 & -\frac{w}{4} & 0 & 0 & 0 & 0 & 0 & 0 \\ \frac{w}{4} & 0 & 0 & 0 & -1 & 0 & 0 & 0 \\ 0 & 0 & 0 & 0 & 0 & -w & 0 & 0 \\ 0 & 0 & 0 & 0 & 0 & 0 & -1 & 0 \end{array}\right). \tag{5.52}$$

It is then easy to check that $\Phi_{\text{T-brane}}$ produces:

- 4 hypers in 5d.
- No preserved discrete symmetry in 5d.

The dimension of the Higgs branch is unaffected, but the discrete symmetry is broken: this is the most simple example of phenomenon 2.

In full generality, one can easily construct Higgs backgrounds living in some subalgebra $\mathcal{M}_{\text{T-brane}} \supset \mathcal{M}$ such that both phenomenon 1 and 2 arise. This fact entails that, given a quasi-homogeneous cDV singularity[17], a plethora of consistent 5d theories, with varying dimension of the Higgs branch, as well as diverse flavor and discrete symmetries, are possible. $\Phi \in \mathcal{M}$ is the choice producing the largest Higgs branch dimension, as well as the smallest breaking of the 7d gauge group. This is another manifestation of the fact that the geometry of the M-theory background does not uniquely fix the effective low dimensional theory [94,95,109,133,135,139,141]. Intuitively one faces the possibilities depicted in Figure 5.12.

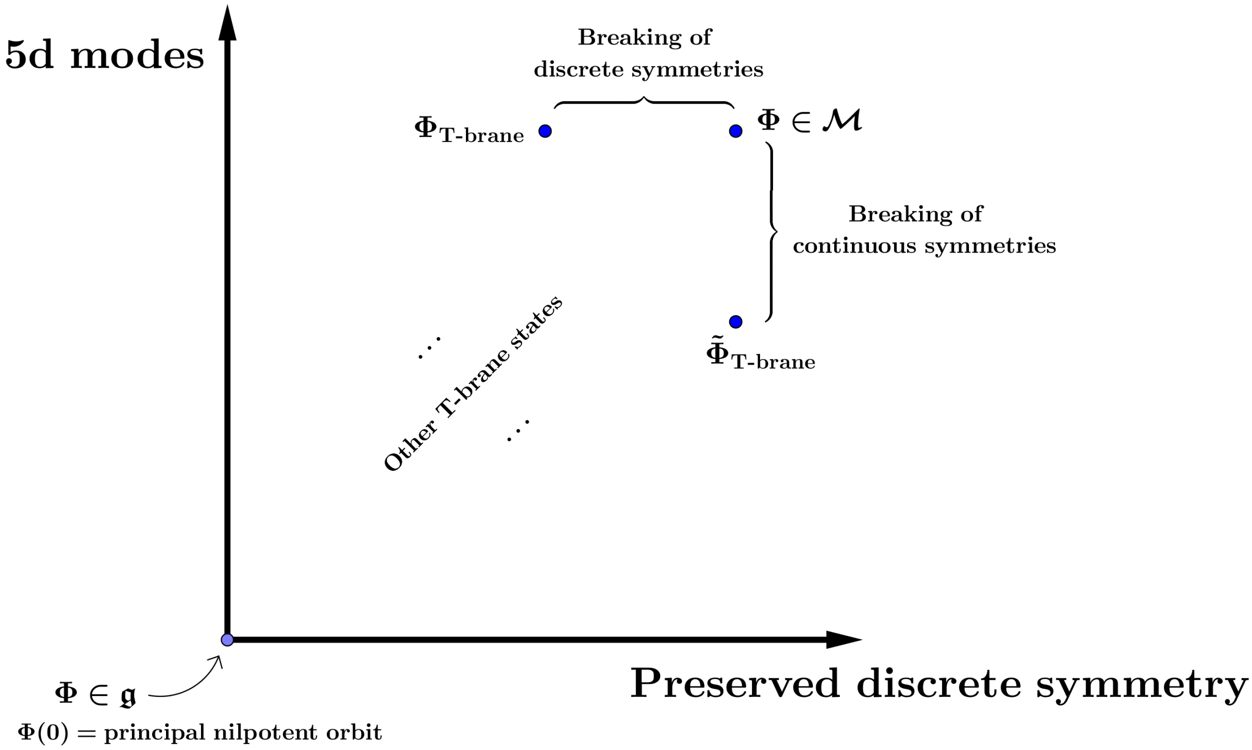

Figure 5.12: *Allowed 5d theories from T-branes.*

It would be extremely interesting to understand the counterpart of the 5d theories arising from T-brane backgrounds in complementary approaches, such as the techniques relying on magnetic quivers.

[17]We remark that T-brane states such as the ones described in the text may appear in *all* one-parameter deformed ADE singularities.

5.5.1 A few general remarks on T-brane backgrounds

In the previous section we have seen that T-brane backgrounds play a pivotal role in the analysis of M-theory on quasi-homogeneous cDV singularities. They are, however, not restricted to those cases, and can potentially arise in *all* one-parameter deformations of ADE singularities, of which quasi-homogeneous cDV singularities are a subclass. Their ubiquitousness makes one wish to find an organizing principle in the apparent chaos of T-brane backgrounds, that can partially break the symmetry of the 5d theories, shrink the dimension of the 5d Higgs branch (in some cases obstructing part of the simultaneous resolution), or display both features at the same time. In Appendix D we propose a partial attempt to classify T-brane backgrounds in quasi-homogeneous cDV singularities, relying on the constraining power of nilpotent orbits. We go along this task by building on a result introduced in Appendix C, dubbed the *codimension formula*. We recap here the gist of the argument, leaving the details for the aforementioned Appendices.

Quasi-homogeneous cDV singularities are ADE fibrations on $\mathbb{C}_w$, that restrict to plain Du Val singularities when evaluated on the origin of $\mathbb{C}_w$. As a consequence, the Higgs backgrounds corresponding to quasi-homogeneous cDV singularities are *nilpotent* when evaluated on $w = 0$ (namely, their Casimirs vanish on $w = 0$), as on top of the origin they should not modify the ADE geometry. As a consequence, we can employ the theory of ADE nilpotent orbits to study the properties of the Higgs backgrounds. In Appendix C, we explain that a Higgs background $\Phi(w) \in \mathfrak{g}$ such that $\Phi(0)$ belongs to some nilpotent orbit $\mathcal{O}_0$ of $\mathfrak{g}$ admits a number of Lie algebra elements n_{ind} supporting 5d modes (in general with multiplicities) that is given by:

$$n_{\text{ind}} = \text{cod}_{\mathbb{C}} \left(\mathcal{O}_0 \hookrightarrow \mathcal{N} \right) , \tag{5.53}$$

where $\mathcal{N}$ is the nilpotent cone defined in Section 2.1.1. (5.53) is the "codimension formula", and it is telling us that Higgs backgrounds that belong to different nilpotent orbits on $w = 0$ localize, in general, a different amount of 5d modes. In this way, we can understand which is the Higgs background localizing the *maximal* amount of modes, that is the one reproducing the dimension of the Higgs branch as intended in the literature, and organize the other Higgs backgrounds, namely the T-brane backgrounds, according to the codimension of the nilpotent orbit to which they belong on top of the origin. This yields a refinement of the discussion presented in the previous section: as we have briefly mentioned in 5.2.2, even Higgses belonging to the same $\mathcal{M}$ can localize a different amount of 5d modes, according to the codimension formula. This means that, for every choice of $\mathcal{M}$ or $\mathcal{M}_{\text{T-brane}}$ in Figure 5.12, there is a further refinement, that allows multiple Higgses corresponding to the *same* subalgebra, but yielding different 5d physics, as they belong to different nilpotent orbits on top of $w = 0$. We provide an explicit example in Appendix C.

This framework also establishes a hierarchy of T-brane backgrounds, starting from the one fixing the maximal amount of modes, and breaking the symmetry the least, to the one with the least 5d modes and the smallest symmetry, which is the one with $\Phi \in \mathcal{M} = \mathfrak{g}$.

As we have mentioned, it is always possible to realize this latter possibility, namely to holomorphically embed a Higgs background in the whole algebra $\mathfrak{g}$: this is guaranteed by a theorem by Slodowy [177], that proves a linear correspondence between the parameters of the Slodowy slice through the *principal nilpotent orbit* of $\mathfrak{g}$ and the Casimirs of $\mathfrak{g}$. In such a way, one can always build a Higgs background in $\mathfrak{g}$ with the desired Casimirs: in the A series, this yields the reconstructible Higgs fields of [94]. For the D and E series, the theorem by Slodowy naturally *defines* a notion of "reconstructible Higgs".

Let us show a brief example in the D_4 case. The reconstructible Higgs is built by turning on a constant background along the principal nilpotent orbit of D_4, built in (2.24), and suitably fixing the parameters of the Slodowy slice through it. The end result reads (in the usual basis of $\mathfrak{so}(8)$ (2.23)):

$$\left(\begin{array}{cccc|cccc} 0 & 1 & 0 & 0 & 0 & 0 & 0 & 0 \\ 0 & 0 & 1 & 0 & 0 & 0 & 0 & 0 \\ 0 & 0 & 0 & 1 & 0 & 0 & 0 & 1 \\ \frac{1}{4}(2\tilde{\delta}_4-\delta_4) & 0 & -\frac{\delta_2}{4} & 0 & 0 & 0 & -1 & 0 \\ \hline 0 & \frac{\delta_6}{4} & 0 & \frac{1}{4}(\delta_4+2\tilde{\delta}_4) & 0 & 0 & 0 & \frac{1}{4}(\delta_4-2\tilde{\delta}_4) \\ -\frac{\delta_6}{4} & 0 & 0 & 0 & -1 & 0 & 0 & 0 \\ 0 & 0 & 0 & \frac{\delta_2}{4} & 0 & -1 & 0 & \frac{\delta_2}{4} \\ \frac{1}{4}(-\delta_4-2\tilde{\delta}_4) & 0 & -\frac{\delta_2}{4} & 0 & 0 & 0 & -1 & 0 \end{array}\right) \tag{5.54}$$

One can immediately check that the (3+4)-dimensional hypersurface equation arising from (5.54) is:

$$x^2+zy^2+z^3+\delta_2 z^2+\delta_4 z+\delta_6+2\tilde{\delta}_4 y = 0, \tag{5.55}$$

that exactly reproduces (1.23), which is written in term of the parameters $\delta, \tilde{\delta} \in \mathcal{T}/\mathcal{W}$. This is precisely what is expected by the reconstructible Higgs, as in the A_n case (4.58). Analogous results can be obtained considering the Slodowy slices through the principal nilpotent orbits of other D_n singularities, as well as for the E_6, E_7, E_8 cases.

It turns out, furthermore, that also the nilpotent orbit to which the w-dependent part of $\Phi(w)$ belongs plays a role in precisely defining the hierarchy of T-brane backgrounds, that can be quite involved. We delve deeper into these ideas, providing precise definitions and concrete examples, in Appendix D.

The results of that Appendix, combined with the analysis of 5.5, make it clear that the T-brane hierarchy can be extremely rich, giving rise to a plethora of different Higgs backgrounds encoding the same geometry, but a different amount of localized modes and unbroken symmetries. Moreover, although we have performed our analysis in the quasi-homogeneous cDV singularities, we expect that the appeareance of a variety of T-brane states holds true in all the one-parameter deformations of ADE singularities, that is the setting in which the "adjoint Higgs" method can be applied. This is reasonably grounded in the mathematical observation that the Casimirs of the Higgs background, that correspond to the M-theory geometry, do not uniquely fix the Higgs background itself, which is an explicit matrix in some representation.

As a result, we have shown that the M-theory geometry is not enough to characterize a T-brane background, and that additional structure is needed: the choice of the Higgs background is intrinsically ambiguous and additional non-geometric data, e.g. the orbits $\mathcal{O}_0$ and $\mathcal{O}_w$ in (D.4), must be specified for a full characterization of the spectrum and of the preserved symmetries in 5d.

CHAPTER 6

A complementary approach: the tachyon condensation formalism

In this chapter, we revisit part of the content of Chapter 4 in a slightly different light: instead of basing the analysis of one-parameter families of deformed ADE singularities on the construction of a Higgs background in Type IIA, we resort to the *tachyon condensation formalism*, first introduced in [178], that allows to perform computations yielding the GV invariants and the hypermultiplet content of the rank-0 5d effective theories arising from M-theory compactification in a quicker and more efficient way, in selected cases[1]. In such a way, we can double-check the results we have already obtained from a similar, and yet inequivalent, perspective.

In Section 6.1 we quickly review the general formalism of tachyon condensation in Type IIA theory, following the approach of [95], in Section 6.2 we apply it to some deformed A cases, while in Section 6.3 we examine deformed D cases, connecting in most instances with the content of Chapter 4.

6.1 Tachyon condensation

Our objective is to explicitly build a setup of D6-branes with or without orientifolds in Type IIA using the tachyon condensation formalism, as this will allow us to describe M-theory compactifications on one-parameter families of A_n and D_n singularities. In this section, we outline the general framework and exhibit its application to the conifold example.

In order to do this, we start with our target space X_{tgt} (in this case, $X_{\text{tgt}} := \mathbb{C}^2$), that encompasses 4 of the 6 extra dimensions of Type IIA theory: we wish to describe D6-branes on a holomorphic subvariety $D \subset X_{\text{tgt}}$, which may be reducible, equipped with a vector bundle over D, that we will specify momentarily. The way to elucidate this setup is to start with a pair of vector bundles $\tilde{E}$ and E defined over all of X_{tgt}, and a linear bundle map

$$T : \tilde{E} \longrightarrow E \tag{6.1}$$

[1]Unfortunately, the tachyon condensation perspective cannot be employed in the E_6, E_7, E_8 cases, that admit no Type IIA dual, and this limits its range of applications.

referred to as the *tachyon map*. Here, E is interpreted as a stack of D8-branes wrapping all of X_{tgt}, as well as the flat 4d spacetime, and $\tilde{E}$ is a stack of anti-D8-branes. T is a matrix that encodes a set of bifundamental strings going from the anti-D8's to the D8's.

If T acquires a vev, then we say that tachyon condensation is taking place, and we get brane-anti-brane annihilation. If T is the identity matrix, then we have total annihilation, and nothing remains. However, if T is a holomorphic matrix, it will typically have complex codimension one loci where it fails to be invertible. At such points, annihilation does not take place, and we are left with D6-branes. An intuitive representation of these phenomena is depicted in Figure 6.1:

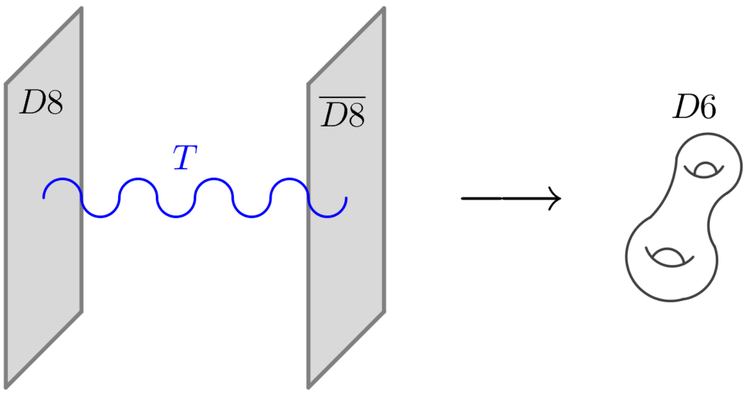

Figure 6.1: *Tachyon condensation.*

In mathematical terms, the cokernel of the map T defines an object with support over the loci where T is not invertible. This is encoded via a short exact sequence as follows:

$$0 \longrightarrow \tilde{E} \xrightarrow{T} E \longrightarrow \text{coker}(T) \longrightarrow 0\,, \tag{6.2}$$

where $\text{coker}(T)$ is the cokernel of the map T, which is a sheaf with support only above the D6-brane locus $\det(T) = 0$. From now on, we will not display exact sequences, but simply the relevant part of the complexes. In this case, we will simply say that this D6-brane is given by the two term complex:

$$\tilde{E} \xrightarrow{T} E\,. \tag{6.3}$$

Now we should consider the fact that there are gauge transformations on the D8 and the anti-D8 stacks, which in turn act bifundamentally on the tachyon field:

$$\begin{array}{ccc} \tilde{E} & \xrightarrow{T} & E \\ \circlearrowleft & & \circlearrowleft \\ G_{\overline{\text{D8}}} & & G_{\text{D8}} \end{array} \qquad \Longrightarrow \qquad T \longrightarrow G_{\text{D8}} \cdot T \cdot G_{\overline{\text{D8}}}^{-1} \tag{6.4}$$

The gauge symmetry on the D6-brane system is given by the subset of transformations

$(g_{\overline{\mathrm{D8}}}, g_{\mathrm{D8}})$ that leave the tachyon map T invariant.

Having defined D6-branes and their gauge symmetries, we are now in a position to discuss the open string spectrum. Concretely it is defined as the vertical map $\delta\varphi$:

$$\begin{array}{ccc} & \tilde{E} & \xrightarrow{T} E \\ & \downarrow{\scriptstyle \delta\varphi} & \\ \tilde{E} \xrightarrow{T} & E & \end{array} \tag{6.5}$$

modulo gauge transformations. If we implement the transformations, it looks as follows:

$$\begin{array}{ccccc} & & \tilde{E} & \xrightarrow{T} & E \\ & \swarrow{\scriptstyle g_{\overline{\mathrm{D8}}}} & \downarrow{\scriptstyle \delta\varphi} & \swarrow{\scriptstyle g_{\mathrm{D8}}} & \\ \tilde{E} & \xrightarrow{T} & E & & \end{array} \tag{6.6}$$

The "fluctuation" field $\delta\varphi$ is defined up to linearized gauge transformations as follows:

$$\delta\varphi \sim \delta\varphi + T \cdot g_{\overline{\mathrm{D8}}} + g_{\mathrm{D8}} \cdot T \,. \tag{6.7}$$

These are referred to as *homotopies* in mathematical language.

Depending on the situation, we can create coincident, intersecting, or so-called *T-branes* with this technology. All three will give rise to different kinds of spectrum. Let us proceed with our example step by step.

First, we build a pair of coincident D6-branes.

We start with two D8-anti-D8 pairs, and a *tachyon map*, as a two-term complex, as follows:

$$\mathcal{O}^{\oplus 2} \xrightarrow{T} \mathcal{O}^{\oplus 2} \,, \tag{6.8}$$

with the choice $T = z \cdot \mathbb{1}_2$, and $\mathcal{O}$ is the *structure sheaf* (trivial line bundle). The tachyon fails to be invertible at $z = 0$. The gauge transformation pairs $(g_{\overline{\mathrm{D8}}}, g_{\mathrm{D8}})$ that leave this tachyon invariant must satisfy

$$g_{\overline{\mathrm{D8}}} = -g_{\mathrm{D8}} \,, \quad \text{with} \quad g_{\mathrm{D8}} \in \mathfrak{sl}(2)_{\perp} \,. \tag{6.9}$$

Initially, we had a $\mathfrak{sl}(2) \oplus \mathfrak{sl}(2)$ gauge algebra, since there was a pair of D8-branes and a pair of anti-D8-branes. The gauge transformation we just identified is one subalgebra $\mathfrak{sl}(2)_{\perp}$. The orthogonal one, defined by the diagonal embedding of $\mathfrak{sl}(2)_{\Delta}$

$$g_{\overline{\mathrm{D8}}} = +g_{\mathrm{D8}} \,, \tag{6.10}$$

gives us our transformation law for the $\delta\varphi$ fluctuations as follows:

$$\delta\varphi \quad \sim \quad \delta\varphi + T \cdot g_{\overline{\mathrm{D8}}} + g_{\mathrm{D8}} \cdot T = \delta\varphi + zg\,, \tag{6.11}$$

with $g \cong \frac{1}{2} g_{\mathrm{D8}} \in \mathfrak{sl}(2)_{\Delta}$. Here, $\delta\varphi \in \mathfrak{sl}(2)$, so this equivalence tells us that we can eliminate all dependence on z in the matter field. In other words

$$\delta\varphi \in \mathfrak{sl}(2) \otimes \mathbb{C}[z] / (z \cdot \mathfrak{sl}(2)) \cong \mathfrak{sl}(2)\,. \tag{6.12}$$

This means that this matter field is localized on the divisor $z = 0$, and is therefore a seven-dimensional adjoint complex scalar on the worldvolume of the two D6-branes.

Now we consider switching on an angle between the two D6-branes. This means choosing

$$T = \begin{pmatrix} z - w & 0 \\ 0 & z + w \end{pmatrix}\,. \tag{6.13}$$

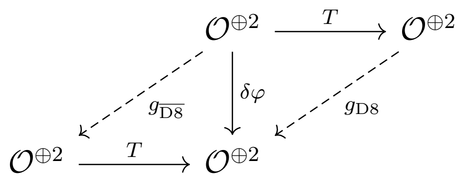

(6.14)

The choice of pair $(g_{\overline{\mathrm{D8}}}, g_{\mathrm{D8}})$ that preserves the tachyon is

$$g_{\mathrm{D8}} = \begin{pmatrix} g & 0 \\ 0 & -g \end{pmatrix}\,, \quad g_{\overline{\mathrm{D8}}} = -g_{\mathrm{D8}} \qquad g \in u_{\mathbb{C}}(1)\,. \tag{6.15}$$

This identifies a $u_{\mathbb{C}}(1) \subset \mathfrak{sl}(2)_{\perp} \subset \mathfrak{sl}(2) \oplus \mathfrak{sl}(2)$, where $\mathfrak{sl}(2)_{\perp}$ is the "relative" linear combination defined earlier.

The broken generators for the $(g_{\overline{\mathrm{D8}}}, g_{\mathrm{D8}})$ pair are then:

$$g_{\overline{\mathrm{D8}}} = \begin{pmatrix} \frac{1}{2} g & a_{+} \\ a_{-} & -\frac{1}{2} g \end{pmatrix}\,, \quad g_{\mathrm{D8}} = \begin{pmatrix} \frac{1}{2} g & b_{+} \\ b_{-} & -\frac{1}{2} g \end{pmatrix}\,. \tag{6.16}$$

These induce the following gauge equivalence for the matter field $\delta\varphi \equiv \begin{pmatrix} \delta\varphi_0 & \delta\varphi_{+} \\ \delta\varphi_{-} & -\delta\varphi_0 \end{pmatrix}$

$$\delta\varphi \sim \delta\varphi + \begin{pmatrix} g(z - w) & (a_{+} + b_{+})z + (a_{+} - b_{+})w \\ (a_{-} + b_{-})z + (b_{-} - a_{-})w & -g(z + w) \end{pmatrix}\,. \tag{6.17}$$

We defined the fluctuation as traceless, since we are not interested in center of mass motion. From this we learn that the $\delta\varphi_0$ mode is localized in codimension one on the target space. In other words, it's a 7d field. On the other hand, the off-diagonal modes are localized in codimension two, and are hence legitimately dynamical from a 5d viewpoint:

$$\delta\varphi_{\pm} \in \mathbb{C}[z,w]/(z,w) \cong \mathbb{C}\,. \tag{6.18}$$

The IIA interpretation is that we have two intersecting flat D6-branes, and there is one 5d hypermultiplet $(\delta\varphi_+, \delta\varphi_-)$, depicted by the following quiver:

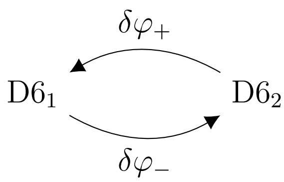

(6.19)

Hence, there is a multiplicity one hypermultiplet of charge one w.r.t. the unbroken $U(1)$ flavor[2] symmetry. In M-theory, this translates to the fact that, on the conifold, there is only the genus zero, degree one GV invariant, and it is equal to one:

$$n_{d=1}^{g=0} = 1\,. \tag{6.20}$$

Of course, this result precisely coincides with the one obtained in Section 4.5.1.

6.2 Deformed A_n singularities

6.2.1 Reid's pagodas

In this section, we revisit the computation for Reid's pagodas, already explored in Section 4.5.3, from the point of view of tachyon condensation.

Let us describe the D6-brane setup corresponding to Reid's pagodas from a IIA perspective as the following complex:

$$\mathcal{O}^{\oplus 2} \xrightarrow{T} \mathcal{O}^{\oplus 2}\,, \tag{6.21}$$

with

$$T := \begin{pmatrix} z^k - w & 0 \\ 0 & z^k + w \end{pmatrix}\,. \tag{6.22}$$

This corresponds to two intersecting D6-branes on the divisors $z^k \pm w = 0$, respectively. Note, however, that these two branes do not intersect transversely, but intersect at a multiplicity k point. In terms of ideals, we write that

$$(z^k - w, z^k + w) = (z^k, w), \tag{6.23}$$

[2]This is a flavor symmetry for the 5d theory; it comes from a 7d gauge symmetry on the worldvolume of the D6-branes.

which is a "fat point" in $\mathbb{C}^2$. Hence, we have no right to expect the spectrum to be one-dimensional, as instead happened in the conifold case. A first hint that this might be so is the fact that the slightest deformation of either brane will split up the fat point into k distinct points:

$$(z^k - w + \delta, z^k + w) = (z^k + \delta, w) \,. \tag{6.24}$$

Hence, we should anticipate k hypermultiplets of charge one under the flavor $U(1)$. Let us compute this with the techniques explained in the previous section.

We have again five broken $\mathfrak{sl}(2)$ generators, meaning that they do not commute with the tachyon:

$$g_{\overline{\mathrm{D8}}} = \begin{pmatrix} \frac{1}{2}g & a_+ \\ a_- & -\frac{1}{2}g \end{pmatrix} \,, \quad g_{\mathrm{D8}} = \begin{pmatrix} \frac{1}{2}g & b_+ \\ b_- & -\frac{1}{2}g \end{pmatrix} \,. \tag{6.25}$$

Now we compute how these generators act as linearized gauged transformations on a fluctuation field $\delta\varphi \equiv \begin{pmatrix} \delta\varphi_0 & \delta\varphi_+ \\ \delta\varphi_- & -\delta\varphi_0 \end{pmatrix}$:

$$\delta\varphi \sim \delta\varphi + \begin{pmatrix} g(z^k - w) & (a_+ + b_+)z^k + (a_+ - b_+)w \\ (a_- + b_-)z^k + (b_- - a_-)w & -g(z^k + w) \end{pmatrix} \,. \tag{6.26}$$

The $\delta\varphi_0$ mode localizes to $w \pm z^k = 0$, and is therefore a 7d field. From the 5d perspective, it is non-dynamical. The bifundamental modes, on the other hand, localize on the ideal

$$(z^k, w) \,. \tag{6.27}$$

So we have that

$$\delta\varphi_\pm \in \mathbb{C}[z,w]/(z^k, w) \cong \mathbb{C}[z]/(z^k) \,. \tag{6.28}$$

This ring can be regarded as a k-dimensional vector space

$$\mathbb{C}[z]/(z^k) \cong \mathbb{C}^k \,. \tag{6.29}$$

Therefore, we conclude that there are k hypermultiplets of charge one. This matches the result already recovered in Section 4.5.3:

$$n^{g=0}_{d=1} = k \,, \tag{6.30}$$

and zero for all other classes and genera.

6.3 Deformed D_n singularities

In this section, we revisit the path through deformed D_n singularities, reviewing the Laufer and Brown-Wemyss examples from the tachyon condensation vantage point, as well as exhibiting a new addition, namely the Morrison-Pinkham threefold.

6.3.1 Tachyon condensation with orientifolds

In order to connect one-parameter families of D_n singularities to IIA constructions, we will need not only D6-branes, but also O6$^-$-planes. O6-planes induce an orientifold projection, that has been described in details in Section 3.5.

In addition, now we need to define the action of the orientifold projection on the tachyon. We refer to [179] for general details. The upshot is that a tachyon complex

$$E \xrightarrow{T} F \tag{6.31}$$

must obey the following:

$$E \cong F^\vee \qquad \text{and} \quad T = -\sigma^*(T^t)\,. \tag{6.32}$$

Consistency requires that left and right gauge transformations be related as follows:

$$T \longrightarrow G{\cdot}T{\cdot}\sigma^*(G^t)\,. \tag{6.33}$$

As we have seen in Section 3.5, the CY threefolds we are looking for are defined as $\mathbb{Z}_2$-quotients of $\mathbb{C}^*$-fibrations over the double-cover IIA geometry. The $\mathbb{Z}_2$-quotient is implemented by the relation $\xi^2 = z$.

From this perspective, all polynomials on the base space of the $\mathbb{C}^*$-fibration can be split into an orientifold even and an odd part: $\gamma(\xi, w, z) = \alpha(w, z) + \xi\beta(w, z)$. Any higher powers in ξ can be eliminated with the hypersurface equation. Combining this with our condition on the tachyon (6.32), we arrive at the following general ansatz:

$$T = A + \xi S\,, \qquad \text{with} \quad A^t = -A \qquad \text{and} \quad S^t = S\,, \tag{6.34}$$

where the entries of A and S are polynomials in $\mathbb{C}[w, z]$.

Let us now go to M-theory. Retracing the path followed in Section 3.5.1, we find that the general geometry is a $\mathbb{C}^*$-fibration degenerating on the D6-brane locus, of the form (3.59), that we rewrite here for convenience:

$$x^2 + zy^2 - P(z, w) + 2yQ(z, w) = 0 \quad \subset \mathbb{C}[x, y, z, w]. \tag{6.35}$$

Let us now revisit Laufer's and Brown-Wemyss' examples through the lens of tachyon condensation.

6.3.2 Laufer's examples

Laufer's singularities read:

$$x^2 - zy^2 - w\left(w^2 - z^{2k+1}\right) = 0 \qquad \text{with } k \geq 1\,. \tag{6.36}$$

Consider the double cover given by $\xi^2 = z$, where the orientifold involution is $\xi \mapsto -\xi$. In the double cover twofold, the D6-brane locus of Laufer's singularities is given by:

$$w\,\xi^2\left(\xi^{2k+1}+w\right)\left(\xi^{2k+1}-w\right)=0 \tag{6.37}$$

and is encoded by the complex

$$\mathcal{O}^{\oplus 4} \xrightarrow{\;T\;} \mathcal{O}^{\oplus 4}, \tag{6.38}$$

where T is

$$T=\begin{pmatrix} 0 & \xi^{2k+1}+w & 0 & 0 \\ \xi^{2k+1}-w & 0 & 0 & 0 \\ 0 & 0 & \xi & 0 \\ 0 & 0 & 0 & w\xi \end{pmatrix}. \tag{6.39}$$

Its determinant correctly reproduces the brane locus (6.37). Notice that the form of the matrix (6.39) is compatible with the orientifold invariance condition (6.34). One may object that (6.37) suggests that there are five D6-branes (one invariant brane at $w = 0$, two branes on top of the O6-plane and a pair of one brane and its orientifold image), and then one would expect a 5×5 tachyon matrix. However there is no way to build a 5×5 matrix that respects (6.34) and that reproduces (6.37). One entry of T must be ξw, which is interpreted as a bound state of two branes (see [94,95]).

The linearized $D8/\overline{D8}$ gauge transformations acts on T as

$$T \mapsto g_{D8}\cdot T + T\cdot \sigma^* g_{D8}^t. \tag{6.40}$$

where the orientifold invariance of the setup forces the relation $G_{\overline{\mathrm{D8}}} = \sigma^* G^t_{\mathrm{D8}}$ at the group level.

The surviving gauge symmetry is again given by the $D8/\overline{D8}$ gauge transformations that leave T invariant. In the present case we still have $U(1)$ gauge symmetry, whose generator is

$$g_{U(1)}=\begin{pmatrix} 1 & 0 & 0 & 0 \\ 0 & -1 & 0 & 0 \\ 0 & 0 & 0 & 0 \\ 0 & 0 & 0 & 0 \end{pmatrix}. \tag{6.41}$$

We are now ready to compute the spectrum of zero modes. The elements of the $\mathfrak{gl}(4)$ $D8/\overline{D8}$ gauge symmetry that act non-trivially on T are given by

$$g_{D8}=\frac{1}{2}\begin{pmatrix} \alpha_{11}+\xi\beta_{11} & \alpha_{12}+\xi\beta_{12} & \gamma_{13} & \gamma_{14} \\ \alpha_{21}+\xi\beta_{21} & \alpha_{11}-\xi\beta_{11} & \gamma_{23} & \gamma_{24} \\ \gamma_{31} & \gamma_{32} & \alpha_{33} & \alpha_{34}+\xi\beta_{34} \\ \gamma_{41} & \gamma_{42} & \alpha_{43}+\xi\beta_{43} & \alpha_{44} \end{pmatrix} \tag{6.42}$$

where α_{ij} and β_{ij} are polynomials invariant under $\xi \mapsto -\xi$, while γ_{ij} are generic polynomials in w, ξ.

The fluctuation field $\delta\varphi$ (that is a matrix with entries $\delta\varphi_{ij}$) is found by modding out the deformations that can be obtained by a linearized gauge transformation (6.40):

$$\delta\varphi \sim \delta\varphi + g_{D8}\cdot T + T\cdot\sigma^* g_{D8}^t \equiv \delta\varphi + \delta_g T \tag{6.43}$$

where we recall that σ^* will force $\xi \mapsto -\xi$.

Let us write $\delta_g T$ in a block-diagonal form (with 2×2 blocks):

$$\delta_g T = \left(\begin{array}{c|c} A & B \\ \hline C & D \end{array}\right). \tag{6.44}$$

Due to the block-diagonal form of the matrix T, the blocks A, D of $\delta_g T$ are affected only by the corresponding 2×2 diagonal blocks of g_{D8}. Moreover the off-diagonal blocks of $\delta_g T$ are related by $C = -\sigma^* B^t$ and depend only on the parameters appearing in the off-diagonal blocks of g_{D8}. Hence, we can study separately the blocks of $\delta_g T$.

We now compute separately each block of $\delta_g T$ and we discuss which modes it can fix. We start with the diagonal block A:

$$A = \begin{pmatrix} 2\alpha_{12}\xi^{2k+1} - 2\beta_{12} w\,\xi & 2\,(\alpha_{11}+\beta_{11}\xi)\left(\xi^{2k+1}+w\right) \\ 2\,(\alpha_{11}-\beta_{11}\xi)\left(\xi^{2k+1}-w\right) & 2\alpha_{21}\xi^{2k+1} + 2\beta_{21} w\,\xi \end{pmatrix}. \tag{6.45}$$

The modes $\delta\varphi_{12}$ and $\delta\varphi_{21}$ localize respectively on the D6-brane loci $w+\xi^{2k+1}$ and $w-\xi^{2k+1}$. They are 7d fields that are non-dynamical in 5d. Due to the orientifold projection condition (6.34), the bifundamental modes are of the form

$$\delta\varphi_{11} = \xi\delta\varphi_{A+} \qquad \text{and} \qquad \delta\varphi_{22} = \xi\delta\varphi_{A-}$$

with $\delta\varphi_{A\pm}$ polynomials that are invariant under $\xi \mapsto -\xi$. The modes $\delta\varphi_{11}$ and $\delta\varphi_{22}$ localize on the ideal

$$(w\xi\,,\ \xi^{2k+1}) \tag{6.46}$$

and then

$$\delta\varphi_{A\pm} \in \mathbb{C}[\xi, w]^{\text{inv}}/(w,\ \xi^{2k}) \cong \mathbb{C}[z, w]/(w,\ z^k) \cong \mathbb{C}[z]/(z^k) \cong \mathbb{C}^k. \tag{6.47}$$

We then conclude that there are k hypermultiplets related to the up-left diagonal block of $\delta\varphi$. They have charge 2 under the $U(1)$ generated by (6.41), as it can be shown by taking $g_{U(1)}\cdot\delta\varphi + \delta\varphi\cdot g_{U(1)}$. This can be understood by noticing that these modes come from strings stretching from one $U(1)$ brane to its image: they live in the symmetric representation of the group on the brane, hence they have charge 2 under the $U(1)$ group.

Let us move to the diagonal block D:

$$D = \begin{pmatrix} 2\alpha_{33}\xi & (\alpha_{34}+\beta_{34}\xi)\,w\xi + (\alpha_{43}-\beta_{43}\xi)\,\xi \\ (\alpha_{34}-\beta_{34}\xi)\,w\xi + (\alpha_{43}+\beta_{43}\xi)\,\xi & 2\alpha_{44}\xi w \end{pmatrix} \tag{6.48}$$

Here we see that none of the modes $\delta\varphi_{33}, \delta\varphi_{34}, \delta\varphi_{43}, \delta\varphi_{44}$ are localized in 5d.

Finally we analyze the block B (the modes in the block C are the orientifold image of the ones in B):

$$B = \begin{pmatrix} \gamma_{13}\xi + \sigma^*\gamma_{32}\left(w+\xi^{2k+1}\right) & \gamma_{14}w\xi + \sigma^*\gamma_{42}\left(w+\xi^{2k+1}\right) \\ \gamma_{23}\xi - \sigma^*\gamma_{31}\left(w-\xi^{2k+1}\right) & \gamma_{24}w\xi - \sigma^*\gamma_{41}\left(w-\xi^{2k+1}\right) \end{pmatrix} \tag{6.49}$$

Here we remind that $\sigma^*\gamma_{ij}(\xi, w) = \gamma_{ij}(-\xi, w)$.

Let us give a name to the different zero modes, related to their charge under the $U(1)$ symmetry (6.41):

$$\delta\varphi_{13} \equiv \delta\varphi_{B+}, \qquad \delta\varphi_{23} \equiv \delta\varphi_{B-}, \qquad \delta\varphi_{14} \equiv \delta\varphi_{B'+}, \qquad \delta\varphi_{24} \equiv \delta\varphi_{B'-}.$$

The modes $\delta\varphi_{B\pm}$ localize on the ideal

$$(\xi\,,\ w\pm\xi^{2k+1}) = (\xi\,,\ w), \tag{6.50}$$

while the modes $\delta\varphi_{B'\pm}$ localize on the ideal

$$(\xi w\,,\ w\pm\xi^{2k+1}) = (\xi^{2k+2}\,,\ w\pm\xi^{2k+1}). \tag{6.51}$$

Hence

$$\delta\varphi_{B\pm} \ \in\ \mathbb{C}[\xi, w]/(\xi, w) \cong \mathbb{C} \tag{6.52}$$

$$\delta\varphi_{B'\pm} \ \in\ \mathbb{C}[\xi, w]/(\xi^{2k+2}, w\pm\xi^{2k+1}) \cong \mathbb{C}[\xi]/(\xi^{2k+2}) \cong \mathbb{C}^{2k+2} \tag{6.53}$$

We then conclude that there are $1+(2k+2) = 2k+3$ hypermultiplets related to the off-diagonal blocks of $\delta\varphi$. They have charge 1 under the $U(1)$ symmetry generated by (6.41). This is understood form the brane point of view from the fact that these modes live on the intersection of the orientifold invariant branes with the $U(1)$ brane: they are bifundamentals of the intersecting branes, i.e. they have charge 1 under the $U(1)$ of the second brane (the first one is invariant and its group is projected out).

Summarizing, we obtained

- ***k* modes** (and k anti-modes) with charge **2**.
- **2*k*+3 modes** (and $2k+3$ anti-modes) with charge **1**.

This perfectly matches the results of Section 4.6.3.

6.3.3 Brown-Wemyss' example

The brane locus for the Brown-Wemyss' singularity (3.67) reads:

$$w\,\xi^2\left(w-\xi(w-\xi^2)\right)\left(w+\xi(w-\xi^2)\right) = 0. \tag{6.54}$$

The corresponding tachyon matrix is

$$T = \begin{pmatrix} 0 & \xi(\xi^2-w)+w & 0 & 0 \\ \xi(\xi^2-w)-w & 0 & 0 & 0 \\ 0 & 0 & \xi & 0 \\ 0 & 0 & 0 & w\xi \end{pmatrix} . \tag{6.55}$$

Again, the $U(1)$ gauge group on the D6-branes is given by (6.41). The zero mode computation follows the steps seen in Section 6.3.2: We have one zero mode $\delta\varphi_{A\pm}$ of charge two localized on the ideal

$$(w\,,\ \xi^2-w) = (w\,,\ \xi). \tag{6.56}$$

Moreover we have one zero mode of charge one localized on

$$(\xi\,,\ w\pm\xi(\xi^2-w)) = (\xi\,,\ w) \tag{6.57}$$

and four zero modes of charge one localized on the ideal

$$(\xi w\,,\ w\pm(\xi^3-\xi w)) = (\xi^4\,,\ w\pm\xi^3). \tag{6.58}$$

We see that we have found the same spectrum that we obtained in Laufer's example with $k=1$. As noticed in [92], the GV invariants of this manifold coincide with those of Laufer's example. This was actually the point of [92], i.e. showing an example of two different varieties with the same GV invariants; they conclude that GV do not determine flops.

6.3.4 Morrison-Pinkham example

A deformation of Laufer's threefold with $k=1$ was first discussed by [180]. Its defining equation is

$$x^2-zy^2+(w+\lambda z)\left(w^2-z^3\right) = 0. \tag{6.59}$$

with λ a complex parameter. This threefold has a singularity with a flop of length 2 at the origin ($x=y=z=w=0$). There is moreover a conifold singularity at the point $x=y=z-\lambda^2=w+\lambda^3=0$.

The corresponding D6-brane locus and tachyon matrix are given by

$$(w+\lambda\xi^2)\,\xi^2\left(\xi^3+w\right)\left(\xi^3-w\right) = 0 \tag{6.60}$$

and

$$T = \begin{pmatrix} 0 & \xi^3+w & 0 & 0 \\ \xi^3-w & 0 & 0 & 0 \\ 0 & 0 & \xi & 0 \\ 0 & 0 & 0 & (w+\lambda\xi^2)\xi \end{pmatrix} . \tag{6.61}$$

One invariant brane has been deformed with respect to Laufer. The gauge symmetry on the

D6-branes is like in Laufer, i.e. the $U(1)$ symmetry generated by (6.41) and living on the brane/image-brane system.

The computation of the zero modes proceeds analogously to Laufer. The only significant difference occurs in the block B of $\delta_g T$: The modes $\delta\varphi_{B'\pm}$ now localize on the ideal

$$(\xi w+\lambda\xi^3\,,\ w\pm\xi^3) = (\xi^3(\lambda\mp\xi)\,,\ w\pm\xi^3). \tag{6.62}$$

Hence, around $\xi = w = 0$ we have

$$\delta\varphi_{B'\pm}\ \in\ \mathbb{C}[\xi, w]/(\xi^3, w) \cong \mathbb{C}[\xi]/(\xi^3) \cong \mathbb{C}^3, \tag{6.63}$$

while around $\xi = \pm\lambda$ and $w = -\lambda^3$

$$\delta\varphi_{B'\pm}\ \in\ \mathbb{C}[\xi, w]/(\xi\mp\lambda, w-\lambda^3) \cong \mathbb{C}. \tag{6.64}$$

All these modes have charge one with respect to the $U(1)$ group living on the brane/image-brane stack. There is also one mode at the origin with charge equal to two: this can be derived with the same computation done in Laufer's example, with $k = 1$.

The deformation from Laufer's example (with $k = 1$) to Morrison-Pinkham's example has separated one conifold point from the singularity at the origin[3]. If we work in the completion of the local ring of the singularity, meaning, we zoom in on the origin, then we essentially move this conifold point infinitely far away. In that case, the GV invariants are

$$n^{g=0}_{d=2} = 1\,, \qquad\qquad n^{g=0}_{d=1} = 4\,, \tag{6.65}$$

and zero for all other invariants.

In the next section, we take a brief detour and further analyze the structure of Laufer's singularity using matrix factorizations, showing how to completely deform it to a series of conifold points, following in some sense the spirit of the Morrison-Pinkham flop.

6.3.5 Completely deformed Morrison-Park

In this section, we aim at further elucidating the structure of Laufer's singularity, showing how it can be deformed into a set of conifold-like singular points, each supporting one hypermultiplet in 5d, or, in a dual language, giving one contribution to the GV computation.

Consider the class of Laufer singularities, defined by the equation[4]:

$$x^2+yz^2+w^3+wz^{2k+1} = 0 \tag{6.66}$$

[3] As we will see in the next section, one can further deform the threefold going to a singular threefold with 1+5 conifold points.

[4] This differs from (4.117) by a trivial change of sign of w and z, done for later convenience.

This hypersurface has only one isolated singularity at the origin, but there exists a deformation that splits the original singularity into $(k)+(2k+3)$ isolated conifold-like singularities. Let us see how this comes about more precisely.

We consider Laufer's singularity labelled by k as deformations of D_{2k+3} singularities, admitting only the resolution of the trivalent node. In this context, the deformation parameters $\varrho_i \in \mathcal{T}/\mathcal{W}'$ (with $\mathcal{W}'$ the Weyl group generated by all the roots except the trivalent one) that totally deform the generalized Laufer singularities are (in the notation of Section 4.6):

$$\boldsymbol{D_{2k+3}}: \begin{cases} \varpi_1 = -w-c_1+c_2 \\ \varpi_2 = -\frac{c_1}{2} \\ \sigma_{2k+1} = w \\ \sigma_{2k} = 0 \\ \sigma_{2k-1} = 1 \\ \sigma_{2k-2} = c_3 \\ \text{all other } \sigma\text{'s} = 0 \end{cases} , \tag{6.67}$$

where the subscript indicates the degree in the parameters of the Cartan subalgebra $\mathcal{T}$, as usual.

The hypersurface equation corresponding to (6.67) reads:

$$\begin{aligned} &\underbrace{\underbrace{x^2+y^2z+wz^{2k+1}+w^3}_{Laufer}-\left(\frac{1}{4}c_1^2z^{2k}+c_1wy+c_2z^{2k+1}-c_2w^2\right)+}_{Morrison-Park} \\ &+c_3^2\left(-\frac{c_1^2z^2}{4}-c_2z^3+wz^3\right)+c_3\left(\frac{1}{2}c_1^2z^{k+1}+2c_2z^{k+2}-2wz^{k+2}\right)=0 \end{aligned} , \tag{6.68}$$

where setting $c_1=c_2=c_3=0$ gives equation (6.66), whereas fixing $c_3=0$ and $k=1$ recovers the Morrison-Park hypersurface, studied in [181].

The hypersurface (6.68) can be interpreted as a determinantal variety, defined by requiring that the matrix

$$M = \begin{pmatrix} x+\frac{c_1}{2}z\left(z^{k-1}-c_3\right) & w & y & z\left(z^{k-1}-c_3\right) \\ -w^2+c_2w+c_1y & x-\frac{c_1}{2}z\left(z^{k-1}-c_3\right) & c_2z\left(z^{k-1}-c_3\right)-wz\left(z^{k-1}-c_3\right) & y \\ -yz & z^2\left(z^{k-1}-c_3\right) & x+\frac{c_1}{2}z\left(z^{k-1}-c_3\right) & -w \\ c_2z^2\left(z^{k-1}-c_3\right)-wz^2\left(z^{k-1}-c_3\right) & -yz & w^2-c_2w-c_1y & x-\frac{c_1}{2}z\left(z^{k-1}-c_3\right) \end{pmatrix}$$

has rank equal or less than 2.

As we will exhibit momentarily, there are two classes of points where the rank of M drops further, signalling that they are singular points:

- There are $2k+3$ points where the rank drops to 1.
- There are k points where the rank drops to 0.

It can be shown that the rank of the matrix drops to 1 on the points that satisfy:

$$\left(x, \text{minors}_{2\times 2}\begin{bmatrix} z^{k+1} & y & -w \\ y & -w+c_2 & \frac{c_1}{2} \\ -w & \frac{c_1}{2} & -z^k \end{bmatrix}\right) = 0 \tag{6.69}$$

which gives $2k+3$ points. Notice that (6.69) is not a complete intersection.

On the other hand the rank of the matrix drops to 0 when:

$$x = y = w = 0, \quad z(z^{k-1}-c_3) = 0, \tag{6.70}$$

which gives k points (including the origin).

The two classes where the rank drops are A_1 singular points (as can be easily seen by "zooming" on the neighborhood of the points): we have succeded in completely deforming Laufer's singularity, "splitting" the singular points into $(k)+(2k+3)$ points. The difference in the rank drop of M to 1 or to 0 signals precisely the fact that such singular points support hypermultiplets of charge 1 and 2, respectively, under the usual flavor $U(1)$ generated by the resolved node of Laufer's singularities. In the Gopakumar-Vafa language, points where the $\text{rk}(M) = 1$ and $\text{rk}(M) = 0$ correspond to degree 1 and 2 GV invariants, respectively. This correctly agrees with the results of section (4.6.3).

Conclusions

A journey through M-theory on deformed ADE singularities: Summary

In the course of this work, devoted to the analysis of M-theory on one-parameter families of ADE singularities, we have employed a *constructive* approach, starting from a description of the simplest Higgs backgrounds associated to deformed ADE singularities (such as the conifold), and slowly building towards more intricate cases, such as the simple flops of Chapter 4 and the quasi-homogeneous compound Du Val singularities of Chapter 5.

In this section, we aim at distillating the technical results of this trip, by summarizing its setting and organically systematizing the outcome of our step-by-step process, that has grown in the preceding chapters: here, we display the final[5] framework for the analysis of M-theory on the one-parameter deformed ADE singularities employing the "adjoint Higgs" technique, fleshing out its power and scope from the vantage point provided by being at the end of the journey, with all the tools at disposal.

The general setting, as we have seen, is the following:

- M-theory on one-parameter families of deformed ADE singularities, with parameter w. These include *all* the compound Du Val singularities, both quasi-homogeneous and not quasi-homogeneous[6].
  To summarize, the "adjoint Higgs" method we have presented works for all ADE singularities deformed with constant or holomorphic w-dependent terms.

We have introduced the Higgs background $\Phi(w)$ as follows: M-theory on an ADE singularity gives rise to a $\mathcal{N} = 1$ 7d theory with three real adjoint scalars ϕ_1, ϕ_2, ϕ_3. Combining two of them into $\Phi = \phi_1 + i\phi_2$ we can describe deformations of the ADE singularity giving a vev to Φ. A vev depending on one complex parameter w corresponds to the one-parameter families of deformed ADE singularities we are considering.

The correspondence is made explicit by the computation of the Casimirs of $\Phi(w)$ (that is taken to live in an explicit matrix representation) which are related to the threefold equation

[5] Final in the extremely limited sense of the work done by the author on the topic, of course.

[6] Provided that we switch on only the parameters of the versal deformation, with w-dependent coefficients.

via:

$$\begin{aligned}
&\boldsymbol{A_n}: \quad x^2+y^2+\det(z\mathbb{1}-\Phi)=0\\
&\boldsymbol{D_n}: \quad x^2+zy^2-\frac{\sqrt{\det(z\mathbb{1}+\Phi^2)}-\mathrm{Pfaff}^2(\Phi)}{z}+2y\,\mathrm{Pfaff}(\Phi)=0\\
&\boldsymbol{E_6}: \quad x^2+z^4+y^3+\epsilon_2 yz^2+\epsilon_5 yz+\epsilon_6 z^2+\epsilon_8 y+\epsilon_9 z+\epsilon_{12}=0\\
&\boldsymbol{E_7}: \quad x^2+y^3+yz^3+\tilde{\epsilon}_2 y^2 z+\tilde{\epsilon}_6 y^2+\tilde{\epsilon}_8 yz+\tilde{\epsilon}_{10} z^2+\tilde{\epsilon}_{12} y+\tilde{\epsilon}_{14} z+\tilde{\epsilon}_{18}=0\\
&\boldsymbol{E_8}: \quad x^2+y^3+z^5+\hat{\epsilon}_2 yz^3+\hat{\epsilon}_8 yz^2+\hat{\epsilon}_{12} z^3+\hat{\epsilon}_{14} yz+\hat{\epsilon}_{18} z^2+\hat{\epsilon}_{20} y+\hat{\epsilon}_{24} z+\hat{\epsilon}_{30}=0,
\end{aligned} \tag{6.71}$$

where the Casimirs $\epsilon_i, \tilde{\epsilon}_i, \hat{\epsilon}_i$ depend on $\Phi(w)$ via the expressions in Appendix B.

This connection is the technical core of the work, and can be represented schematically as:

$$\boxed{\text{Casimirs of Higgs background } \Phi(w)} \quad \longleftrightarrow \quad \boxed{\begin{array}{c}\text{one-parameter families of}\\ \text{deformed ADE singularities}\end{array}} \tag{6.72}$$

The relationship (6.72) can also be inferred using Slodowy slices, introduced in Chapter 2 and employed in the construction of Higgs backgrounds in Chapter 4, 5 and 6. It can be proven that Slodowy slices $\mathcal{S}_{\text{subreg}}$ through subregular nilpotent orbits of the ADE algebras encode the versal deformations of the very same ADE singularities, parameterized by coordinates $u_i \in \mathcal{T}/\mathcal{W}$, with $\mathcal{T}$ and $\mathcal{W}$ the Cartan subalgebra and the Weyl group of the given ADE algebra, respectively. The u_i are related to the Casimirs of the Slodowy slice. Cutting the versal deformation with a choice $u_i = u_i(w)$ produces a one-parameter deformation of an ADE singularity. In this picture, the Casimirs of the Slodowy slice play the role of the Casimirs of the Higgs background in (6.71). Slodowy slices, in turn, are the tool at the core of Springer resolutions, which yield the partial (or complete) simultaneous resolution corresponding to the threefold given by the explicit choice of Casimirs. We have then a correspondence between the Higgs background and the Slodowy slice tools, that can be depicted as follows:

$$\text{Casimirs of } \mathcal{S}_{\text{subreg}} \quad \longleftrightarrow \quad \text{Casimirs of } \Phi \tag{6.73}$$

Physically, triggering a vev for $\Phi(w)$ higgses the 7d theory, yielding an effective theory in five spacetime dimensions: this is the 5d $\mathcal{N}=1$ SCFT arising from M-theory on the one-parameter deformed ADE singularity corresponding to the Higgs background[7]. Our objective has been to study, using the information contained in the Higgs background:

- The Higgs branch of the 5d SCFT.
- The GV invariants of the compactification threefold.

[7]Here, we are considering deformed ADE families admitting an *isolated singularity*.

In Chapter 4, we have seen that the two tasks are intimately related, as the GV invariants encode the number of hypermultiplets in the 5d Higgs branch, and their degrees correspond to the flavor charges of the hypers. Concretely, the Higgs background encodes the Higgs branch data as follows:

- Fluctuations around the Higgs background that cannot be gauge fixed to zero, and that are localized on[8] $w = 0$, are five-dimensional hypermultiplets.
- The preserved group G_{5d} is given by the stabilizer of[9] $\Phi(w)$. The charges of the hypers under the symmetry are given by the adjoint action of G_{5d} on the hypers.

Once the relationship between the Casimirs of $\Phi(w)$ and the threefold equation has been established, the problem of writing down the explicit form of $\Phi(w)$ comes about. Unfortunately, (6.72) is not sufficient to accomplish this task: linear-algebraically, the Casimirs *do not* uniquely fix the form of the Higgs background matrix. Given a threefold, the possible Higgs backgrounds with compatible Casimirs fall into two categories:

1. The Higgs background that breaks the 7d gauge group in the *least* brutal way, and localizes the *maximal* amount of modes in 5d.
2. All other Higgs backgrounds.

In the course of the work, we have mostly focused on 1: namely, we have searched for the Higgs vev $\Phi(w)$ leaving as much of the 7d symmetry unbroken as possible, and that yields the Higgs branch of maximal dimension. In turn, this implies that such Higgs background inflates the maximal number of nodes in the corresponding ADE Dynkin diagram. The results obtained choosing this Higgs background agree, when an overlap is present, with other approaches in the literature, both as regards the Higgs branches[10] and the GV invariants[11].

Given a threefold built as a one-parameter deformation of an ADE singularity $\mathfrak{g}$, finding the correct subalgebra $\mathcal{M}$ of $\mathfrak{g}$ in which the Higgs background satisfying 1 lives is a formidable task. In general, $\mathcal{M}$ is of the form:

$$\mathcal{M} = \bigoplus_h \mathcal{M}_h \oplus \mathcal{H}, \tag{6.74}$$

where the $\mathcal{M}_h$ are simple addends and $\mathcal{H}$ is a sum of elements in the Cartan subalgebra: the roots dual to these elements are inflated by the simultaneous resolution corresponding to the given Higgs vev. The Casimirs of $\Phi(w)$ can then be expressed as functions of the *partial*

[8] In case after a suitable shift of the variable w.

[9] An ambiguity, due to the global structure of the theory, is present in the choice of the gauge group G_{7d} in 7d, that gives different outcomes for G_{5d}. We have showed the different results due to this subtlety in Chapter 4.

[10] As is the case for a few quasi-homogeneous deformed A singularities in [59], and the systematic analysis of the (A, A), (A, D) and (A, E) singularities, examined from a magnetic quiver perspective, in [175] and [176].

[11] Computed for various examples of simple flops in [86, 89–92]. In general, our results for simple flops of all lengths comply with the lower bounds on the GV invariants imposed by [182].

Casimirs of $\mathcal{M}$, namely the Casimirs ϱ_i of its addends. The choice of $\mathcal{M}$ automatically fixes the stabilizer of $\Phi(w)$, including its discrete part:

$$\boxed{\text{Stab}_{G_{7d}}(\Phi(w))} \quad \longleftrightarrow \quad \boxed{\text{minimal } \mathcal{M} \text{ containing } \Phi(w)} \tag{6.75}$$

In addition, $\mathcal{M}$ can be embedded in some Levi subalgebra $\mathcal{L}$ of $\mathfrak{g}$:

$$\mathcal{L} = \bigoplus_h \mathcal{L}_h \oplus \mathcal{H}. \tag{6.76}$$

The minimal $\mathcal{L}$ containing $\mathcal{M}$ is precisely the Levi subalgebra corresponding to the Springer simultaneous resolution of the roots dual to $\mathcal{H}$. As a consequence, for the Higgs background Φ conforming to prescription 1, we have a web of correspondences between its Casimirs, the Levi subalgebra of $\mathfrak{g}$ in which it is embedded, and the simultaneous resolution that is unobstructed by Φ. Namely, we can extend the graph (6.73) as:

$$\begin{array}{ccc} \text{Casimirs of } \mathcal{S}_{\text{subreg}} & \longleftrightarrow & \text{Casimirs of } \Phi \\ \updownarrow & & \updownarrow \\ \text{Springer resolution} & \longleftrightarrow & \text{Levi subalgebra containing } \Phi \end{array} \tag{6.77}$$

In selected cases, such as the *quasi-homogeneous* cDV singularities of Chapter 5, we have found completely automatic techniques to pinpoint $\mathcal{M}$, solely relying on the degrees of the deformation parameter in the ADE versal deformation. Once $\mathcal{M}$ is fixed, one can proceed and explicitly build a Higgs background focusing on the single addends and concentrating on tuning only the entries comprised in the Slodowy slice through the nilpotent orbit related to the single addend[12]. In general, many different nilpotent orbits are compatible with the threefold equation, yielding a different spectrum in 5d, according to the *codimension formula* of Appendix C. To conform to presciption 1, one takes the nilpotent orbit with biggest codimension inside the nilpotent cone.

In more general cases, though, the procedure is not straightforward, and some guesswork must be employed, embarking on a recursive strategy: one first tries choosing $\mathcal{M} = \mathcal{T}$, that is the subalgebra corresponding to a complete resolution, and checks if there exists a holomorphic choice of the partial Casimirs of $\mathcal{M}$ that reproduce the threefold. If it exists, the job is concluded and one has found the correct $\mathcal{M}$: otherwise, the algorithm goes on, picking a bigger $\mathcal{M}$, that corresponds to some partial resolution, until a suitable Higgs background is found. In the "worst" case, one ends up with $\mathcal{M} = \mathfrak{g}$.

As a byproduct, embedding a Higgs background in a subalgebra $\mathcal{M} \subset \mathfrak{g}$ corresponding to a given simultaneous resolution of $\mathfrak{g}$, and keeping the dependence of the resulting threefold on the partial Casimirs of $\mathcal{M}$, one automatically obtains the expression of the versal deformation of the $\mathfrak{g}$-singularity in coordinates adapted to the simultaneous resolution, a task that can

[12] This strategy turns out to work in all the examined examples, although a definitive proof is yet to be found.

pose significant computational challenges, especially for the exceptional algebras.

On the other hand, if one drops assumption 1, a plethora of possible Higgs backgrounds arise, corresponding to choice 2: these are the T-brane backgrounds. They might give rise to a smaller unbroken symmetry in five dimensions, to a smaller dimension of the 5d Higgs branch, or to a combination of both phenomena. As we have seen in Chapter 5, T-brane backgrounds display an intricate structure, which is, in cases such as the cDV singularities, interestingly classified by the theory of nilpotent ADE orbits.

In the next section, we conclude with some more general remarks concerning the work performed so far.

Final remarks

In the course of this thesis, we have focused on a narrow corner of M-theory geometric engineering, namely on the study of M-theory compactifications on one-parameter deformations of ADE singularities, displaying an isolated singularity. Picking this somewhat restrictive environment, though, has been extremely beneficial: we have been able to compute the Higgs branches of the rank-0 5d SCFTs for wide classes of non-toric threefolds built as deformed ADE singularities, many of which were previously unexplored. We have employed an extremely explicit technique, based on an adjoint Higgs background associated to the threefold singularity, that has reduced the task to a straightforward linear algebra computation[13]. The outcome has confirmed that these rank-0 5d SCFTs possess a Higgs branch that is composed of free hypers or discrete gaugings of free hypers[14]. In this fashion, we have constructed examples of simple threefold flops of all lengths, and completely exahusted the classification of the Higgs branches of quasi-homogeneous compound Du Val singularities.

On a dual side, these computations have furnished an alternative physics-based interpretation of the Gopakumar-Vafa invariants of the compactification threefolds: the counting of the GV invariants, which is usually performed in the mathematics literature employing sophisticated techniques, or via correspondences with sheaf-theoretic data, has been reformulated as a zero-mode computation of fluctuations around a Higgs background (that lends itself to an open string states interpretation in the A and D cases, that admit a Type IIA counterpart), based exclusively on linear algebra. This has confirmed existing results from the mathematical literature, as well as adding the knowledge of the GV invariants for the classes of threefolds we have analyzed in the main body of the thesis. Besides, our computations naturally yield an interpretation of charge 0 hypermultiplets as "degree 0" GV invariants, which are not properly defined in the mathematical literature. This is an aspect that requires further investigation.

Moreover, we have also shown a complementary approach for the characterization of

[13] Moreover, as we have mentioned in the first section of the Conclusions, this technique in principle applies to *all* possible one-parameter deformations of ADE singularities, and not only to the classes examined in the text.

[14] With the caveat, which is yet to be completely understood, that the flavor symmetry in 5d turns out to be smaller than the expected one for a bunch of free hypers.

Higgs branches and GV invariants, relying on the tachyon condensation formalism, that has allowed quicker computations for singularities admitting a Type IIA dual, thanks to the reduced sizes of the tachyon matrices with respect to their Higgs counterpart. We have shown this in action for a few examples of simple flops, but nothing forbids an application also to other cDV singularities.

On a side note, the work of the preceding chapters has further elucidated the role of nilpotent orbits in the classification of 5d SCFTs, as they have been one of the key organizing principles in the explicit construction of the Higgs backgrounds, via the theory of Slodowy slices and Grothendieck-Springer resolutions, as well as in the analysis of T-brane backgrounds. In particular, the T-brane backgrounds seem to be governed by a Hasse diagram-like hierarchical structure. As welcome byproducts, the theory of ADE nilpotent orbits has also produced a direct and automatic way to compute deformed ADE families admitting a given simultaneous partial resolution, based on the "adjoint Higgs method", as well as a natural definition of reconstructible Higgs backgrounds in the D and E series, expanding upon the definition in the A case.

The results recapped in the previous paragraph offer natural avenues for extensions and generalizations: the somewhat limited scope of rank-0 5d SCFTs arising from hypersurface equations built as one-parameter deformed ADE singularities, for example, ineherently calls for a generalization of the "adjoint Higgs" technique to higher-rank 5d SCFTs, with the due adaptations, and hopefully transferring much of its computational power. This is particularly relevant also in light of applications to the (D, D) and (D, E) singularities, which are not cDV, and that as such require an updated approach with respect to the one outlined in this work.

On a slightly more mathematics-oriented side, considering M-theory on *two-parameter* deformations of ADE singularities, a setting that could be aptly dealt with the adjoint Higgs method, could shed some light on Gopakumar-Vafa invariants for Calabi-Yau fourfolds, as introduced by Klemm and Pandharipande [183] and later developed in the mathematical literature [184–186]. The properties of the 3d effective theories arising from these setups, previously considered in [157] in some special cases, but that remain largely uninvestigated, could also be analyzed in this fashion.

APPENDIX A

ADE Lie algebras

In this Appendix we review a few basic facts about Lie algebras that we need in the main body of the work: we start from strolling through some definitions, and end up giving explicit matrix presentations for the Lie algebra in the A_n and D_n series.

Among the countless reviews of the topic, we mainly draw from the crystal clear lectures of Benini [187] and the book of Collingwood, MacGovern [112].

A.1 Basic facts on Lie algebras

For our purposes, a Lie algebra $\mathfrak{g}$ is a vector space over $\mathbb{C}$ that comes with an antisymmetric bilinear operation, usually called commutator:

$$[\cdot,\cdot]: \quad \mathfrak{g}\times\mathfrak{g} \to \mathfrak{g}. \tag{A.1}$$

The Lie algebra can be explicitly defined by a set of generators T^a, satisfying the commutation relations:

$$[T^a, T^b] = i f^{abc} T^c, \tag{A.2}$$

where repeated indices are summed, and the factor i is needed to make the generators hermitian, i.e. $(T^a)^\dagger = T^a$. The coefficients f^{abc} are called structure constants, they are antisymmetric in the first two indices, and completely define the Lie algebra $\mathfrak{g}$. In other words, given the set of all f^{abc} we can completely reconstruct the commutation relations, and so also the algebra.

A representation ρ of the Lie algebra $\mathfrak{g}$ associates every element of the Lie algebra to an element of the endomorphisms of a vector space V:

$$\rho: \quad \mathfrak{g} \to \mathrm{End}(V). \tag{A.3}$$

The dimension of V is the dimension of the representation, and ρ is said to be a *faithful* representation if it is an injective map.

The most natural representation of the Lie algebra, that takes V as the Lie algebra itself, is the *adjoint representation* "ad", defined as:

$$\mathrm{ad}: \quad \mathfrak{g}\times\mathfrak{g} \to \mathfrak{g} \qquad \mathrm{ad}(X) = [X, Y]. \tag{A.4}$$

The generators of the adjoint representation are nothing but the structure constants if^{abc}.

Using the adjoint representation we can also define the *Killing form* κ, a symmetric bilinear form on $\mathfrak{g}$:

$$\kappa: \quad \mathfrak{g}\times\mathfrak{g} \to \mathbb{C}, \qquad \kappa(X,Y) = \mathrm{Tr}\left(\mathrm{ad}(X)\mathrm{ad}(Y)\right). \tag{A.5}$$

In the following, we will only be concerned about *simple* Lie algebras, namely non-abelian algebras that do not contain any proper ideal. In this setting, we take a look at a specific choice of basis for the generators in (A.2), known as Cartan-Weyl base, that is extremely convenient for our ends.

Given a Lie algebra $\mathfrak{g}$ of rank n, we can always find a set of n mutually commuting generators, that we denote by H^i. Namely, they satisfy:

$$\left[H^i, H^j\right] = 0, \qquad \forall i, j = 1, \dots, n. \tag{A.6}$$

The generators H^i are called Cartan generators, and they define the Cartan subalgebra $\mathfrak{h}$ of $\mathfrak{g}$, which is maximal. Being a set of commuting generators, they can always be simultaneously diagonalized up to an appropriate change of basis. We set ourselves in such basis, and consider the remaining generators of the algebra, denoted by E_α. They can be chosen in such a way as to be eigenvectors of the Cartan generators, namely:

$$[H^i, E_\alpha] = \alpha^i E_\alpha. \tag{A.7}$$

The vectors $\alpha = (\alpha^1, \dots, \alpha^n)$ are the *roots* of the Lie algebra $\mathfrak{g}$, and it can be proven that they are non-zero and all different. The set of all the root vectors α constitutes the *root system* Δ of $\mathfrak{g}$, and it can be seen that the dimension of the Lie algebra is connected to the number of root and Cartan generators, that is:

$$\dim(\mathfrak{g}) = \underbrace{n}_{Cartan} + \underbrace{|\Delta|}_{roots}. \tag{A.8}$$

With some work, one can show that the full commutation relations of the Lie algebra in the Cartan-Weyl basis are given by:

$$\begin{aligned}[][H^i, H^j] &= 0 \\ [H^i, E_\alpha] &= \alpha^i E_\alpha \\ [E_\alpha, E_\beta] &= N_{\alpha,\beta} \quad \text{if } \alpha+\beta \in \Delta \\ &= 2\tfrac{\alpha\cdot H}{|\alpha|^2} \quad \text{if } \alpha = -\beta \\ &= 0 \qquad \text{otherwise,}\end{aligned} \tag{A.9}$$

where $N_{\alpha,\beta}$ are some constants, and $\alpha\cdot H \equiv \alpha_i H^i$.

Making use of the Killing form (A.5) we can establish a correspondence between the Cartan subalgebra $\mathfrak{h}$ spanned by H^i and the roots α. More precisely, the roots α can be seen as operators living in the dual $\mathfrak{h}^*$ of $\mathfrak{h}$. In other words, we associate to every element $H^\alpha \in \mathfrak{h}$ an operator:

$$\alpha = \kappa(H^\alpha, \cdot). \tag{A.10}$$

In this way, we can define a scalar product $(\cdot,\cdot)$ between roots using the Killing form:

$$(\alpha,\beta) = \kappa(H^\alpha, H^\beta) = \sum_i \alpha^i \beta^i, \tag{A.11}$$

where the last step is made possible by a suitable normalization of the elements of the Cartan subalgebra. In particular, the square module of a root is defined as:

$$(\alpha,\alpha) = \kappa(H^\alpha, H^\alpha) = |\alpha|^2. \tag{A.12}$$

Consider now the root system Δ, that comprises all the roots as defined in (A.9): the total number of roots is higher than the rank of $\mathfrak{g}$, and so they are linearly dependent. We can then choose an ordered basis $(\beta_1, \ldots, \beta_n)$ and expand each generic root α accordingly:

$$\alpha = \sum_i c_i \beta_i, \tag{A.13}$$

with c_i some numerical coefficients. This allows us to split the root system Δ into two sets of same cardinality: the positive roots (i.e. roots whose first non-vanishing c_i is positive) Δ_+ and the negative roots Δ_-. These two sets are related by:

$$\Delta_+ = -\Delta_-. \tag{A.14}$$

We further define a *simple root* as a root that cannot be written as the sum of any other set of roots. There are exactly n positive simple roots, and they form the preferred basis $(\alpha_1, \ldots, \alpha_n)$ in which to perform the expansion (A.13). It can be proven that all the roots in Δ can be generated as sums of the simple roots, and there exists an easy algorithm to perform the computation in any Lie algebra (for details, we refer to [187]). Finally, the choice of simple roots provides us with the last ingredient needed to tackle the characterization of the algebras in the ADE classification.

Indeed, each Lie algebra is uniquely defined by its Cartan matrix A_{ij}, defined as:

$$A_{ij} = \frac{2(\alpha_i, \alpha_j)}{|\alpha_j|^2} \quad \in \{0, -1, \pm 2, -3\}. \tag{A.15}$$

More specifically, the ADE Lie algebras are simply laced, meaning that the Cartan matrix is symmetric and that its only possible entries are 2 on the diagonal, as well as 0 or -1 outside:

$$A_{ij}^{\text{ADE}} = \frac{2(\alpha_i, \alpha_j)}{|\alpha_j|^2} \quad \in \{0, -1, 2\}. \tag{A.16}$$

The Cartan matrix, in turn, can be neatly represented graphically introducing the Dynkin diagram, in which each node corresponds to a simple root and each line connecting two nodes corresponds to a non-vanishing entry (i.e. a -1 entry in our cases) in the Cartan matrix. We conclude this section by listing the Dynkin diagrams for the ADE classification, that will be extensively used in the main text:

$\boldsymbol{A_n}$ 

$\boldsymbol{D_n}$ 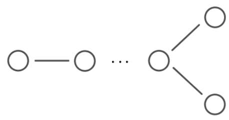

$\boldsymbol{E_6}$ 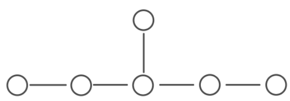

$\boldsymbol{E_7}$ 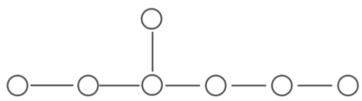

$\boldsymbol{E_8}$ 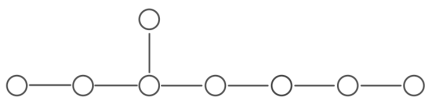

In the next section we report another useful tool, namely the standard matrix representation basis for the Lie algebras in the A_n and D_n series, along with recipes to explicitly build the Cartan and root generators.

A.2 Explicit Cartan and root generators for A and D algebras

In this section we give explicit rules to construct the matrices of the fundamental representation of A_n and D_n, and to express the elements of the Cartan subalgebra $\mathfrak{h}$ and all the root generators E_α for $\alpha \in \Delta$ in our preferred basis, following Collingwood and MacGovern [112]. This will make up the backbone of all the computations carried out in the main chapters.

A_n series

The preferred basis for the fundamental representation of $A_n = \mathfrak{sl}(n+1)$ is the standard $(n+1)$-dimensional representation given by traceless matrices. The Cartan elements in $\mathfrak{h}$ are chosen to lie on the diagonal. In order to express the root generators, define linear functionals $e_i \in \mathfrak{h}^*$ as:

$$e_i(H) = i^{\text{th}} \text{ diagonal entry of } H. \tag{A.17}$$

The root system of A_n is therefore defined as:

$$\Delta = \{e_i - e_j \mid 1 \leq i, j \leq n+1, i \neq j\}. \tag{A.18}$$

The positive roots are spanned by $\Delta = \{e_i - e_j \quad | \quad i < j\}$, and the simple roots are the positive roots where i and j are consecutive numbers. We denote the simple positive roots as:

$$\alpha_i = \{e_i - e_j \mid i, j \text{ consecutive}\}. \tag{A.19}$$

As a result, the root generators $E_{e_i - e_j}$ associated to the roots $e_i - e_j \in \Delta$ can be defined as:

$$E_{e_i - e_j} = X_{i,j}, \tag{A.20}$$

where $X_{i,j}$ is a matrix of $\mathfrak{sl}(n+1)$ having 1 as its (i,j) entry and 0 elsewhere.

To conclude this section, let us give an explicit example, taking into account the $A_5 = \mathfrak{sl}(6)$ algebra. A_5 has rank 5, and consequently possesses 5 simple roots. They can be written as:

$$\Delta_{\text{simple roots}} = \{e_1 - e_2, e_2 - e_3, e_3 - e_4, e_4 - e_5, e_5 - e_6\}. \tag{A.21}$$

Each simple root intersects, via the Killing form (A.11), only with its neighboring simple roots, and hence the Lie algebra A_5 can be represented by a linear Dynkin diagram with 5 nodes, each corresponding to a simple root. The matrix representation of the simple roots goes as (where we have highlighted the non-vanishing entries referred to the generator of the simple roots α_i):

$$\begin{pmatrix} 0 & \alpha_1 & 0 & 0 & 0 & 0 \\ -\alpha_1 & 0 & \alpha_2 & 0 & 0 & 0 \\ 0 & -\alpha_2 & 0 & \alpha_3 & 0 & 0 \\ 0 & 0 & -\alpha_3 & 0 & \alpha_4 & 0 \\ 0 & 0 & 0 & -\alpha_4 & 0 & \alpha_5 \\ 0 & 0 & 0 & 0 & -\alpha_5 & 0 \end{pmatrix} \tag{A.22}$$

The other roots in the root system Δ can be written down either by using the representations of the simple roots as linear functionals (A.19), or commuting their explicit matrix representations (A.22).

D_n series

For the D_n series, let us start by giving our preferred basis for the fundamental representation of $\mathfrak{so}(2n)$. A generic $2n$-dimensional matrix in the fundamental of $\mathfrak{so}(2n)$ is expressed in this basis as:

$$\left\{ M = \begin{pmatrix} Z_1 & Z_2 \\ Z_3 & -Z_1^t \end{pmatrix} \mid Z_2, Z_3 \text{ antisymmetric} \right\}, \tag{A.23}$$

where Z_1, Z_2, Z_3 are complex-valued matrices. It is easy to show that matrices of the kind (A.23) satisfy the Lie algebra of $\mathfrak{so}(2n)$:

$$M\mathcal{Q}+\mathcal{Q}M^t = 0. \tag{A.24}$$

with $\mathcal{Q}$ the quadratic form:

$$\mathcal{Q} = \begin{pmatrix} 0 & \mathbb{1} \\ \mathbb{1} & 0 \end{pmatrix}. \tag{A.25}$$

which has superseded the identity in the definition of the Lie algebra in the new basis (A.23).

The Cartan subalgebra is given by the diagonal matrices, that by construction are of the form:

$$H = \begin{pmatrix} D & 0 \\ 0 & -D \end{pmatrix}, \tag{A.26}$$

with:

$$D = \begin{pmatrix} h_1 & 0 & 0 & \dots & 0 \\ 0 & h_2 & 0 & \dots & 0 \\ \vdots & \vdots & \vdots & \ddots & \vdots \\ 0 & 0 & 0 & \dots & h_n \end{pmatrix}. \tag{A.27}$$

Now define functionals $e_i \in \mathfrak{h}^*$ similarly to the A_n case (notice that the index goes until n, not $2n$):

$$e_i(H) = h_i. \tag{A.28}$$

The root system Δ of D_n is then spanned by:

$$\Delta = \{\pm e_i \pm e_j \mid 1 \leq i, j \leq n, i \neq j\}. \tag{A.29}$$

The set of positive roots is therefore:

$$\Delta_+ = \{e_i \pm e_j \mid 1 \leq i < j \leq n\}, \tag{A.30}$$

and the n simple positive roots are:

$$\Delta_{\text{simple roots}} = \{e_1 - e_2, \dots, e_{n-1} - e_n, e_{n-1} + e_n\}. \tag{A.31}$$

The simple roots intersect in the shape of the Dynkin diagram of D_n, the "upper" node being given by the simple root $\alpha_n = e_{n-1}+e_n$.

Explicit matrix representations of the root generators can be produced using the following dictionary:

$$\begin{aligned} E_{e_i-e_j} &= X_{i,j}-X_{n+j,n+i}, \\ E_{e_i+e_j} &= X_{i,n+j}-X_{j,n+i}, \\ E_{-e_i-e_j} &= X_{n+i,j}-X_{n+j,i}. \end{aligned} \tag{A.32}$$

where $X_{i,j}$ has 1 as its (i,j) entry and 0 elsewhere.

Finally, let us give a concrete example of such representation basis. Take into account the rank 4 algebra D_4, that possesses four simple roots:

$$\Delta_{\text{simple roots}} = \{e_1-e_2, e_2-e_3, e_3-e_4, e_3+e_4\}. \tag{A.33}$$

The matrix representation associated to the simple roots turns out to be:

$$\left(\begin{array}{cccc|cccc} 0 & \alpha_1 & 0 & 0 & 0 & 0 & 0 & 0 \\ 0 & 0 & \alpha_2 & 0 & 0 & 0 & 0 & 0 \\ 0 & 0 & 0 & \alpha_3 & 0 & 0 & 0 & \alpha_4 \\ 0 & 0 & 0 & 0 & 0 & 0 & -\alpha_4 & 0 \\ \hline 0 & 0 & 0 & 0 & 0 & 0 & 0 & 0 \\ 0 & 0 & 0 & 0 & -\alpha_1 & 0 & 0 & 0 \\ 0 & 0 & 0 & 0 & 0 & -\alpha_2 & 0 & 0 \\ 0 & 0 & 0 & 0 & 0 & 0 & -\alpha_3 & 0 \end{array}\right) \tag{A.34}$$

A.3 Borel and Levi subalgebras

In this section we define three classes of subalgebras of an ADE Lie algebra $\mathfrak{g}$: the Borel, parabolic and Levi subalgebras, that are extremely relevant in the context of Springer resolutions, dealt with in Chapter 2. As we only need an operative understanding of such concepts, mathematical details will be avoided.

Let us start by defining Borel subalgebras of a Lie algebra $\mathfrak{g}$:

Def A.1. *A Borel subalgebra $\mathfrak{b}$ of $\mathfrak{g}$ can always be decomposed (modulo conjugation) as a direct sum $\mathfrak{h}\oplus\mathfrak{n}$, where $\mathfrak{h}$ is a Cartan subalgebra of $\mathfrak{g}$ and $\mathfrak{n} = [\mathfrak{b}, \mathfrak{b}]$ is a subalgebra composed of nilpotent elements. Furthermore, the nilpotent subalgebra $\mathfrak{n}$ can always be decomposed as a sum of positive root generators of $\mathfrak{g}$, namely:*

$$\mathfrak{n} = \sum_{\alpha\in\Delta_+} E_\alpha. \tag{A.35}$$

An example helps in clarifying the meaning of the above definition: consider the A_n algebras and their standard matrix representation, given in the previous section. Borel subalgebras of A_n are nothing but subalgebras formed by upper triangular matrices (up to conjugation by G_{ad}). For instance, in the $A_3 = \mathfrak{sl}(4)$ case, Borel subalgebras are all conjugate to:

$$\mathfrak{b} = \begin{pmatrix} * & * & * & * \\ 0 & * & * & * \\ 0 & 0 & * & * \\ 0 & 0 & 0 & * \end{pmatrix}, \tag{A.36}$$

where a $*$ entry can take any value in $\mathbb{C}$.

Notice that each Borel subalgebra $\mathfrak{b}$ highlights a choice of simple roots $\Delta_{\text{simple roots}}$ (for instance, in the A_3 case, the simple roots $\alpha_1, \alpha_2, \alpha_3$ in the canonical matrix representation). Now, picking a subset $\Theta \subseteq \Delta_{\text{simple roots}}$ we can define *parabolic subalgebras*:

Def A.2. *Given a Borel subalgebra $\mathfrak{b} = \mathfrak{h} \oplus \mathfrak{n}$, a parabolic subalgebra $\mathfrak{p}$ containing $\mathfrak{b}$ can always be generated, up to conjugation, by a direct sum of:*

- $\mathfrak{h}$
- *the root generators contained in $\mathfrak{b}$*
- *the simple roots generators $E_{-\alpha}$, if $\alpha \in \Theta$.*

The definition of parabolic subalgebra naturally takes us to the last relevant class of subalgebras we will need, the so-called *Levi subalgebras*:

Def A.3. *Given a parabolic subalgebra $\mathfrak{p}$ associated to a subset Θ of simple roots, and to the subroot system $\langle\Theta\rangle$ generated by Θ, the maximal Levi subalgebra $\mathcal{L}$ contained in $\mathfrak{p}$ is given by:*

$$\mathcal{L} = \mathfrak{h} \oplus \sum_{\alpha \in \langle\Theta\rangle} E_\alpha. \tag{A.37}$$

Again, let us give a clarifying example, in the algebra $A_3 = \mathfrak{sl}(4)$.
Pick $\Theta = \{\alpha_1, \alpha_3\}$. Then the subroot system generated by Θ is:

$$\langle\Theta\rangle = \{\alpha_1, -\alpha_1, \alpha_3, -\alpha_3\}. \tag{A.38}$$

The parabolic subalgebra relative to Θ is obtained summing to the Borel subalgebra (A.36) the generators of all the roots $-\alpha$ such that $\alpha \in \Theta$, namely $-\alpha_1$ and $-\alpha_3$:

$$\mathfrak{p}_\Theta = \begin{pmatrix} * & * & * & * \\ * & * & * & * \\ 0 & 0 & * & * \\ 0 & 0 & * & * \end{pmatrix}. \tag{A.39}$$

The Levi subalgebra relative to Θ is instead given by the sum of the Cartan subalgebra in

$\mathfrak{b}$ with the subroot system $\langle\Theta\rangle$, yielding:

$$\mathcal{L}_\Theta = \begin{pmatrix} * & * & 0 & 0 \\ * & * & 0 & 0 \\ 0 & 0 & * & * \\ 0 & 0 & * & * \end{pmatrix}. \tag{A.40}$$

For further intuition, a remarkably eloquent classification of parabolic and Levi subalgebras in the A_3 case is contained in a table of [112].

A.4 Casimir invariants for ADE Lie algebras

It is a well-known fact [188] that an ADE Lie algebra $\mathfrak{g}$ of rank n possesses n Casimir invariant operators, i.e. operators made up of Lie algebra generators that commute with the whole algebra. One of the easiest and most influential examples is the spin operator, i.e. the Casimir invariant operator of the $\mathfrak{su}(2)$ algebra.

In general, one can define n independent Casimir operators for all the ADE Lie algebras. In turn, it can be shown that this implies that there exist n independent tensors, invariant under the whole Weyl group $\mathcal{W}$ of $\mathfrak{g}$. More precisely, given the Lie algebra generators T^a, we can define n tensors $C^{(m)}_{i_1,\dots,i_m}$ of degree m of the form:

$$\begin{aligned} C^{(m)}: \quad \underbrace{\mathfrak{g}\times\cdots\times\mathfrak{g}}_{m \text{ times}} \quad &\to \quad \mathbb{C} \\ (T^{i_1},\dots,T^{i_m}) \quad &\to \quad C^{(m)}_{i_1,\dots,i_m} = \mathrm{sTr}(T^{i_1}\dots T^{i_m}), \end{aligned} \tag{A.41}$$

where:

$$\mathrm{sTr}(T^{i_1}\dots T^{i_m}) = \frac{1}{m!}\sum_{\sigma\in S_m}\mathrm{Tr}(T^{i_{\sigma_1}}\dots T^{i_{\sigma_m}}), \tag{A.42}$$

with σ the elements of the permutation group of m elements S_m.

In the following, we will treat the tensors $C^{(m)}$ and the $C^{(m)}_{i_1,\dots,i_m}\in\mathbb{C}$ as the same object, and will often call them (with some abuse of notation) “Casimir invariants”.

We proceed now in giving the explicit expressions of the Casimirs $C^{(m)}$ for all the ADE Lie algebras. Having in mind the applications of the main text, where we want to compute the “Casimir invariants” of the Higgs background Φ, we give the expressions for $C^{(m)}(\underbrace{\Phi,\dots\Phi}_{m \text{ times}})$, keeping the notation of the main text.

For the A_n algebras we have:

$$\begin{array}{c} \boldsymbol{A_n} \\ \hline k_i = \mathrm{Tr}(\Phi^{i+1}),\ \ i=1,\dots,n \end{array} \tag{A.43}$$

For the D_n algebras we have:

$$\begin{array}{c} \boldsymbol{D_n} \\ \hline \tilde{k}_i = \mathrm{Tr}(\Phi^{2i}), \;\; i = 1, \ldots, n-1 \\ \tilde{k}_n = \mathrm{Pfaff}(\Phi) \end{array} \tag{A.44}$$

For the E_6, E_7, E_8 algebras we have:

$$\begin{array}{c|l} \boldsymbol{E_6} & c_i = \mathrm{Tr}(\Phi^i) \;\; \text{for } i = 2, 5, 6, 8, 9, 12 \\ \boldsymbol{E_7} & \tilde{c}_i = \mathrm{Tr}(\Phi^i) \;\; \text{for } i = 2, 6, 8, 10, 12, 14, 18 \\ \boldsymbol{E_8} & \hat{c}_i = \mathrm{Tr}(\Phi^i) \;\; \text{for } i = 2, 8, 12, 14, 18, 20, 24, 30 \end{array} \; . \tag{A.45}$$

APPENDIX B

Explicit deformation coordinates for exceptional Lie algebras

In this section we show how to compute the explicit form of the equations (3.79), after having briefly recapped how they are obtained.

Our aim is to exhibit a simple way to relate the Casimirs of the Higgs background Φ with the coefficients of the versal deformations of the E_6, E_7, E_8 singularities, thus allowing to write down explicitly the equation that corresponds to a given Φ. In principle, this entails that we can reproduce both the deformed E families over the partial Casimirs $\varrho_i \in \mathcal{T}/\mathcal{W}'$, for some partial simultaneous resolution $\mathcal{W}'$, and the explicit threefold equations, once a dependence $\varrho_i(w)$ has been chosen.

To ground our reasoning, we work with a Higgs field Φ in the representations (3.77). This is not compulsory, but the coefficients that we will show in the following lines are subject to change according to the representation in which Φ resides. Take Φ to live in the Cartan subalgebra of one among E_6, E_7, E_8[1], i.e.

$$\Phi_{\text{cartan}} = \sum_{i=1}^{n} a_i \tilde{H}^i, \tag{B.1}$$

where $\tilde{H}^i$ are the Cartan elements in some basis and the a_i are generic coefficients. Imposing that the action of Φ_{cartan} on the simple roots generators E_{α_i} respects the volumes (1.26) of the 2-cycles associated to the simple roots, namely:

$$[\Phi_{\text{cartan}}, E_{\alpha_i}] = \text{vol}_{\alpha_i} \cdot E_{\alpha_i}, \tag{B.2}$$

and recalling that the volumes are functions of the parameters t_i, we can solve for the coefficients $a_i = a_i(t_i)$ and find the "canonical" basis of the Cartan subalgebra, that is the

[1]This can always be achieved by diagonalizing (eventually with non-holomorphic eigenvalues) the Higgs field.

one in which the coefficients are precisely the parameters t_i. In this way we can rewrite:

$$\Phi_{\text{cartan}} = \sum_{i=1}^{n} t_i H^i, \tag{B.3}$$

with H^i the "canonical" Cartan subalgebra generators. We can further compute the Casimirs of Φ_{cartan}, as defined in (3.78), that we rewrite here for convenience:

$$\begin{array}{c|l} \boldsymbol{E_6} & c_i = \text{Tr}(\Phi^i_{\text{cartan}}) \;\; \text{for } i = 2,5,6,8,9,12 \\ \boldsymbol{E_7} & \tilde{c}_i = \text{Tr}(\Phi^i_{\text{cartan}}) \;\; \text{for } i = 2,6,8,10,12,14,18 \\ \boldsymbol{E_8} & \hat{c}_i = \text{Tr}(\Phi^i_{\text{cartan}}) \;\; \text{for } i = 2,8,12,14,18,20,24,30 \end{array} . \tag{B.4}$$

We stress that now the Casimirs of Φ_{cartan} are functions of the parameters t_i.

Now consider the deformed E singularities in equation (1.24). In each one, we have n deformation parameters:

$$\begin{array}{c|l} \boldsymbol{E_6} & \epsilon_i \;\; \text{for } i = 2,5,6,8,9,12 \\ \boldsymbol{E_7} & \tilde{\epsilon}_i \;\; \text{for } i = 2,6,8,10,12,14,18 \\ \boldsymbol{E_8} & \hat{\epsilon}_i \;\; \text{for } i = 2,8,12,14,18,20,24,30 \end{array} , \tag{B.5}$$

which are functions of the parameters t_i. Following the recipe of the A and D series, we know that it should be possible to write the parameters (B.5) as functions of the Casimirs (B.4) of Φ_{cartan}. For example, given $\Phi_{\text{cartan}} \in E_6$ we should have:

$$\begin{aligned} \epsilon_2 &= \beta_1 c_2 \\ \epsilon_5 &= \beta_2 c_5 \\ \epsilon_6 &= \beta_3 c_6 + \beta_4 c_2^3 \\ &\vdots \\ \epsilon_{12} &= \dots \end{aligned} \tag{B.6}$$

with β_i some numerical coefficients to be determined imposing the equality of (B.6) with the explicit expressions of $\epsilon_i, \tilde{\epsilon}_i, \hat{\epsilon}_i$ as functions of the t_i, which can be found in [111]. Performing this kind of computation for all the E_6, E_7, E_8 cases we find the relationships (B.7), (B.8) and (B.9) between the Casimirs of Φ_{cartan} and the deformation parameters $\epsilon_i, \tilde{\epsilon}_i, \hat{\epsilon}_i$.

It is crucial to highlight that the equations (B.7), (B.8) and (B.9) are valid for any Higgs field configuration Φ, and that the use of Φ_{cartan} is a mere computational tool useful to obtain the final expression. This is the case because the traces of Φ are invariant under diagonalization, and of course it can be explicitly checked in the threefolds we have analyzed in the main text. Moreover, using (B.7), (B.8) and (B.9) for Higgs configurations corresponding to simple flops examined in Chapter 4, one immediately obtains the expressions of the deformation parameters (B.5) in terms of the partial Casimirs of the Higgs. In this way, one can construct a generic deformed E_6, E_7, E_8 family admitting a simple flop.

Summing up, once one has built an explicit Higgs configuration $\Phi(w)$, *corresponding to an arbitrary simultaneous resolution, the explicit expression of the resulting threefold can be obtained computing its Casimirs and plugging them into* (B.7), (B.8) *and* (B.9).

The end result for the E_6 case is:

$$\begin{aligned}
\epsilon_2 &= -\frac{c_2}{24} \\
\epsilon_5 &= \frac{c_5}{60} \\
\epsilon_6 &= \frac{c_2^3}{13824} - \frac{c_6}{144} \\
\epsilon_8 &= -\frac{c_2^4}{110592} + \frac{13c_2c_6}{8640} - \frac{c_8}{240} \\
\epsilon_9 &= \frac{c_9}{756} - \frac{c_2^2c_5}{11520} \\
\epsilon_{12} &= -\frac{c_{12}}{3240} + \frac{109c_2^6}{4299816960} - \frac{847c_2^3c_6}{134369280} + \frac{109c_2^2c_8}{3732480} + \frac{13c_2c_5^2}{466560} + \frac{61c_6^2}{933120}.
\end{aligned} \tag{B.7}$$

For the E_7 case:

$$\epsilon_2 = \frac{\tilde{c}_2}{18}$$

$$\epsilon_6 = \frac{\tilde{c}_2^3}{139968} - \frac{\tilde{c}_6}{72}$$

$$\epsilon_8 = -\frac{7\tilde{c}_2^4}{25194240} + \frac{11\tilde{c}_2\tilde{c}_6}{16200} - \frac{\tilde{c}_8}{300}$$

$$\epsilon_{10} = -\frac{2\tilde{c}_{10}}{315} + \frac{\tilde{c}_2^5}{151165440} - \frac{17\tilde{c}_2^2\tilde{c}_6}{583200} + \frac{\tilde{c}_2\tilde{c}_8}{1400}$$

$$\epsilon_{12} = -\frac{16\tilde{c}_{10}\tilde{c}_2}{1148175} + \frac{\tilde{c}_{12}}{12150} - \frac{149\tilde{c}_2^6}{10579162152960} + \frac{167\tilde{c}_2^3\tilde{c}_6}{3401222400} + \frac{737\tilde{c}_2^2\tilde{c}_8}{881798400} - \frac{31\tilde{c}_6^2}{437400}$$

$$\epsilon_{14} = \frac{8303\tilde{c}_{10}\tilde{c}_2^2}{14935460400} - \frac{2201\tilde{c}_{12}\tilde{c}_2}{217314900} + \frac{4\tilde{c}_{14}}{62601} + \frac{11083\tilde{c}_2^7}{24082404724998144} - \frac{11609\tilde{c}_2^4\tilde{c}_6}{5530387622400}$$
$$- \frac{1289\tilde{c}_2^3\tilde{c}_8}{1433804198400} + \frac{353\tilde{c}_2\tilde{c}_6^2}{142242480} - \frac{31\tilde{c}_6\tilde{c}_8}{1463400}$$

$$\epsilon_{18} = \frac{121826345 87\tilde{c}_{10}\tilde{c}_2^4}{7780651466388 4339200} - \frac{564449\tilde{c}_{10}\tilde{c}_2\tilde{c}_6}{3418744644000} + \frac{1844\tilde{c}_{10}\tilde{c}_8}{3956880375} - \frac{27233975\tilde{c}_{12}\tilde{c}_2^3}{11321053720935552}$$
$$+ \frac{301\tilde{c}_{12}\tilde{c}_6}{452214900} + \frac{307855\tilde{c}_{14}\tilde{c}_2^2}{13588370378352} - \frac{2\tilde{c}_{18}}{1507383} - \frac{886993691\tilde{c}_2^9}{31364416064086741984 7393280}$$
$$+ \frac{4713945967\tilde{c}_2^6\tilde{c}_6}{7202660214599578828 8000} - \frac{14715122551\tilde{c}_2^5\tilde{c}_8}{2334195439916530176000} - \frac{579011753\tilde{c}_2^3\tilde{c}_6^2}{23156700792822720000}$$
$$+ \frac{2313866297\tilde{c}_2^2\tilde{c}_6\tilde{c}_8}{222355151645760000} - \frac{77393\tilde{c}_2\tilde{c}_8^2}{3376537920000} - \frac{15011\tilde{c}_6^3}{97678418400}. \tag{B.8}$$

For the E_8 case:

$$
\begin{aligned}
\epsilon_2 &= \frac{\hat{c}_2}{120} \\
\epsilon_8 &= \frac{13\hat{c}_2^4}{24883200000} - \frac{\hat{c}_8}{5760} \\
\epsilon_{12} &= \frac{\hat{c}_{12}}{181440} + \frac{101\hat{c}_2^6}{3224862720000000} - \frac{\hat{c}_2^2\hat{c}_8}{64512000} \\
\epsilon_{14} &= -\frac{71\hat{c}_{12}\hat{c}_2}{798336000} + \frac{\hat{c}_{14}}{1108800} - \frac{2531\hat{c}_2^7}{9029615616000000000} + \frac{103\hat{c}_2^3\hat{c}_8}{696729600000} \\
\epsilon_{18} &= -\frac{4451\hat{c}_{12}\hat{c}_2^3}{689762304000000} + \frac{1523\hat{c}_{14}\hat{c}_2^2}{12454041600000} - \frac{\hat{c}_{18}}{47174400} - \frac{26399\hat{c}_2^9}{2080423437926400000000000} \\
&\quad + \frac{4747\hat{c}_2^5\hat{c}_8}{722369249280000000} + \frac{331\hat{c}_2\hat{c}_8^2}{1672151040000} \\
\epsilon_{20} &= \frac{191071\hat{c}_{12}\hat{c}_2^4}{2121019084800000000} + \frac{127\hat{c}_{12}\hat{c}_8}{174569472000} - \frac{1165063\hat{c}_{14}\hat{c}_2^3}{612738846720000000} + \frac{236627\hat{c}_{18}\hat{c}_2}{434023349760000} \\
&\quad + \frac{10249681\hat{c}_2^{10}}{614140998875873280000000000000} - \frac{2994007\hat{c}_2^6\hat{c}_8}{3554056706457600000000} - \frac{323371\hat{c}_2^2\hat{c}_8^2}{82269831168000000} - \frac{\hat{c}_{20}}{220809600} \\
\epsilon_{24} &= -\frac{193\hat{c}_{12}^2}{17793312768000} + \frac{228270563\hat{c}_{12}\hat{c}_2^6}{29320967828275200000000000} + \frac{234189517\hat{c}_{12}\hat{c}_2^2\hat{c}_8}{945465467240448000000} \\
&\quad - \frac{9171869023\hat{c}_{14}\hat{c}_2^5}{5267593317482496000000000} - \frac{23281\hat{c}_{14}\hat{c}_2\hat{c}_8}{9150846566400000} + \frac{561557071\hat{c}_{18}\hat{c}_2^3}{829158207381504000000} \\
&\quad + \frac{8268193432181\hat{c}_2^{12}}{580761207304971815485440000000000000000} - \frac{20976434911\hat{c}_2^8\hat{c}_8}{305535146940746956800000000000} \\
&\quad - \frac{16935675593\hat{c}_2^4\hat{c}_8^2}{3300533994730291200000000} - \frac{666323\hat{c}_2^2\hat{c}_{20}}{721337268326400000} + \frac{\hat{c}_{24}}{10061694720} - \frac{593\hat{c}_8^3}{887354818560000} \\
\epsilon_{30} &= -\frac{636328729\hat{c}_{12}^2\hat{c}_2^3}{3676467835511164108800000000} - \frac{189107437\hat{c}_{12}\hat{c}_{14}\hat{c}_2^2}{2779760018939904000000000} + \frac{2521\hat{c}_{12}\hat{c}_{18}}{319072545792000000} \\
&\quad + \frac{122785779721089347\hat{c}_{12}\hat{c}_2^9}{5354576379380206927872000000000000000000} + \frac{374760114643099\hat{c}_{12}\hat{c}_2^5\hat{c}_8}{685159914799807856640000000000000} \\
&\quad - \frac{199931513\hat{c}_{12}\hat{c}_2\hat{c}_8^2}{944585637101568000000000} + \frac{28501673\hat{c}_{14}^2\hat{c}_2}{386077780408320000000000} - \frac{16345135784075712229\hat{c}_{14}\hat{c}_2^8}{3206548401263100769075200000000000000000} \\
&\quad - \frac{3442332938170993\hat{c}_{14}\hat{c}_2^4\hat{c}_8}{5938052594931668090880000000000000} + \frac{1223\hat{c}_{14}\hat{c}_8^2}{112201334784000000} + \frac{15587535288859801\hat{c}_{18}\hat{c}_2^6}{763463905062643040256000000000000000} \\
&\quad - \frac{1051350791\hat{c}_{18}\hat{c}_2^2\hat{c}_8}{12433108448349388800000000} + \frac{38736013334814563129113\hat{c}_2^{15}}{91917141325413107393723923169280000000000000000000000} \\
&\quad - \frac{966205043352894287\hat{c}_2^{11}\hat{c}_8}{464971941598543059773030400000000000000000000} - \frac{53516928494297557\hat{c}_2^7\hat{c}_8^2}{4200288541992258895872000000000000000} \\
&\quad - \frac{2159242595767\hat{c}_2^5\hat{c}_{20}}{737984035215212544000000000000} + \frac{21328481\hat{c}_2^3\hat{c}_{24}}{583320714375168000000000} + \frac{225239997090599\hat{c}_2^3\hat{c}_8^3}{1195915487650573713408000000000000} \\
&\quad + \frac{72667\hat{c}_2\hat{c}_{20}\hat{c}_8}{4518107320320000000} - \frac{\hat{c}_{30}}{1978376400000}.
\end{aligned}
\tag{B.9}
$$

APPENDIX C

Higgs branches from M-theory on (A_{M-1}, A_{N-1}) singularities

In this Appendix we aim at obtaining the Higgs branch of M-theory on a generic (A_{M-1}, A_{N-1}) singularity, given by the following threefold, explicitly expressed as a $\mathbb{C}^*$-fibration:

$$uv = z^M + w^N. \tag{C.1}$$

In order to achieve this task, we decompose the brane locus, which is the r.h.s of (C.1), into irreducible factors (namely, polynomials in (w, z) that do not admit further factorization). Each factor corresponds, geometrically, to an irreducible component of the brane locus (seen as a one-dimensional subvariety of $\mathbb{C}_w \times \mathbb{C}_z$).

We write (A_{M-1}, A_{N-1}) as (A_{mp-1}, A_{mq-1}), with p, q coprimes, $p \geq q$, and $m = \gcd(M, N)$. It then becomes manifest that we can always factor the brane locus as follows:

$$\Delta = z^{mp} + w^{mq} = \prod_{s=1}^{m} (z^p + e^{2\pi i s/m} w^q). \tag{C.2}$$

The factor $(z^p + e^{2\pi i s/m} w^q)$ in (C.2) can be realised, for all the (p, q), as the characteristic polynomial of a $p \times p$ matrix $\mathcal{A}_s$, with matrix entries being polynomials in w *of degree at most one.*

The blocks "$\mathcal{A}_s$" (they are, indeed, characterized by the four integers p, q, s, m, appearing in each factor of (C.2) but we omit p, q, m for ease of notation) whose characteristic polynomials are the irreducible factors appearing in (C.2) can be put in the following canonical shape[1]:

[1]Notice that the canonical form (C.3) is precisely in the shape of a companion matrix, as usually understood in the mathematical literature.

$$\mathcal{A}_s(w) = \begin{pmatrix} 0 & * & 0 & \cdots & 0 \\ 0 & 0 & * & 0 & 0 \\ \vdots & 0 & \ddots & \ddots & 0 \\ 0 & 0 & 0 & 0 & * \\ -e^{2\pi i s/m} w & 0 & 0 & 0 & 0 \end{pmatrix}, \tag{C.3}$$

where the $*$ entries are filled either with w, or are constants (that can be set to 1); to reproduce the right characteristic polynomial, we have to fill $q-1$ $*$-entries with "w".

Depending on the position where we place the "w", one has a different number of zero-modes. D-brane states realizing the same brane locus (or, analogously, dual to the same M-theory geometry) but with a different number of zero-modes are known in this context as *T-brane states*.

There exists a fast criterium to understand (without performing any computation[2]) if the chosen $\mathcal{A}_s$ describes a T-brane background. The argument holds more generally for any Higgs field Φ. Indeed, we can think of $\mathcal{A}_s$ itself as the Higgs field associated to the singularity $uv = \chi(\mathcal{A}_s)$, with $\mathcal{A}_s \in A_{p-1}$ and χ the characteristic polynomial. Keeping the characteristic polynomial fixed, we associate to Φ the nilpotent orbit $\mathcal{O}_0$ obtained acting with the seven-dimensional gauge group on $\Phi|_{w=0}$. We find that the number n_{ind} of linearly independent elements of the seven-dimensional gauge algebra $\mathfrak{g}$ supporting a five-dimensional zero-mode always equals the complex codimension of $\mathcal{O}_0$ in the nilpotent cone of $\mathfrak{g}$:

$$n_{\text{ind}} = \text{cod}_{\mathbb{C}}\Big(\mathcal{O}_0 \hookrightarrow \mathcal{N}\Big). \tag{C.4}$$

(C.4) holds also for the Higgs fields associated to the threefolds analyzed in Chapter 5, namely all quasi-homogeneous cDV singularities. Notice that if there are 5d localized modes supported on $\mathbb{C}[w]/(w^k)$ with $k > 1$, then n_{ind} *does not* coincide with the total number of 5d modes localized in the Higgs background.

Furthermore, we find that in all the (A_j, A_l) cases the Higgs maximizing n_{ind} also maximizes the total number of five-dimensional modes. Consequently, the Higgs field Φ displaying the maximum number of five-dimensional modes is the block-diagonal sum of blocks $\mathcal{A}_s$ corresponding to the $\mathcal{O}_0$ that sits at the lowest position in the A_{p-1} nilpotent orbits Hasse diagram, while the other Higgs fields have obstructed five-dimensional modes[3]. Let us consider the example of the (A_1, A_4) quasi-homogeneous cDV singularity. The threefold is:

$$uv = z^5 + w^2, \quad (u, v, w, z) \in \mathbb{C}^4. \tag{C.5}$$

[2] Of course, one can always run the gauge fixing analysis to check this a posteriori. The codimension formula for A_j-fibered threefolds simply shortens this process. Unfortunately, the same argument cannot be applied in the D_k case.

[3] A more precise geometric proof of this is given in [98].

We have two possible Higgs backgrounds[4] reproducing the same geometry:

$$\Phi^{(I)} = \begin{pmatrix} 0 & 1 & 0 & 0 & 0 \\ 0 & 0 & w & 0 & 0 \\ 0 & 0 & 0 & 1 & 0 \\ 0 & 0 & 0 & 0 & 1 \\ -w & 0 & 0 & 0 & 0 \end{pmatrix}, \quad \Phi^{(II)} = \begin{pmatrix} 0 & w & 0 & 0 & 0 \\ 0 & 0 & 1 & 0 & 0 \\ 0 & 0 & 0 & 1 & 0 \\ 0 & 0 & 0 & 0 & 1 \\ -w & 0 & 0 & 0 & 0 \end{pmatrix}. \tag{C.6}$$

If we want to have no obstructed five-dimensional modes we have to pick the first Higgs, $\Phi^{(I)}$. Indeed, the orbit corresponding to $\Phi^{(I)}$ is, in the notation of [112], the one with partition $[3, 2]$, that is below the orbit $[4, 1]$ (associated to $\Phi^{(II)}$) in the A_4 nilpotent orbits Hasse diagram. It also turns out that $[3, 2]$ is the tiniest orbit that contains a matrix (that is, $\mathcal{A}_s|_{w=0}$) realizing (z^5+w^2) as its characteristic polynomial.

Summing up, *if we want to maximize five-dimensional modes*, for a given factor $z^p + e^{2\pi i s/m} w^q$ in (C.2) we pick the block $\mathcal{A}_s$ such that $\mathrm{cod}_{\mathbb{C}} \mathcal{O}_0 \hookrightarrow \mathcal{N}_{A_{p-1}}$ is maximized (with $\mathcal{N}_{A_{p-1}}$ the nilpotent cone of A_{p-1})[5]. To obtain the m factors of the brane locus corresponding to the full Higgs field, we take the block direct sum of all the $\mathcal{A}_s$ blocks[6]:

$$\Phi_{(A_{mp-1}, A_{mq-1})} \equiv \underbrace{\left(\begin{array}{c|c|c|c} \mathcal{A}_{s=1} & \mathbb{0}_p & \mathbb{0}_p & \mathbb{0}_p \\ \hline \mathbb{0}_p & \mathcal{A}_{s=2} & \vdots & \\ \hline & \vdots & \ddots & \mathbb{0}_p \\ \hline & \vdots & \vdots & \mathcal{A}_{s=m} \end{array}\right)}_{m \text{ blocks}}. \tag{C.7}$$

The previous procedure applies similarly for all the (A_{mp-1}, A_{mq-1}) singularities, and we can describe it in general terms as follows:

1. the five-dimensional modes localize with the following pattern:

$$\varphi \equiv \underbrace{\left(\begin{array}{c|cc|c} (p-1)(q-1)\text{modes} & p\cdot q \text{ modes} & \cdots & p\cdot q \text{ modes} \\ p\cdot q \text{ modes} & \ddots & & \vdots \\ \vdots & & \ddots & p\cdot q \text{ modes} \\ p\cdot q \text{ modes} & \cdots & p\cdot q \text{ modes} & (p-1)(q-1) \text{ modes} \end{array}\right)}_{m \text{ blocks}}; \tag{C.8}$$

[4]With polynomial entries of degree at most one in w.

[5]This also implies that the codimension of the *whole* Higgs (living in A_{mp-1}) in $\mathcal{N}$ is maximized.

[6]The integers p, q are the same for all the blocks, the phase $e^{2\pi i s/m}$ multiplying the lowest-left entry in (C.3) is opportunely tuned in such a way that each block $\mathcal{A}_s$ reproduces each of the factors of (C.2).

2. the discrete group (starting with $G_{7d} = SU(mp)$) is always isomorphic to $\mathbb{Z}_p$. We can pick the generator to be:

$$G_{\text{gauge}} \equiv \underbrace{\left(\begin{array}{c|c|c|c} e^{\frac{2\pi i}{p}}\mathbb{1}_p & \mathbb{0}_p & \mathbb{0}_p & \mathbb{0}_p \\ \hline \mathbb{0}_p & \mathbb{1}_p & \vdots & \\ \hline & \vdots & \ddots & \mathbb{0}_p \\ \hline & \vdots & \vdots & \mathbb{1}_p \end{array}\right)}_{m \text{ blocks}}; \tag{C.9}$$

3. the flavor group matrix $G_{\text{flavor}} \in U(1)^m / U(1)_{diag}$ is:

$$G_{\text{flavor}} \equiv \underbrace{\left(\begin{array}{c|c|c|c} e^{i\alpha_1}\mathbb{1}_p & \mathbb{0}_p & \dots & \mathbb{0}_p \\ \hline \mathbb{0}_p & e^{i\alpha_2}\mathbb{1}_p & \vdots & \vdots \\ \hline \vdots & \vdots & \ddots & \mathbb{0}_p \\ \hline \mathbb{0}_p & \dots & \mathbb{0}_p & e^{i\alpha_m}\mathbb{1}_p \end{array}\right)}_{m \text{ blocks}}, \quad \sum_{s=1}^{m} \alpha_s = \frac{2\pi n}{p}; \tag{C.10}$$

4. $G_{\text{gauge}}, G_{\text{flavor}}$ act on the modes by adjoint action:

$$\varphi \to G_{\text{gauge}}\varphi(G_{\text{gauge}})^{-1}, \qquad \varphi \to G_{\text{flavor}}\varphi(G_{\text{flavor}})^{-1}; \tag{C.11}$$

The data in the matrix (C.8) allows us to completely reconstruct the Higgs branches *as complex varieties*[7]. That matrix and the shape of the flavor and discrete gauging are already sufficient to reconstruct completely the Higgs branch, and determine the action of the flavor group.

For the (A_{mp-1}, A_{mq-1}), we can do more, and recollect the result in a closed compact formula. Looking at (C.8), we get the following general formula for the Higgs branch:

$$\text{HB}_{m,p,q} = \mathbb{C}^{\left(m^2-2m+2\right)pq+m(1-p-q)} \times \frac{\mathbb{C}^{2(m-1)pq}}{\mathbb{Z}_p}. \tag{C.12}$$

The $\mathbb{Z}_p$ acts multiplying the first half of the $\mathbb{C}^{2(m-1)pq}$ complex coordinates (corresponding to, say, the chiral complex scalars inside the hypers) by $e^{\frac{2\pi i}{p}}$, and the second half of the $\mathbb{C}^{2(m-1)pq}$ complex coordinates (that correspond to the complex scalars in the anti-chiral part of the hyper) by $e^{-\frac{2\pi i}{p}}$. As we have remarked in the main text, the discrete gauging group might disappear if we make a different choice for the seven-dimensional gauge group global structure.

[7] In particular, we cannot determine the hyper-Kähler metric.

In Chapter 5, we indeed take a different choice, namely we pick as starting 7d gauge group $SU(mp)/\mathbb{Z}_{mp}$. This leaves no discrete group in 5d.

The flavor group is $U(1)^m/U(1)_{diag}$, as we saw in (C.10). These abelian factors correspond, in the resolved CY geometry, to the $\mathbb{P}^1$'s inflated in the resolution. These $\mathbb{P}^1$'s correspond to the roots at positions $r\times p$, with $r = 1, .., m-1$ in the Dynkin diagram of the A_{mp-1} ADE singularity. Each of the flavor $U(1)$ of (C.10) acts linearly, with charge one, on $m(q-1)(p-1)$ modes:

$$Q_i \to e^{i\alpha_s} Q_i, \quad \tilde{Q}_i \to e^{-i\alpha_s} \tilde{Q}_i, \quad i = 1, ..., n_{\text{charged hypers}}, \quad s = 1, ..., m. \tag{C.13}$$

To conclude, we quickly recap our strategy to get to (C.12). Given, as input datum, the equation of the (A_{mp-1}, A_{mq-1}) singularity:

1. We *computed the brane locus* Δ looking where the $\mathbb{C}^*$-fibers of the threefold degenerate.

2. We *factored the brane locus* (C.2) in polynomials that can be represented by the characteristic polynomials of a traceless matrix $\mathcal{A}_s$ with entries being $w-$dependent polynomials of degree at most one. We found that *any* polynomial that enters in the factorization of the brane locus of the (A_{mp-1}, A_{mq-1}) singularity is the characteristic polynomial of some block $\mathcal{A}_s$ of the shape (C.3).

3. We *counted the number of five-dimensional modes that are localized in the diagonal blocks*. More precisely, each of the $\mathcal{A}_s$ selects a minimal $\mathfrak{sl}(p) \hookrightarrow A_{mp-1}$ subalgebra that corresponds to the block containing $\mathcal{A}_s$ (C.8) (we highlighted the $\mathfrak{sl}(p)$ subalgebras corresponding to the various $\mathcal{A}_s$ with different colours in (C.7)). The localization of modes inside a certain $\mathfrak{sl}(p)$ subalgebra is determined just by the corresponding block $\mathcal{A}_s$, and is always the same for all the s.

4. We *counted the number of five-dimensional modes that a pair $\mathcal{A}_s$, $\mathcal{A}_s$ localizes in the corresponding off-diagonal blocks* of the block decomposition of the $\mathfrak{sl}(mp, \mathbb{C}[w])$ matrix, finding:

$$\left(\begin{array}{c|cc|c} (p-1)(q-1)\text{ modes} & \dots & \cdots & p\cdot q\text{ modes} \\ \vdots & \ddots & & \vdots \\ \vdots & & \ddots & \vdots \\ p\cdot q\text{ modes} & \dots & \dots & (p-1)(q-1)\text{ modes} \end{array}\right). \tag{C.14}$$

APPENDIX D

T-branes and nilpotent orbits in (A, D) singularities

As we have briefly mentioned in the case of (A_j, A_l) singularities of Appendix C, the choice of the Higgs background Φ deforming the stack of D6-branes is not unique. This means that in general many different Higgs fields $\Phi(w)$ realizing the brane-loci of the (A_j, A_l) singularities, called T-brane backgrounds, are allowed. These various choices can be labelled using the Lie algebra formalism involving nilpotent orbits: given a Higgs field $\Phi(w)$, we define as $\Phi_0 = \Phi(w = 0)$ its constant component. As on $w = 0$ we wish to obtain the undeformed singularity, we find that Φ_0 is always nilpotent for all the (A_j, A_l) and (A_k, D_n), and thus belongs to some nilpotent orbit $\mathcal{O}_0$ of A_j (supposing $j > l$) or D_n, respectively. Consequently we can label every Higgs $\Phi(w)$ using the nilpotent orbit $\mathcal{O}_0$ in which its constant component resides. This argument indeed holds for all the quasi-homogeneous cDV singularities. Furthermore, the codimension formula (C.4) relates the nilpotent orbit $\mathcal{O}_0$ to the number of linearly independent elements of the 7d gauge algebra that support 5d modes localized at the intersection of the D6-branes. For the (A_j, A_l) singularities the story ends here: in order to obtain the Higgs background for (A_j, A_l) yielding the maximal number of modes, we take the blocks in $\mathcal{A}$ in (C.3), evaluated on $w = 0$, to lie in the biggest-codimension nilpotent orbit $\mathcal{O}_0$ compatible with the geometry, namely reproducing the brane locus. We remark that in general the total number modes for this Higgs configuration need not be equal to the number of linearly independent elements in the 7d gauge algebra (i.e. there could be modes supported on $\mathbb{C}[w]/(w^k)$ with $k > 1$).

This is an example of a more general phenomenon: whenever we tackle the anaylsis of a quasi-homogeneous cDV singularity, the Higgs background producing the maximal amount of 5d modes lies in the nilpotent orbit of minimal dimension, when evaluated on $w = 0$. All the Higgses that localize *less* 5d modes are T-brane states. Namely, we find that:

For quasi-homogeneous cDV singularities, the Higgs field localizing the maximal amount of 5d modes satisfies:

$$\Phi(w)|_{w=0} = \Phi_0 \in \mathcal{O}_0^{low},$$

with $\mathcal{O}_0^{low}$ the nilpotent orbit of lowest dimension (that is, biggest codimension in $\mathcal{N}$) allowed by the compatibility with the threefold equation.

This is equivalent to requiring that every addend $\Phi_h(0)$ in (5.21) lies in the smallest allowed nilpotent orbit of the corresponding subalgebra, compatibly with the threefold equation.

In addition, the number of localized modes can be influenced by the distribution of the w-dependent entries of the Higgs background. In the example of the (A_k, D_n) singularities, this makes the hierarchy of the different Higgs backgrounds much more complicated. The goal of this section is to show how a classification of the allowed Higgs backgrounds is possible, providing an explicit example.

The starting point, as always, is the threefold equation for the (A_k, D_n) singularities in Table (5.1). The threefold equation, in turn, fixes the D6-brane locus, according to (3.62), that we reproduce here for convenience:

$$\det\,(\xi\mathbb{1}+\Phi(w)) = \Delta(\xi^2, w) = \xi^2(\xi^{2n-2}+w^{k+1}). \tag{D.1}$$

As we have said, there is vast space for ambiguities in the choice of a Higgs compatible with the brane locus (D.1), giving rise to a hierarchy governed by the nilpotent orbits that can be associated to the Higgs itself. Let us see how this precisely comes about.

Generally speaking, each Higgs comprises constant entries, along with entries depending on w (w-entries).

Correspondingly, by considering the constant and w-entries separately, we can analyze their orbit structure. In particular, for all the cases in (D.1), we now show how to associate both the constant entries and the w-entries to **nilpotent orbits**, that can be classified by suitable partitions of $[2n]$ as the Higgs Φ lives in the algebra $\mathfrak{so}(2n)$. As is well known in the mathematical literature, nilpotent orbits are organized hierarchically along Hasse diagrams, and this structure will be reflected in the possible choices for the Higgs background, giving rise in general to different spectrums in 5d. Following the notation for the (A_j, A_l) cases, we denote the nilpotent orbit associated to the constant entries as $\mathcal{O}_0$, and the one related to the w-entries as $\mathcal{O}_w$. More precisely, we define:

$$\begin{aligned} \mathcal{O}_0 &= \text{nilpotent orbit in which } \Phi(0) \text{ lives}, \\ \mathcal{O}_w &= \text{nilpotent orbit in which } \Phi-\Phi(0) \text{ lives}. \end{aligned} \tag{D.2}$$

Consequently, the full Higgs field Φ can be decomposed as:

$$\Phi = \Phi(0)+(\Phi-\Phi(0)) \equiv \Phi_0+\Phi_w, \tag{D.3}$$

where $\Phi_0 \in \mathcal{O}_0$ and $\Phi_w \in \mathcal{O}_w$.

When trying to pick a choice for Φ satisfying (D.1) for a given brane locus related to some (A_k, D_n) singularity, one is confronted with the following logical steps:

- In general, each brane locus is compatible with many choices of $\mathcal{O}_0$[1], thus giving rise

[1] Here by compatible we mean that we can build an Higgs field Φ with Φ_0 belonging to $\mathcal{O}_0$.

to an ambiguity. There is always a *minimal* $\mathcal{O}_0$, giving rise to the largest spectrum. Mathematically this is the lowest-lying orbit, among the compatible ones, in the Hasse diagram.
Most notably, *the choice of* $\mathcal{O}_0$ *completely fixes the number of linearly independent elements inside the 7d gauge algebra supporting 5d localized modes*, according to the codimension formula (C.4).

- In general, each $\mathcal{O}_0$ is compatible with many *bottom* orbits $\mathcal{O}_w$, namely with many different choices of w-entries, barely sufficient to reproduce the correct brane locus (where "barely" means that no "w" entry can be removed without affecting the brane locus). Among the bottom orbits $\mathcal{O}_w$ there is always a minimal $\mathcal{O}_w$, lying at the lowest position in the Hasse diagram, giving rise to the maximal number of modes.
Each bottom $\mathcal{O}_w$ gives rise, in general, to a different number of total 5d modes.

- By deforming each bottom $\mathcal{O}_w$, tuning zero-entries into w-entries while keeping the brane locus and $\mathcal{O}_0$ fixed, we find a *tower* of allowed $\mathcal{O}_w$, starting from the bottom one and terminating on a top one (there always is a top orbit, as the size of the Higgs is fixed by the brane locus).
Most importantly, *each* $\mathcal{O}_w$ *belonging to the same tower*[2] *gives rise to the same number of total modes*. In addition, towers starting from different bottom $\mathcal{O}_w$ need not be disjoint (meaning that the same $\mathcal{O}_w$ can appear in many different towers, producing different amounts of modes. What counts for the number of modes is the *bottom* $\mathcal{O}_w$ at the base of the tower).

Summing up, given a brane locus in the (A_k, D_n) series, a choice of the Higgs is completely determined once one picks:

$$\begin{cases} \text{a nilpotent orbit } \mathcal{O}_0, \text{ corresponding to the constant entries of } \Phi, \\ \text{a bottom orbit } \mathcal{O}_w, \text{ corresponding to the } w\text{-entries of } \Phi. \end{cases} \tag{D.4}$$

In order to understand this hierarchy of choices in a more intuitive way, it is instructive to depict it graphically, indicating with segments the possible choices, and with arrows the nilpotent orbits hierarchy in the Hasse diagram sense. Notice that we have explicitly indicated the minimal $\mathcal{O}_0$ and minimal $\mathcal{O}_w$ orbits, that when combined in the choice of the Higgs yield the M-theory dynamics with the maximal number of modes. In an extensive case by case analysis we have always found that such choice is unique, but we cannot rule out the possibility that there is more than one minimal choice of $\mathcal{O}_0$ and $\mathcal{O}_w$ yielding the maximal number of modes, as there could be more than one orbit on the same level of the Hasse diagram hierarchy. We finally stress that each bottom orbit $\mathcal{O}_w$ in the picture is the starting point of a tower of orbits, obtained deforming the Higgs configuration corresponding to the bottom orbit, with the same number of total 5d modes as the ones given by the bottom

[2] We stress that this means that the Higgs associated to the $\mathcal{O}_w$ in the tower is obtained turning on some w-entries in the Higgs associated to the bottom orbit, without modifying its brane locus.

orbit. We have omitted such towers for a better graphical depiction.

Finally, notice that for every choice of $\mathcal{O}_0$ we have indicated the total number of linearly independent elements of the 7d gauge algebra supporting localized 5d hypers (namely, the number of 7d elements supporting localized 5d modes given by the codimension formula (C.4) is *twice* the number we have indicated), and that for every bottom $\mathcal{O}_w$ we have highlighted the total number of hypers.

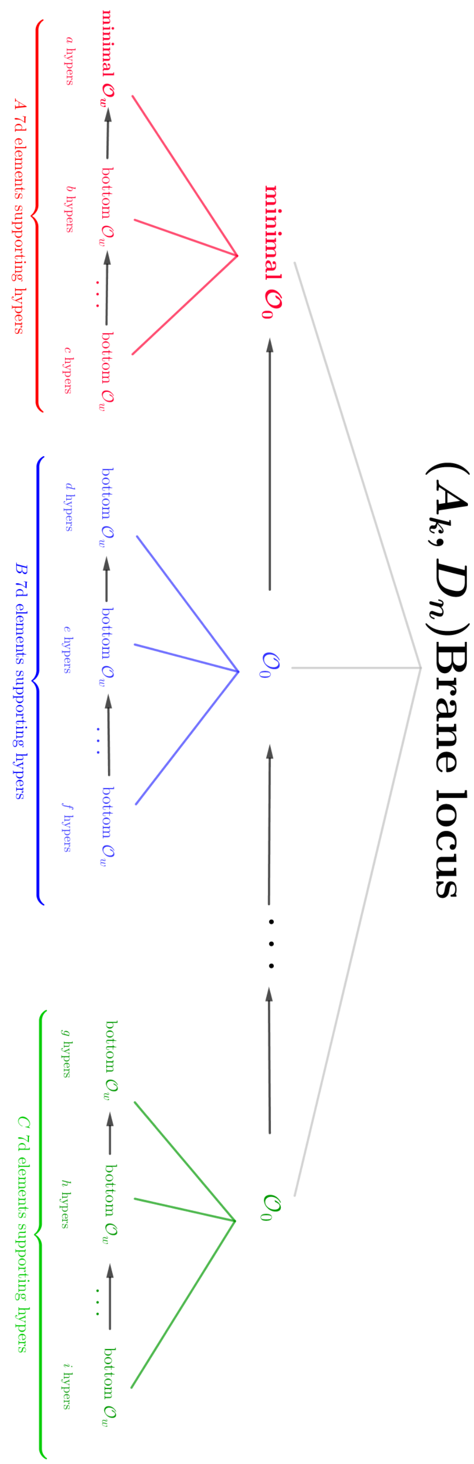

Let us now examine a concrete example, so as to make the abstract remarks above a bit more grounded. An interesting instance of brane locus giving rise to a T-brane hierarchy is (A_8, D_8), that displays a remarkable structure. This singularity is non-resolvable and its brane locus is:

$$\Delta(\xi^2, w) = \underbrace{\xi^2(\xi^{14}+w^9)}_{\text{type (b)}} = 0. \tag{D.5}$$

In the following picture, the red color refers to the $\mathcal{O}_0$, the blue color to bottom $\mathcal{O}_w$ and the dark arrows to dominance in the Hasse diagram sense. We have instead omitted towers with the same number of total hypers for the sake of graphical clarity. As before, we have indicated the total number of 7d gauge algebra elements supporting localized 5d hypers for every choice of $\mathcal{O}_0$ in the hierarchy, as well as the total number of hypers for every bottom $\mathcal{O}_w$. As it can be seen from the picture, the M-theory dynamics with maximal modes is reproduced by the lowest $\mathcal{O}_0$ with the lowest $\mathcal{O}_w$ in the Hasse diagram, yielding 32 total hypers. All the other partitions are instead T-brane configurations with a lower amount of modes.

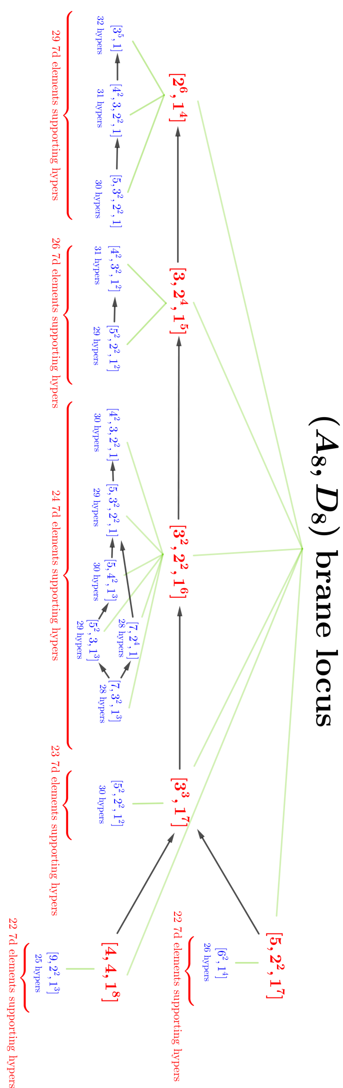

Bibliography

[1] M. B. Green and J. H. Schwarz, "Anomaly cancellations in supersymmetric d = 10 gauge theory and superstring theory", *Physics Letters B* **149** (1984), no. 1, 117–122.

[2] E. Witten, "String theory dynamics in various dimensions", *Nucl. Phys. B* **443** (1995) 85–126, hep-th/9503124.

[3] J. Polchinski, "Dirichlet Branes and Ramond-Ramond charges", *Phys. Rev. Lett.* **75** (1995) 4724–4727, hep-th/9510017.

[4] E. Palti, "The Swampland: Introduction and Review", *Fortsch. Phys.* **67** (2019), no. 6, 1900037, 1903.06239.

[5] E. Witten, "Quantum Field Theory and the Jones Polynomial", *Commun. Math. Phys.* **121** (1989) 351–399.

[6] P. S. Aspinwall, B. R. Greene, and D. R. Morrison, "Calabi-Yau moduli space, mirror manifolds and space-time topology change in string theory", *Nucl. Phys. B* **416** (1994) 414–480, hep-th/9309097.

[7] M. Kontsevich, "Homological Algebra of Mirror Symmetry", alg-geom/9411018.

[8] R. Gopakumar and C. Vafa, "M theory and topological strings. 1.", hep-th/9809187.

[9] R. Gopakumar and C. Vafa, "M theory and topological strings. 2.", hep-th/9812127.

[10] R. Gopakumar and C. Vafa, "On the gauge theory / geometry correspondence", *Adv. Theor. Math. Phys.* **3** (1999) 1415–1443, hep-th/9811131.

[11] E.-N. Ionel and T. H. Parker, "The gopakumar-vafa formula for symplectic manifolds", *Annals of Mathematics* **187** (2018), no. 1, 1–64.

[12] R. Pandharipande and R. P. Thomas, "13/2 ways of counting curves", *Lond. Math. Soc. Lect. Note Ser.* **411** (2014) 282–333, 1111.1552.

[13] S. H. Katz, A. Klemm, and C. Vafa, "Geometric engineering of quantum field theories", *Nucl. Phys. B* **497** (1997) 173–195, hep-th/9609239.

[14] S. H. Katz and C. Vafa, "Geometric engineering of N=1 quantum field theories", *Nucl. Phys. B* **497** (1997) 196–204, hep-th/9611090.

[15] N. Seiberg and E. Witten, "Electric - magnetic duality, monopole condensation, and confinement in N=2 supersymmetric Yang-Mills theory", *Nucl. Phys. B* **426** (1994) 19–52, hep-th/9407087. [Erratum: Nucl.Phys.B 430, 485–486 (1994)].

[16] N. Seiberg and E. Witten, "Monopoles, duality and chiral symmetry breaking in N=2 supersymmetric QCD", *Nucl. Phys. B* **431** (1994) 484–550, hep-th/9408099.

[17] D. Gaiotto, "N=2 dualities", *JHEP* **08** (2012) 034, 0904.2715.

[18] D. Gaiotto, G. W. Moore, and A. Neitzke, "Wall-crossing, Hitchin Systems, and the WKB Approximation", 0907.3987.

[19] A. D. Shapere and C. Vafa, "BPS structure of Argyres-Douglas superconformal theories", hep-th/9910182.

[20] P. C. Argyres and M. R. Douglas, "New phenomena in SU(3) supersymmetric gauge theory", *Nucl. Phys. B* **448** (1995) 93–126, hep-th/9505062.

[21] P. C. Argyres, M. R. Plesser, N. Seiberg, and E. Witten, "New N=2 superconformal field theories in four-dimensions", *Nucl. Phys. B* **461** (1996) 71–84, hep-th/9511154.

[22] N. Seiberg, "Notes on theories with 16 supercharges", *Nucl. Phys. B Proc. Suppl.* **67** (1998) 158–171, hep-th/9705117.

[23] M. Henningson, "Self-dual strings in six dimensions: Anomalies, the ADE-classification, and the world-sheet WZW-model", *Commun. Math. Phys.* **257** (2005) 291–302, hep-th/0405056.

[24] C. Cordova, T. T. Dumitrescu, and X. Yin, "Higher derivative terms, toroidal compactification, and Weyl anomalies in six-dimensional (2, 0) theories", *JHEP* **10** (2019) 128, 1505.03850.

[25] J. J. Heckman, D. R. Morrison, and C. Vafa, "On the Classification of 6D SCFTs and Generalized ADE Orbifolds", *JHEP* **05** (2014) 028, 1312.5746. [Erratum: JHEP 06, 017 (2015)].

[26] L. Bhardwaj, "Classification of 6d $\mathcal{N} = (1, 0)$ gauge theories", *JHEP* **11** (2015) 002, 1502.06594.

[27] J. J. Heckman, D. R. Morrison, T. Rudelius, and C. Vafa, "Atomic Classification of 6D SCFTs", *Fortsch. Phys.* **63** (2015) 468–530, 1502.05405.

[28] P. Jefferson, S. Katz, H.-C. Kim, and C. Vafa, "On Geometric Classification of 5d SCFTs", *JHEP* **04** (2018) 103, 1801.04036.

[29] N. Seiberg, "Five-dimensional SUSY field theories, nontrivial fixed points and string dynamics", *Phys. Lett. B* **388** (1996) 753–760, hep-th/9608111.

[30] D. R. Morrison and N. Seiberg, "Extremal transitions and five-dimensional supersymmetric field theories", *Nucl. Phys. B* **483** (1997) 229–247, hep-th/9609070.

[31] K. A. Intriligator, D. R. Morrison, and N. Seiberg, "Five-dimensional supersymmetric gauge theories and degenerations of Calabi-Yau spaces", *Nucl. Phys. B* **497** (1997) 56–100, hep-th/9702198.

[32] O. Aharony and A. Hanany, "Branes, superpotentials and superconformal fixed points", *Nucl. Phys. B* **504** (1997) 239–271, hep-th/9704170.

[33] O. Aharony, A. Hanany, and B. Kol, "Webs of (p,q) five-branes, five-dimensional field theories and grid diagrams", *JHEP* **01** (1998) 002, hep-th/9710116.

[34] O. DeWolfe, A. Hanany, A. Iqbal, and E. Katz, "Five-branes, seven-branes and five-dimensional E(n) field theories", *JHEP* **03** (1999) 006, hep-th/9902179.

[35] O. Bergman, D. Rodríguez-Gómez, and G. Zafrir, "5-Brane Webs, Symmetry Enhancement, and Duality in 5d Supersymmetric Gauge Theory", *JHEP* **03** (2014) 112, 1311.4199.

[36] G. Zafrir, "Duality and enhancement of symmetry in 5d gauge theories", *JHEP* **12** (2014) 116, 1408.4040.

[37] O. Bergman and G. Zafrir, "5d fixed points from brane webs and O7-planes", *JHEP* **12** (2015) 163, 1507.03860.

[38] G. Zafrir, "Instanton operators and symmetry enhancement in 5d supersymmetric USp, SO and exceptional gauge theories", *JHEP* **07** (2015) 087, 1503.08136.

[39] H. Hayashi, S.-S. Kim, K. Lee, M. Taki, and F. Yagi, "A new 5d description of 6d D-type minimal conformal matter", *JHEP* **08** (2015) 097, 1505.04439.
[40] H. Hayashi, S.-S. Kim, K. Lee, and F. Yagi, "Dualities and 5-brane webs for 5d rank 2 SCFTs", *JHEP* **12** (2018) 016, 1806.10569.
[41] H. Hayashi, S.-S. Kim, K. Lee, and F. Yagi, "5-brane webs for 5d $\mathcal{N} = 1$ G_2 gauge theories", *JHEP* **03** (2018) 125, 1801.03916.
[42] O. Bergman and D. Rodríguez-Gómez, "The Cat's Cradle: deforming the higher rank E_1 and $\tilde{E}_1$ theories", *JHEP* **02** (2021) 122, 2011.05125.
[43] M. Bertolini and F. Mignosa, "Supersymmetry breaking deformations and phase transitions in five dimensions", *JHEP* **10** (2021) 244, 2109.02662.
[44] L. Bao, E. Pomoni, M. Taki, and F. Yagi, "M5-Branes, Toric Diagrams and Gauge Theory Duality", *JHEP* **04** (2012) 105, 1112.5228.
[45] M. Taki, "Seiberg Duality, 5d SCFTs and Nekrasov Partition Functions", 1401.7200.
[46] M. van Beest, A. Bourget, J. Eckhard, and S. Schafer-Nameki, "(Symplectic) Leaves and (5d Higgs) Branches in the Poly(go)nesian Tropical Rain Forest", *JHEP* **11** (2020) 124, 2008.05577.
[47] C. Closset, M. Del Zotto, and V. Saxena, "Five-dimensional SCFTs and gauge theory phases: an M-theory/type IIA perspective", *SciPost Phys.* **6** (2019), no. 5, 052, 1812.10451.
[48] V. Saxena, "Rank-two 5d SCFTs from M-theory at isolated toric singularities: a systematic study", *JHEP* **04** (2020) 198, 1911.09574.
[49] F. Apruzzi, C. Lawrie, L. Lin, S. Schäfer-Nameki, and Y.-N. Wang, "5d Superconformal Field Theories and Graphs", *Phys. Lett. B* **800** (2020) 135077, 1906.11820.
[50] M. Van Beest, A. Bourget, J. Eckhard, and S. Schäfer-Nameki, "(5d RG-flow) Trees in the Tropical Rain Forest", *JHEP* **03** (2021) 241, 2011.07033.
[51] L. Bhardwaj and P. Jefferson, "Classifying 5d SCFTs via 6d SCFTs: Arbitrary rank", *JHEP* **10** (2019) 282, 1811.10616.
[52] F. Apruzzi, C. Lawrie, L. Lin, S. Schäfer-Nameki, and Y.-N. Wang, "Fibers add Flavor, Part I: Classification of 5d SCFTs, Flavor Symmetries and BPS States", *JHEP* **11** (2019) 068, 1907.05404.
[53] F. Apruzzi, C. Lawrie, L. Lin, S. Schäfer-Nameki, and Y.-N. Wang, "Fibers add Flavor, Part II: 5d SCFTs, Gauge Theories, and Dualities", *JHEP* **03** (2020) 052, 1909.09128.
[54] L. Bhardwaj, "On the classification of 5d SCFTs", *JHEP* **09** (2020) 007, 1909.09635.
[55] P. Jefferson, H.-C. Kim, C. Vafa, and G. Zafrir, "Towards Classification of 5d SCFTs: Single Gauge Node", 1705.05836.
[56] F. Apruzzi, L. Lin, and C. Mayrhofer, "Phases of 5d SCFTs from M-/F-theory on Non-Flat Fibrations", *JHEP* **05** (2019) 187, 1811.12400.
[57] L. Bhardwaj and P. Jefferson, "Classifying 5d SCFTs via 6d SCFTs: Rank one", *JHEP* **07** (2019) 178, 1809.01650. [Addendum: JHEP 01, 153 (2020)].
[58] D. Xie and S.-T. Yau, "Three dimensional canonical singularity and five dimensional $\mathcal{N} = 1$ SCFT", *JHEP* **06** (2017) 134, 1704.00799.
[59] C. Closset, S. Schafer-Nameki, and Y.-N. Wang, "Coulomb and Higgs Branches from Canonical Singularities: Part 0", *JHEP* **02** (2021) 003, 2007.15600.
[60] C. Closset, S. Giacomelli, S. Schafer-Nameki, and Y.-N. Wang, "5d and 4d SCFTs: Canonical Singularities, Trinions and S-Dualities", *JHEP* **05** (2021) 274, 2012.12827.

[61] C. Closset, S. Schäfer-Nameki, and Y.-N. Wang, "Coulomb and Higgs branches from canonical singularities. Part I. Hypersurfaces with smooth Calabi-Yau resolutions", *JHEP* **04** (2022) 061, 2111.13564.
[62] S. Cremonesi, A. Hanany, and A. Zaffaroni, "Monopole operators and Hilbert series of Coulomb branches of $3d$ $\mathcal{N}=4$ gauge theories", *JHEP* **01** (2014) 005, 1309.2657.
[63] M. Bullimore, T. Dimofte, and D. Gaiotto, "The Coulomb Branch of 3d $\mathcal{N}=4$ Theories", *Commun. Math. Phys.* **354** (2017), no. 2, 671–751, 1503.04817.
[64] S. Cremonesi, G. Ferlito, A. Hanany, and N. Mekareeya, "Coulomb Branch and The Moduli Space of Instantons", *JHEP* **12** (2014) 103, 1408.6835.
[65] A. Braverman, M. Finkelberg, and H. Nakajima, "Coulomb branches of $3d$ $\mathcal{N}=4$ quiver gauge theories and slices in the affine Grassmannian", *Adv. Theor. Math. Phys.* **23** (2019) 75–166, 1604.03625.
[66] G. Ferlito, A. Hanany, N. Mekareeya, and G. Zafrir, "3d Coulomb branch and 5d Higgs branch at infinite coupling", *JHEP* **07** (2018) 061, 1712.06604.
[67] S. Cabrera and A. Hanany, "Quiver Subtractions", *JHEP* **09** (2018) 008, 1803.11205.
[68] S. Cabrera, A. Hanany, and F. Yagi, "Tropical Geometry and Five Dimensional Higgs Branches at Infinite Coupling", *JHEP* **01** (2019) 068, 1810.01379.
[69] A. Bourget, J. F. Grimminger, A. Hanany, M. Sperling, and Z. Zhong, "Magnetic Quivers from Brane Webs with O5 Planes", *JHEP* **07** (2020) 204, 2004.04082.
[70] A. Bourget, J. F. Grimminger, A. Hanany, R. Kalveks, M. Sperling, and Z. Zhong, "Magnetic Lattices for Orthosymplectic Quivers", *JHEP* **12** (2020) 092, 2007.04667.
[71] M. Akhond, F. Carta, S. Dwivedi, H. Hayashi, S.-S. Kim, and F. Yagi, "Five-brane webs, Higgs branches and unitary/orthosymplectic magnetic quivers", *JHEP* **12** (2020) 164, 2008.01027.
[72] M. Akhond, F. Carta, S. Dwivedi, H. Hayashi, S.-S. Kim, and F. Yagi, "Factorised 3d $\mathcal{N}=4$ orthosymplectic quivers", *JHEP* **05** (2021) 269, 2101.12235.
[73] M. Akhond, F. Carta, S. Dwivedi, H. Hayashi, S.-S. Kim, and F. Yagi, "Exploring the orthosymplectic zoo", *JHEP* **05** (2022) 054, 2203.01951.
[74] M. Akhond and F. Carta, "Magnetic quivers from brane webs with $O7^+$-planes", *JHEP* **10** (2021) 014, 2107.09077.
[75] A. Bourget, S. Cabrera, J. F. Grimminger, A. Hanany, M. Sperling, A. Zajac, and Z. Zhong, "The Higgs mechanism — Hasse diagrams for symplectic singularities", *JHEP* **01** (2020) 157, 1908.04245.
[76] F. Albertini, M. Del Zotto, I. n. García Etxebarria, and S. S. Hosseini, "Higher Form Symmetries and M-theory", *JHEP* **12** (2020) 203, 2005.12831.
[77] D. R. Morrison, S. Schafer-Nameki, and B. Willett, "Higher-Form Symmetries in 5d", *JHEP* **09** (2020) 024, 2005.12296.
[78] F. Apruzzi, L. Bhardwaj, J. Oh, and S. Schafer-Nameki, "The Global Form of Flavor Symmetries and 2-Group Symmetries in 5d SCFTs", 2105.08724.
[79] P. Benetti Genolini and L. Tizzano, "Instantons, symmetries and anomalies in five dimensions", *JHEP* **04** (2021) 188, 2009.07873.
[80] P. B. Genolini and L. Tizzano, "Comments on Global Symmetries and Anomalies of $5d$ SCFTs", 2201.02190.

[81] M. Del Zotto, J. J. Heckman, S. N. Meynet, R. Moscrop, and H. Y. Zhang, "Higher Symmetries of 5d Orbifold SCFTs", 2201.08372.
[82] M. Del Zotto, I. n. G. Etxebarria, and S. Schafer-Nameki, "2-Group Symmetries and M-Theory", 2203.10097.
[83] M. Cvetič, J. J. Heckman, M. Hübner, and E. Torres, "0-Form, 1-Form and 2-Group Symmetries via Cutting and Gluing of Orbifolds", 2203.10102.
[84] M. Reid, "Minimal models of canonical 3-folds", *Adv. Stud. Pure Math* **1** (1981) 131–180.
[85] M. Aganagic, A. Klemm, M. Marino, and C. Vafa, "The Topological vertex", *Commun. Math. Phys.* **254** (2005) 425–478, hep-th/0305132.
[86] S. H. Katz, "Genus zero Gopakumar-Vafa invariants of contractible curves", *J. Diff. Geom.* **79** (2008), no. 2, 185–195, math/0601193.
[87] W. Donovan and M. Wemyss, "Noncommutative deformations and flops", *Duke Mathematical Journal* **165** (2016), no. 8, 1397–1474.
[88] W. Donovan, "Contractions of 3-folds: Deformations and invariants", *International Journal of Mathematics* **27** (2016), no. 07, 1640004.
[89] Y. Toda, "Non-commutative width and Gopakumar-Vafa invariants", *Manuscripta Mathematica* **148** (11, 2014).
[90] C. Curto and D. Morrison, "Threefold flops via matrix factorization", *Journal of Algebraic Geometry* **22** (12, 2006).
[91] J. Karmazyn, "The length classification of threefold flops via noncommutative algebras", *Advances in Mathematics* **343** (2019) 393–447.
[92] G. Brown and M. Wemyss, "Gopakumar-Vafa invariants do not determine flops", *Commun. Math. Phys.* **361** (2018), no. 1, 143–154, 1707.01150.
[93] T. Gomez and E. R. Sharpe, "D-branes and scheme theory", hep-th/0008150.
[94] S. Cecotti, C. Cordova, J. J. Heckman, and C. Vafa, "T-Branes and Monodromy", *JHEP* **07** (2011) 030, 1010.5780.
[95] A. Collinucci and R. Savelli, "T-branes as branes within branes", *JHEP* **09** (2015) 161, 1410.4178.
[96] A. Collinucci, A. Sangiovanni, and R. Valandro, "Genus zero Gopakumar-Vafa invariants from open strings", *JHEP* **09** (2021) 059, 2104.14493.
[97] A. Collinucci, M. De Marco, A. Sangiovanni, and R. Valandro, "Higgs branches of 5d rank-zero theories from geometry", *JHEP* **10** (2021), no. 18, 018, 2105.12177.
[98] M. De Marco and A. Sangiovanni, "Higgs Branches of rank-0 5d theories from M-theory on $(\mathrm{A}_j, \mathrm{A}_l)$ and $(\mathrm{A}_k, \mathrm{D}_n)$ singularities", *JHEP* **03** (2022) 099, 2111.05875.
[99] A. Collinucci, M. De Marco, A. Sangiovanni, and R. Valandro, "Flops of any *length*, Gopakumar-Vafa invariants, and 5d Higgs Branches", 2204.10366.
[100] M. De Marco, A. Sangiovanni, and R. Valandro, "5d Higgs Branches from M-theory on quasi-homogeneous cDV threefold singularities", 2205.01125.
[101] E. Cartan, "Sur la structure des groupes de transformations finis et continus", *Oevres Complètes, 1, CNRS* (1984) 789–855.
[102] W. Killing, "Die zusammensetzung der stetigen endlichen transformationsgruppen i", *Math. Ann.* **31** (1888) 252–290.
[103] W. Killing, "Die zusammensetzung der stetigen endlichen transformationsgruppen ii", *Math. Ann.* **33** (1889) 1–48.

[104] W. Killing, "Die zusammensetzung der stetigen endlichen transformationsgruppen iii", *Math. Ann.* **34** (1889) 57–122.

[105] W. Killing, "Die zusammensetzung der stetigen endlichen transformationsgruppen iv", *Math. Ann.* **36** (1890) 161–189.

[106] J. McKay, "Graphs, singularities, and finite groups", *Proc. Symp. Pure Math.* **37** (1980).

[107] P. Du Val, "On isolated singularities of surfaces which do not affect the conditions of adjunction (part i)", *Mathematical Proceedings of the Cambridge Philosophical Society* **30** (1934), no. 4, 453–459.

[108] D. Eisenbud, "Homological algebra on a complete intersection, with an application to group representations", *Transactions of the American Mathematical Society* **260** (1980), no. 1, 35–64.

[109] A. Collinucci and R. Savelli, "F-theory on singular spaces", *JHEP* **09** (2015) 100, 1410.4867.

[110] M. F. Atiyah, "On analytic surfaces with double points", *Proceedings of the Royal Society of London. Series A, Mathematical and Physical Sciences* **247** (1958), no. 1249, 237–244.

[111] S. Katz and D. R. Morrison, "Gorenstein threefold singularities with small resolutions via invariant theory for weyl groups", *J. Alg. Geom.* **1** (1992) 449–530, alg-geom/9202002.

[112] D. H. Collingwood and W. M. McGovern, "Nilpotent orbits in semisimple lie algebra: An introduction", *Chapman and Hall/CRC* (1993).

[113] A. Henderson, "Singularities of nilpotent orbit closures", 1408.3888.

[114] Z. Yun, "Lectures on Springer theories and orbital integrals", 1602.01451.

[115] T. A. Springer, "The unipotent variety of a semi-simple group", in *Algebraic geometry*, pp. 373–391, Oxford Univ. Press London. (1969).

[116] R. Steinberg and V. Deodhar, *Conjugacy Classes in Algebraic Groups.* Lecture Notes in Mathematics. Springer, (1974).

[117] R. Steinberg, "On the desingularization of the unipotent variety.", *Inventiones mathematicae* **36** (1976) 209–224.

[118] E. Brieskorn, "Singular elements of semi-simple algebraic groups", in *Actes du Congres International des Mathématiciens (Nice, 1970)*, vol. 2, pp. 279–284. 1970.

[119] B. Conrad, "Math 249b. standard parabolic subgroups: theory and examples".

[120] A. C. Cadavid, A. Ceresole, R. D'Auria, and S. Ferrara, "Eleven-dimensional supergravity compactified on Calabi-Yau threefolds", *Phys. Lett. B* **357** (1995) 76–80, hep-th/9506144.

[121] S. S. Gubser, "TASI lectures: Special holonomy in string theory and M theory", in *Theoretical Advanced Study Institute in Elementary Particle Physics (TASI 2001): Strings, Branes and EXTRA Dimensions*, pp. 197–233. 1, 2002. hep-th/0201114.

[122] B. S. Acharya and S. Gukov, "M theory and singularities of exceptional holonomy manifolds", *Phys. Rept.* **392** (2004) 121–189, hep-th/0409191.

[123] S. H. Katz, D. R. Morrison, and M. R. Plesser, "Enhanced gauge symmetry in type II string theory", *Nucl. Phys. B* **477** (1996) 105–140, hep-th/9601108.

[124] A. Sen, "A Note on enhanced gauge symmetries in M and string theory", *JHEP* **09** (1997) 001, hep-th/9707123.

[125] P. K. Townsend, "The eleven-dimensional supermembrane revisited", *Phys. Lett. B* **350** (1995) 184–187, hep-th/9501068.

[126] A. Sen, "Kaluza-Klein dyons in string theory", *Phys. Rev. Lett.* **79** (1997) 1619–1621, hep-th/9705212.

[127] A. Sen, "Dynamics of multiple Kaluza-Klein monopoles in M and string theory", *Adv. Theor. Math. Phys.* **1** (1998) 115–126, hep-th/9707042.

[128] E. Witten, "Branes, Instantons, And Taub-NUT Spaces", *JHEP* **06** (2009) 067, 0902.0948.

[129] E. Witten, "Phase transitions in M theory and F theory", *Nucl. Phys. B* **471** (1996) 195–216, hep-th/9603150.

[130] D. Xie and S.-T. Yau, "4d N=2 SCFT and singularity theory Part I: Classification", 1510.01324.

[131] Y. Wang and D. Xie, "Classification of Argyres-Douglas theories from M5 branes", *Phys. Rev. D* **94** (2016), no. 6, 065012, 1509.00847.

[132] C.-C. Chiou, A. E. Faraggi, R. Tatar, and W. Walters, "T-branes and Yukawa Couplings", *JHEP* **05** (2011) 023, 1101.2455.

[133] L. B. Anderson, J. J. Heckman, and S. Katz, "T-Branes and Geometry", *JHEP* **05** (2014) 080, 1310.1931.

[134] M. Cicoli, F. Quevedo, and R. Valandro, "De Sitter from T-branes", *JHEP* **03** (2016) 141, 1512.04558.

[135] A. Collinucci, S. Giacomelli, R. Savelli, and R. Valandro, "T-branes through 3d mirror symmetry", *JHEP* **07** (2016) 093, 1603.00062.

[136] I. Bena, J. Blåbäck, R. Minasian, and R. Savelli, "There and back again: A T-brane's tale", *JHEP* **11** (2016) 179, 1608.01221.

[137] F. Marchesano and S. Schwieger, "T-branes and α'-corrections", *JHEP* **11** (2016) 123, 1609.02799.

[138] N. Mekareeya, T. Rudelius, and A. Tomasiello, "T-branes, Anomalies and Moduli Spaces in 6D SCFTs", *JHEP* **10** (2017) 158, 1612.06399.

[139] L. B. Anderson, J. J. Heckman, S. Katz, and L. P. Schaposnik, "T-Branes at the Limits of Geometry", *JHEP* **10** (2017) 058, 1702.06137.

[140] I. Bena, J. Blåbäck, and R. Savelli, "T-branes and Matrix Models", *JHEP* **06** (2017) 009, 1703.06106.

[141] A. Collinucci, S. Giacomelli, and R. Valandro, "T-branes, monopoles and S-duality", *JHEP* **10** (2017) 113, 1703.09238.

[142] F. Marchesano, R. Savelli, and S. Schwieger, "Compact T-branes", *JHEP* **09** (2017) 132, 1707.03797.

[143] F. Carta, S. Giacomelli, and R. Savelli, "SUSY enhancement from T-branes", *JHEP* **12** (2018) 127, 1809.04906.

[144] F. Marchesano, R. Savelli, and S. Schwieger, "T-branes and defects", *JHEP* **04** (2019) 110, 1902.04108.

[145] I. Bena, J. Blåbäck, R. Savelli, and G. Zoccarato, "The two faces of T-branes", *JHEP* **10** (2019) 150, 1905.03267.

[146] R. Barbosa, M. Cvetič, J. J. Heckman, C. Lawrie, E. Torres, and G. Zoccarato, "T-branes and G_2 backgrounds", *Phys. Rev. D* **101** (2020), no. 2, 026015, 1906.02212.

[147] F. Hassler, J. J. Heckman, T. B. Rochais, T. Rudelius, and H. Y. Zhang, "T-Branes, String Junctions, and 6D SCFTs", *Phys. Rev. D* **101** (2020), no. 8, 086018, 1907.11230.

[148] F. Marchesano, R. Moraru, and R. Savelli, "A vanishing theorem for T-branes", *JHEP* **11** (2020) 002, 2007.02960.

[149] I. n. García Etxebarria, B. Heidenreich, and D. Regalado, "IIB flux non-commutativity and the global structure of field theories", *JHEP* **10** (2019) 169, 1908.08027.
[150] J. Dixmier, "Enveloping algebras", *North-Holland, Amsterdam* (1977).
[151] S. Okubo and J. Patera, "General indices of representations and casimir invariants", *J. Math. Phys.* **25** (1984).
[152] K. Hori, S. Katz, C. Vafa, R. Thomas, A. M. Society, C. M. Institute, R. Pandharipande, A. Klemm, R. Vakil, and E. Zaslow, "Mirror Symmetry", *Clay mathematics monographs*, American Mathematical Society, (2003).
[153] E. Witten, "Topological Sigma Models", *Commun. Math. Phys.* **118** (1988) 411.
[154] I. Antoniadis, E. Gava, K. S. Narain, and T. R. Taylor, "Topological amplitudes in string theory," *Nucl. Phys. B* **413** (1994) 162–184, hep-th/9307158.
[155] M. Caibar, "Minimal models of canonical singularities and their cohomology", (2011).
[156] M. Caibar, "Minimal models of canonical 3-fold singularities and their betti numbers", *International Mathematics Research Notices* (2005) 1563–1581.
[157] S. Gukov, C. Vafa, and E. Witten, "CFT's from Calabi-Yau four folds", *Nucl. Phys. B* **584** (2000) 69–108, hep-th/9906070. [Erratum: Nucl.Phys.B 608, 477–478 (2001)].
[158] P. S. Aspinwall and D. R. Morrison, "Quivers from Matrix Factorizations", *Commun. Math. Phys.* **313** (2012) 607–633, 1005.1042.
[159] F. Cachazo, S. Katz, and C. Vafa, "Geometric transitions and N=1 quiver theories", hep-th/0108120.
[160] A. Collinucci, M. Fazzi, and R. Valandro, "Geometric engineering on flops of length two", *JHEP* **04** (2018) 090, 1802.00813.
[161] H. Laufer, "On cp1 as an exceptional set", *Ann. of Math. Stud. Vol. 100, Princeton Univ. Press, Princeton, NJ* (1981).
[162] M. Reid, "Minimal models of canonical 3-folds", *North-Holland, Amsterdam* (1983).
[163] H. Clemens, J. Kollár, and S. Mori, "Higher-dimensional complex geometry", *Astérisque* (1989).
[164] D. S. Freed, G. W. Moore, and G. Segal, "Heisenberg Groups and Noncommutative Fluxes", *Annals Phys.* **322** (2007) 236–285, hep-th/0605200.
[165] D. S. Freed, G. W. Moore, and G. Segal, "The Uncertainty of Fluxes", *Commun. Math. Phys.* **271** (2007) 247–274, hep-th/0605198.
[166] A. Collinucci, M. Fazzi, D. R. Morrison, and R. Valandro, "High electric charges in M-theory from quiver varieties", *JHEP* **11** (2019) 111, 1906.02202.
[167] T. Banks and N. Seiberg, "Symmetries and Strings in Field Theory and Gravity", *Phys. Rev. D* **83** (2011) 084019, 1011.5120.
[168] M. van Beest, J. Calderón-Infante, D. Mirfendereski, and I. Valenzuela, "Lectures on the Swampland Program in String Compactifications", 2102.01111.
[169] A. P. Braun, A. Collinucci, and R. Valandro, "The fate of U(1)'s at strong coupling in F-theory", *JHEP* **07** (2014) 028, 1402.4054.
[170] T. W. Grimm, M. Kerstan, E. Palti, and T. Weigand, "Massive Abelian Gauge Symmetries and Fluxes in F-theory", *JHEP* **12** (2011) 004, 1107.3842.
[171] S. Cecotti, A. Neitzke, and C. Vafa, "R-Twisting and 4d/2d Correspondences", 1006.3435.

[172] P. Bala and R. W. Carter, "Classes of unipotent elements in simple algebraic groups. i", *Mathematical Proceedings of the Cambridge Philosophical Society*, vol. 79, pp. 401–425, Cambridge University Press, (1976).

[173] P. Bala and R. W. Carter, "Classes of unipotent elements in simple algebraic groups. ii", *Mathematical Proceedings of the Cambridge Philosophical Society*, vol. 80, pp. 1–18, Cambridge University Press, (1976).

[174] D. I. Stewart, "On the minimal modules for exceptional lie algebras: Jordan blocks and stabilizers", *LMS Journal of Computation and Mathematics* **19** (2016), no. 1, 235–258.

[175] F. Carta, S. Giacomelli, N. Mekareeya, and A. Mininno, "Conformal manifolds and 3d mirrors of Argyres-Douglas theories", *JHEP* **08** (2021) 015, 2105.08064.

[176] F. Carta, S. Giacomelli, N. Mekareeya, and A. Mininno, "Dynamical consequences of 1-form symmetries and the exceptional Argyres-Douglas theories", 2203.16550.

[177] P. Slodowy, "Simple Singularities and Simple Algebraic Groups", *Lecture notes in mathematics*, Springer-Verlag, (1980).

[178] A. Sen, "Tachyon condensation on the brane anti-brane system", *JHEP* **08** (1998) 012, hep-th/9805170.

[179] A. Collinucci, F. Denef, and M. Esole, "D-brane Deconstructions in IIB Orientifolds", *JHEP* **02** (2009) 005, 0805.1573.

[180] H. C. Pinkham, "Factorization of birational maps in dimension-3", *Proceedings of Symposia in Pure mathematics*, vol. 40, pp. 343–371, American Mathematical Society, (1983).

[181] D. R. Morrison and D. S. Park, "F-Theory and the Mordell-Weil Group of Elliptically-Fibered Calabi-Yau Threefolds", *JHEP* **10** (2012) 128, 1208.2695.

[182] W. Donovan and M. Wemyss, "Stringy Kähler moduli, mutation and monodromy", 1907.10891.

[183] A. Klemm and R. Pandharipande, "Enumerative geometry of Calabi-Yau 4-folds", *Commun. Math. Phys.* **281** (2008) 621–653, math/0702189.

[184] Y. Cao and Y. Toda, "Gopakumar–Vafa Type Invariants on Calabi–Yau 4-Folds via Descendent Insertions", *Commun. Math. Phys.* **383** (2021), no. 1, 281–310, 2003.00787.

[185] Y. Cao, M. Kool, and S. Monavari, "Stable Pair Invariants of Local Calabi–Yau 4-folds", *Int. Math. Res. Not.* **2022** (2022), no. 6, 4753–4798, 2004.09355.

[186] Y. Cao, G. Oberdieck, and Y. Toda, "Gopakumar-Vafa type invariants of holomorphic symplectic 4-folds", 2201.10878.

[187] F. Benini, "Basics of Differential Geometry & Group Theory".

[188] G. Racah, "Group Theory and Spectroscopy", Institute for Advanced Study, Princeton, (1951).